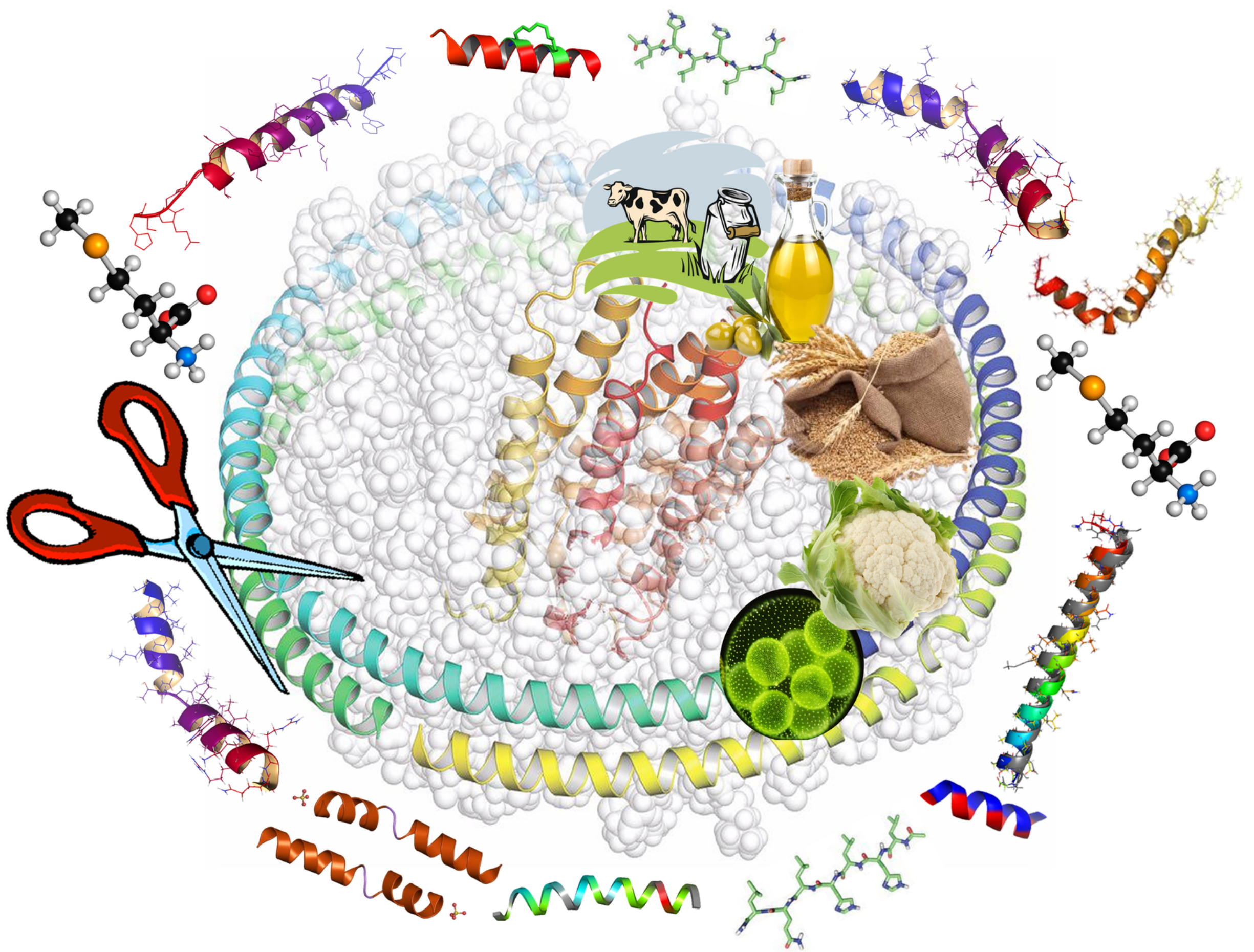


PH.D. IN CHEMISTRY

BIOACTIVE COMPOUNDS ANALYSIS IN FOOD MATRICES AND WASTE PRODUCTS



Tutor Prof. Aldo Laganà

CARMELA MARIA MONTONE



University of Rome "SAPIENZA"



SAPIENZA
UNIVERSITÀ DI ROMA

Faculty of Mathematical, Physical and Natural Sciences



Department of Chemistry

**Bioactive compounds analysis in food matrices and waste
products**

Carmela Maria Montone

Supervisor

Prof. Aldo Laganà

Coordinator

Prof. Osvaldo Lanzalunga

Ph.D. in Chemistry

Cycle XXXII

Registration number: 1674043

2019

Table of contents

TABLE OF FIGURES	IV
PH.D. THESIS PUBLICATIONS	VII
ABBREVIATIONS	IX
ABSTRACT	XII
CHAPTER 1: BACKGROUND	1
1.1 Food quality, nutrition and valorization of waste products	1
1.2 Applications in nutraceuticals, pharmaceuticals, and medicine	3
1.2.1 Bioactive peptides.....	4
1.2.1.1 Short peptides.....	5
1.2.2 Seleno-amino acids	6
1.2.3 Phosphopeptides	7
CHAPTER 2: BIOACTIVE PEPTIDES	10
2.1 Protein extraction	11
2.2 Bioactive peptides by enzymatic hydrolysis	12
2.2.1 Bioactive peptides from agro-industrial wastes.....	13
2.3 Peptide purification by multidimensional liquid-chromatography.....	13
2.4 Peptidomics and identification of bioactive peptides	14
2.4.1 Characterization of Antioxidant and Angiotensin-Converting Enzyme Inhibitory Peptides Derived from Cauliflower by-products by Multidimensional Liquid Chromatography and Bioinformatics (Paper I).....	16
2.4.2 A Peptidomic strategy for purification and identification of potential ACE-Inhibitory and antioxidant peptides in Tetrademus obliquus microalgae (Paper II).....	22
CHAPTER 3: SHORT PEPTIDES	31
3.1 Chromatographic separation of short peptides on PGC (Paper III)	31
3.1.1 Effect of organic modifier and acidic additives	33
3.1.2 Effect of temperature.....	35

3.1.3 Post-column addition of 3-NBA	36
3.2 Data analysis and peptide identification	38
3.3 Identification of bioactive short peptides in cow milk by high performance liquid chromatography on C18 and porous graphitic carbon coupled to high resolution mass spectrometry (Paper IV)	39
3.3.1 Peptide purification with cotton-HILIC tips	39
3.3.2 Ultra-high performance liquid chromatography-HRMS analysis	40
3.3.3 Identification of bioactive short peptides in cow milk	44
CHAPTER 4: SELENO-AMINO ACIDS	47
4.1 Targeted analysis	47
4.2 On-line and off-line methods.....	47
4.3 Encrypted and free seleno-amino acids.....	48
4.4 Data analysis	50
4.4.1 Simultaneous Preconcentration, Identification, and Quantitation of Selenoamino Acids in Oils by Enantioselective High Performance Liquid Chromatography and Mass Spectrometry (Paper V) ..	55
4.4.2 Investigation of free seleno-amino acids in extra-virgin olive oil by mixed mode solid phase extraction cleanup and enantioselective hydrophilic interaction liquid chromatography-tandem mass spectrometry (Paper VI)	61
4.4.3 Investigation of free and conjugated seleno-amino acids in wheat bran by hydrophilic interaction liquid chromatography-tandem mass spectrometry (Paper VII).....	67
CHAPTER 5: PHOSPHOPEPTIDES	73
5.1 Molecularly imprinted polymers (MIP).....	73
5.2 MIP for phosphoproteomics	75
5.2.1 Synthesis of phosphate-imprinted magnetic nanoparticles (Fe ₃ O ₄ @FB1@PPA).....	75
5.2.2 Data analysis.....	78
5.3 Application.....	79
APPENDIX 1	86
1.1 Liquid chromatography	86
1.2 Ionization source	87
1.2.1 ESI.....	87
1.2.2 MALDI.....	89
1.3 Mass analyzers.....	89
1.3.1 Triple quadrupole	90
1.3.2 Orbitrap.....	93
1.3.2.1 LTQ-Orbitrap XL.....	94
1.3.2.2 Orbital Velos and Elite	95
1.3.2.3 Q Exactive Orbitrap.	96
1.3.3 Time of flight (TOF).....	98

CONCLUSIONS	100
OUTLOOKS	103
BIBLIOGRAPHY	104

Table of Figures

Figure 1 Linear economy and circular economy.....	2
Figure 2 Structures of phosphoserine, phosphothreonine and phosphotyrosine.....	8
Figure 3 Approaches in bioactive peptides analysis.....	10
Figure 4 Chromatograms related to the optimization of cauliflower waste proteins digestion by Alcalase at pH 7 for 2 h (a), pH 7 for 4 h (b), pH 8 for 2 h (c) or pH 8 for 4 h (d).....	17
Figure 5 Fractionation scheme adopted for preparative RP-HPLC of cauliflower waste hydrolysates	19
Figure 6 Bioactivity percentage of the 12 fractions for the antioxidant assay.....	20
Figure 7 Bioactivity percentage of the 12 fractions for the antihypertensive assay.....	20
Figure 8 Protein yields for the 7 extractive protocols.....	24
Figure 9 The MS/MS spectra of the four identified and synthesized peptides.....	30
Figure 10 Schematic representation of the optimization experiments performed on PGC for short peptide separation. Final conditions are marked in red.....	32
Figure 11 Variation of the retention time (t_R) of short peptide standards as a function of TFA% in H ₂ O/ACN gradient.....	33
Figure 12 Variation of the retention time (t_R) of short peptide standards as a function of TFA% in H ₂ O/MeOH gradient.....	34
Figure 13 Variation of the retention time (t_R) of short peptide standards as a function of temperature in H ₂ O/ACN gradient.....	35
Figure 14 Variation of the retention time (t_R) of short peptide standards as a function of temperature in H ₂ O/MeOH gradient.....	36
Figure 15 Extracted ion chromatogram of the short peptide mixture under the final conditions. Analyte order: SH (1), KH (2), PL (3), LP and PI (4), KHK (5), VEP (6), GDLE (7), VRGP (8), RF (9), LPL (10), RKKH (11), IPI (12), IPPL (13).....	37
Figure 16 Extracted ion chromatogram of the short peptide mixture by C18 column.....	41
Figure 17 Extracted ion chromatogram of the short peptide mixture by PGC column.....	42
Figure 18 MS/MS spectra showing diagnostic fragments for the dipeptide Xle-Trp, for the tripeptide Val-Glu-Phe and for the tetrapeptide Xle-Pro-Met-Trp, respectively identified in the C18 separation	43

Figure 19 MS/MS spectra showing diagnostic fragments for the di-peptide Tyr-Gln, for the tri peptide Xle-Xle-Val and for the tetrapeptide Xle-Pro-Val-Pro, respectively identified in the PGC separation	44
Figure 20 Distribution of the short peptides identified in the C18 and PGC experiments.....	45
Figure 21 Structures of seleno-amino acids.....	49
Figure 22 CHIROBIOTIC TAG: Glycopeptide Teicoplanin Aglycone	50
Figure 23 L-Selenomethionine (peak 1), D-selenomethionine (peak 3), Se-methyl-L-selenocysteine (peak 2), L-selenocystine (peak 4), D-selenocystine (peak 6), and meso-selenocystine (peak 5).....	53
Figure 24 Racemic tryptophan trapping and enantioresolution in DCM. Trapping efficiency as calculated by the estimated recovery: 60% for L-tryptophan and 60% for D-tryptophan	56
Figure 25 Image of the capture system	57
Figure 26 High pressure vessel preconcentration on 500 mg fish oil supplement (blue) and sunflower oil (orange) and on 50 mg soybean oil (green) sample	60
Figure 27 Recovery (%) for different loaded sample and cleanup conditions (a–e) for the OASIS MCX (150 mg) cartridge	63
Figure 28 A: Enantioresolution of the target seleno-amino acids (0.4 ng injected of each standard) on the CHIROBIOTIG TAG. Elution order: L-SeMet (1), L-MeSeCys (2), D-SeMet (3), L-SeCys ₂ (4), meso-SeCys ₂ (5), D-SeCys ₂ (6). B: mass chromatograms of two representative EVOO samples, one containing 0.72 µg kg ⁻¹ L-SeMet (sample 27) and an apparently empty sample (sample 33).....	64
Figure 29 Correlation between Selenium and Selenium-methionine.....	66
Figure 30 Comparison between the different procedures	69
Figure 31 SRM acquisition of sample spiked at LOQ value. L-Selenomethionine (peak 1) 3.9min, D-selenomethionine (peak 3) 6.9min, Se-methyl-L-selenocysteine (peak 2) 4.1min, L-selenocystine (peak 4) 8.6min, D-selenocystine (peak 6) 11min, and meso-selenocystine (peak 5) 9.5min;.....	70
Figure 32.....	71
Figure 33 Chromatograms showing the separation of seleno-amino acids in bran: A) free seleno-amino acids B) conjugated seleno-amino acids obtained by digestion with protease k; C) conjugated seleno-amino acids obtained by digestion with protease XIV. L-Selenomethionine (peak 1) 3.9min, D-selenomethionine (peak 3) 6.9min, Se-methyl-L-selenocysteine (peak 2) 4.1min, L-selenocystine (peak 4) 8.6min, D-selenocystine (peak 6) 11min, and meso-selenocystine (peak 5) 9.5min.....	72
Figure 34 Schematic representation of the molecular imprinting process	74
Figure 35 Synthesis of phosphate-imprinted magnetic nanoparticles (Fe ₃ O ₄ @FB1@PPA)	77
Figure 36 SEM image of phosphate-imprinted magnetic nanoparticles (Fe ₃ O ₄ @FB1@PPA)	78
Figure 37 MALDI MS spectrum of the standard peptide mixture (reference) for each step of the enrichment process (loading and elution) with reference solution	81

Figure 38 MALDI MS spectrum of each fraction form the enrichment of standard phosphopeptides from a mixture of casein and BSA digests; the reference is a tryptic digest of casein and BSA spiked with the 8 standard phosphopeptides. Stars label pTyr peptides	82
Figure 39. ESI ionization process [120].....	88
Figure 40 Basic scheme of a mass spectrometer [123]	90
Figure 41 Diagram of a quadrupole	90
Figure 42 QqQ mass spectrometer.....	91
Figure 43 Acquisition modes of a QqQ instrument	92
Figure 44 Scheme of Orbitrap analyzer FT mass analyzer [125]	94
Figure 45 Ion trap/Orbitrap hybrid mass spectrometer architecture	95
Figure 46 Schematic representation of Orbitrap Elite.....	96
Figure 47 Schematic representation of Orbitrap Q-Exactive.....	97
Figure 48 MALDI TOF/TOF instrumentation.....	99

Ph.D. thesis publications

[I] **C. M. Montone**, A. L. Capriotti, C. Cavaliere, G. La Barbera, S. Piovesana, R. Zenezini Chiozzi, A. Laganà. *Characterization of Antioxidant and Angiotensin-Converting Enzyme Inhibitory Peptides Derived from Cauliflower by-products by Multidimensional Liquid Chromatography and Bioinformatics*, Journal of functional foods 2018, 44, 40-47 doi: 10.1016/j.jff.2018.02.022

[II] **C. M. Montone**, A. L. Capriotti, C. Cavaliere, G. La Barbera, S. Piovesana, R. Zenezini Chiozzi A. Laganà, *A Peptidomic strategy for purification and identification of potential ACE-Inhibitory and antioxidant peptides in Tetradismus obliquus microalgae*, Analytical and Bioanalytical Chemistry 2018, 410 (15) 3573-3586 doi: 10.1007/s00216-018-0925-x

[III] S. Piovesana, **C.M. Montone**, C. Cavaliere, C. Crescenzi, G. La Barbera, A. Laganà, A.L.Capriotti, *Sensitive untargeted identification of short hydrophilic peptides by high performance liquid chromatography on porous graphitic carbon coupled to high resolution mass spectrometry*, Journal of Chromatography A 2019, 1590 73-79 doi: 10.1016/j.chroma.2018.12.066

[IV] **C. M. Montone**, A. L. Capriotti, A. Cerrato, M. Antonelli, G. La Barbera, S. Piovesana A. Laganà,,C. Cavaliere, *Identification of bioactive short peptides in cow milk by high performance liquid chromatography on C18 and porous graphitic carbon coupled to high resolution mass spectrometry* Analytical and Bioanalytical Chemistry 2019 411 (15) 3395-3404 doi: 10.1007/s00216-019-01815-0

[V] A.L. Capriotti, **C.M. Montone**, M. Antonelli, C. Cavaliere, G. La Barbera, F. Gasparrini, S. Piovesana, A. Laganà, *Simultaneous Preconcentration, Identification, and Quantitation of Selenoamino Acids in Oils by Enantioselective High Performance*

Liquid Chromatography and Mass Spectrometry, Analytical Chemistry 2018, 90 (14) 8326-8330 doi: 10.1021/acs.analchem.8b02089

[VI] S. Piovesana, **C.M. Montone**, M. Antonelli, C. Cavaliere, G. La Barbera, S., Canepari, R. Samperi, A. Laganà, A.L. Capriotti, *Investigation of free seleno-amino acids in extra-virgin olive oil by mixed mode solid phase extraction cleanup and enantioselective hydrophilic interaction liquid chromatography-tandem mass spectrometry*, Food Chemistry 2019, 278 17-25 doi: 10.1016/j.foodchem.2018.11.053

[VII] **C. M. Montone**, M. Antonelli, A. L. Capriotti, C. Cavaliere, G. La Barbera, S. Piovesana, A. Laganà, *Investigation of free and conjugated seleno-amino acids in wheat bran by hydrophilic interaction liquid chromatography-tandem mass spectrometry*, Journal of separation science 2019, 42 (10) 1938-1947 doi: 10.1002/jssc.201900047

[VIII] G. La Barbera, A. L. Capriotti, C. Cavaliere, **C. M. Montone**, S. Piovesana, R. Samperi, R. Zenezini Chiozzi, A. Laganà *Liquid chromatography-high resolution mass spectrometry for the analysis of phytochemicals in vegetal-derived food and beverages*, Food Research International 2017, 100 28-52 doi: 10.1016/j.foodres.2017.07.080

[IX] C. Cavaliere, A.L. Capriotti, G. La Barbera, **C.M. Montone**, S. Piovesana, A. Laganà, *Liquid chromatographic strategies for separation of bioactive compounds in food matrices*, Molecules 2018, 23 (12) 27 doi: 10.3390/molecules23123091

[X] S. Piovesana, A. L. Capriotti, C. Cavaliere, G. La Barbera, **C. M. Montone**, R. Zenezini Chiozzi A. Laganà, *Recent trends and analytical challenges in plant bioactive peptides separation, identification and validation*, Analytical and Bioanalytical Chemistry 2018, 410 (15) 2018, 3425-3444 doi: 10.1007/s00216-018-0852-x

Abbreviations

BPs bioactive peptides

PTM post-translational modification

SPE solid-phase extraction

Se-AAs seleno-amino acids

RP reversed phase

MS mass spectrometry

HR high-resolution

NIH National Institutes of Health

SeCys Se-cysteine

SeMet Se-methionine

MeSeCys methyl-Se-cysteine

SeCys² Se-cystine

pTyr Tyrosine phosphopeptides

pSer Serine phosphopeptides

pThr Threonine phosphopeptides

MIPs molecularly printed polymers

BAP bioactive peptides

UHPLC ultra-high-pressure liquid chromatography

SDS sodium dodecyl sulphate

HILIC Hydrophilic interaction chromatography

ABTS (2,2'-Azino-bis(3-ethylbenzothiazoline-6-sulfonic acid)

DPPH (2,2-diphenyl-1-picrylhydrazyl)

ACE-inhibitor angiotensin-converting-enzyme inhibitor

PGC porous graphitic carbon

3-NBA 3-nitro benzyl alcohol

TFA Trifluoroacetic acid

FA Formic acid

MeOH Methanol

ACN Acetonitrile

GRAVY grand average of hydropathy index

SRM Selected Reaction Monitoring

LLE Liquid-liquid extraction

S/N signal-to-noise ratio

DCM dichloromethane

R% recovery

ME% matrix effect

PE% process efficiency

LOQ quantification limit

LOD identification limit

Oasis MCXTM SPE Sorbents Mixed-mode, strong Cation-eXchange

OASIS HLB SPE Sorbents Hydrophilic-Lipophilic Balance

EVOO extra virgin olive oil,

HCl chloridric acid

ESI electrospray ionization

FDA Food and Drug Administration

PPA phenylphosphonic acid

black magnetic nanoparticles (MagNPs)

TEOS (10%) (Tetraethyl orthosilicate)

FB1 (PABA (4-Aminobenzoic acid) + 3,5-Bis(trifluoromethyl)phenyl isocyanate)

BSA bovine serum albumin

DTT dithiothreitol

IAA iodoacetamide

MALDI matrix-assisted laser desorption/ionization

HCD high-energy collisional dissociation cell

TOF Time of flight

2D 2 dimension

Abstract

Food and nutrition research have grown exponentially over the past two decades, changing the way food is considered. In fact, it is no longer considered simply energy for the body but provides components with specific functions and nutritional properties, which include potential benefits, as well as possible harmful effects on health; among these, fatty acids, vitamins, phenolic acids, and flavonoids have been studied in recent years. In recent years, proteins, peptides and lipids have also played an important role in the study of components with high nutritional value, giving way to a new branch of the omic sciences, namely nutritional proteomics (nutriproteomics) and lipidomics. The study of bioactive peptides present in various food products represents a new field of research and field of application of proteomic analysis. Some peptides are able to trigger physiological activities that promote skin health, such as stimulating collagen synthesis, controlling angiogenesis and melanogenesis and modulating cell proliferation. Peptides are often classified as multifunctional peptides, i.e. they are capable of inducing more than one physiological activity. These characteristics make them suitable for use as therapeutic agents in the pharmaceutical field or as functional compounds, food additives, bio-preservatives in the field of nutraceuticals. These peptides can be released in different ways: they can be naturally present (i.e. endogenous) in matrices due to the presence of enzymes or bacteria, they can be released during gastrointestinal digestion, they can be formed following processes that occur in foods such as maturation, fermentation, storage or cooking, or by *in vitro* hydrolysis with the selection of a specific and appropriate enzyme. Except in the case in which the digestion is carried out *in vitro* by site-specific proteases, the obtained peptides can have a wide range of terminal amino acids and sizes. Of interest are both the bioactive peptides derived from enzymatic digestion, but also the short peptides naturally present within the matrix. Another very interesting class of molecules, not widely studied but specifically analyzed in this work are: seleno-amino acids. These compounds regulate many biological activities, and are important against various diseases. Another important goal is the study of waste. This type of product is normally seen as a problem for the economy and the

environment, because it must be disposed of waste could be better used, though, not only as feed for animals but, for example, as a source of bioactive compounds.

Therefore, the purpose of this doctoral project was to develop effective and innovative analytical strategies for the study of bioactive molecules and identification of compounds not abundant or not yet identified in different food matrices.

Chapter 1: Background

1.1 Food quality, nutrition and valorization of waste products

Food and nutrition research has been growing exponentially over the last twenty years, changing the way in which food is considered. In fact, it is no longer considered simply energy for the body but provides components with specific function and nutritional properties, which include potential benefits, as well as possible harmful effects on health; this is demonstrated by a rapid proliferation of studies examining nutritional exposures in relation to different diseases [1]. The health and efficiency of the person depend largely on nutrition. Eating too much and incorrectly can cause overweight, hypercholesterolemia, high blood pressure, diabetes and, therefore, increase the risk of cardiovascular disease. If on the one hand an incorrect diet significantly affects the development of some diseases, on the other hand some foods can protect us [2]. Antioxidants compounds, for example, are important in the prevention of cancer since they are capable of buffering DNA damage at the base of the development of tumors caused by free radicals. Other compounds that have an important nutritional value and should be regularly introduced into the body are vitamin C, contained in fruit and vegetables, vitamin E, contained in vegetable oils, polyphenolic antioxidants such as resveratrol, contained in fruits and grapes, and finally carotenoids such as lycopene, which is also contained in vegetables [3]. These classes of substances have been widely studied over the past decades [4]. More recently, research has moved on components with a high nutritional value such as proteins, peptides and lipids, starting a new class of omic sciences, namely nutritional proteomics (nutriproteomics) and lipidomics. Along with the extraction of compounds useful for health and with a high nutritional value, the conversion of wastes, biomass and various residues into energy, fuels and other useful materials has recently become an important research field. This concept is known as re-valorization [5]. From this point of view, waste

becomes precious raw materials from which to derive new resources; in this way, the foundations are built for the transition to a new type of economic model: the circular economy, in which what is produced is thought to have a new life, becoming new raw materials. This model differs from the previous linear economy, based on the assumption that the products which we use follow a life cycle that begins with the extraction of raw materials, proceeds through the transformation of these into goods that are then placed on the market and ends with the elimination of the "waste".

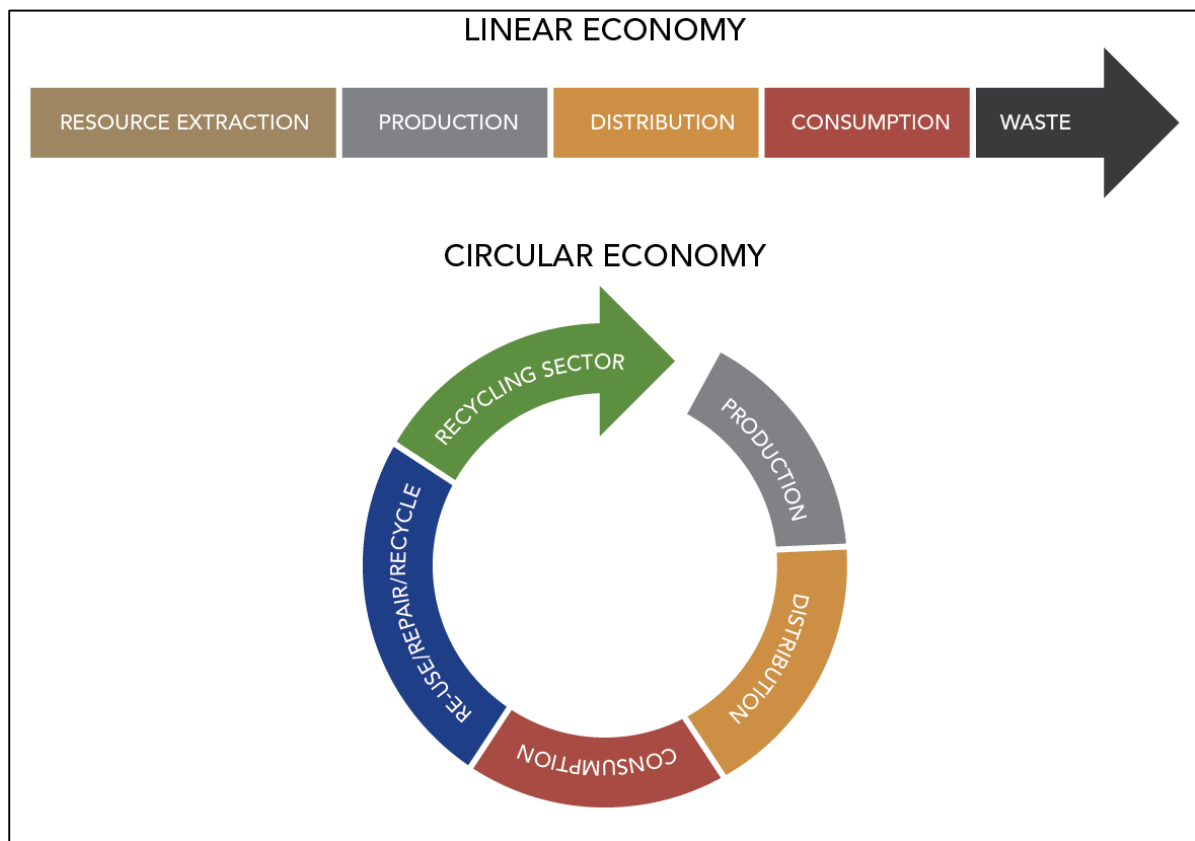


Figure 1 Linear economy and circular economy

It is easy to understand how the circular economy is an important component of the transition towards sustainable development: it is based, in fact, on renewable energy sources and aims to reduce the use of substances that are harmful to the environment, to minimize the waste production maximizing the conversion of products.

1.2 Applications in nutraceuticals, pharmaceuticals, and medicine

The beneficial properties of food have been studied for years [6]. Modern nutraceuticals have been first developed in Japan in 1980 and they differ from medicinal herbs used for years in Asia. Until a few years ago, food analysis was limited to the analysis of flavor (taste and sensory consistency) and its nutritional value (carbohydrates, vitamins, fats, water and minerals). Scientists have instead shown that food can play a key role in health [7]. Consumption of therapeutic food is a viable alternative to reverse situation due to poor eating habits and sedentary lifestyle, mainly in industrialized countries where population consumes diets with extra calories and nutrients imbalance. In fact, therapeutic food has specific characteristics that contribute to the prevention and treatment of diseases due to the presence of bioactive compounds. The action of bioactive compounds in therapeutic food in reducing the risk of diseases is directly related to the bioactivity of metabolites, such as polyunsaturated fatty acids, triglycerides, steroids, flavonoids, isoflavones, carotenoids, vitamin C, and other antioxidants. In general, they are present in low concentrations in food, consequently they have low bioactivity when compared to pharmaceuticals products; however, once they are ingested regularly as part of the diet, they may present long-term noticeable physiological effects. These bioactive compounds are the subject of recent studies and further research to elucidate their effects and benefits is extremely important [8]. Therefore, due to the importance of these compounds, innovative strategies for extracting and enriching these substances find application in the field of human health. The interaction between modern food science and disciplines such as pharmacology, medicine or biotechnology, offers new challenges and impressive opportunities. Research in the field of food science and nutrition use nowadays advanced analytical approaches which involved omic science, bioinformatic tools and *in vitro* and *in vivo* assays [3]. Different compounds play an important role in the nutraceuticals and pharmaceuticals fields. A detailed description of the classes of interest in this thesis dissertation will be provided below. In particular, bioactive peptides (BPs), seleno-amino acids (Se-AAs) and phosphopeptides will be described with a particular focus on structure, functions and bioactivity properties.

1.2.1 Bioactive peptides

The interest in bioactive peptides (BPs) has been greatly increasing in the last 10 years. As evidence of it, more than 800 publications have been published on this topic since 2014 (PubMed search). BPs are protein fragments which usually have a minimum of 2 and a maximum of 20 amino acids (AAs) in their sequences. They are usually classified into two main categories as medium size peptides (6-20 aa) and short peptides (2-5 aa). BPs can be released and generated in different ways: they can be naturally present in the matrices (endogenous BPs) due to the presence, for instance, of enzymes or bacteria, or they can be released during gastrointestinal digestion or even they can be formed as a result of processes that occur in foods such as maturation, fermentation, storage or cooking, or by *in vitro* hydrolysis with the selection of a specific enzyme. Except when the digestion is carried out *in vitro* by site-specific proteases (for instance, trypsin), in most cases peptides obtained in other ways can have a wide range of terminal amino acids and sizes.

BPs are inactive within the native protein, but once formed they can show numerous biological activities; a wide range of biological activities are known to be induced by these peptides, such as antioxidant, cytomodulatory, immunomodulatory, antihypertensive, antidiabetic, anti-inflammatory, antithrombotic, metal-chelating, antimicrobial, emulsifying agents, and anti-cholesterolemic [9,10]. Some peptides are able to trigger physiological activities that promote skin health, such as stimulating collagen synthesis, controlling angiogenesis and melanogenesis and modulating cell proliferation. Peptides are often classified as multifunctional peptides, i.e. they are capable of inducing more than one physiological activity [11]. These characteristics make them suitable for use as therapeutic agents in the field of pharmaceutical production or as functional compounds, food additives, bio-preservatives in the field of nutraceuticals.

Fruit and vegetable BPs have been less studied [12,13] compared to those derived from milk [14–16], eggs [17], fish [10] and meat [18]. However, plant peptides have good potential since they are continuously subjected to biotic and abiotic stresses, which can lead to the development of an efficient defense system in plants consisting of secondary metabolites such as phenols, substituted oxygen derivatives, terpenoids, quinines, tannins and BPs [19]. Proteins and peptides play a role as secondary metabolites, because they show many properties, such as slowing the progression of the disease, inhibiting pathophysiological mechanisms or

suppressing the activity of pathogenic molecules [20]. Moreover, the search for BP in plants is of considerable importance, because it possibly represents an re-valorization of waste products [21]. In the perspective of biosustainable development and renewable resource technologies, by-products and waste from plants and fruits represent a relatively cheap source of material suitable for BP production, which would reduce both the amount of waste and the related costs of disposal, while producing added-value nutritional products [22]. In this dissertation thesis Chapter 2 will be dedicated to the extraction, separation and identification of BPs in vegetable matrices, in particular microalgae and cauliflowers by-products.

1.2.1.1 Short peptides

Short peptide sequences (< 5 AAs) are emerging as promising compounds in different research fields, such therapeutics [23], diagnostics [24] and nutraceuticals [25]. One of the most important and studied research field is in the area of nutraceutical, being BPs in food or food by-products health promoters, with antioxidant, antihypertensive and antimicrobial properties [16,26]. Another interesting application in the food area is the discovery of short peptides as biomarkers for food traceability [27]. Another emerging and promising field is the identification of short peptide biomarkers of disease [24], because peptides can have specific functions, for instance, in modulating cancer cells aggressiveness [28].

Until now, just few papers in the literature were focused on the analysis of short peptides, despite their importance in many fields. There are, in fact, several issues related to the analysis and identification of short peptide sequences. The first one concerns the wide range of polarity of these peptides. The common analytical strategies employed for purification and separation are usually based on conventional reversed phase (RP) systems, which is not directly applicable to all short peptides due to a wide range of polarity which results with short amino acidic sequences being eluted with the dead volume or lost during the enrichment, purification and separation step [29]. The second issue concerns MS detection. Differently from larger peptides, short peptides do not easily become at least doubly positively charged, a limitation which reduces the information acquired by MS/MS experiments as background noise is increased and fragmentation of the backbone is reduced. Such behaviour places short peptides at the interface between macromolecules and small molecule analysis. A different MS approach needs to be pursued, and fragmentation energy becomes a fundamental parameter to be evaluated to optimize fragmentation and peptide identification [30]. This feature, typical of

small molecule analysis, is particularly relevant when considering that short peptides can also be identified within metabolomics studies and are commonly included within metabolite databases [31,32]. The third challenge concerns the identification and the bioinformatic interpretation of spectra for their identification. Common proteomic databases cannot confidently identify sequences shorter than 5 amino acids [33]. Some solutions have been found to overcome the problem. For example, a targeted analysis with standards for which retention times (tR) and mass data are recorded; or identification by *de novo* sequence [34] or, as recently described by Fitzgerald and his co-workers, retention time validation by retention time prediction models [35].

For these reasons, one of the main goal of this thesis was the development of a specific analytical platform able to solve the challenges related to the separation and identification of short amino acidic sequences. Chapter 3 will be entirely dedicated to this topic.

1.2.2 Seleno-amino acids

Selenium (Se) is a micronutrient which possesses a high influence on human health [36]. Selenium can be essential but at the same time harmful. The amount of total selenium has been extensively studied in food, dietary and biological food supplements [37–39]. It has an important biochemical role in the synthesis of seleno-proteins (25 in humans), which generally have redox functions and are involved in scavenging free radicals, immune function, thyroid function, spermatogenesis, cancer prevention and resistance to pathogens [40]. For the National Institutes of Health (NIH) [41] the recommended daily dose of Se is in the range of 55-70 $\mu\text{g day}^{-1}$ for adults and 15-40 $\mu\text{g day}^{-1}$ for children, while the largest level of intake in adults is set at 400 μg per day. Intake of Se in human occurs with the diet. Food of animal origin is richer in Se compared to plants.

Plants assimilate and metabolize Se (VI) by sulfur uptake and biochemical pathways [42,43]. Selenate anion (SeO_4^{2-}) is firstly reduced to selenite (SeO_3^{2-}), then to selenide (Se^{2-}) and finally metabolized to organic forms, which are mainly seleno-amino acids, i.e. Se-cysteine (SeCys), Se-methionine (SeMet), methyl-Se-cysteine (MeSeCys), Se-cystine (SeCys^2) and sometime other more complex Se organic forms [44].

Determining the total content of Se of a given food is incomplete information, because the bioavailability of this nutrient depends on the form in which it is present, being better assimilated by humans as an organic species [45].

Another very important aspect to consider is related to the chirality of seleno-amino acid compounds. In fact, amino acids have a single asymmetric carbon atom therefore they can exist as a pair of enantiomers. Instead, for the Se-Cys₂, which consists of two molecules of Se-Cys, with a Se-Se bond, there are three enantiomeric forms D-, L- and meso-form. Chirality can play an important role in bio-distribution and bioactivity. Amino acids found conjugated to proteins are L-amino acids and it has been studied that D- and L-amino acids have different intestinal absorption and different metabolic pathways; more specifically, the absorption of D-isomers is slower than L-isomers [46]. Furthermore, even the D-isomers must convert into L-forms before protein insertion, this conversion has been described for all amino acids [47].

The analytical methodologies for the extraction, enrichment and chiral separation of Se-AAs in olive oil and in wheat bran samples will be discussed and described in Chapter 4.

1.2.3 Phosphopeptides

Phosphopeptides derive from a post-translational modification (PTM): phosphorylation. Phosphorylation is a dynamic and reversible post translational modification, one of the most widely studied, affecting basic biological processes such as cell growth, proliferation, differentiation, and apoptosis as well as cellular signal transduction [48]. It can occur on nine AAs, i.e. serine, threonine, tyrosine, histidine, lysine, arginine, aspartic acid, glutamic acid, and cysteine. However, in proteins it is most frequently found on serine, threonine, tyrosine, which are actually the most investigated.

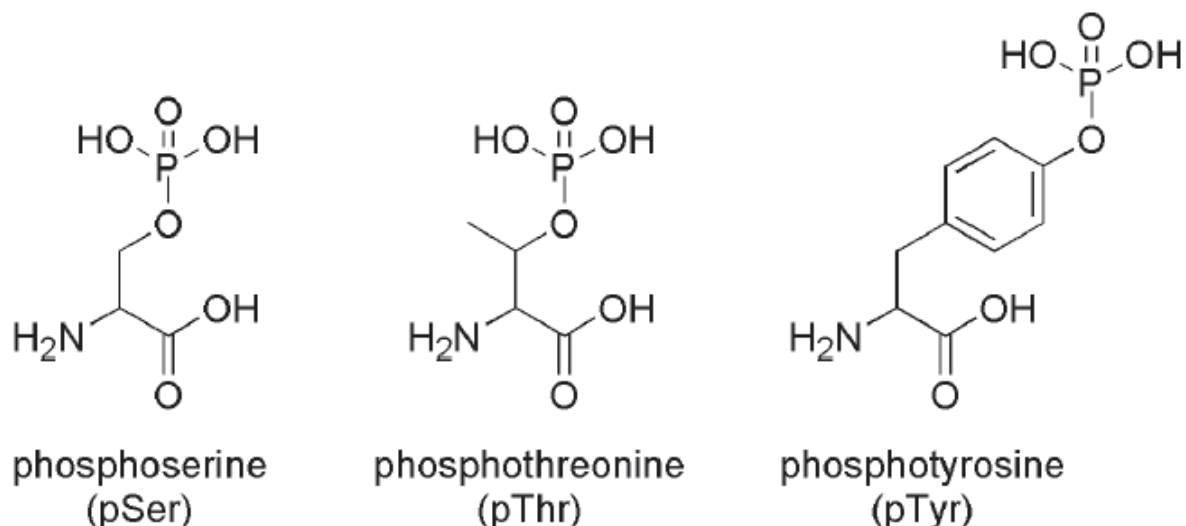


Figure 2 Structures of phosphoserine, phosphothreonine and phosphotyrosine

Phosphorylation is responsible for regulation of many important processes such as cell proliferation, differentiation and apoptosis and plays a vital role in signal transduction. Disruptions in signaling pathways, regulated by kinases and phosphatases, are often recognized as a cause or a consequence of various diseases, including cancer [49,50], neurodegenerative diseases [51], cardiovascular diseases [52,53], inflammatory diseases [54,55], and diabetes [56]. This has led to an increasing effort to identify kinases and phosphorylated proteins that could serve as disease biomarkers or drug targets, especially in cancer [49].

Proteomic technologies and mass spectrometry are the main techniques for the study of PTMs. Due to the low abundance of phosphopeptides and the suppression caused by the more abundant non-phosphorylated peptides during ionization and MS analysis, direct analysis using HPLC-MS/MS cannot be performed without prior peptide enrichment [57]. Different approaches are described in the literature, such as the immobilized metal-ion affinity chromatography (IMAC), metal-oxide affinity chromatography (MOAC), inorganic affinity chromatography with lanthanide salt ions, coprecipitation, ion exchange chromatography, chemical derivatization and immunoprecipitation [58]. Affinity chromatography is the most used, based on the affinity of the phosphate to an ionic metal. The metal ions used in IMAC include Fe³⁺ [57], Ga³⁺ [59], Ti⁴⁺ [60], and Zr⁴⁺ [61]. As far as MOAC is concerned, the metal oxides TiO₂ [49] and ZrO₂ are the most popular [62].

Tyrosine phosphopeptides (pTyr) are very important and can be used as biomarker for cancer diagnostics and therapies [63,64]. However, the abundance of pTyr is generally very low (<1%) compared to pSer (90%) and pThr (10%) in most eukaryote cells [65], which makes it difficult to analyze pTyr by common pre-concentration techniques. The common pre-concentration techniques have two disadvantages: insufficient specificity and the interference of non-phosphorylated peptides. For this reason, it is important to develop absorbents for the selective enrichment of pTyr, based, for example, on molecularly printed polymers (MIPs), which possess some advantages over the above mentioned approaches, such as chemical stability, specific recognition and reusability [66]. Molecular imprint technology is a strategy to create tailored target binding sites to recognize the target and represents a valuable alternative to antibodies.

This part of thesis was performed in Sweden in the research group of Prof. Sellergren at the Department of Biomedical Sciences, Malmö University.

Chapter 2: Bioactive Peptides

Approaches for the identification of new bioactive peptides (BAP) have been described in the scientific literature [15,67]. Most of these approaches are empirical and involve a stepwise process (Fig.3) in which peptides are fractionated one or more times, assayed for a given bioactivity and only the most active fraction identified. Empirical approaches resulted in the successful identification and evaluation of dietary BAPs. However, several limitations exist, which are summarised in Fig.3. These will be discussed in further detail in the following thesis subsections. Specific examples will be also provided (paper I and paper II).

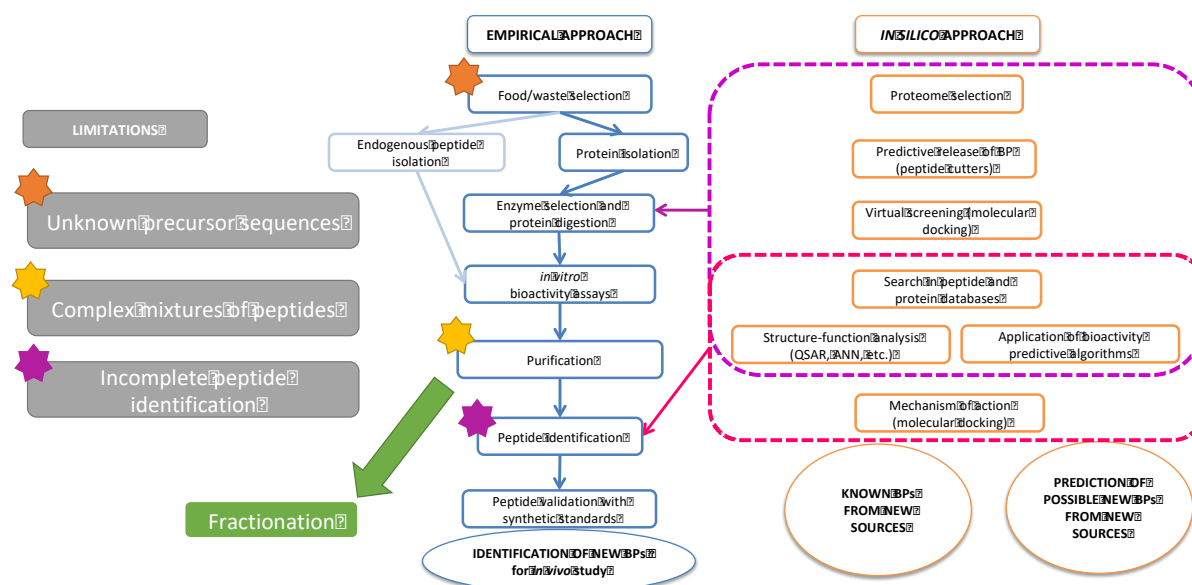


Figure 3 Approaches in bioactive peptides analysis

The first step of the empirical approach in BAP discovery consists in the selection of the food matrices and of the proteolytic enzyme for the preparation of protein hydrolysates. In many cases a site-specific enzyme is not necessary because some matrices directly contain endogenous peptides, therefore digestion is not required.

After extraction of the endogenous peptides or protein hydrolysis, specific *in vitro* bioactivity assays should be carried out to test an investigated bioactivity. The peptide composition of many hydrolysates may be highly complex. Indeed, the complexity of the peptide mixture represents a difficulty in understanding which peptides within complex mixtures are exerting a specific bioactivity. For this reason, fractionation or enrichment techniques may be employed to reduce the complexity of hydrolysates and subsequently allow identification of those peptides contributing to the bioactive properties. Peptides may be further fractionated with techniques based on different physicochemical properties such as molecular weight, hydrophobicity or charge. When a highly bioactive fraction has been obtained, it can be further characterized by identification of the peptide sequences. This generally involves the utilization of separative techniques such as, UHPLC or nano-liquid chromatography (LC) or capillary electrophoresis (CE) coupled to high resolution mass spectrometry (MS). The obtained data are analyzed with specific bioinformatics software which provide a list of peptide identification. These identifications are then processed by software and algorithms able to give a probability score of potential bioactivity, useful in order to select specific amino acidic sequences for the subsequent synthesis and validation of the identification, *in vitro* bioactivity assay and ultimately finishing with *in vivo* bioactivity assays.

2.1 Protein extraction

Protein extraction is a crucial challenge, mostly in recalcitrant tissues, as vegetables, where it is not possible to provide a universal and simple sample preparation method. An efficient protein extraction obviously influences the recovery of BAPs.

The presence of interfering substances such as polysaccharides, lipids, phenolic compounds and secondary metabolites, can impact on the protein separation and analysis. Moreover, the low concentration of soluble proteins and the abundance of proteases hinder proteomic and peptidomic analyses. Finally, owing to the diversity of protein abundance, molecular weight, charge, isoelectric point, hydrophobicity, post-translational processing and modifications, and complexation with other molecules, no single extraction protocol is effective for all proteins. For this reason a number of protein extraction protocols have been published [68,69]; those most often employed are the trichloroacetic acid (TCA)-acetone extraction and the phenol extraction. The first one is based on protein denaturation under acidic and hydrophobic conditions, and has the advantage of to separate proteins from other analytes,

avoiding contamination.; the second involves protein solubilization in the phenol phase, followed by precipitation with methanol and ammonium acetate and centrifugation. This method has been shown to generate high-quality protein extracts from a variety of plant species, but it is more time consuming, and it can be difficult to solubilize the pellet. Several strategies, based on biochemical, biophysical, or cellular properties, have been developed to improve the coverage and detection of specific groups of proteins, such as membrane proteins and low-abundant proteins. A few examples of extraction reagents and methods for specific classes of proteins include: phase partitioning by using organic solvents or Triton X-114 detergent, 3-[(3-cholamidopropyl)dimethylammonio]-1-propanesulfonate (CHAPS), sodium dodecyl sulphate (SDS), LC fractionation and isolation of highly enriched organelles or subcellular compartments.[70]

The elimination of interfering compounds after protein extraction involves the use of aqueous or phenol buffers for the extraction of proteins and their subsequent precipitation by acetone or methanol. Sometimes neither of these strategies is efficient enough, especially when the sample contains a great number of interfering compounds and a low percentage of proteins.

2.2 Bioactive peptides by enzymatic hydrolysis

Once the peptides are extracted from the selected matrix, the hydrolysis of precursor protein can be carry out by a single or multiple proteases, used either sequentially or as mixture, or by fermentation. Enzymes provide interesting advantages over fermentation approaches, especially in the case of BAP small-scale investigations. Compared with microorganisms, the hydrolysis performed by enzymes is generally faster and can be controlled. Indeed, by optimization of the hydrolysis parameters (temperature, pH, buffer composition and reaction time), reproducible molecular weight profiles and peptide composition can be obtained [13]. This makes enzymatic digestion the method of choice to produce peptides with target functionalities.

On a laboratory scale, the hydrolysis is usually performed by the traditional in solution approach, but other approaches are available, such as the use of immobilized enzymes, which allow to reduce enzyme costs and scale-up the process.

Enzymes can be site specific or unspecific. From a discovery perspective, enzymes are not equivalent to one another. In particular, the use of site-specific enzymes, such as trypsin,

allows the established proteomics technologies for peptide identification to be used, as the search space is strongly reduced when the cleavage site is known. On the other hand, in large-scale production, the use of such enzymes is not usually affordable because of the high costs. Alternatively, less specific enzymes, such as alcalase, can be used, but the specificity information is lost, complicating the final step of data management. In recent years, much has been done in this sense, and the modern approaches based on peptidomics can greatly help in peptide identification in the latter cases. In the field of vegetable-derived BAPs, proteases such as alcalase and alkaline protease and proteinases have been used to obtain BAPs on a commercial basis as their lower cost is compatible with large-scale applications [13].

In the field of peptide generation by hydrolysis, the simulation of gastrointestinal digestion is a subfield, in which the digestion conditions are mimicked to discover potential BAPs thus produced or potential inhibitory peptides of enzymes involved in the metabolic syndrome obtained by simulated gastrointestinal digestion of fermented bean (*Phaseolus vulgaris* L.) seeds [71].

In this case, the combination of pepsin–pancreatin or pepsin–chymotrypsin–trypsin is usually used to simulate the gastrointestinal degradation of food proteins in humans.

2.2.1 Bioactive peptides from agro-industrial wastes

In the perspective of biosustainable development and renewable resource technologies, by-products and waste represent a relatively cheap source of material suitable for BAP production, which would reduce both the amount of waste and the related costs of disposal, while producing added-value nutritional products. BAP production from waste and by-products does not significantly differ from the production from food vegetables, and enzymes are commonly used to hydrolyse proteins [22].

2.3 Peptide purification by multidimensional liquid-chromatography

As the peptide composition of many hydrolysates can be highly complex, there is a difficulty in understanding which peptides are exerting a certain bioactivity. For this reason, different fractionation techniques may be employed in order to enrich specific peptide sequences, allowing easier identification of peptides. The employed techniques are based on

different physicochemical properties such as molecular mass for ultrafiltration membrane systems or size exclusion chromatography, hydrophobicity for reversed phase and HILIC chromatography and charge for ion exchange chromatography [22]. Nowadays, the chromatographic techniques result to be the best choice to reduce the complexity of peptide mixtures. Chromatographic separation can be carried out in mono-dimensional or bi-dimensional (2D) set ups, the latter used to increase the separation efficiency, resolution and peak capacity. 2D-LC can be “comprehensive” when the whole sample is subjected to the two distinct separations or “heart-cutting” if only a part of the sample eluting from the first dimension is sent to the second one [72]. A representative example of how 2D-LC workflows could provide a valuable contribution to BAP analysis was provided by the work of Sommella and co-workers in the separation of peptides of milk-soluble fractions after their expiration date [73]. They used an online comprehensive LC × UHPLC platform and compared the results to those of a classical highly efficient 1D separation with the same analysis time, showing that peak capacity and resolution can be greatly enhanced in 2D-LC. Other examples using 2D-LC separation are well described in a review by Sanchez-Rivera and co-workers [74]. The separation and purification of bioactive peptides which will involve development of automated and continuous systems is an important field for food chemists. Much effort has been given to develop selective column chromatography methods that can replace batch methods of salting out or solvent extraction for BAP isolation and purification. Advancement here would improve BP recovery and would enable one to produce functional food with such peptides or employ them for specific nutraceutical applications.

2.4 Peptidomics and identification of bioactive peptides

The approach usually used to identify peptides is based on proteomics technologies, which in turn exploit nanoLC coupled to high resolution mass spectrometry and bioinformatics for spectra matching. This allows proteomic analysis to be carried out without the need for pure standards for analysis, also bypassing the laborious approach based on Edman degradation. When mass spectrometry is used for the identification of peptides in complex matrices, the correlation between experimental fragmentation spectra and those present in protein databases is the most common approach. Database search is a valuable application of proteomic approaches to identify peptides in complex samples, although it is very successful when it

comes to complete protein databases and a known enzymatic cleavage rule. However, this approach is not always applied to BAP studies, as the enzyme is not often site-specific, which in turn requires longer identification times, and the probability associated with the identification of peptides may also be lower. These problems are particularly evident in non-sequenced organisms, as in most plants. In this case, a commonly used approach is the extension of the database search to higher taxonomy entries, which enlarges the search space further hindering high confidence peptide identifications. In this latter case, the reduction of the complexity of the identified mixture is often a good strategy to increase the number of peptide identifications and improve the quality of identifications, especially when the protease is not specific (paper I and paper II). De novo identification is a valid alternative to database-driven peptide identification in peptidomic studies, and it is possible to carry it out using new fragmentation techniques, such as the dissociation of electron transfer and dissociation spectra with electron capture [115]. De novo peptide identification can be used in conjunction with traditional database search.

Once peptide sequences have been identified, it is very important to assess the probability of the associated bioactivity. A valuable tool to assess a possible bioactivity associated with each peptide sequence is provided by bioinformatics; one major advantage of bioinformatics is the possibility to search the experimental peptide sequences against databases of known bioactive sequences; for instance, searching the BIOPEP database can help identify the sequences that are already known for their bioactivity. Alternatively, bioinformatics also includes algorithms able to predict peptide-based bioactivity and assign a statistical probability of bioactivity to each sequence, although the latter approach is not applicable to all any bioactivity. However, there are limitations in both approaches, which in turn require validation of both peptide identification and bioactivity. For instance, often experimental sequences only partially correspond to the BIOPEP entries, so the synthesis and validation of each individual peptide is the only means for validating both the peptide sequence and the bioactivity and it would be necessary for undoubted conclusions.

Many freely available bioactive peptide databases have been designed to store information such as sequence, reference to published work, EC50, source and more. Three are the most interesting and were used during my PhD:

- BioPep [http://www.uwm.edu.pl/biochemia/index_en.php, is a database containing information on bioactive peptides (3271 sequences) with any kind of activity and 135 major allergens
- PeptideDB (<http://www.peptides.be>) is a database that assembles all naturally occurring signaling peptides from animal source (20,027 sequences).

In the two articles presented below, different extraction and digestion protocols were developed. Specific bioactivity assays were carried out; then, in order to try to simplify the obtained peptide hydrolysates, peptide mixtures were fractionated by preparative chromatography. This is useful for arriving to a possible bioactive sequence to be synthesized, tested and to select possible aminoacidic sequence for pharmaceutical or nutraceutical applications.

2.4.1 Characterization of Antioxidant and Angiotensin-Converting Enzyme Inhibitory Peptides Derived from Cauliflower by-products by Multidimensional Liquid Chromatography and Bioinformatics (Paper I)

In paper I, the main objective of the work was the development of a peptidomic approach for the recovery, identification and isolation of BAPs from cauliflower by-products and for the characterization of their antioxidant and anti-hypertensive biological activity. These molecules could then be used as nutraceuticals, drugs for the prevention or treatment of pathologies, cosmetic ingredients, active agents for smart packaging, etc., thus turning waste into valuable products able to improve the ecosustainability of the entire cultivation by waste disposal reduction.

Brassicaceae represent in fact a good model for the search of bioactive molecules in waste. Indeed, both food and industrial use of Brassicaceae results in large amounts (up to about 50%) of waste, which is rich in bioactive compounds. Brassicaceae contain heterogeneous classes of bioactive compounds, such as glucosinolates (a unique component of the brassicaceous vegetable metabolome), polyphenols, complex alcohols, S-containing volatile compounds, peptides, etc. [75]. Some of these compounds have not been extensively characterized, yet, which also applies to peptides.

Starting from this concept, in the present paper, BAPs from cauliflower by-products (leaves and stems) were investigated. Alcalase protein hydrolysis conditions were optimized. In particular, two pH conditions (7 and 8) and two hydrolysis times (2 h and 4 h) were tested starting from the same protein extract and the results were compared with the classical trypsin digestion (Fig 4 e tab. 1).

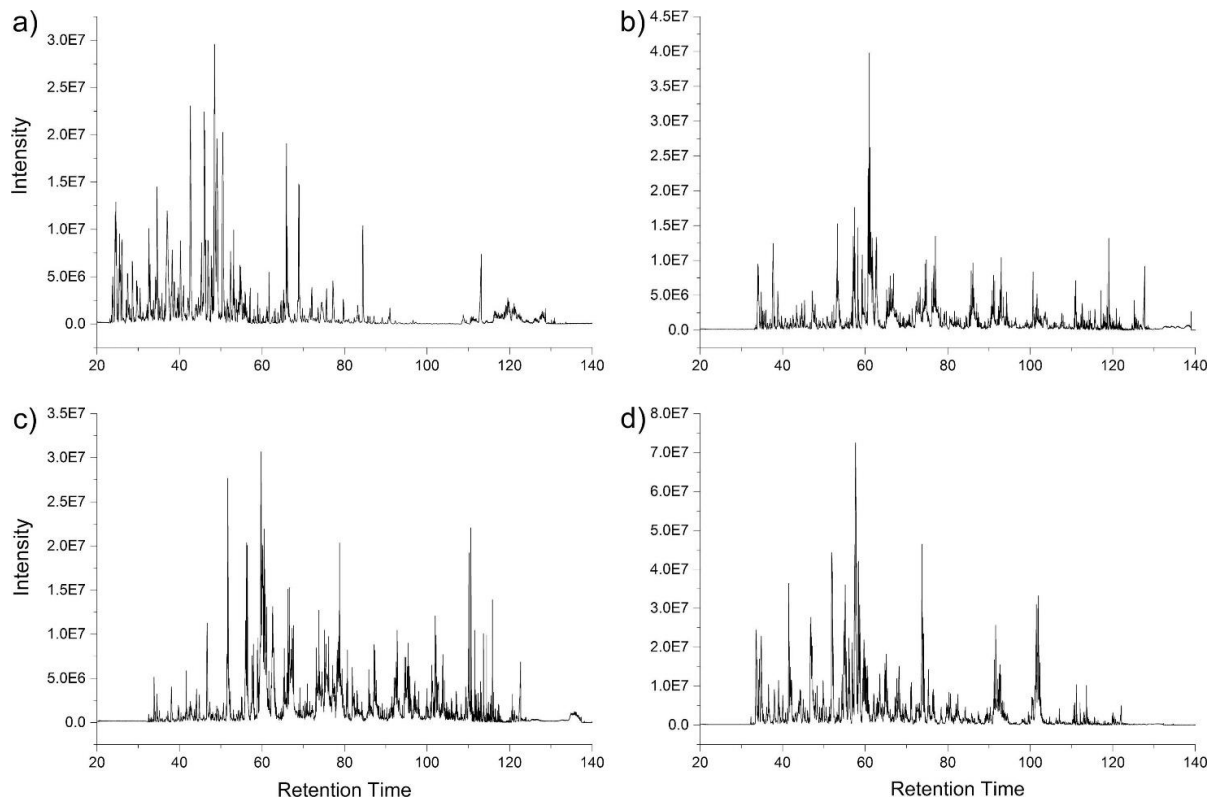


Figure 4 Chromatograms related to the optimization of cauliflower waste proteins digestion by Alcalase at pH 7 for 2 h (a), pH 7 for 4 h (b), pH 8 for 2 h (c) or pH 8 for 4 h (d)

Table 1. MS/MS spectra of chromatograms obtained from 5 μ g cauliflower waste digest by alcalase at two pH conditions (pH 7 and 8) and two hydrolysis times (2 h and 4 h). The last row provides MS/MS spectra for the same sample digested by trypsin.

Digestion conditions	Average intensity \pm SD	Full scan spectra \pm SD	MS/MS spectra \pm SD
pH7_2h	4656121 \pm 235462	9423 \pm 198	16039 \pm 330
pH7_4h	4705293 \pm 250381	9541 \pm 219	16581 \pm 325
pH8_2h	5265321 \pm 300654	9221 \pm 175	17012 \pm 381
pH8_4h	8523595 \pm 441680	8247 \pm 164	21807 \pm 463
trypsin	8125511 \pm 425945	7569 \pm 151	28623 \pm 570

The use of alcalase provided protein hydrolysates more bioactive than the hydrolysates provided by trypsin, which was used in the previous work [76]; in the present work the ACE-inhibitor activity was maintained (90.5% for trypsin vs 92.6% for alcalase), while significantly increasing the antioxidant activity, at least for the DPPH assay (7.4% for trypsin vs 38.6% for alcalase). A direct comparison indicated an improved bioactivity for alcalase hydrolysates than trypsin hydrolysates, as the above-mentioned results are normalized on the same amount of precursor proteins, 1 mg in both experiments.

After alcalase digestion, the peptide mixture was fractionated by preparative RP-HPLC (Xbridge BEH preparative C18 5 μ m OBD 19 \times 250 mm, Waters) into 12 fractions following the gradient shown in Fig 5.

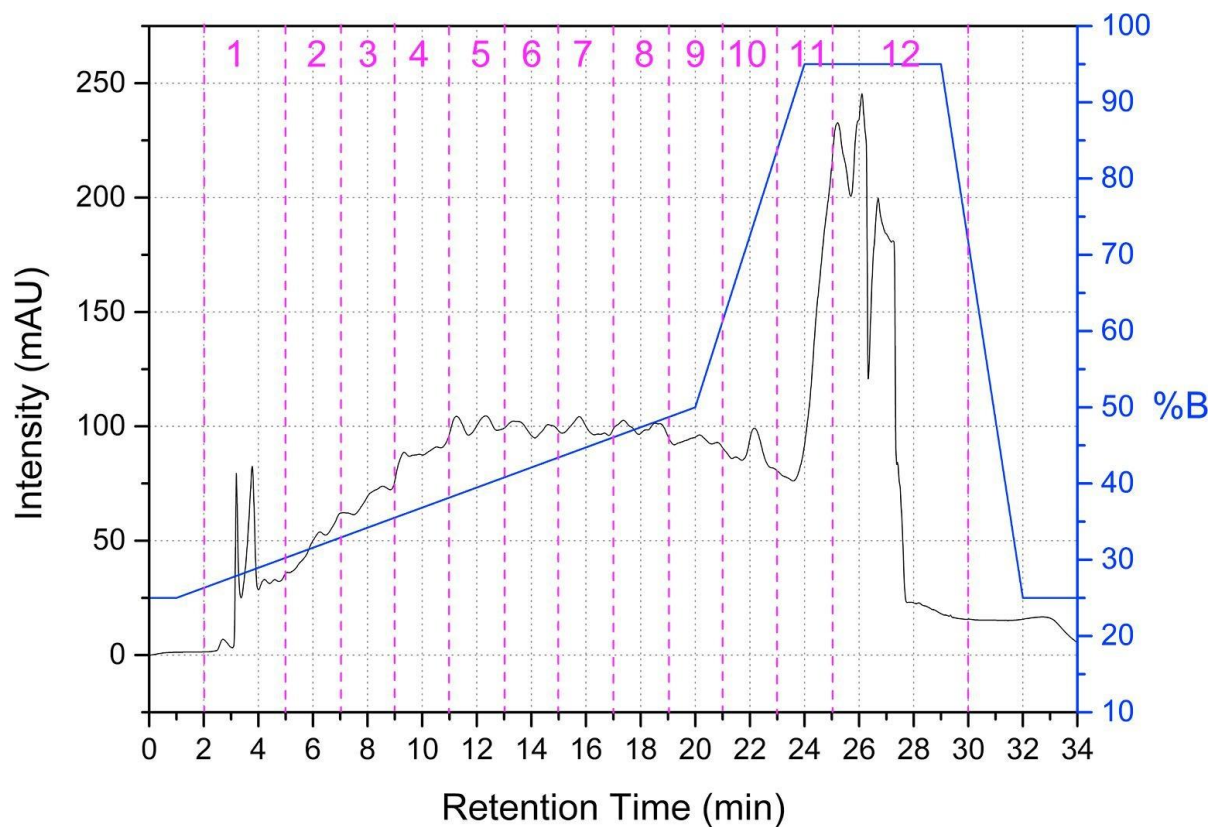


Figure 5 Fractionation scheme adopted for preparative RP-HPLC of cauliflower waste hydrolysates

Each fraction was tested for the ABTS (2,2'-Azino-bis(3-ethylbenzothiazoline-6-sulfonic acid)), and DPPH (2,2-diphenyl-1-picrylhydrazyl) radical scavenging activity and for ACE (angiotensin-converting enzyme) inhibitor activity.

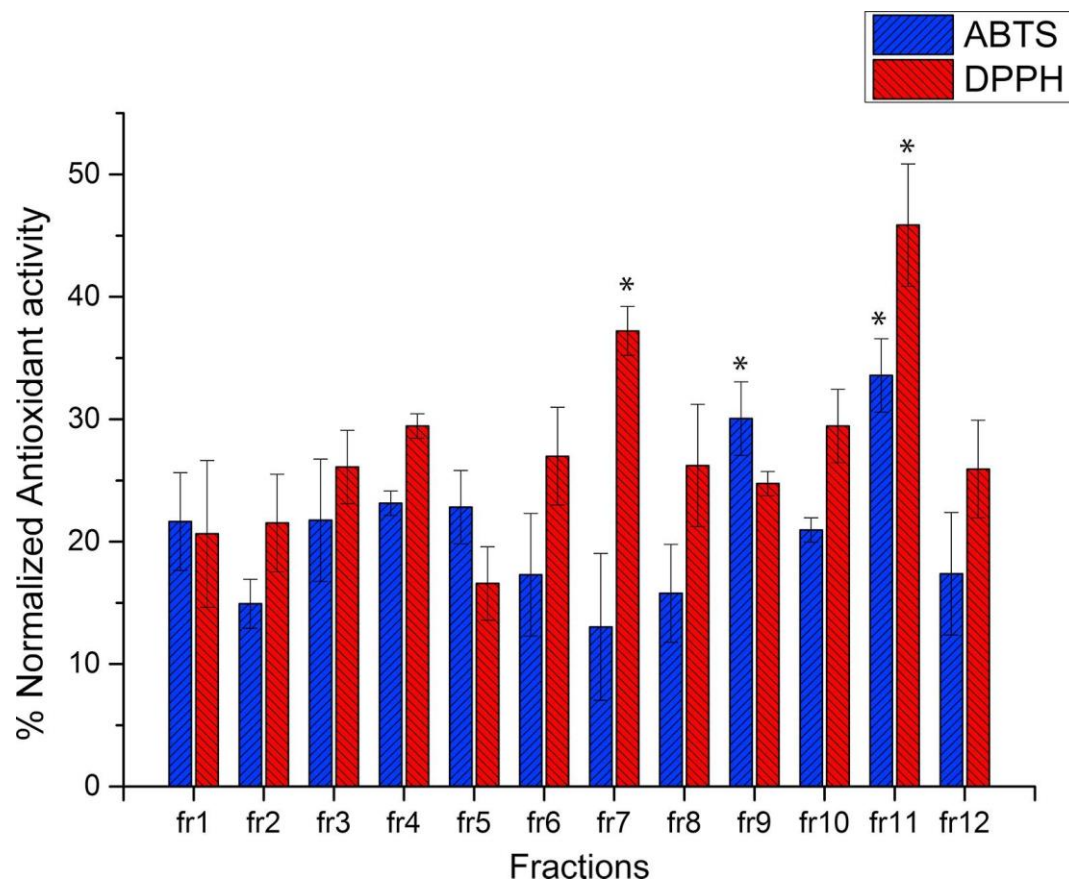


Figure 6 Bioactivity percentage of the 12 fractions for the antioxidant assay

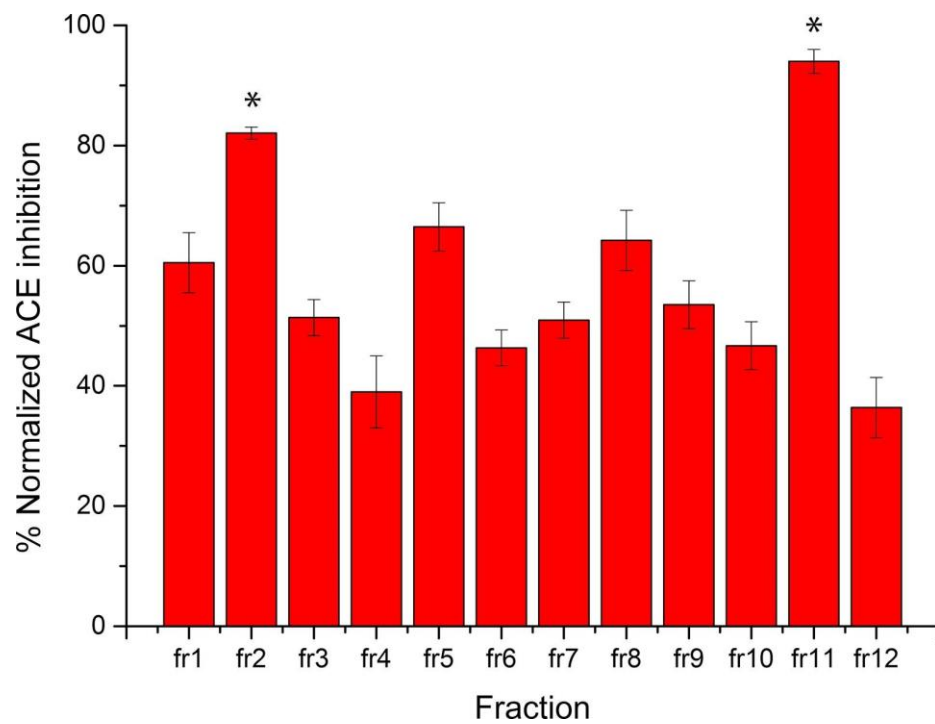


Figure 7 Bioactivity percentage of the 12 fractions for the antihypertensive assay

As is possible to see in Fig 6, for the antioxidant bioactivity, both assays provided a similar distribution with the exception of fraction 7, where the DPPH assay provided a significant higher activity than the ABTS assay (37% vs 13%) while for ACE-inhibitory activity (Fig 7) the bioactivity was generally much higher than the antioxidant activity for all fractions (Fig. 6). Only fraction 12 and 4 were below 40% ACE-inhibition. The most potent fraction reached 82% (fraction 2) and 94% (fraction 11) ACE-inhibition.

The peptides in the most active fractions were identified by peptidomics technologies and screened for bioactivity by the use of bioinformatics. Fraction 2 was selected for ACE-inhibitor activity, fraction 7 for DPPH radical scavenging activity, fraction 9 for ABTS radical scavenging activity and fraction 11 for all tested activities. The 4 selected fractions were finally analyzed by nanoHPLC-MS/MS with Orbitrap Elite (settings as described in the appendix) and the identification was made by Mascot. From this identification, a total number of 461 peptides were identified and distributed as follows: 128 peptides were found in fraction 2, 114 in fraction 7, 76 in fraction 9 and 72 in fraction 11. As the number of peptide identifications was very high, the PeptideRanker algorithm was used [77] to rank the sequences and attribute a score of probability on peptide sequences, in order to select possible candidates for the subsequent synthesis. PeptideRanker searches the specific query in online databases, trying to find similarity with other active sequences and giving back a score from 0 to 1. We decided to put the conservative limit of 0.8 to avoid false positive cases. After this screening, 5 peptides were selected for the synthesis then tested individually (Tab. 2).

Table 2. Sequence of peptides with the best score from PeptideRanker and related bioactivity, mass and original fraction from which they were identified. Color scale: in blue are marked the hydrophobic residues, in green are marked the negatively charged residues and in red are marked the positively charged residues. The EC₅₀ values obtained from in vitro assays of each peptide standard are also reported.

Sequence	Fraction	Mass	PeptideRanker score	Potential bioactivity	EC ₅₀ [$\mu\text{mol L}^{-1}$] \pm SD
SKGFTSPLF	11	983.12	0.85	AO DPPH	8.20 \pm 0.95
				ACE-inhibitor	15.26 \pm 1.60
				AO ABTS	10.35 \pm 1.21
APYDPDWYYIR	2	1458.58	0.84	ACE-inhibitor	2.59 \pm 0.29
LRAPPGWTGR	7	1110.27	0.82	AO DPPH	5.26 \pm 0.33
LDDPVFRPL	9	1071.23	0.81	AO ABTS	8.29 \pm 1.38

For ACE-inhibitor activity, two peptides were synthesized, APYDPDWYYIR and SKGFTSPLF, which provided an EC₅₀ value of 2.59 $\mu\text{mol L}^{-1}$ and 15.26 $\mu\text{mol L}^{-1}$, respectively. For the ABTS radical scavenging activity, SKGFTSPLF and LDDPVFRPL were tested, and provided an EC₅₀ of 10.35 $\mu\text{mol L}^{-1}$ and 8.29 $\mu\text{mol L}^{-1}$, respectively. For the DPPH radical scavenging activity, SKGFTSPLF and LRAPPGWTGR were tested and provided an EC₅₀ of 8.2 $\mu\text{mol L}^{-1}$ and 5.26 $\mu\text{mol L}^{-1}$, respectively. Furthermore the peptides were validated, by adding the synthesized standards to the cauliflower extract and by checking that the retention time and the fragmentation spectrum matched between the sample not supplemented with the synthetic standard and the supplemented one.

2.4.2 A Peptidomic strategy for purification and identification of potential ACE-Inhibitory and antioxidant peptides in *Tetrademus obliquus* microalgae (Paper II)

In paper II the BAPs derived from microalgae were identified. Microalgae peptides are very important because they come from high quality proteins that, due to their structural diversity, contain a series of new bioactive peptides yet to be discovered. In this work, a peptidomic platform was developed for the extraction, separation and identification of BAPs in protein hydrolysates. The extraction of proteins from recalcitrant tissues is still a challenge due to their strong cell walls and the high levels of non-protein interfering compounds. Seven extractive protocols based on organic and non-organic solvents and mechanical methods were thus compared (Tab. 3).

Table 3: Summary of tested extracted protocols:

Protocol name	Protocol description	Type of method
Protocol I	Suspension in lysis buffer and sonication using a commercial sonic bath	Chemical method
Protocol II	Milling in presence of glass beads	Mechanical method
Protocol III	Alkaline process	Chemical method
Protocol IV	HCl-Bligh and Dyer method (MeOH/CH ₃ Cl/H ₂ O)	Chemical method using organic solvent
Protocol V	Hexane/ethanol	Chemical method using organic solvent
Protocol VI	MTBE	Chemical method using green organic solvent
Protocol VII	Osmotic shock	Mechanical method

The best extraction protocol was evaluated by calculating the total protein percentage extracted by each protocol. The quantitative analysis of proteins was carried out using a BCA assay.

Protocols I and III were based on simple chemical process and resulted to be the worst, with a protein recovery of 1.7 and 0.4% respectively (the results are shown in fig 8). Protocol II used glass beads that are a well known effective system for releasing intracellular proteins from recalcitrant samples. Protocols IV used organic solvents but showed lower protein yields. Protocol VI with esano ethanol, therefore with organic solvents, it produced good results, but it was not the best protocol. In protocol VI, the solvent usually used for extraction, chloroform or hexane, were replaced with green solvents, namely MTBE, but the recovery of proteins was rather low with a yield percentage of 6.4%. Finally, protocol VII was based on protein extraction by osmotic shock.

Protocols II and VII were those with a higher protein percentage 12.7% and 11.6% and were both based on mechanical methods that break the cell wall. For the subsequent petidomic experiments, protocol II was chosen, because protocol VII is a laborious time-consuming method and provided a slightly lower protein recovery. However, protocol VII can be used to repeat the experiment on a large scale.

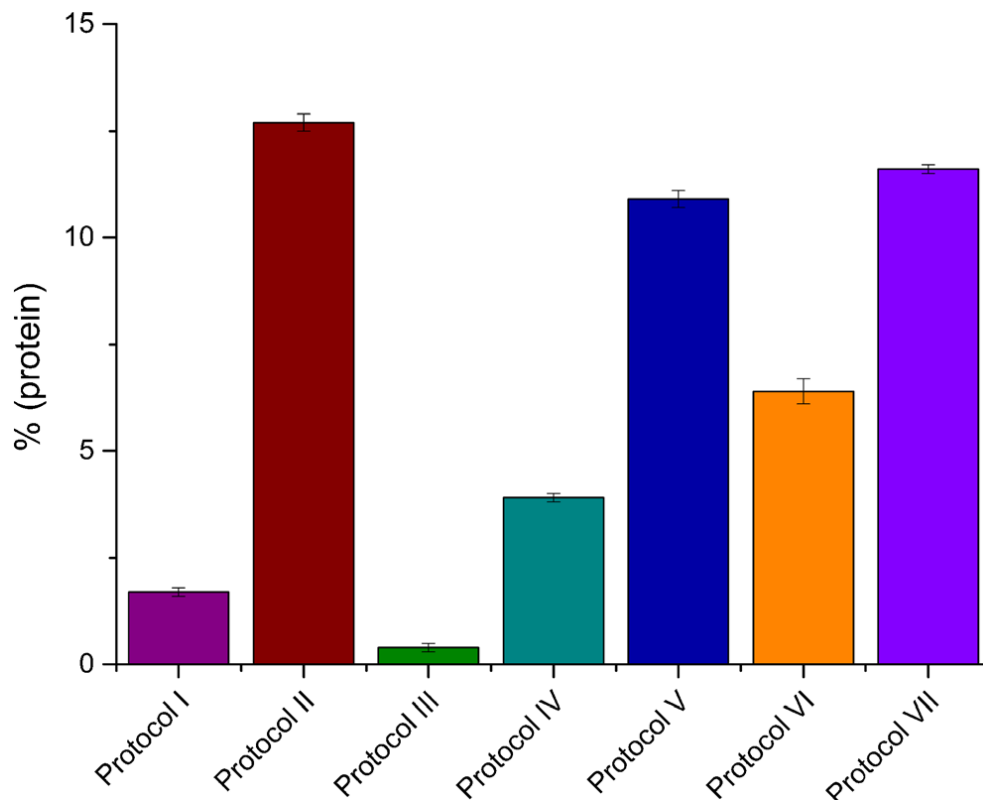


Figure 8 Protein yields for the 7 extractive protocols

Protocol III has a very low protein yield, this because the extracted proteins have been precipitated by adjusting the pH to 3.3 with HCl; the pI of most proteins is usually in the pH range between 4 and 7. At pH 3.3, only the proteins that have an isoelectric point around 3 were precipitated, which greatly restricts the number of proteins which statistically can fall into this category. Another possible explanation could be that acids tend to denature proteins.

The results of Protocol I and II are also interesting, as these protocols are the same and differ only in the presence of glass beads and high temperature in Protocol II. These devices used in Protocol II are more useful for cell lysis.

The methods commonly used to quantify proteins are the methods of Bradford [78] and Lowry [79] González López et al. [80] quantified the protein yield of *Scenedesmus* at 40% but the precipitation phase was neglected. This value could be a fake, due to the presence of non-protein compounds that absorb at the same wavelength. Our best extractive agent showed a protein yield of 12%, this value seems very low compared to the literature values, but performing the same test without precipitating the proteins, the protein content of the biomass was about 47% of the dry weight and the result was in line with those reported by many authors

highlighting that precipitation is clearly needed to remove contaminants and to have a reliable result of the protein content.

As previously described for cauliflower wastes, also in this paper a digestion was carried out using alcalase. This enzyme is cheap and allows the method to be scaled to an industrial level. The digestion was carried out only on the extract from protocol II, which resulted the best based on protein yield; the digestion parameters were optimized, including the incubation time with alcalase and pH, they were carefully monitored in order to understand how they affect the speed and the completeness of digestion. The hydrolysate was purified by semi-preparative reversed phase 2D LC. This process has made it possible to simplify the hydrolysate to have a better identification. The fractions from the first and second chromatographic dimensions were tested for antioxidant and antihypertensive tests.

The fractions with the greatest bioactivity score in the second dimension were analyzed by nano-HPLC coupled with high resolution mass spectrometry, and about 500 peptide sequences were identified. The identified peptides were subjected to an *in silico* analysis using the PeptideRanker algorithm in order to assign a bioactivity probability score. Twenty-five sequenced peptides were found with potential antioxidant activity and ACE-inhibitory activity. Four of these peptides, WPRGYFL, GPDRPKFLGPF, WYGPDRPKFL, SDWDRF, were selected for synthesis and tested *in vitro* for specific bioactivity, exhibiting good values of antioxidant and ACE inhibitory activity.

WPRGYFL and SDWDRF were analyzed for antioxidant activity, they came from the F5f9 fraction (fraction 5, first dimension, fraction 9, second dimension) and F10f10 (fraction 10, first dimension, fraction 10, second dimension), which gave higher values of radical scavenging activity by ABTS and DPPH assays, respectively. Antioxidant peptides usually have 5 to 11 amino acid residues of. The amino acid composition can cause some biological activity, for example a peptide sequence with high amounts of hydrophobic residues in the N-terminal position and probably aromatic, amphiphilic and polar amino acid residues at the C-terminal influencing the antioxidant properties [81]. The two peptides selected in the microalga possess a large number of aromatic residues, two of which were also hydrophobic and had a low molecular weight of 937 and 824 Da respectively. WPRGYFL gave an EC₅₀ value of 4405 ng mL⁻¹ (4.70 μmol L⁻¹), while the DPPH radical washing activity of the SDWDRF peptide was 11.532 ng mL⁻¹ (13.97 μmol L⁻¹). The results obtained are significantly higher than the antioxidant trolox standard (EC₅₀ value 1 μmol L⁻¹) [82]. GPDRPKFLGPF and

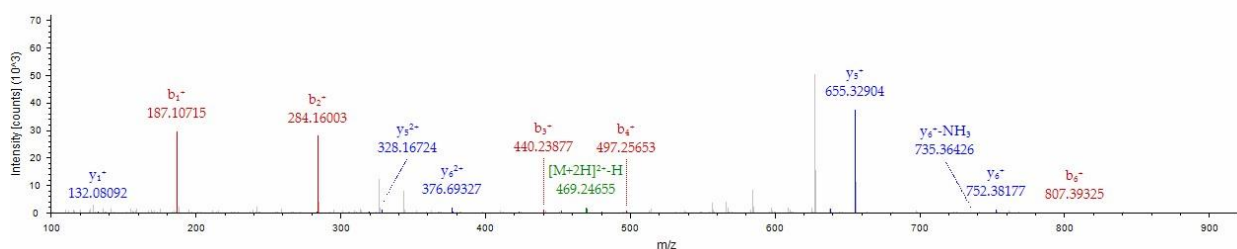
WYGPDRPKFL came from the F9f6 fraction, which had an ACE inhibitory percentage of 80%. Usually, a strong antihypertensive activity is correlated to the presence of hydrophobic and aromatic residues at the N- and C-terminals [83]; the two peptides had a large number of this type of residue. In fact, they showed a powerful activity, with EC50 values of 5.73 and 0.82 $\mu\text{mol L}^{-1}$, which were better than the results reported for *Chlorella vulgaris*.

The results reported in paper II have therefore allowed to identify two new antioxidant peptides and two ACE inhibitors. High values for biological activities make them good candidates in the nutritional field. Furthermore, the development of this analytical approach allows to identify the compounds with greater sensitivity and resolution.

Another improvement with respect to papers already present in the literature is provided by the validation of peptide sequences, which was achieved by synthesis of the peptide candidates, assays made on synthetic peptides to compare them with those performed on the fractions where they were identified, and then added to the microalgae extract to confirm the consistency with the peptides in the matrix. The certainty on the identification of the peptide was given by the comparison between the extract supplemented with the synthetic peptide standard and the extract without supplementation, by checking the consistency between the fragmentation, mass and retention time of standard and native peptide. The peptides corresponded to the synthetic standards, as reported below:

1. Sequence: WPRGYFL, Charge: +2, Monoisotopic m/z : 469.74564 Da (-2.17 mmu/- 4.62 ppm), MH+: 938.48400 Da

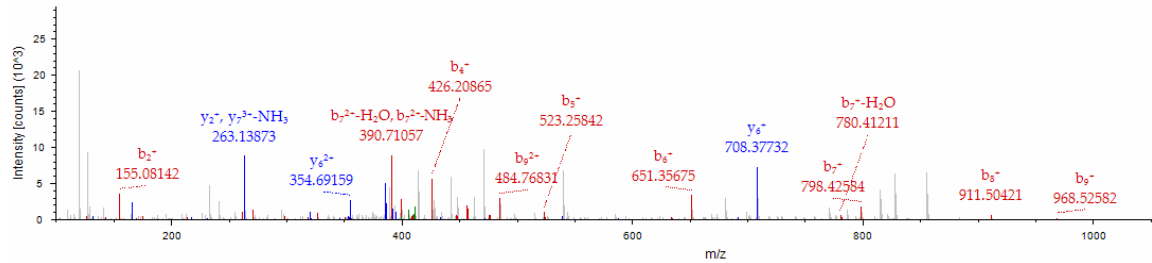
b+	b2+		y+	y2+
187.08660	94.04694	W		
284.13937	142.57332	P	752.40901	376.70814
440.24049	220.62388	R	655.35624	328.18176
497.26196	249.13462	G	499.25512	250.13120
660.32528	330.66628	Y	442.23365	221.62046
807.39370	404.20049	F	279.17033	140.08880
		L	132.10191	66.55459



2. Sequence: GPDRPKFLGPF, Charge: +3,
 Monoisotopic m/z : 410.89304 Da (+0.51 mmu/+1.23 ppm), MH+:
 1230.66455 Da

b+	b2	b3		y+	y2	y3
	+	+			+	+
58.0	29.	20.				
2875	51801	01443				
155.	78.	52.		117	587	39
08152	04440	36536		3.64157	.32442	1.88537
270.	135	90.		107	538	35
10847	.55787	70767		6.58880	.79804	9.53445
426.	213	14		961.	481	32
20959	.60843	2.74138		56185	.28456	1.19213
523.	262	17		805.	403	26
26236	.13482	5.09230		46073	.23400	9.15843
651.	326	21		708.	354	23
35733	.18230	7.79063		40796	.70762	6.80750
798.	399	26		580.	290	19
42575	.71651	6.81343		31299	.66013	4.10918
911.	456	30		433.	217	14
50982	.25855	4.50812		24457	.12592	5.08637
968.	484	32		320.	160	10
53129	.76928	3.51528		16050	.58389	7.39168
106	533	35		263.	132	88.
5.58406	.29567	5.86620		13903	.07315	38453

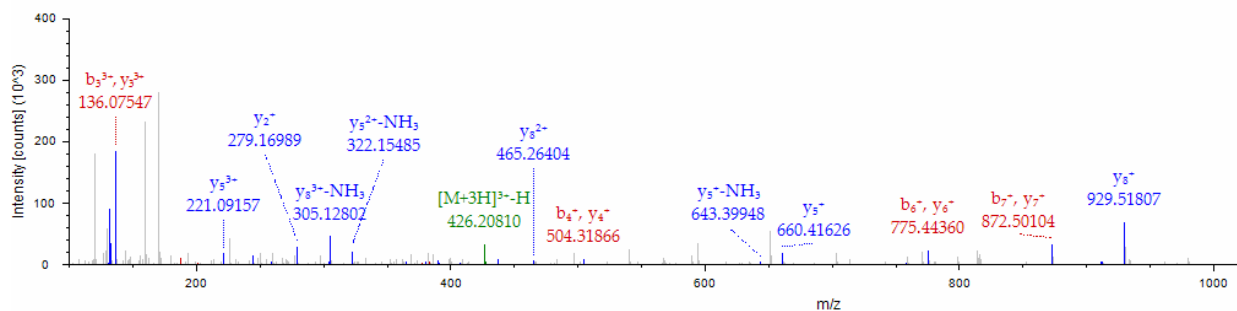
				166.	83.	56.
				08626	54677	03360



- Sequence: WYGPDRPKFL, Charge: +3,
 Monoisotopic m/z : 426.89343 Da (+0.91 mmu/+2.13 ppm),
 MH+: 1278.66574 Da

b+	b2	b3		y+	y2	y3
	+	+			+	+
187.	94.	63.				
08660	04694	03372				
350.	175	11		109	54	364
14992	.57860	7.38816		2.58370	6.79549	.86608
407.	204	13		929.	46	310
17139	.08933	6.39531		52038	5.26383	.51164
504.	252	16		872.	43	291
22416	.61572	8.74624		49891	6.75309	.50449
619.	310	20		775.	38	259
25111	.12919	7.08855		44614	8.22671	.15356
775.	388	25		660.	33	220
35223	.17975	9.12226		41919	0.71323	.81125
872.	436	29		504.	25	168
40500	.70614	1.47318		31807	2.66267	.77754
100	500	33		407.	20	136
0.49997	.75362	4.17151		26530	4.13629	.42662
114	574	38		279.	14	93.

7.56839	.28783	3.19431		17033	0.08880	72829
				132.	66.	44.
				10191	55459	70549



- Sequence: SDWDRF, Charge: +2, Monoisotopic
 m/z : 413.17978 Da (-0.18 mmu/- 0.42 ppm), MH⁺: 825.35228 Da,

b+	b2		y+	y2
	+			+
88. 03931	44. 52329	S		
20 3.06626	10 2.03677	D	73 8.32060	36 9.66394
38 9.14558	19 5.07643	W	62 3.29365	31 2.15046
50 4.17253	25 2.58990	D	43 7.21433	21 9.11080
66 0.27365	33 0.64046	R	32 2.18738	16 1.59733
		F	16 6.08626	83. 54677

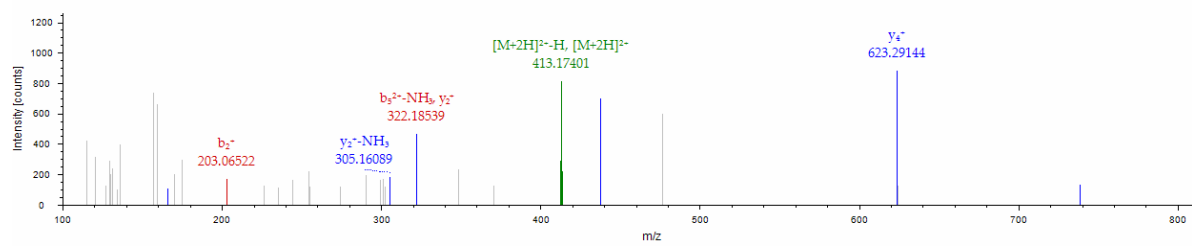


Figure 9 The MS/MS spectra of the four identified and synthesized peptides

Chapter 3: Short Peptides

Short peptides still represent an analytical challenge, in particular shorter peptide sequences (<5 long amino acids). The problems encountered in the identification and analysis of short peptides has been described in chapter 1, the problems are essentially consist in low retention under conventional reversed phase (RP) chromatographic separation, and in lack of automated software for the identification of short amino acid sequences. Firstly, chromatographic issues were solved using porous graphitic carbon (PGC) as a stationary phase for the separation of di-, tri- and tetra-peptides (paper III). The chromatographic conditions (composition of the mobile phase, ion-coupling modifiers, column temperature) have been optimized to improve the shape and resolution of the peak under conditions compatible with mass spectrometry. Secondly, the separation of the small peptides on PGC was coupled with high-resolution (HR) MS. Ionization is enhanced by the post-column addition of 3-nitro benzyl alcohol (3-NBA) to increase sensitivity. HR tandem MS was used for data acquisition using the data-dependent mode. Thirdly, an untargeted MS spectra acquisition was devised based on a suspect screening approach to improve quality of spectra and enable the confident identification of short peptides. Finally, a database with all the possible combinations of the 20 natural amino acids within di-, tri- and tetrapeptides was compiled with exact masses of both precursors and fragments and used to search the experimental spectra for peptide identification.

3.1 Chromatographic separation of short peptides on PGC (Paper III)

PGC in paper III was used to optimize the chromatographic separation of 14 short standard peptides. Different organic solvents and additives were evaluated. 1% tetrahydrofuran (THF) was added to phase B to prevent column contamination by peptides with aromatic side chains, and to restore the theoretical conditions. Initially neutral phases were used, but many

peptides did not elute and others eluted in peaks wider than one minute. Several acid additives have thus been tested, to exploit the double nature of reverse phase and electronic interaction [84] (Fig. 10). The general model described by Knox and Ross [85] for the retention of polar molecules also describes the retention of inorganic and organic anions by charge interactions with the polarized graphitic surface [86,87] which could be eluted by the addition of TFA (used as a competitor); on the contrary, cations were reported to have little electronic interaction; for cation the retention depended on the charge distribution and could be increased by TFA, which this time is used as an ionic coupling reagent [87]. In the case of peptides, their zwitterionic nature will make their retention dependent on their charge states and mobile phase composition.

Given the above, after preliminary tests for separation of short peptides on PGC using un-buffered mobile phases, the general scheme reported in Fig. 10 was used to optimize the separation conditions and detection by MS. Two acid modifiers (TFA and FA) were tested, at three nominal concentrations and three temperature conditions.

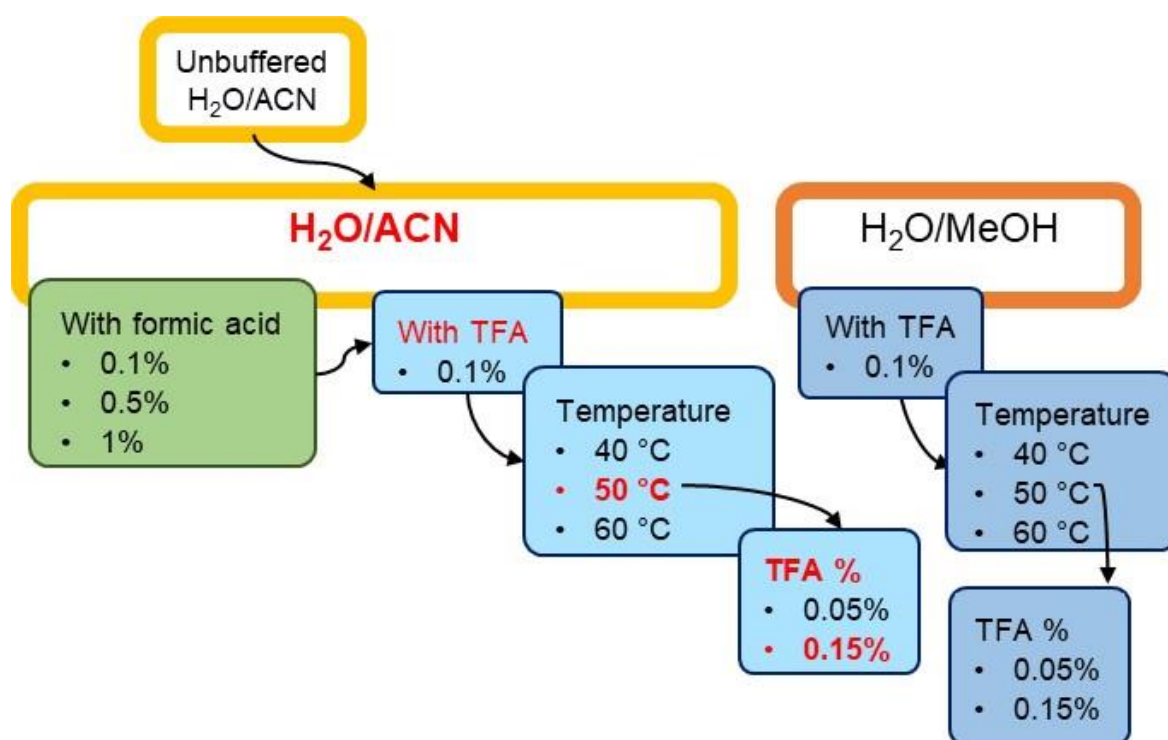


Figure 10 Schematic representation of the optimization experiments performed on PGC for short peptide separation. Final conditions are marked in red

3.1.1 Effect of organic modifier and acidic additives

Formic acid on PGC reduced the retention time of all analyzed peptides; indeed, some peptides eluted with the dead volume (KH, RKKH, KHK and SH), a phenomenon that can be attributed to the little hydrophobic of formic acid as a coupling agent. In contrast, with TFA retention was improved in all cases, as well as peak areas, peak height, efficiency and peak capacity. The increase in the percentage of TFA from 0.05% to 0.1% and 0.15% increased t_R for all peptides (Fig. 11), respectively at 4.24-10.67 min and 4.91-12.28 min, while the detection of 13 peptides out of 14 was allowed: RKKH was not detected at 0.1% of TFA and PI and LP could not be completely resolved at 0.15% of TFA. Despite the reduced selectivity for the separation of the isomers, 0.15% of TFA was selected because the RKKH could be identified while remaining undetected in all the other tested conditions.

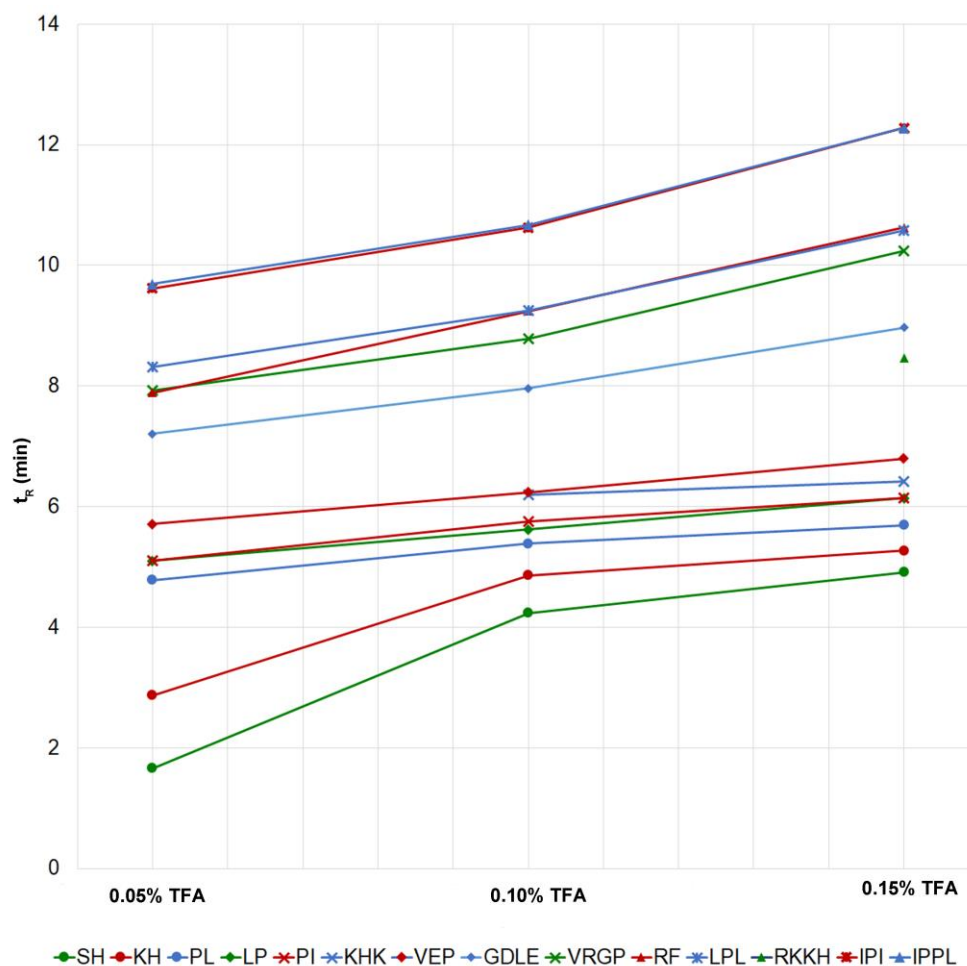


Figure 11 Variation of the retention time (t_R) of short peptide standards as a function of TFA% in H₂O/ACN gradient

Increase of TFA from 0.05% to 0.15% also increased retention of the analytes, but some exceptions were observed, for SH and VEP, for which the retention initially decreased from 0.05% to 0.1% of TFA but then increased again to 0.15% of TFA. This behavior was probably due to the role of the hydrogen bond both in the retention and in the resolution attributed to the multiple PGC retention mechanisms. The mechanism of interaction is therefore explained by an ionic couple mechanism and interaction with hydrogen bonds.

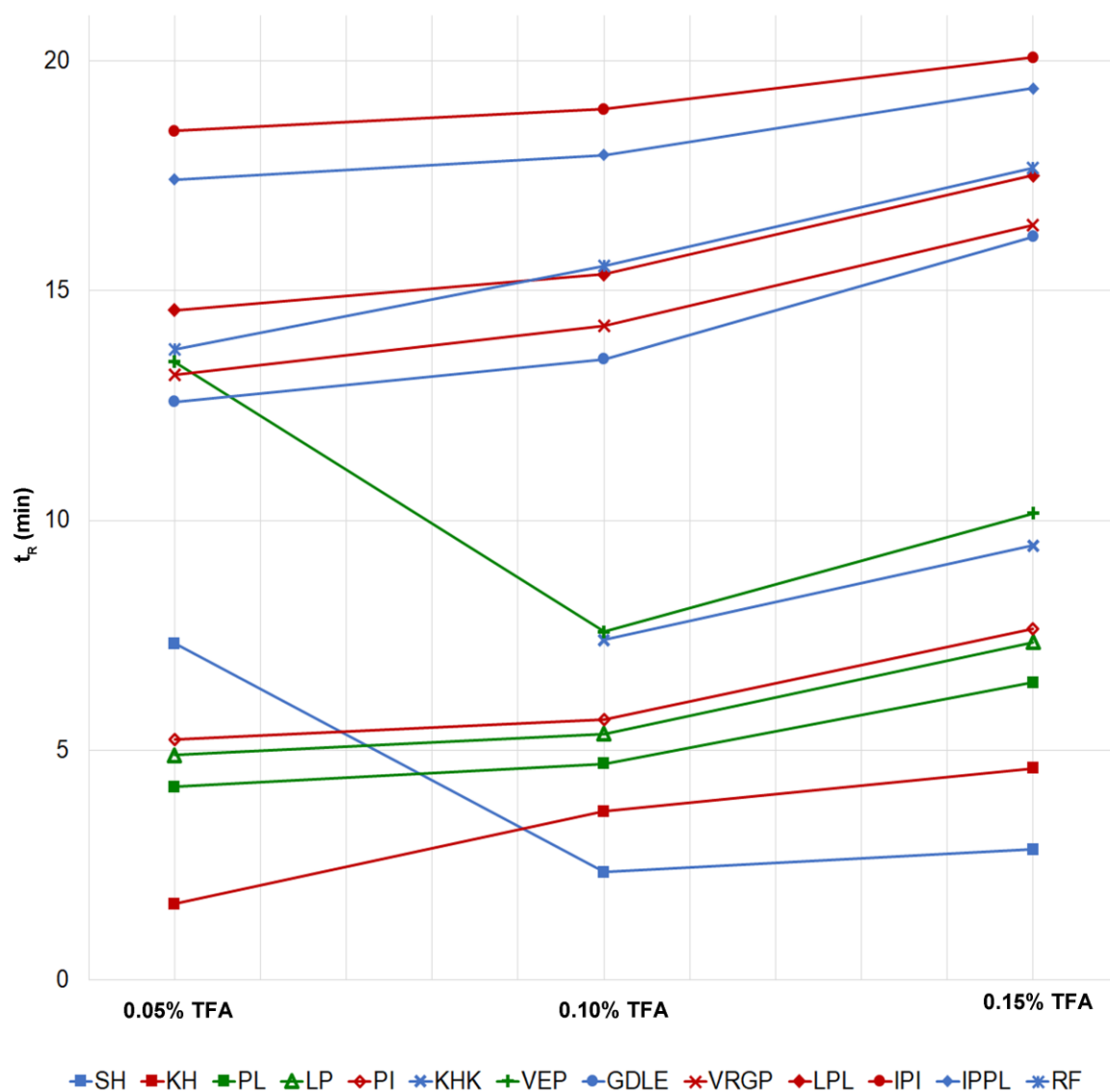


Figure 12 Variation of the retention time (t_R) of short peptide standards as a function of TFA% in H₂O/MeOH gradient

3.1.2 Effect of temperature

The temperature was studied at three different values (40 °C, 50 °C, 60 °C) and TFA concentration of 0.1% (for MeOH, studies at 40 °C could not be carried out as the back pressure exceeded the maximum allowed for the column in use). The temperature allowed to have narrower peaks. In ACN at 60 °C, sharp peaks were observed, the isobaric compounds LP and PI were not separated, and correct acquisition of the peak was often difficult, because the peptides in these conditions coeluted. The condition at 40 °C was the best for peak areas, but at 50 °C efficiency and peak capacity were better. Methanol showed a greater decrease in retention times when the temperature was increased. The best condition was therefore 50 °C in acetonitrile (Fig. 13).

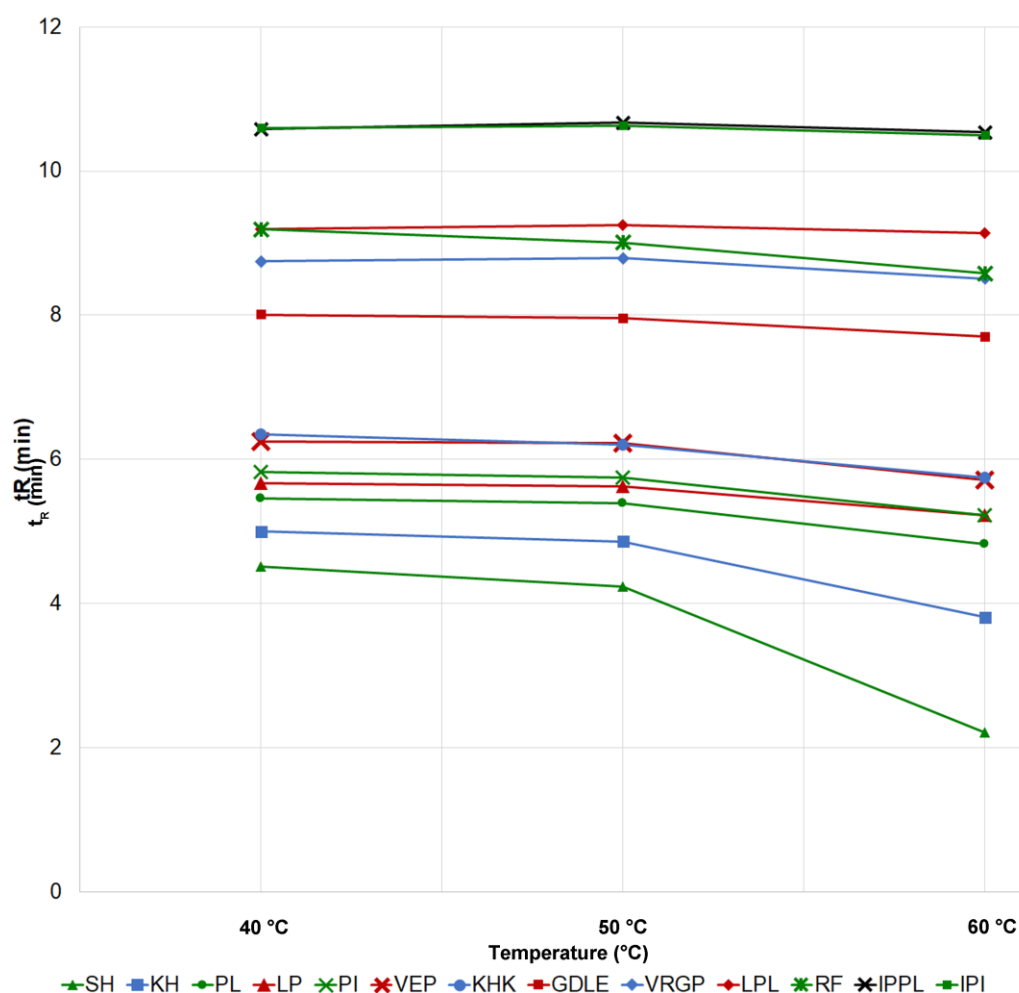


Figure 13 Variation of the retention time (t_R) of short peptide standards as a function of temperature in H₂O/ACN gradient

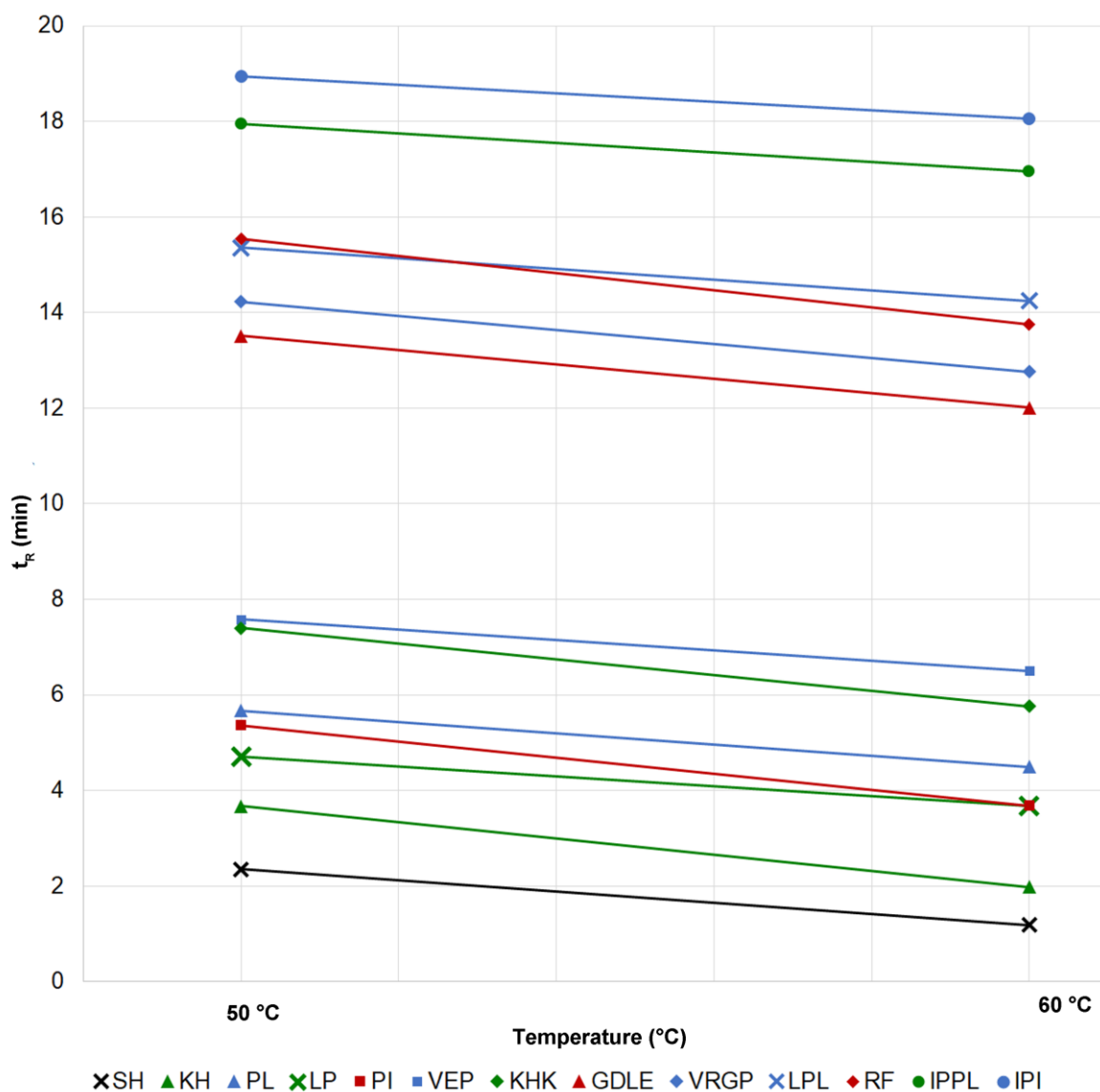


Figure 14 Variation of the retention time (t_R) of short peptide standards as a function of temperature in H₂O/MeOH gradient

3.1.3 Post-column addition of 3-NBA

Methanol was no longer used to optimize chromatographic separation, because it did not allow to separate RKKH, which was detected only in acetonitrile. Acetonitrile with 0.15% of TFA was tested with a post-column addition of 3-NBA, this allowed to improve the signal. Despite TFA is known to decrease ionization in ESI source, this was not observed in the separation of short peptides, as the areas increased with the percentage of TFA, in comparison to the use of neutral phases. The peptides ionize themselves as singly loaded species, this influences the subsequent fragmentation, moreover many contaminants are monocaricate and

generate a high background noise. The 3-NBA, as a super-charge agent [88], was therefore post-column added in order to improve ESI detection without affecting the chromatographic separation. 3-NBA generated a consistent increase of the signal for all analytes up to 18 times.

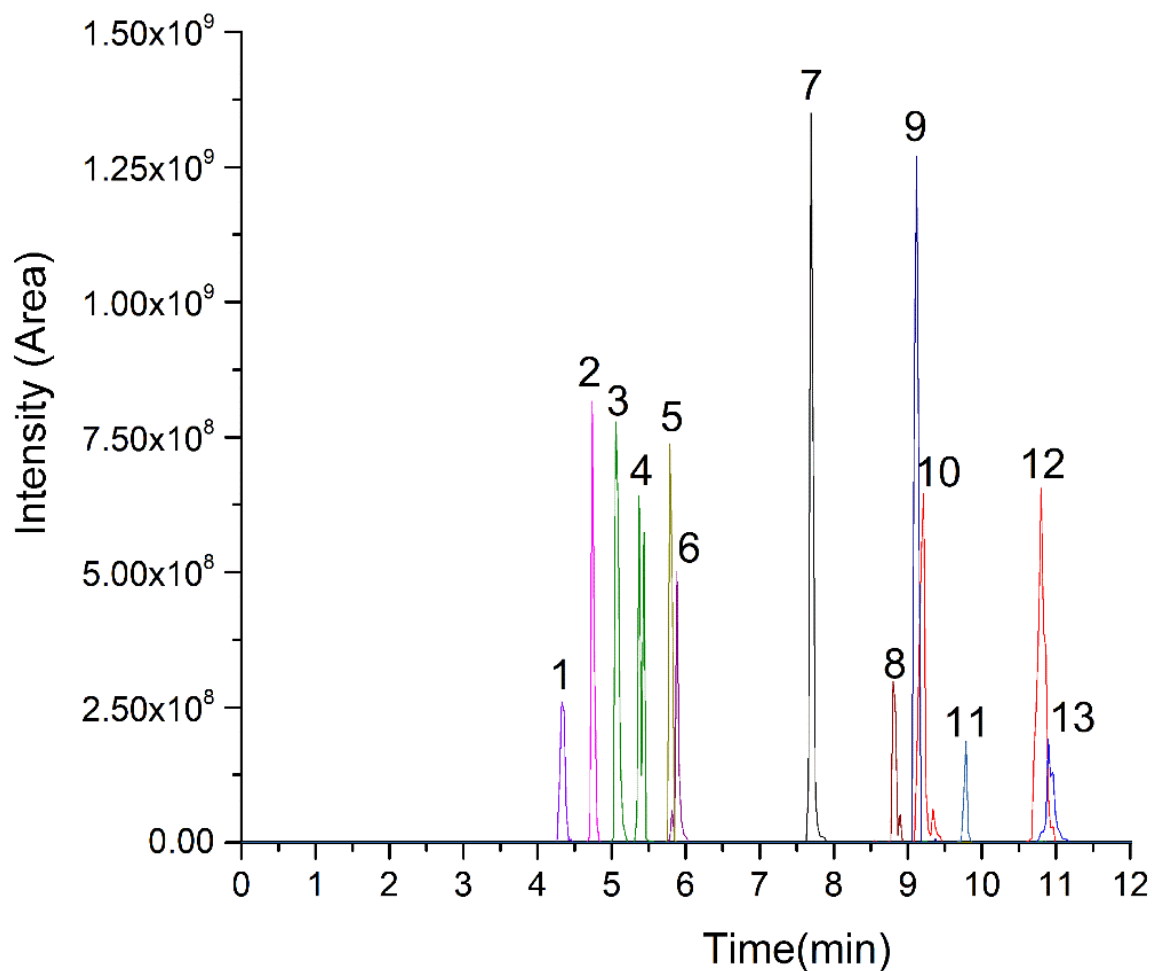


Figure 15 Extracted ion chromatogram of the short peptide mixture under the final conditions. Analyte order: SH (1), KH (2), PL (3), LP and PI (4), KHK (5), VEP (6), GDLE (7), VRGP (8), RF (9), LPL (10), RKKH (11), IPI (12), IPPL (13)

Table 4. Effect of NBA postcolumn addition on the peak area and peak height of short peptide standards monitored by MS detection

Peptide	Peak Area with NBA/without NBA	Peak Height with NBA/without NBA
SH	2.8	2.2
KH	1.2	0.9

PL	9.9	12.3
LP/PI	6.5	7.0
KHK	5.1	3.7
VEP	6.0	7.3
GDLE	3.3	3.8
VRGP	18.2	18.7
RF	5.6	5.2
LPL	10.3	10.9
IPI	13.2	10.7
IPPL	10.2	10.5
RKKH	1.2	3.1

3.2 Data analysis and peptide identification

A suspect screening approach was performed to identify the short peptides in complex matrices. This approach can be used when no reference standards are available, but some information of the target compounds is known to create a database containing molecular formulae, isotope model, structure and mass spectra, if available. The database is used to search suspect compounds in high-resolution mass experimental spectra. In this context, the 20 natural amino acids were considered and used to compute all the possible combinations in which they can be found in dipeptides, tripeptides and tetrapeptides, using the software MATLAB to make the combinations and calculate the related molecular formula and weight. The resulting combinations were used to prepare an inclusion list of m/z precursors and acquire MS/MS spectra in suspect screening analysis mode. The list was also used for data analysis and identification of the possible precursors associated with the m/z observed in the full scan. To confirm the identification, the experimental MS/MS spectrum was matched to the fragmentation spectrum generated in silico for the putative peptide sequences corresponding

to the exact precursor mass. The identification is shown both as a table and as a visual identification of the product ions combined between the lists of *in silico* and experimental product ions. a, b, and y, and immonium ions product ions were considered for peptide identification. If for the same mass there were more candidate peptides, the identification was based on the total number of corresponding product ions and on the intensity of the signals. The peptide with the largest number of corresponding product ions, particularly the most intense ones, was selected as identified. This approach is different from the targeted analysis, because it presents a wider range of research for peptide identification, identification is done by a database with all the possible short peptide sequences. The comparison of the fragmentation model is fundamental for the identification also of isomers [30,88,89]. Another approach is the prediction of retention time, this requires a large number of synthetic peptides to establish a model, it is limited to the chromatographic conditions used and can be used for unknown sequences [35]. The approach described in document III is independent of chromatographic conditions, can be automated to match spectral precursors and fragments to the resulting complete database.

3.3 Identification of bioactive short peptides in cow milk by high performance liquid chromatography on C18 and porous graphitic carbon coupled to high resolution mass spectrometry (Paper IV)

The short peptides were searched in a sample of cow milk as they are particularly interesting due to the many bioactivities which have been reported for short peptides. The innovation of paper IV is that before this, no work had ever been done on cow milk for the identification of endogenous hydrophilic short peptides.

3.3.1 Peptide purification with cotton-HILIC tips

Milk was defatted and deproteinized before being treated. The resulting solution was evaporated and reconstituted with an ACN/H₂O solution (85:15, v/v) with 0.1% TFA (v/v). Peptides were purified on cotton-HILIC microtips to remove carbohydrates. Ten mg of cotton was placed in a 200 μ L microtip using a steel piston, the microtip was washed five times with

water, and conditioned three times with the same loading phase. The milk sample (treated as described above) was then loaded, washed twice with the loading phase. The loading phase was evaporated and reconstituted with an aqueous solution of 0.1% (v/v) TFA.

3.3.2 Ultra-high performance liquid chromatography-HRMS analysis

For the chromatographic analysis, two different columns were tested: a Kinetex XB-C18 column (100 × 2.1 mm, particle size 2.6 μm) and a Hypercarb™ PGC column (150 × 2.1 mm, 5 μm particle size). The second column is the one whose chromatographic conditions have been optimized in paper III. The chromatographic method for the Kinetex XB-C18 was optimized as previously seen with the PGC column. The same mixture of standard peptides was used which covers a wide range of grand average of hydropathy index (GRAVY) values. The flow was 0.5 mL min⁻¹ with post-column addition of MeOH with NBA percentages (v/v) from 1.2% to 3% at 0.1 mL min⁻¹ for both column runs. The C18 column was maintained at 40 °C and the mobile phases were water and acetonitrile with 0.1% (v/v) TFA. For the Hypercarb column the chromatographic conditions were the same optimized in the previous work with a small modification (paper III). The Hypercarb column was maintained at 50 °C, the water and acetonitrile mobile phases were both with 0.2% TFA (v/v). The chromatographic system was coupled to a hybrid quadrupole-Orbitrap mass spectrometer (Q Exactive, Thermo Fisher Scientific) using a heated electrospray ionization (ESI) source. For all chromatographic conditions the ESI source was used in positive mode. To obtain a significant fragmentation for the peptides, an exclusion list was created with the 150 most abundant ions acquired in three empty samples, which consisted of ultra pure water, while the inclusion list was obtained using MATLAB R2018a as previously described (18,533 combinations). The database contained exact *m/z* values for singly charged precursor ions, doubly charged ions (only for tri- and tetrapeptides), triply charged ions and quadruply charged ions (tetrapeptides only).

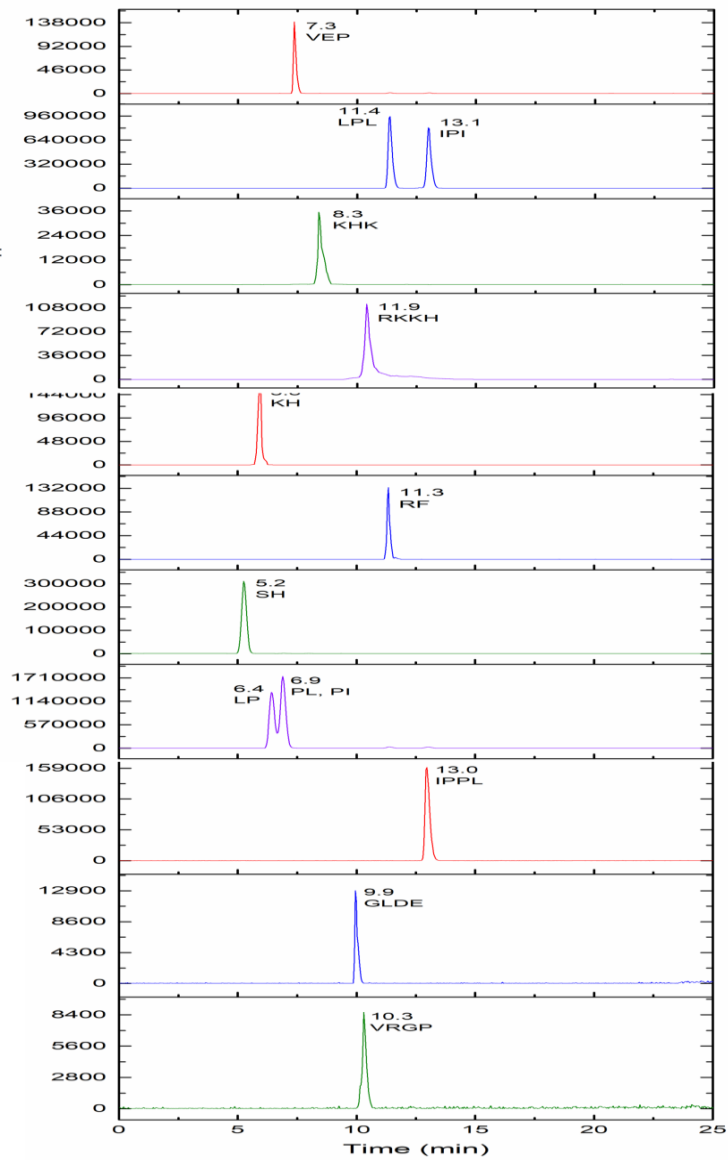


Figure 16 Extracted ion chromatogram of the short peptide mixture by C18 column

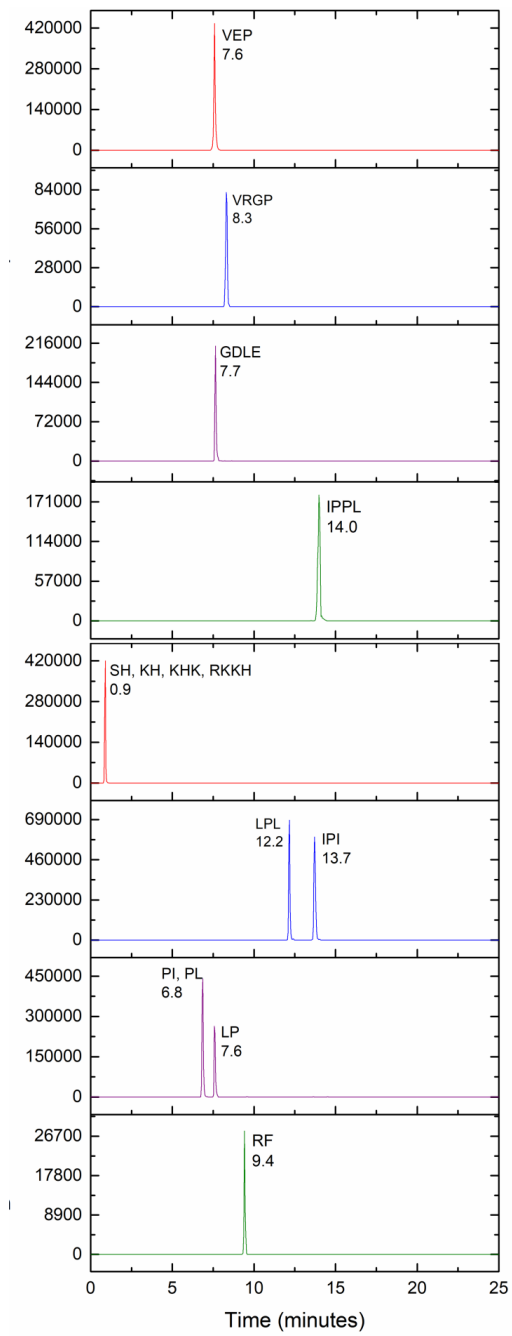


Figure 17 Extracted ion chromatogram of the short peptide mixture by PGC column

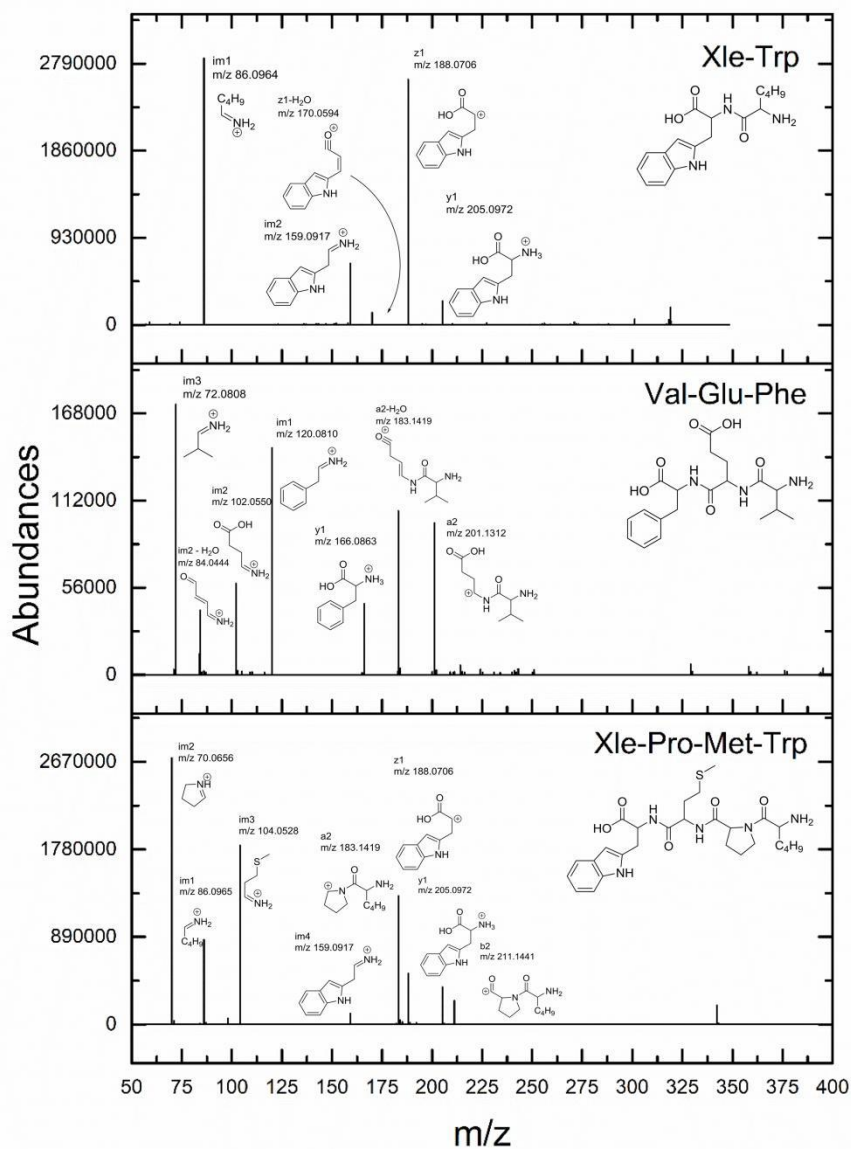


Figure 18 MS/MS spectra showing diagnostic fragments for the dipeptide Xle-Trp, for the tripeptide Val-Glu-Phe and for the tetrapeptide Xle-Pro-Met-Trp, respectively identified in the C18 separation

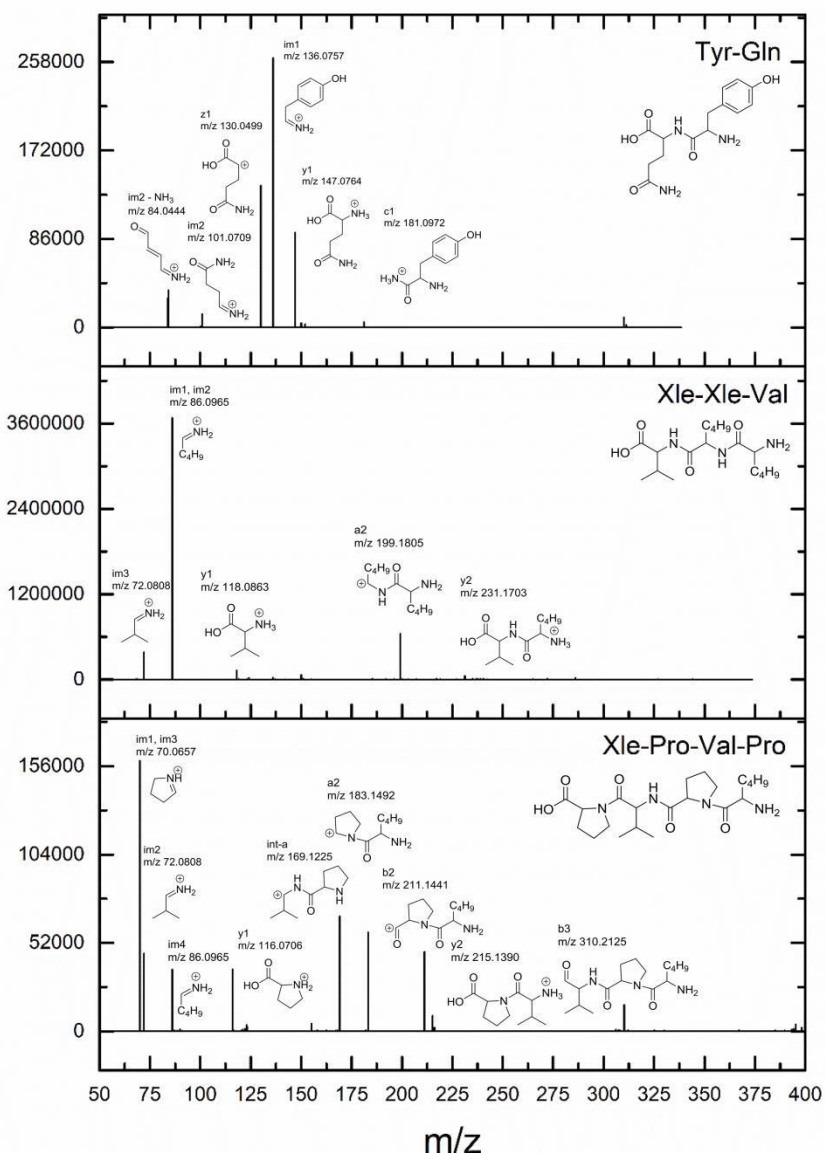


Figure 19 MS/MS spectra showing diagnostic fragments for the di-peptide Tyr-Gln, for the tri peptide Xle-Xle-Val and for the tetrapeptide Xle-Pro-Val-Pro, respectively identified in the PGC separation

3.3.3 Identification of bioactive short peptides in cow milk

The purpose of this work was to completely characterize peptides in cow milk. In the first part of the work, an evaluation of two columns, with different retention mechanisms, was performed. The separation by reversed phase chromatography is the most used for the separation of peptide mixtures. However, the more hydrophilic fractions are not retained under

these conditions. PGC is a valid alternative for the retention of hydrophilic compounds [90]. In fact the mixture of 14 standard peptides was optimally separated on PGC, but not on C18, where some peptides eluted with dead volume. The chromatographic conditions for PGC were already optimized in paper III. In cow milk samples, 57 peptides were identified using by C18 RP separation and 41 peptides by PGC separation (Table 1 and 2 in paper IV). Uncleaned samples were also tested on cotton microtips, carried out only to remove sugars and avoid ion suppression. The cotton-HILIC procedure was employed as clean-up: the samples were loaded and flowthrough recovered for further analysis, while the elution was skipped. The comparison between peptide identifications obtained with and without the cotton-HILIC clean-up indicated an improvement due to the removal of sugars for both column separation, with 550 vs 57 peptides identified by the C18 separation and 30 vs 41 peptides identified for the PGC separation. Significant improvement was shown in the areas (ca. + 60%). In the comparison between the two columns, only 26 peptides were identified with both separation strategies, 31 unique peptides were identified exclusively with C18, and 15 with PGC. The GRAVY values were compared to clarify the behavior of the two columns. The GRAVY value is defined as the sum of the hydropathy values of all the amino acids divided by the length of the protein. The GRAVY values are discussed on the basis of four intervals, i.e. $x > 1$, $1 \geq x > 0$, $0 \leq x < -1$ or $x \leq -1$ (arbitrary units). A positive GRAVY value indicates a hydrophobic peptide, while a negative value indicates a hydrophilic peptide. The bar graph in Fig. 20 shows the distribution of the short peptides identified in the C18 and PGC experiments as a percentage of peptides out of the total for each category.

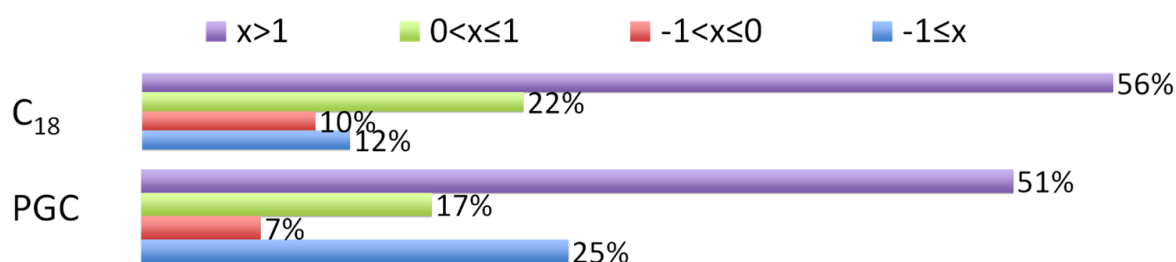


Figure 20 Distribution of the short peptides identified in the C18 and PGC experiments

The results obtained for the two columns are different, 56% of the peptides separated with C18 showed a GRAVY value > 1 , the percentage fell to 51% with PGC. As far as hydrophilic peptides were concerned, the results were more interesting, as the PGC column

had a GRAVY value ≤ -1 against only 12% for separation with C18. Analyzing the GRAVY value, it was shown that the two columns have a different selectivity mechanism, to improve the number of identifications an integrated approach may be useful because of the wide polarity of the short peptides.

In milk the peptides could be generated by the action of some non-specific endogenous proteases, such as plasmin, cathepsins B and D; the plasmin usually generates longer peptides unlike cathepsins that have a wide splitting capacity. Short peptides can form in the pasteurization process. Some of the identified peptides were already present on BIOPEP, and their bioactivity was confirmed. The others were analyzed with peptide ranker, which indicated that C18 peptides potentially displayed antihypertensive activity, while those separated with PGC displayed antioxidant activity. To the best of our knowledge, this is the first work done on endogenous short peptide in cow milk samples.

Chapter 4: Seleno-Amino acids

4.1 Targeted analysis

The targeted analysis involves the use of reference standards, for qualitative and quantitative analysis. For the unique identification of a compound, the retention time, mass and fragmentation spectrum are compared with that of the reference standard, measured under the same experimental conditions. Obviously this type of approach involves the knowledge of the substances present in the matrix and the availability of pure standards. As described in detail in appendix 1 (paragraph 2.3.1) the identification and quantification of compounds at low concentrations requires high sensitivity and good selectivity. The study presented here, on seleno-amino acids, since the transitions to be followed are few, it is possible to perform experiments with a low-resolution MS instrument in SRM mode, taking advantage of the instrument without losing sensitivity and selectivity.

4.2 On-line and off-line methods

Sample preparation is one of the most important steps in the analysis of bioactive compounds, and often requires 80% of the total analysis time. Sample purification includes different processes such as, dilution, precipitation, filtration and centrifugation, which could affect the final measurement. The extraction is typically necessary to separate the analytes from interfering components present in the matrix and enrich them if they are present in the samples at low concentration [91].

The choice of the sample preparation method is very important in the qualitative and quantitative determination of the target compounds, because it allows choosing a suitable

method to obtain the right sensitivity for analysis. In nature there are a wide variety of compounds, which can be lipophilic, moderately polar, can have basic, acidic or neutral properties. The preparation of the sample is necessary to eliminate possible interferences and to concentrate and stabilize the target analytes and finally to bring the sample to conditions optimally sufficient for chromatographic analysis or other analyzes[92].

Liquid-liquid extraction (LLE) is a traditional method of extraction, which is based on the partition of the analyte between water and an immiscible organic solvent. The disadvantage of LLE is that relatively large volumes of organic solvents are required. This poses use and disposal problems. In addition, this technique requires a trained analyst with good hand-eye coordination to carefully pipet immiscible layers of similar appearance and each time a drug is extracted between an aqueous and organic layer, some loss will occur. In the 1960's and 1970's, solid-phase extraction (SPE) was initially performed by toxicologists who made their own columns using sodium sulfate and cotton balls or materials containing silicon, such as diatomaceous earth [93]. This is an alternative method of extraction which finds a large number of applications because it is a very versatile technique; by the use of different stationary phases it is possible to analyze different analytes with different physico-chemical properties. Online SPE methods have been developed in recent years and have many advantages over off-line SPE methods, such as reducing sample handling and analysis time. The SPE coupled to HPLC-MS/MS and UHPLC-MS/MS provides very sensitive and specific methods for the detection of trace analytes [94]. In this thesis, work two different enrichment methods were studied: one was an online method, which allowed a direct analysis by pre-concentrating the sample in the chromatographic column for analysis; the second method was an off-line method optimized on commercial SPE cartridges. The online method (paper 5) uses CHIROBIOTIC TAG to focus and concentrate the analytes in the column; moreover, the same stationary phase has also been exploited for chiral separation. The off-line method (paper 6-7), despite having longer analysis times, allows to perform trace analyzes, since the LOQ values obtained are much lower.

4.3 Encrypted and free seleno-amino acids

The importance and biotransformation of seleno-amino acids has been extensively described in section 1.2.3. As the chirality of these molecules is expected to affect the

biological role of these molecules, the objective of this work was to separate all the enantiostereoisomeric forms of these compounds and enrich them in order to allow their identification. The chirality of seleno-amino acids is rarely considered. Amino acids with a selenium atom have a single chiral center so they exist as a pair of enantiomers. Se-Cys₂ consists of two Se-Cys molecules linked by a Se-Se bond, so it can exist as a pair of enantiomers and a (meso) form. Chirality can have a major impact on the biodistribution of seleno-amino acids. The presence of L-forms has been demonstrated in proteins, and the amino acids D- and L- have different intestinal absorption and different metabolic pathways. Specifically, the absorption of D-isomers is slower than that of L-isomers [46], which causes the L-seleno-amino acids to be more toxic than the D-forms [95]. Furthermore, the D-isomers before incorporation into proteins also require conversion to L-isomers, although this conversion has not been described for all amino acids [47].

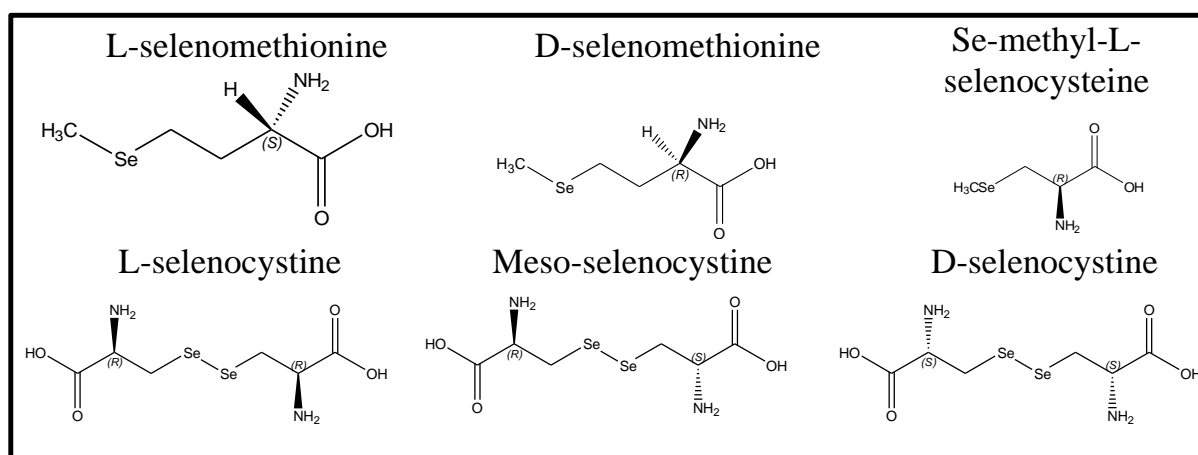


Figure 21 Structures of seleno-amino acids

Seleno-amino acids can be naturally present in plant matrices, due to the process of metabolizing selenium into organic selenium forms. Protein-conjugation of seleno-amino acids is also nutritionally relevant, considering that free Se-AAs are more readily available for humans than protein-conjugated Se-AAs [96]. Some works in the literature have already studied free or conjugated Se-AA, for instance in green bean sprouts, which had been grown under conditions enriched with Se [97], and in *Brassica juncea* but without any system of preconcentration which is fundamental for the identification of all the species present in the sample at relatively low concentrations (ppb) [98]. Protein digestion is necessary for the

determination of seleno-amioacids conjugated to proteins, using non-specific enzymes able to extensively digest proteins into amino acids and very small sequences (paper 7)

4.4 Data analysis

Chromatographic separation of seleno-amino acids is a study reason as it is not possible to perform it on common C18-based stationary phases due to the low retention of analytes. In this thesis work, attention is also focused on the enantiomeric forms of seleno-amino acids. For this reason, particular stationary phases have been studied. For example, the CHIROBIOTIC TAG has been considered superior for various aspects to the phases already used for the separation of selenoamino acids [43,99,100].

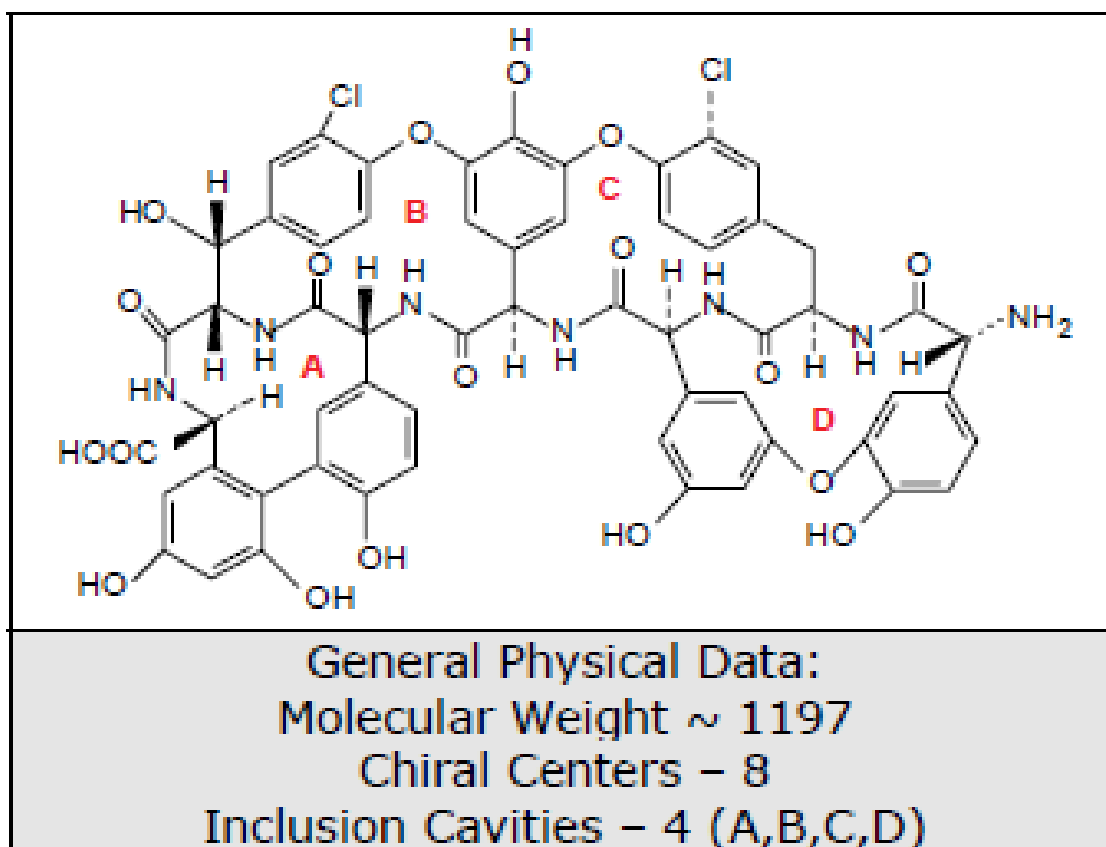


Figure 22 CHIROBIOTIC TAG: Glycopeptide Teicoplanin Aglycone

The CHIROBIOTIC TAG consists of teicoplanin aglycone molecules, each of which provides seven polyhydroxy groups (including six phenols), free carboxylic fractions, six polar amide bonds and seven benzene rings [101]. Thanks to the presence of these groups it is possible to increase interaction and increase retention; without the need for derivatization reactions or the use of combination reagents, which in turn increase analysis time and potentially interfere with ionization and mass spectrometry detection. For chromatographic separation using the CHIROBIOTIC TAG column, the studied seleno-amino acids were eluted using a very polar aqueous mobile phase. The composition of the mobile phases, the temperature and the gradient have been studied to obtain the best retention and chromatographic separation.

The optimization studies indicated that the water percentage in both mobile phases and pH were essential. The percentage of water in phase B was increased from 80 to 85% to 95%, showing that retention was compromised at 95% of water and retention was no longer observed. Furthermore, selectivity was also compromised for SeCys₂ stereoisomers, as all three forms eluted together, indicating that the electrostatic interactions necessary for the chiral recognition was totally compromised in water when the CHIROBIOTIC TAG column was used. This depends on the multiple interactions through hydrogen bonds that are established between the aglycone basket and the carboxylate portion of seleno-amino acids; such hydrogen bonds are disrupted in the presence of water and recognition is no longer possible, since the interaction between the seleno-amino acid and the chiral selector is weakened. The optimized conditions differed a lot for those used for CHIROBIOTIC T, in this case reverse phase conditions were used and seleno-methionine enantiomers were resolved by 0–40% (v/v) MeOH gradient in water [102].

The pH strongly influenced the bandwidth: larger bands were obtained without an acid modifier; the lowering of the pH of phase B to 4 and the addition of 0.5% formic acid to phase A significantly improved the separation, especially for D-, L- and meso-SeCys₂. This result was obtained for the first time from this thesis work, it had never been obtained with previous reports on the enantioresolution of seleno-methionine on the T CHIROBIOTIC column [102]. In the case of the CHIROBIOTIC T columns, the retention times and resolution were not influenced in the pH range of 4–7. This discrepancy can be attributed to the complementarity of CHIROBIOTIC T and TAG columns.

The temperature was tested between 37 and 50 °C. The increase in temperature improved bandwidth and peak symmetry, in particular for the seleno-methionine and SeCys₂stereoisomers, reducing retention.

To improve the separation between Se-methyl-L-selenocysteine and L-seleno-methionine, a ternary solvent mixture was used in phase A: ethanol, isopropanol and MeOH were tested and the two compounds were completely separated only using MeOH. The separation was obtained both with a high concentration of analyte and a low concentration of analyte (Fig. 23).

After optimization, the final chromatographic conditions for the CHIROBIOTIC TAG column: 0.5 mL min⁻¹, 50 °C; mobile phase A: MeOH/ACN/H₂O, 45:45:10 (v/v/v) with 10 mmol L⁻¹ of ammonium formate and 0.5% formic acid; mobile phase B: ACN/H₂O, 20:80 (v/v) with 20 mmol L⁻¹ of ammonium formate at apparent pH 4 by formic acid; linear gradient separation: 0% B (0–2 min), 15% B (2–4 min), 100% (4–14 min); 5 min column washing at 100% B, equilibration at 0% B for 5 min; SRM detection.

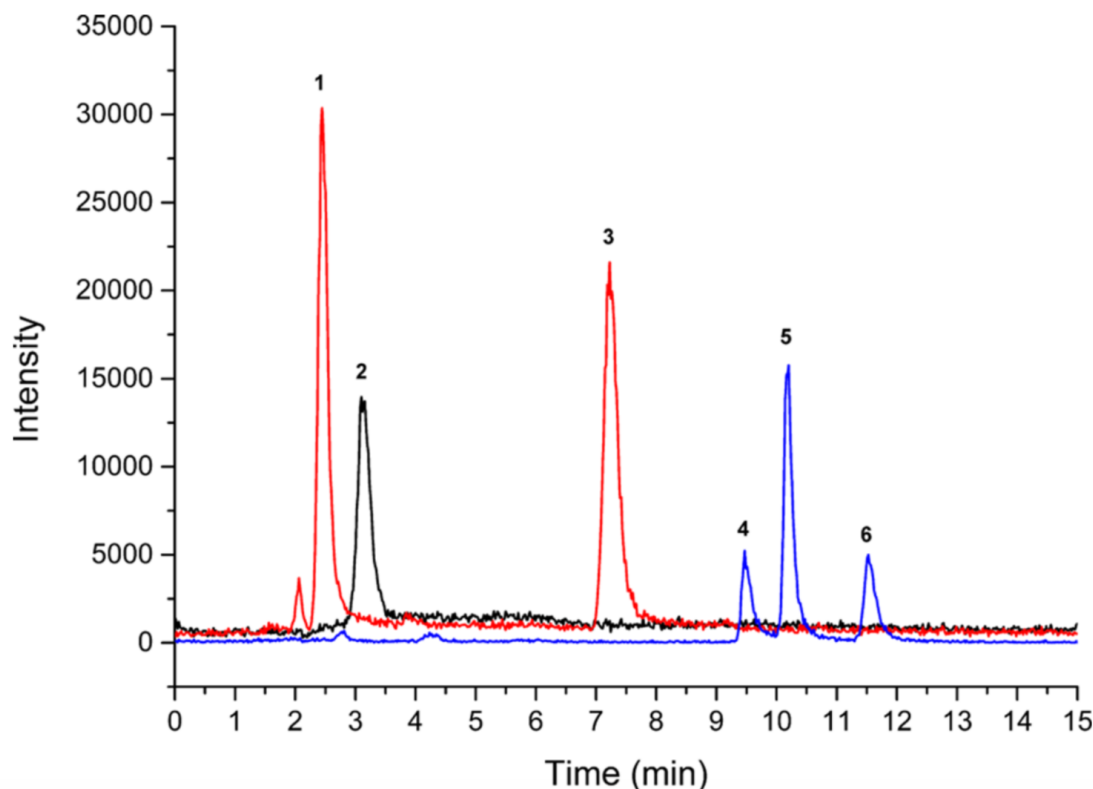


Figure 23 L-Selenomethionine (peak 1), D-selenomethionine (peak 3), Se-methyl-L-selenocysteine (peak 2), L-selenocystine (peak 4), D-selenocystine (peak 6), and meso-selenocystine (peak 5)

The complete elution of the analytes in the optimized conditions occurred in 15 min, the objectives of enantioselective separation were achieved with a Column 5 cm long.

In paper V-VI-VII a method will be described by using (CHIROBIOTIC TAG) which allows the separation of all chiral species, furthermore in paper V this stationary phase will also be used to enrich and focus species before analysis.

The detection method used is low-resolution mass spectrometry, a triple quadrupole was used in SRM acquisition mode (described in detail in appendix 1 paragraph 1.3.1)

The source used is ESI was used in positive ionization with the following settings: 3.0 kV spray voltage, 280 °C vaporizer temperature and capillary temperature (ion transfer tube) 280 °C. The sheath gas pressure, the ion sweep gas pressure and the auxiliary gas pressures were set to 40, 0 and 20 (arbitrary units) respectively. The conditions of the source, the parameters of the objective and the transitions of the analytes were optimized by infusing standard solutions at 10 ng μL^{-1} in mobile phase A at 10 $\mu\text{L min}^{-1}$. The ions $[\text{M} + \text{H}]^+$ were

selected from the first quadrupole and fragmented in the collision cell with optimized collision energy. The two transitions showing the highest signal-to-noise ratio (S/N) were selected for the SRM setting (see Table 1). The UHPLC-MS system was managed by the Xcalibur software (v.2.1, Thermo Fisher Scientific).

Table 5: SRM transitions optimized

Compound	Parent ion	Product ion	Collision energy	S-lens
Se ⁷⁸ -methyl-seleno-cysteine	182	121	20	40
	182	165	6	
Se ⁸⁰ -methyl-seleno-cysteine	184	123	19	40
	184	167	6	
Se ⁷⁸ -selenomethionine	196	56	22	64
	196	179	9	
Se ⁸⁰ -selenomethionine	198	56	20	64
	198	181	9	
Se ⁷⁸ -selenocystine	335	86	33	80
	335	246	33	
Se ⁸⁰ -selenocystine	337	88	33	80
	337	248	18	
¹³ C-Se-methionine	199	110	22	64

4.4.1 Simultaneous Preconcentration, Identification, and Quantitation of Selenoamino Acids in Oils by Enantioselective High Performance Liquid Chromatography and Mass Spectrometry (Paper V)

Selenoamino acids are present in trace amounts in oil [103], moreover oil represents an analytical challenge, because it is a very complex matrix, rich in triacylglycerols, free fatty acids, phenols, sterols and phospholipids [104]. For this reason the determination of selenoamino acids in oil is particularly complex, only a few methods have been developed and none of these involves the chiral determination of the species [103,105]. Therefore, the novelty of this paper is represented by the chiral separation (described in paragraph 4.4), and also by the optimization of a method for the enrichment of the target seleno-amino acids directly on the CHIROBIOTICA TAG pre-column after simple dilution of oils with dichloromethane (DCM). Preconcentration was achieved by operating the CHIROBIOTICA TAG pre-column in normal phase conditions (NP). The key point of this paper is the optimization of the trapping and focusing of the seleno-amino acids under NP conditions. The chiral stationary phase (CSP) CHIROBIOTIC TAG is a multimodal CSP; therefore, the enrichment of the analytes in oil could be theoretically be achieved without sample pretreatment by direct loading of the analytes onto the pre-column. This approach is much simpler and faster than conventional SPE; moreover, it is very convenient for easily degradable low concentration analytes, such as seleno-amino acids, and would also be applicable to stationary phases, which are not available in packaged cartridges or are too expensive to be used in disposable devices.

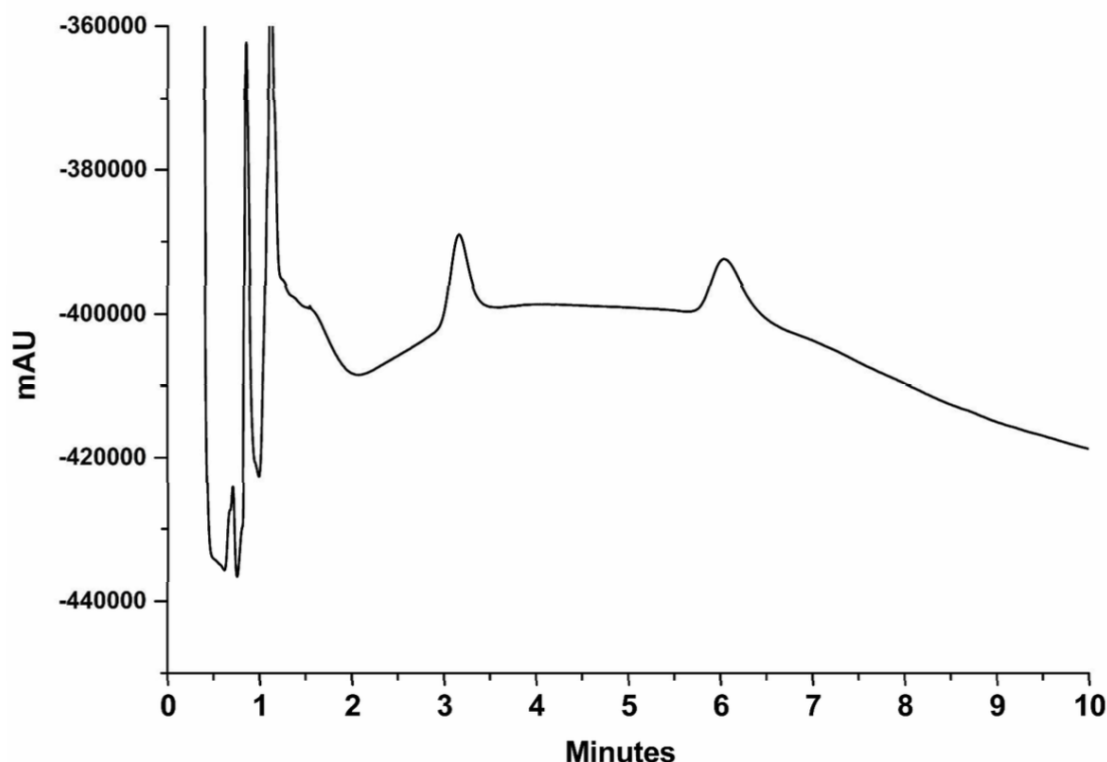


Figure 24 Racemic tryptophan trapping and enantioresolution in DCM. Trapping efficiency as calculated by the estimated recovery: 60% for L-tryptophan and 60% for D-tryptophan

The trapping conditions were optimized using tryptophan as a surrogate analyte (data shown here, not present in the attached paper), since elution could be easily monitored by UV-vis detection and since L-tryptophan had a close retention time to the less restrained analyte (L-seleno-methionine).

Dichloromethane was used to dilute the oil, to ensure compatibility between the chromatographic separation (described in section 4.4) and the NP entrapment procedure; the precolumn conditioning was performed using miscible solvents with decreasing polarity. For the wash after loading the same approach cannot be used because it would lead to the elution of the analytes. Dichloromethane was used to eliminate traces of oil and avoid the elution of the target analytes; finally, drying of the stationary phase was carried out using nitrogen gas to ensure compatibility between NP trapping and elution conditions.

The apparatus used for focusing the seleno-amino acids on the CHIROBIOTIC TAG pre-column is shown in Fig. 25: it consisted of a high-pressure stainless steel container (15 ×

1 cm) which was connected to a nitrogen cylinder by means of a three-way valve. Nitrogen was used as a pressurizing gas, at 2-3 MPa, to allow the sample and solvents to enter the high-pressure vessel and being forced through the pre-column.



Figure 25 Image of the capture system

The optimized final conditions are the following: the high-pressure vessel was washed twice with 6 mL of water, successively with 6 mL of ethanol and finally with 6 mL of DCM. The high-pressure vessel was connected to the stainless steel filter (porosity of 0.45 μm , the filter was previously passivated with nitric acid to avoid adsorption of the analyte) and to the pre-column by a practically zero-dead volume Viper high performance liquid chromatography (UHPLC) fitting (50 \times 0.1 mm, Thermo Scientific, Fig. 25). The precolumn was conditioned with 4 mL of ethanol and 4 mL of DCM (each passage for dryness) and was finally balanced with 6 mL of hexane. Oil samples (500 mg) were dissolved in 9 mL of DCM and loaded. Then, the precolumn was washed with 3 mL of DCM and finally dried for 15 minutes by washing with nitrogen. The precolumn was connected to the column by the virtually zero dead-volume Viper fitting and to an Ultimate 3000 LC system (Thermo Fisher Scientific, Bremen, Germany) into the thermostated column compartment at 50 ° C. (chromatographic conditions described in paragraph 4.4). In the optimized conditions, problems of phase miscibility were solved and analyte loss or band diffusion were avoided. The recovery of tryptophan was 60% (Fig. 24). The final procedure was used to trap the target seleno-amino acids.

Compared to the direct analysis, the preconcentration on the pre-column influenced the retention times of the analytes, which eluted up to 2.5 minutes before in the case of selenomethionine. Regardless of the changes of time, the seleno-amino acid enantioresolution was not affected.

The optimized method was used to construct calibration curves in matrix and in solvent, and validated in terms of recovery (R%), matrix effect (ME%), process efficiency (PE%), quantification limit (LOQ), identification limit (LOD). Then applied to samples of commercial oil.

The recovery (R%) could not be calculated using the reference methods [106], therefore it was calculated using the formula: $R\% = (\text{standard area high pressure vessel} / \text{area direct injection}) \times 100$. Similarly, matrix effect (ME) was estimated based on the formula: $ME\% = (\text{high pressure container for oil area} / \text{high pressure container for standard area}) \times 100$; Process efficiency (PE) was estimated according to the formula: $PE\% = (\text{area oil high pressure vessel} / \text{area direct injection}) \times 100$. The determination limits (LOD) and the quantification limits (LOQ) were calculated as a signal to noise ratio (S / N) = 3 for the second most intense transition and (S / N) = 10 for the sum of the two most intense transitions, respectively.

Table 6. Mean recovery (R, %), matrix effect (ME, %) and process efficiency (PE, %), with the relative standard deviations, for each seleno-amino acid isomer at either 1.88 ng and 5.00 ng or 0.94 ng and 2.50 ng.

SELENOAMINO ACID	R±RSD	ME±RSD	PE±RSD	R±RSD	ME±RSD	PE±RSD
	1.88 ng			5.00 ng		
SE-METHYL-L-SELENOCYSTEINE	65±2%	74±7%	48±9%	63±5%	79±6%	50±11%
L-SELENOMETHIONINE	69±5%	74±3%	51±8%	73±4%	81±4%	59±8%
D-SELENOMETHIONINE	72±7%	77±8%	55±15%	68±6%	76±7%	51±13%
MESO-SELENOCYSTEINE	69±5%	95±6%	65±11%	62±4%	81±1%	50±6%
SELENOAMINO ACID	R±RSD	ME±RSD	PE±RSD	R±RSD	ME±RSD	PE±RSD
	0.94 ng			2.50 ng		
L-SELENOCYSTEINE	64±8%	115±10%	74±18%	70±7%	112±9%	84±16%
D-SELENOCYSTEINE	62±11%	110±9%	68±20%	65±5%	107±10%	69±15%

Table 7. LOD and LOQ values for each seleno-amino acid are reported as concentration in the original 500 mg extra virgin olive oil sample preconcentrated by the high pressure vessel procedure; calibration curves of Se-AAs for preconcentration by high pressure vessel of spiked extra virgin olive oil samples

Selenoamino acid	LOD	LOQ	calibration curve	R ²
	ng g ⁻¹	ng g ⁻¹		
Se-methyl-L-selenocysteine	1.50	1.92	y = 3052x - 3111.9	0,9688
L-selenomethionine	0.96	1.25	y = 17618x - 7596,4	0,9773
D-selenomethionine	0.84	1.02	y = 9232,3x - 441	0,9725

meso-selenocystine	0.62	0.93	$y = 2033,7x - 1362,7$	0,9758
L-selenocystine	0.56	0.75	$y = 2428,6x - 858,39$	0,9695
D-selenocystine	0.78	0.84	$y = 1635,3x + 37265$	0,958

The protocol was applied to samples of commercial oil purchased in a local supermarket, i.e. extra virgin olive oil, cold-pressed unrefined maize, soy and sunflower oils, and fish oil from commercial omega-3 supplements.

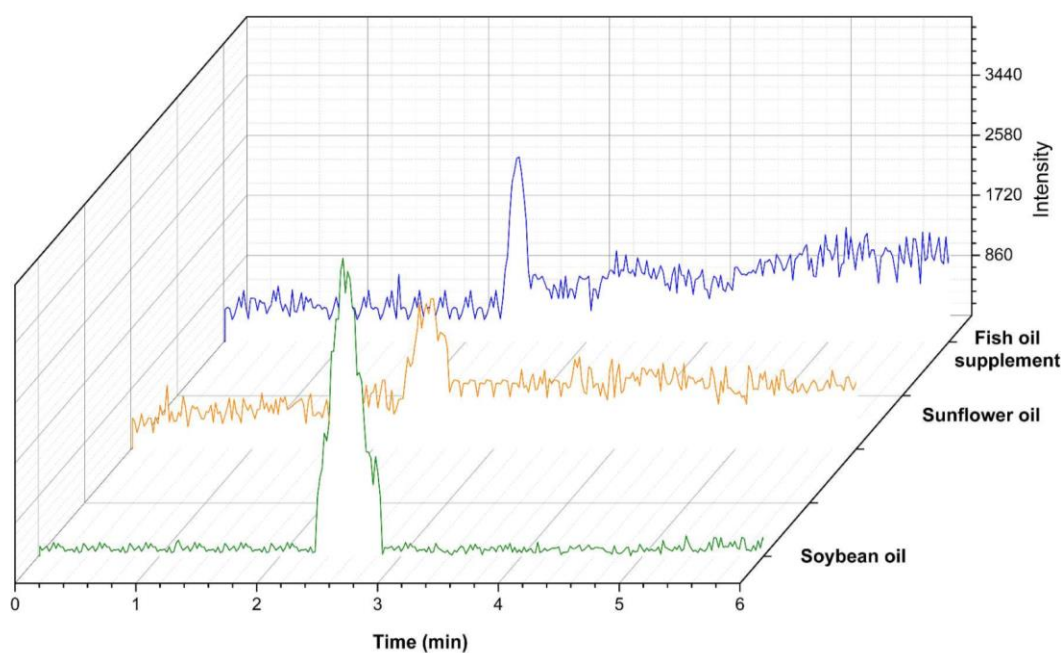


Figure 26 High pressure vessel preconcentration on 500 mg fish oil supplement (blue) and sunflower oil (orange) and on 50 mg soybean oil (green) sample

Two ng of L-seleno-methionine was found in 500 mg of sunflower oil (4 ng g^{-1}) and 1.8 ng of L⁻¹ seleno-methionine was found in the fish oil from supplements (3.6 ng g^{-1}). Soybean oil was the most naturally rich with L-seleno-methionine; thus, the oil amount employed for preconcentration was reduced 10-fold, to fit within the calibration curve. In this way, 3.1 ng of L-seleno-methionine was quantified in 50 mg of soybean oil (62 ng g^{-1}).

4.4.2 Investigation of free seleno-amino acids in extra-virgin olive oil by mixed mode solid phase extraction cleanup and enantioselective hydrophilic interaction liquid chromatography-tandem mass spectrometry (Paper VI)

The purpose of this paper was to develop an enrichment method for the determination of trace seleno-amino acids in olive oil, as showed in paper III, where the on-line enrichment method allowed the determination of seleno-methionine in soybean oil, sunflower oil, and in fish oil supplements, but not in olive oil. The method described in this paper was applied to 32 extra virgin olive oils, coming from various geographical testimonies in Italy. In this paper, the total Se determination was also performed along with the selected seleno-amino acid quantitation and the two were correlated with each other .

In the preliminary experiments, the samples were extracted by a liquid-liquid extraction with 10 mL of MeOH/H₂O, 80:20 (v/v). Two different commercial cartridges were tested, i.e. OASIS HLB and OASIS MCX; in the case of OASIS HLB, a concentration of the extract was needed to reduce the MeOH content. The stability of the analytes during solvent evaporation was also tested, along with a possible oxidation of SeCys and SeMet, which was avoided by addition of dithiothreitol (DTT). Stability was also studied after elution, the eluent volume was set at 2 mL of MeOH, to ensure quantitative elution after SPE. Therefore, 10 mL of MeOH/H₂O, 80:20 (v/v) (loading phase) and 2 mL of MeOH (elution phase) were tested for evaporation under neutral, acidic conditions (0.01 mol L⁻¹ HCl) and basic (3% NH₃) conditions, with or without the addition of 1% (w/v) DTT. The solvent evaporation was performed at 25 °C in Speed-Vac to guarantee equal conditions for all the samples. For the evaporation of the eluate, the analytes were stable without adding DTT in both acid and basic conditions, provided that the samples were not evaporated to dryness. From a practical point of view, this means that: i) the acidified extract can be evaporated up to 5 mL before OASIS HLB SPE and ii) a basified eluate from the cleaning cartridge can be evaporated to the level of μL without degradation of the analytes. For the eluates, evaporation was stopped at 150 μL of residual volume, which considered a safe safety limit. Although you can directly inject up to 20 μL without widening the peak, in the final procedure the samples were diluted with ACN to ensure compatibility with the HPLC mobile phase; 10 μL was injected from the resulting solution, since no improvement in the S/N ratio was obtained by doubling the injection volume. After establishing the possibility of analyte concentration, OASIS MCX was preferred between the two commercial cartridges, as percentage recovery values were better; OASIS MCX has the

same polymeric backbone as OASIS HLB, but is functionalized with sulfonic acid and can therefore be considered a mixed mode absorbent. All these experiments were conducted by adding the analytes to the extract, in order to test recovery after cleaning of the complex matrix.

For this reason, Oasis MCXTM SPE cartridges were used. The first experiments were carried out on water fortified with standard, subsequently the same were carried out on fortified oil, all the tests are shown in the paper VI. The oil results are shown here following the protocol suggested by the manufacturer, i.e. loading: 5 mL of water at pH 2 with HCl; first wash: 5 mL at pH 2 for HCl; second wash: 5 mL MeOH; elution: 2 mL MeOH, 3% NH₃. Under these conditions, recoveries ranged from 85% (MeSeCys) to 103% (meso-SeCys₂); however, the recoveries decreased drastically when the procedure was applied to 30 mg of oil, diluted with hexane and extracted with 10 mL of MeOH/H₂O, 80:20 (v/v); all other conditions have been kept constant (Tab. 8, condition a). A significant improvement was achieved using only 15 mg of EVOO (Extra virgin olive oil) sample (Tab. 8, condition b), but for SeMet and MeSeCys the recovery remained unsatisfactory; therefore, the acidity of the first wash phase was decreased (Tab. 8, condition c) which provided a small improvement, then the acidity was further decreased (Tab. 8, condition d). At this point, the first washing step with acid water was replaced by 2 mL of neutral H₂O, generating a significant improvement in the recovery of the analyte in the elution phase. (Tab. 8, condition e).

Table 8: Recovery (%) for different loaded sample and cleanup conditions (a-e) (W1^a first wash)

MeSeCys	L- SeMet	D- SeMet	L- SeCys	meso- SeCys ₂	D- SeCys ₂
a) 30 g EVOO sample and W1 ^a with 5 mL 0.01 mol L ⁻¹ HCl					
25%	32%	29%	71%	75%	70%
b) 15 g EVOO sample and W1 ^a with 5 mL 0.01 mol L ⁻¹ HCl					
51%	48%	53%	95%	91%	94%
c) 15 g EVOO sample and W1 ^a with 5 mL 0.050 mol L ⁻¹ HCl					
40%	42%	41%	93%	95%	89%
d) 15 g EVOO sample and W1 ^a with 5 mL 0.005 mol L ⁻¹ HCl					
43%	39%	44%	86%	87%	90%

e) 15 g EVOO sample and W1 ^a with 2 mL H ₂ O					
67%	70%	68%	102%	96%	101%

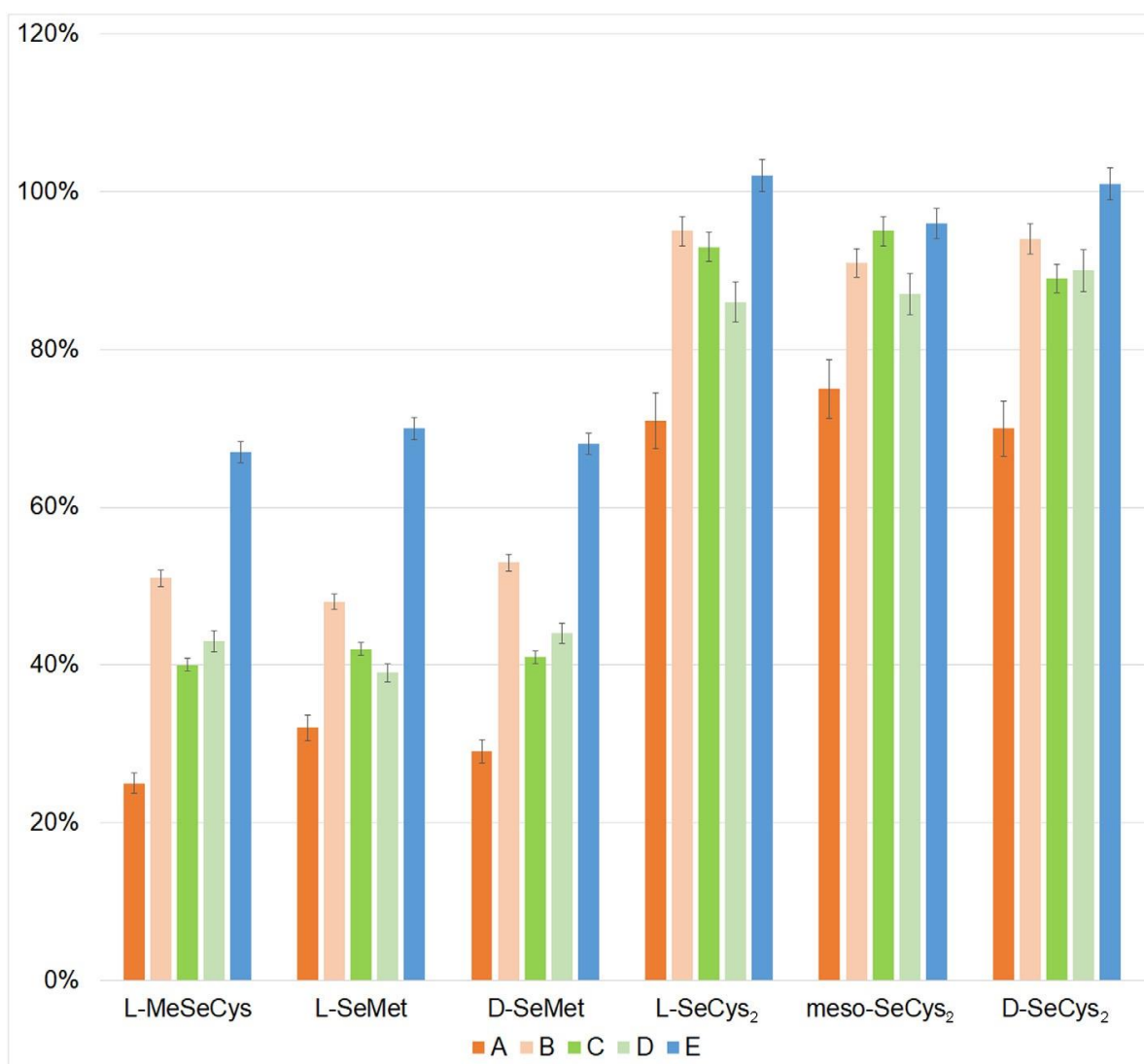


Figure 27 Recovery (%) for different loaded sample and cleanup conditions (a–e) for the OASIS MCX (150 mg) cartridge

The final conditions used for the 32 oil samples were: 15 g of oil were added with 100 μL of the IS solution ($0.1 \text{ ng } \mu\text{L}^{-1}$) and 15 mL of hexane and the mixture was stirred manually for about 30 seconds; 10 mL of MeOH/H₂O (80:20, v/v) were added and the mixture was vortexed for 20 minutes, then centrifuged for 10 minutes at $3000 \times g$ at $15 \text{ }^\circ\text{C}$. The oil/hexane supernatant was discarded and lower layer was acidified with 20 μL of 6 mol mL^{-1} HCl and the mixture was stirred for 30 seconds. The extract thus formed was loaded onto an MCXTM SPE cartridge, after activation with 5 mL of MeOH and 5 mL of 10 mmol L^{-1} HCl solution.

The cartridge was washed with 2 mL of ultrapure water followed by 5 mL of MeOH (by gravity), the analytes were eluted with 2 mL of MeOH with 3% of NH₃ (v/v). The solvent was evaporated up to approx. 150 μL at 25 °C in the Speed-Vac SC 250 Express (Thermo, Holbrook, NY, USA); finally, 100 μL of ACN containing 0.5% HCOOH (v/v) were added, the solution obtained was forced through a PTFE syringe filter and 10 μL were injected into the UHPLC-MS/MS system.

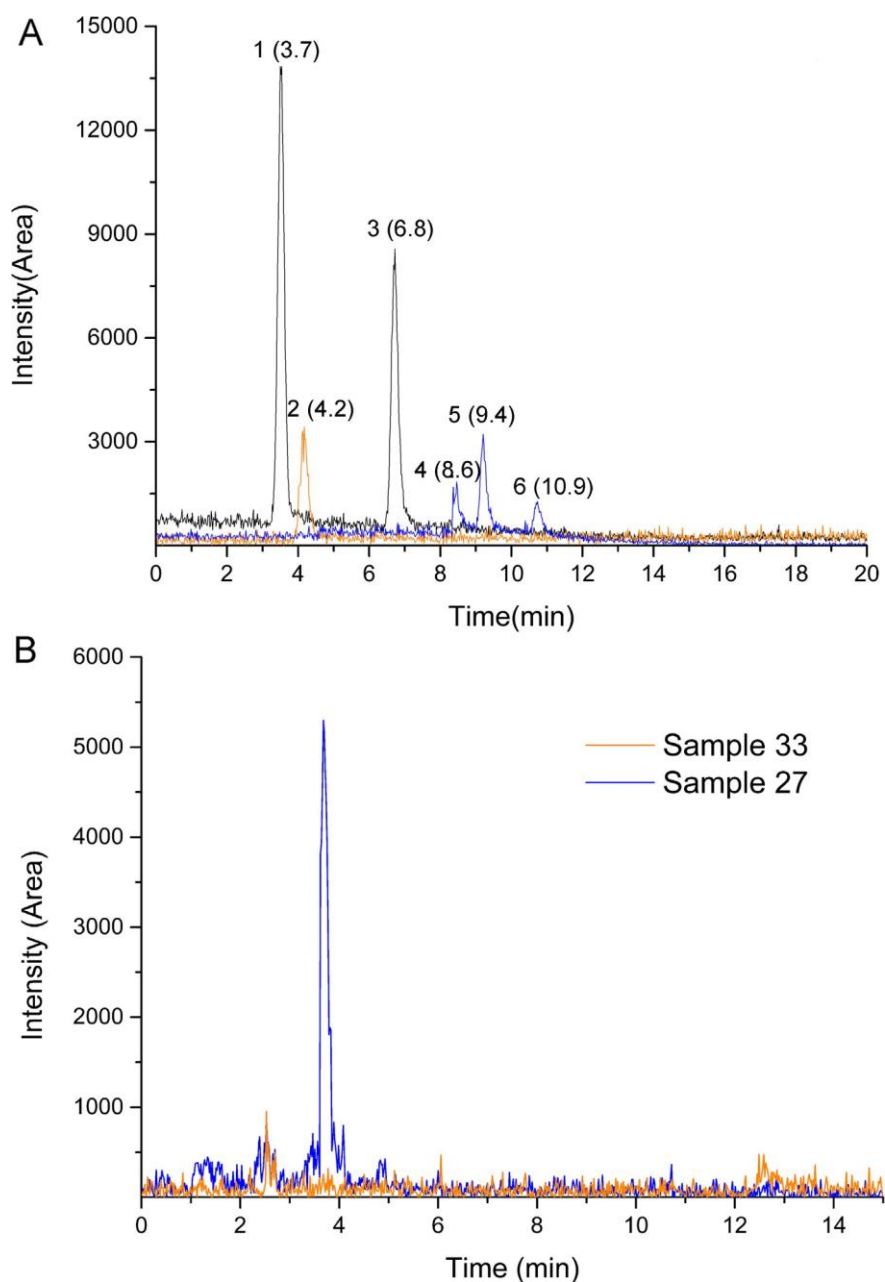


Figure 28 A: Enantioresolution of the target seleno-amino acids (0.4 ng injected of each standard) on the CHIROBIOTIG TAG. Elution order: L-SeMet (1), L-MeSeCys (2), D-

SeMet (3), L-SeCys₂ (4), meso-SeCys₂ (5), D-SeCys₂ (6). B: mass chromatograms of two representative EVOO samples, one containing 0.72 µg kg⁻¹ L-SeMet (sample 27) and an apparently empty sample (sample 33).

Thirty-two samples of extra virgin olive oil of various certified geographical origins were analyzed for both the total Se and the seleno-amino acid content. L-SeMet was quantified in 7/32 samples. This does not agree with the only paper available on this topic [103], in which MeSeCys was the only compound detected. This difference cannot be explained by the geographical origin, but could derive from the total Se content. Both SeMet and MeSeCys have been synthesized in plant systems starting from SeCys; to overcome the toxic level, the biosynthesis of SeCys increases, activating the detoxifying enzyme Se-cysteine methyltransferase, which combines with SeCys, which turns into volatile dimethylselenide[44].

Another interesting discovery is the excellent correlation ($R^2 = 0.996$) between Se and SeMet (Fig. 29) . This correlation cannot be easily explained. If incorporated into proteins it should be in the approximate maximum quantity of 15 ng of L⁻¹, therefore, as reported elsewhere [105]. Most of Se should be bound or transported by the fraction lipid or other minor EVOO compounds in the form of selenite, selenate and selenolipids.

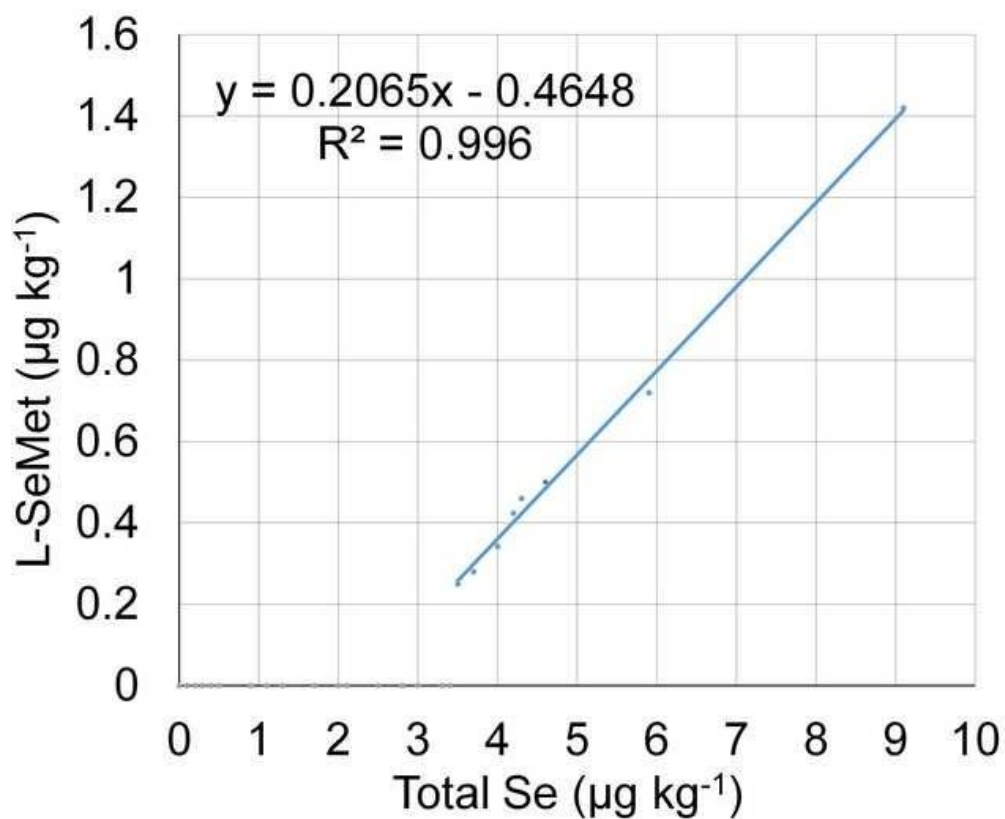


Figure 29 Correlation between Selenium and Selenium-methionine

The method was validated following the guidelines in the commission Decision 2002/657/EC (Decision 2002/657/CE, 2002) in terms of linear dynamic range, recoveries, matrix effect, limit of quantification, limit of identification, trueness, process efficiency and precision.

This paper described a new method for the determination of seleno-amino acids in EVOO which includes the enantioresolution of seleno-amino acid isomers, no enomers in oil were determined. The method, based on HPLC-ESI-MS/MS, has been developed and validated. The total concentration range of Se was 0.5-9.1 µg kg⁻¹ and L-SeMet at a concentration in the range 0.2–1.42 µg kg⁻¹.

4.4.3 Investigation of free and conjugated seleno-amino acids in wheat bran by hydrophilic interaction liquid chromatography-tandem mass spectrometry (Paper VII)

After developing an enantioselective chromatographic method for separation of seleno-amino acids and enrichment methods for both abundant and low-abundant seleno-amino acids in oils, one final topic was left behind, which is why a method for the determination of both free and protein-conjugated seleno-amino acids was developed in paper VII. More specifically, in paper VII a more comprehensive method was developed, for free and conjugated seleno-amino acid extraction from wheat bran. Four different methods were compared, also including two different proteolytic enzymes, i.e. proteinase K and protease XIV, to release the conjugated Se-AA. The samples were purified and enriched by solid phase extraction (optimized method in VI paper) and analyzed by HPLC-ESI-MS/MS (see section 4.4). The method was then validated in the raw matrix.

Bran samples were frozen in liquid nitrogen to break the cell walls, powdered with a pestle in a mortar, and stored at 4 °C in a refrigerator in a 50 mL polypropylene tube wrapped with aluminum foil until extraction or digestion.

Table 9: Summary of the extraction protocols

Extraction protocol	Obtained Samples	Brief Method Description
Protocol A	A_free	This protocol allowed to identify free and conjugated Se-AA. Sonication temperature 55° C
	A_Proteinase K	
	A_Protease XIV	
Protocol B	B_free	This protocol allowed to identify free and conjugated Se-AA. Sonication in ice bath.
	B_Proteinase K	
	B_Protease XIV	
Protocol C	C_Proteinase K	Digestion was carried out directly on wheat bran. No free Se-AAs analyzed.
	C_Protease XIV	
Protocol D	D_Proteinase K	Proteomic experiment. Only conjugated Se-AAs were analyzed.
	D_Protease XIV	

In this paper, four different extraction processes were compared for the simultaneous identification of free Se-AA and conjugates in wheat bran because a significant amount of Se is conjugated to proteins, therefore enzymatic hydrolysis is fundamental to free the Se-AA inside the protein molecule. Based on the data in our possession, this study is the only one conducted on this matrix by HPLC-MS/MS analysis; a previous study on cereals, always carried out on seleno-amino acids, did not differentiate between free and protein-conjugated seleno-amino acids [107]. The first challenge to consider is the recalcitrant nature of plant tissues, which makes it necessary to grind it as finely as possible to obtain a high recovery of compounds of interest before any solvent extraction, and to achieve the breakdown of cell walls. Compared to works of literature [97,98], in this paper the bran is first mixed with glass beads. The use of a mechanical extraction method promotes the solubilization of the seleno-amino acids. After mechanical extraction, extraction is essential, and hot water is one of the most used strategies [97,108,109], due to the polar nature of these compounds. Protocol A uses a temperature of 55 °C, which is reported to be the optimal one in the literature. Protocol B was performed on ice, to see if the extraction at high temperatures could degrade seleno-amino acids. Protocol C [98] was performed according to a literature method, and consisted in the digestion of bran directly with enzymes, without protein extraction or isolation. The method was used in order to compare a literature method with our procedures even if it was not possible to obtain the free fractions of seleno-amino acids. In the last protocol (Protocol D), a stronger extraction buffer was tested, which included a detergent such as sodium dodecyl sulfate (SDS), which is commonly employed in proteomics workflows for protein extraction. In this experiment only digested fractions were obtained, since the supernatant contained a high amount of salts and interfering compounds and could not be analyzed by mass spectrometry.

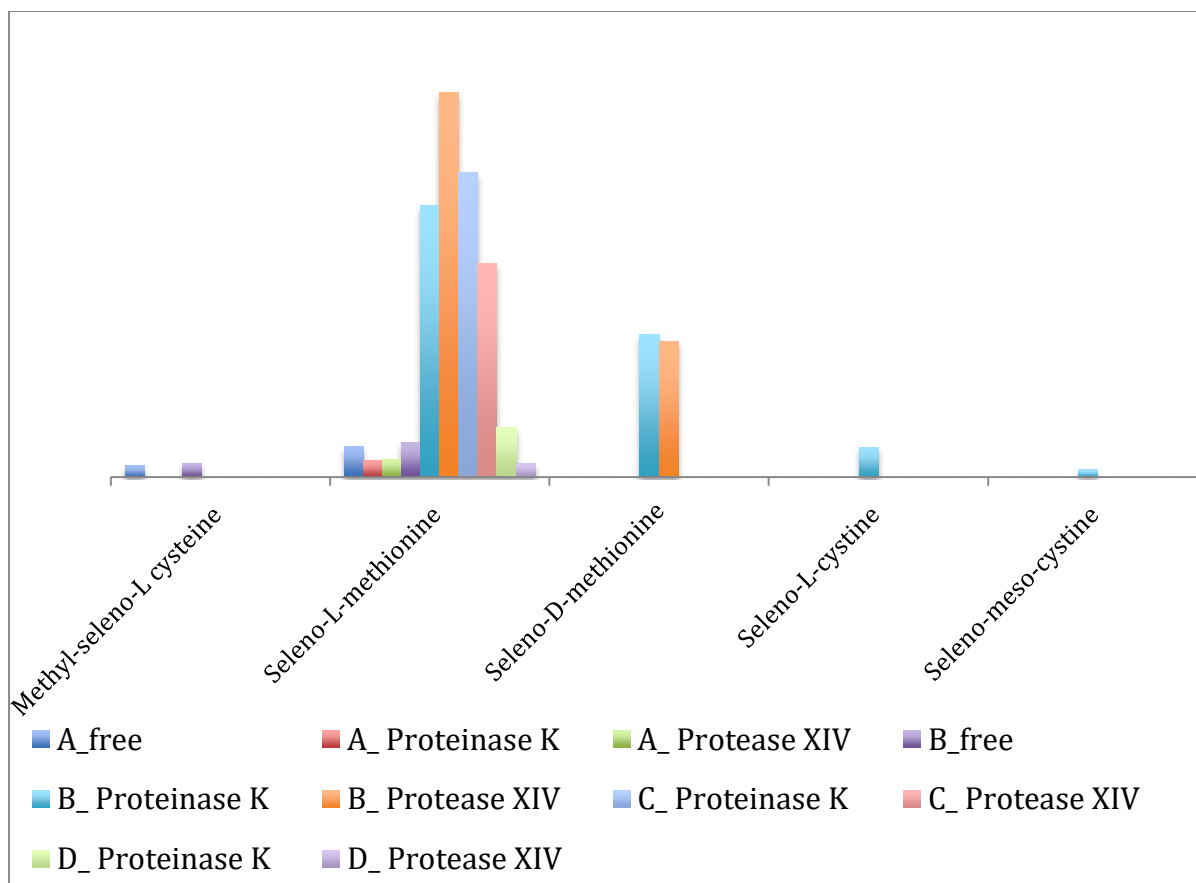


Figure 30 Comparison between the different procedures

It is known that the D-series of amino acids is not found naturally in eukaryotic organisms but they are commonly synthesized by bacteria. Racemization of amino acids can occur when food matrices are exposed to high temperatures or fermentation during production. It is possible to see in Fig.30 that Se-L-Cys₂ and Se-meso-Cys₂ were detected only by application of protocol B with proteinase K digestion, a result which can be attributed to the different action of enzymes. Another possible explanation for the presence of Se-L-Cys₂ and Se-meso-Cys₂ could be related to the fact that in plants and animals, most of the amino acids incorporated into proteins are L-forms, this is why the corresponding D-form or meso-form can be potentially toxic. The motivation can also be procedural. Water extraction is considered a commonly used procedure that does not induce racemization, but it has been reported that strong acids convert 0-10% of Se-L-Met into the D-enantiomer [110].

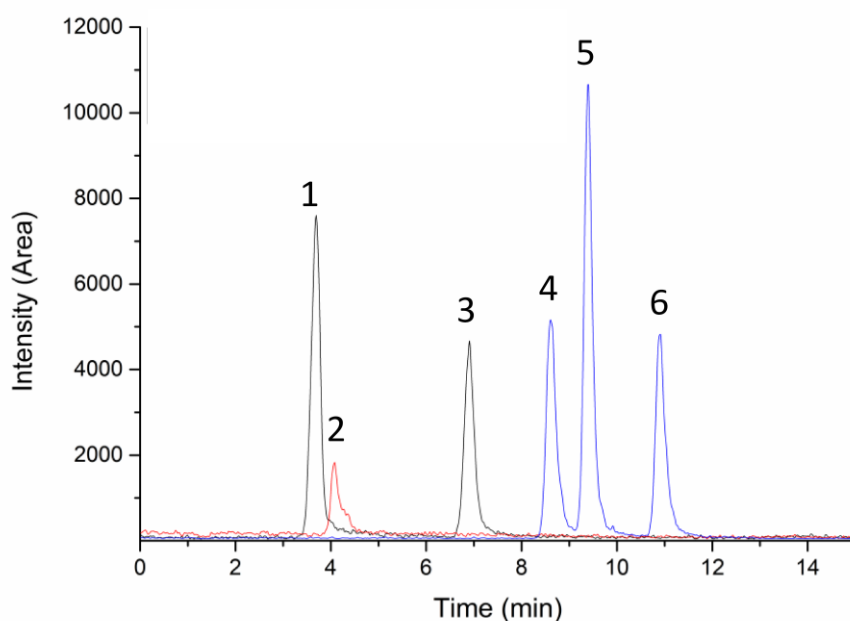


Figure 31 SRM acquisition of sample spiked at LOQ value. L-Selenomethionine (peak 1) 3.9min, D-selenomethionine (peak 3) 6.9min, Se-methyl-L-selenocysteine (peak 2) 4.1min, L-selenocystine (peak 4) 8.6min, D-selenocystine (peak 6) 11min, and meso-selenocystine (peak 5) 9.5min;

The samples showed a Se concentration range of 4.41–5.36 ng/g for free seleno-amino acids and 45.61–53.87 ng/g for conjugated seleno-amino acids. Se-L-Met was more abundant in all the samples analyzed with a concentration range of 7.42-9.21 ng/g in the free fractions and 67.21–100.02 ng/g for the conjugates, showing that cereals convert Se mainly into Se-Met and incorporate it into proteins instead of methionine because tRNA-Met does not discriminate between methionine and Se-Met [111]. We finally evaluated the speciation of Se in the analyzed samples, discovering that 7% of the total Se was represented by free seleno-amino acids, while 60-70% belonged to conjugate fractions. The remaining 20-30% is due to other compounds, which were not included in this study.

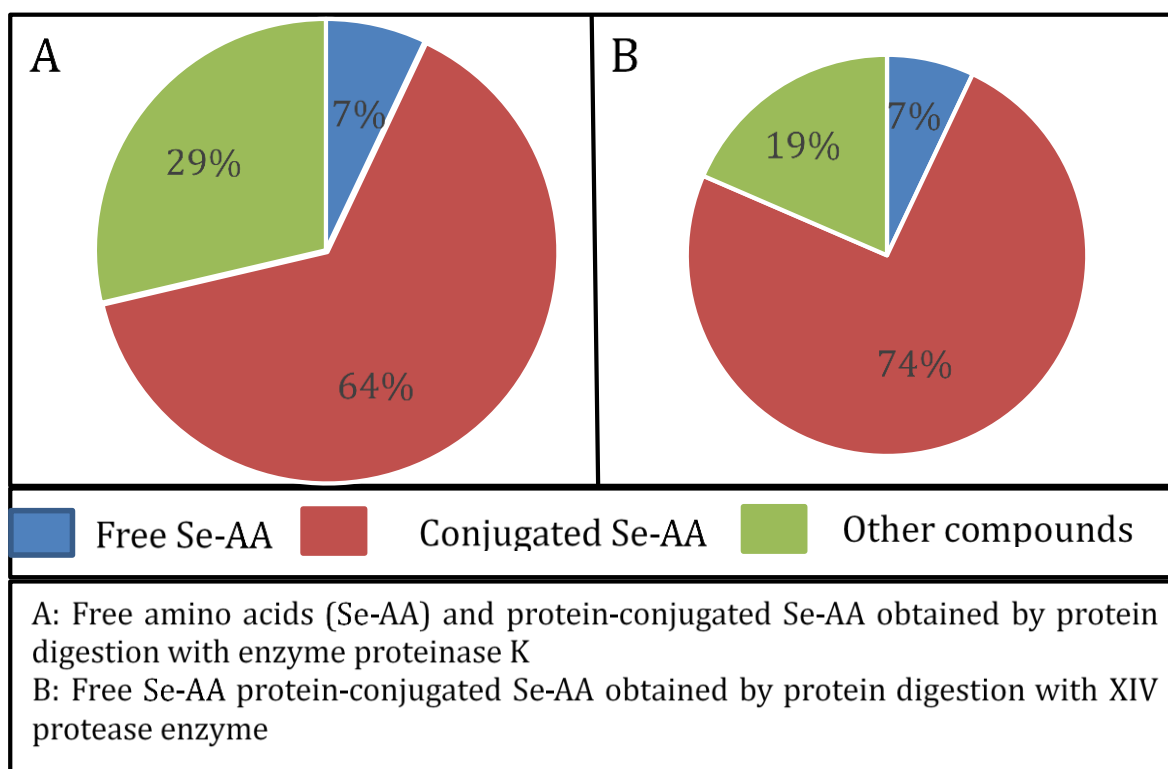


Figure 32 Distribution of seleno-amino acids in wheat bran

The best extraction was found to be protocol B in which an aqueous solution buffer and ice sonication cycles were used. This protocol allowed the recovery of high concentrations of Se-AA avoiding losses and degradation caused by high temperatures. The best protocol was then applied to the analysis of four real samples collected in different local markets.

Also the best protocol has been optimized according to the main FDA guidelines. The method was verified by determination of its linear dynamic range, limit of quantification, identification limit, recovery, matrix effect, process efficiency, precision and robustness. (The validation results are in the VII paper)

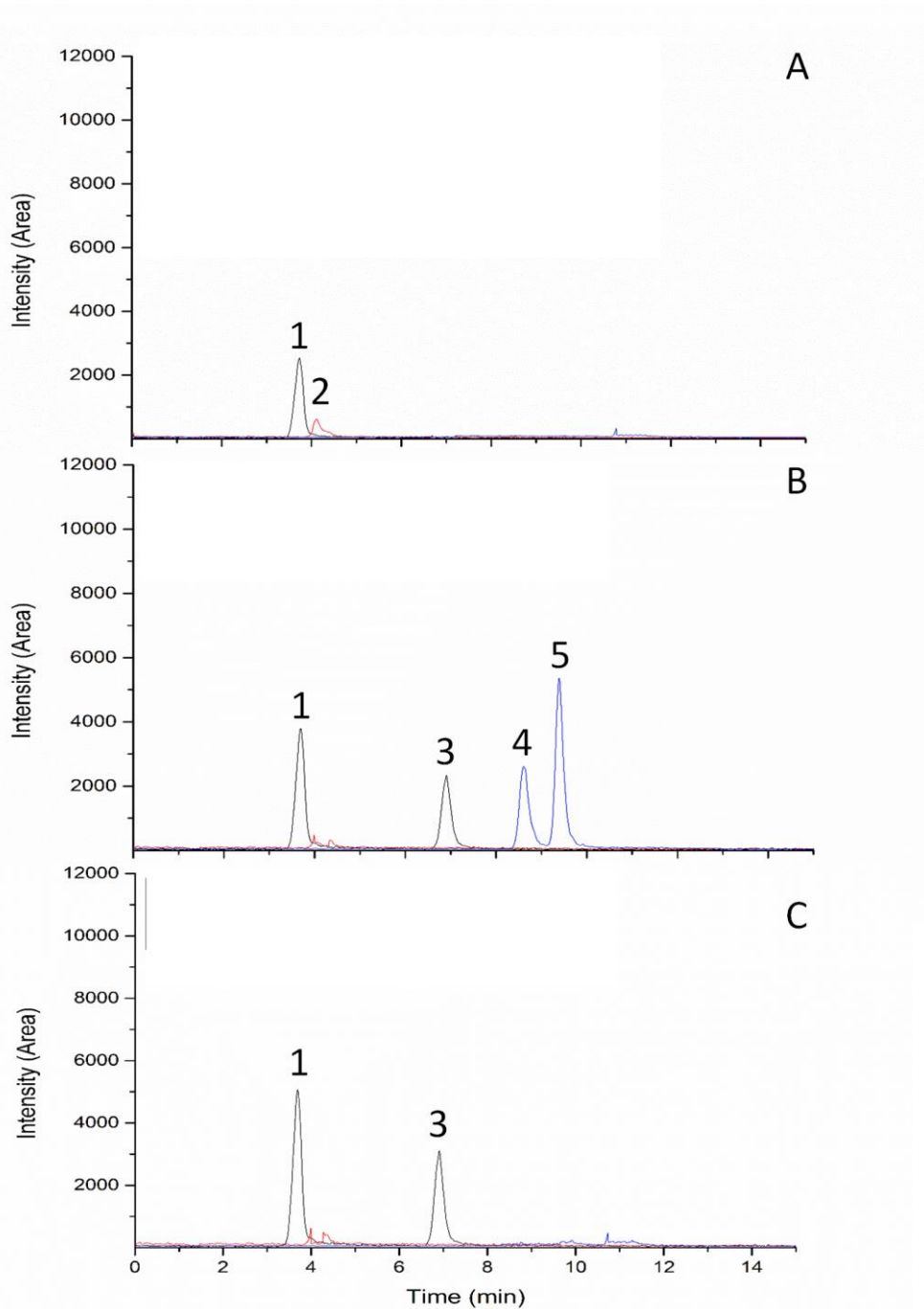


Figure 33 Chromatograms showing the separation of seleno-amino acids in bran: A) free seleno-amino acids B) conjugated seleno-amino acids obtained by digestion with protease k; C) conjugated seleno-amino acids obtained by digestion with protease XIV. L-Selenomethionine (peak 1) 3.9min, D-selenomethionine (peak 3) 6.9min, Se-methyl-L-selenocysteine (peak 2) 4.1min, L-selenocystine (peak 4) 8.6min, D-selenocystine (peak 6) 11min, and meso-selenocystine (peak 5) 9.5min

Chapter 5: Phosphopeptides

5.1 Molecularly imprinted polymers (MIP)

Molecular imprinting is an innovative approach to create synthetic materials with molecular recognition properties [112]. This technique is based on the copolymerization of functional monomer and crosslinker in the presence of a model, which is subsequently removed. A MIP has cavities of a size and shape complementary to the model, allowing the re-binding of the model and its similar analogues (Fig. 34). This basic concept is applicable to a wide variety of molecules, ions, small molecules, macromolecules and microorganisms. The interaction between functional and template can be weak or strong, for example covalent and non-covalent interactions and ligand exchange.

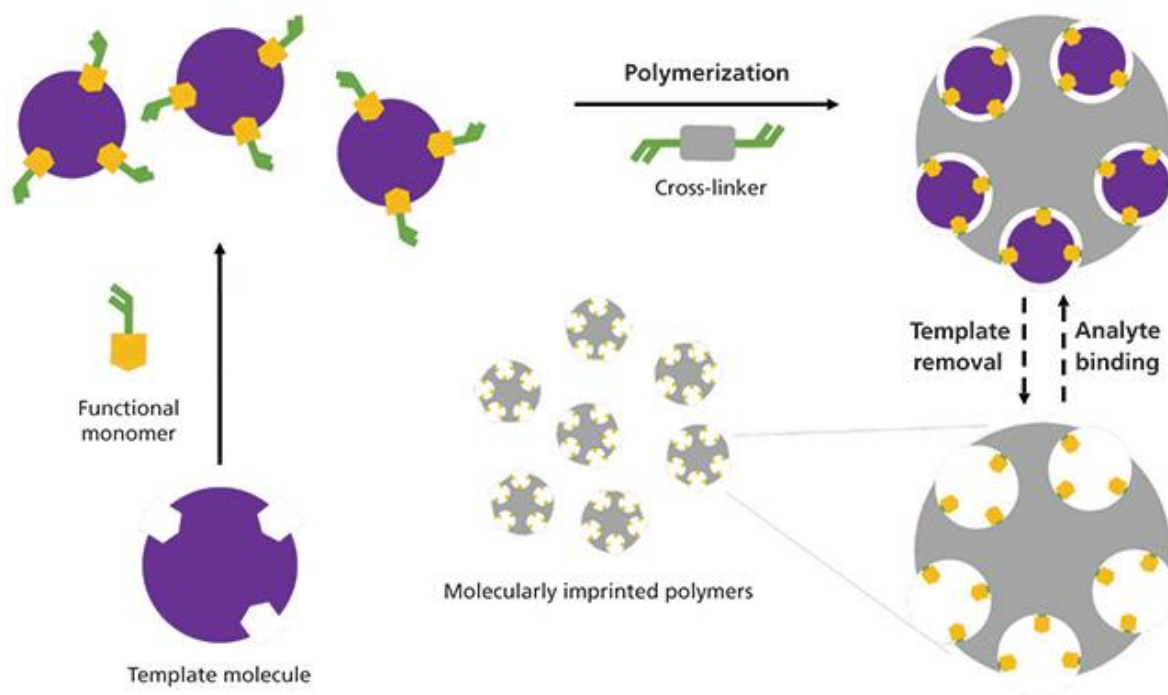


Figure 34 Schematic representation of the molecular imprinting process

Due to the unique properties of MIP recognition, characterized by a high specificity and affinity for the target molecule, the molecular imprinting technology has found application in different fields, including sample preparation, preparation of purification and separation phases [113], in sensor chemistry [114] and in the delivery of drugs [115]. MIPs are robust materials with high stability at different temperatures and solvents. The low production cost and the possibility of multiple re-use of the material are further interesting features of MIPs.

The imprinting of water-soluble biological macromolecules, such as proteins [116], represents a great analytical challenge, due to the large size and complexity of these objectives with subsequent slow mass transfer to the binding site. Two main approaches have been developed to overcome these difficulties: epitope imprinting and surface imprinting. The imprinting of epitopes uses a small fragment of proteins or peptides as a model [117]. This allows not only the recognition of the model, but also larger molecules that have that imprinted fragment.

5.2 MIP for phosphoproteomics

Several approaches for the development of phosphopeptide-selective molecular polymers have been reported in literature [63]. The goal of my time in Sweden was to develop a new material for phosphorylated peptides. In particular, polymers with imprinted phenylphosphonic acid (PPA), for the selective recognition of phospho-tyrosine (pY) peptides, have been synthesized; pY peptides are found at low levels in protein digests. The development of the method involved the evaluation of the properties of PPA-MIP and the commercial kit based on titanium dioxide (TiO₂-Kit) for the enrichment of low-level microgram phosphopeptides.

5.2.1 Synthesis of phosphate-imprinted magnetic nanoparticles (Fe₃O₄@FB1@PPA)

The synthesized material in this thesis work, i.e. PPA-MIP, is a magnetic material. The use of magnetic materials is particularly interesting and attracting attention, as the magnetic properties can be exploited to automate the enrichment process. For this reason, a magnetite core was initially created by hydrothermal reaction as described below.

0.99g of Iron(II) chloride tetrahydrate (FeCl₂*4H₂O) and 2.73 g of Iron(III) chloride hexahydrate (FeCl₃*6H₂O) were dissolved in 25 mL of milliQ water at room temperature. The mixture was stirred vigorously at 80 °C for 15 min and then 10 mL of ammonium hydroxide solution (NH₄OH) was quickly added into mixture until the pH reached to 10. The black precipitate was separated by magnetic decantation and washed several times with milliQ water and 3 times with ethanol. The black magnetic nanoparticles (MagNPs) were finally dried at 60 °C overnight. Before the amino-functionalization, a silica core was synthesized around the magnetic nanoparticles (MagNPs@SiO₂). One g of dry MagNPs was dispersed in 25 mL of milliQ water by sonication. The collected MagNPs were subsequently dissolved in 115 mL of aqueous solution of TEOS (10%) (Tetraethyl orthosilicate). One-hundred mL of glycerol was added. The pH was adjusted to 4,6 with glacial acetic acid. The dispersion was heated to 90 °C under N₂ atmosphere and vigorously stirred for 2h. The resulted product was collected by external magnet and washed several times with milliQ water and ethanol and dried at 60 °C.

For amino-functionalization of MagNPs, 1 g of MagNPs@SiO₂ was suspended in 30 mL of ethanol/milliQ water (1:1, v/v) under sonication at room temperature for 30 min. The flask was sealed with septum and the solution was heated to 40 °C under mechanical stirring and N₂ atmosphere. Four mL of APTMS (3-Aminopropyl)trimethoxysilane) was injected into the flask, and the mixture was allowed to react overnight. After the amino-functionalization, the MagNPs were collected by external magnet and washed with ethanol and 3 times with milliQ water until a neutral pH value was obtained. The ninhydrin test was positive, the amino-functionalization was successfully achieved. The particles were dried under vacuum at 60 °C for 8h. At the same time, the functional monomer (FB1) was synthesized, as follows: 1 g of PABA (4-Aminobenzoic acid) was dissolved in 20 mL of THF (tetrahydrofuran) under N₂ atmosphere; 1.26 mL of 3,5-Bis(trifluoromethyl)phenyl isocyanate was added to mixture. The reaction mixture was stirred overnight at room temperature under N₂ atmosphere. The solvent was evaporated by rotavapor. The product was recrystallized by hot acetone. The product was closed in a flask and then re-dried to get the product. This was tested with a mass spectrometric analysis. The product was synthesized without impurities. The functionalized amino-particles were reacted with the functional monomer (MagNPs-NH₂-FB1). One-hundred mg of MagNPs-NH₂ were suspended in 45 mL of anhydrous THF under N₂ atmosphere. Then 245 mg of FB1 (pre-dissolved in THF) was added dropwise to the magNP-NH₂ solution. The mixture was stirred 24 h at room temperature under N₂ atmosphere. MagNPs-NH₂-FB1 were separated from the bulk solution using a permanent magnet and then washed 5 times with acetone. The particles were dried overnight. On the external surface of the synthesized material, phenylphosphonic acid was imprinted to create a cavity for selective recognition. Phosphate-imprinted magnetic nanoparticles (PMNPs) were synthesized by dissolving 20 mg of MagNPs-NH₂-FB1 in 10 mL of buffer solution A (50% acetonitrile ACN containing 3% trifluoroacetic acid (TFA)), following by addition of 30 mg of phenylphosphonic acid (PPA) and shaken for 3 h. Subsequently, the products were obtained by magnetic separation and washed with buffer solution A and buffer solution B (50% ACN containing 0.1% TFA) for three times. Finally, a silica layer was prepared via Stöber sol-gel process to oriented imprint PPA. The obtained products were dispersed in a solution of ethanol/water/TEOS/UPTES (100.52 mL, 80/20/0.5/0.02, v/v/v/v), and then 2.0 mL of ammonia solution (NH₃·H₂O) was added dropwise under stirring, followed by mechanical stirring for 10 min at room temperature. Subsequently, the products were separated using a magnet and washed with ethanol. The step was repeated three times before drying at 40 °C in a vacuum overnight. To remove the imprinting template,

the particles were washed with 10 mL of 5% ammonia solution ($\text{NH}_3 \cdot \text{H}_2\text{O}$) and shaken for 1 h at room temperature, which was repeated four times. After removing the templates, the imprinted products were collected magnetically, washed with ethanol for three times and then dried at 40 °C overnight. Non-imprinted magnetic nanoparticles (NMNPs) were prepared as described above, except that the template molecule was omitted.

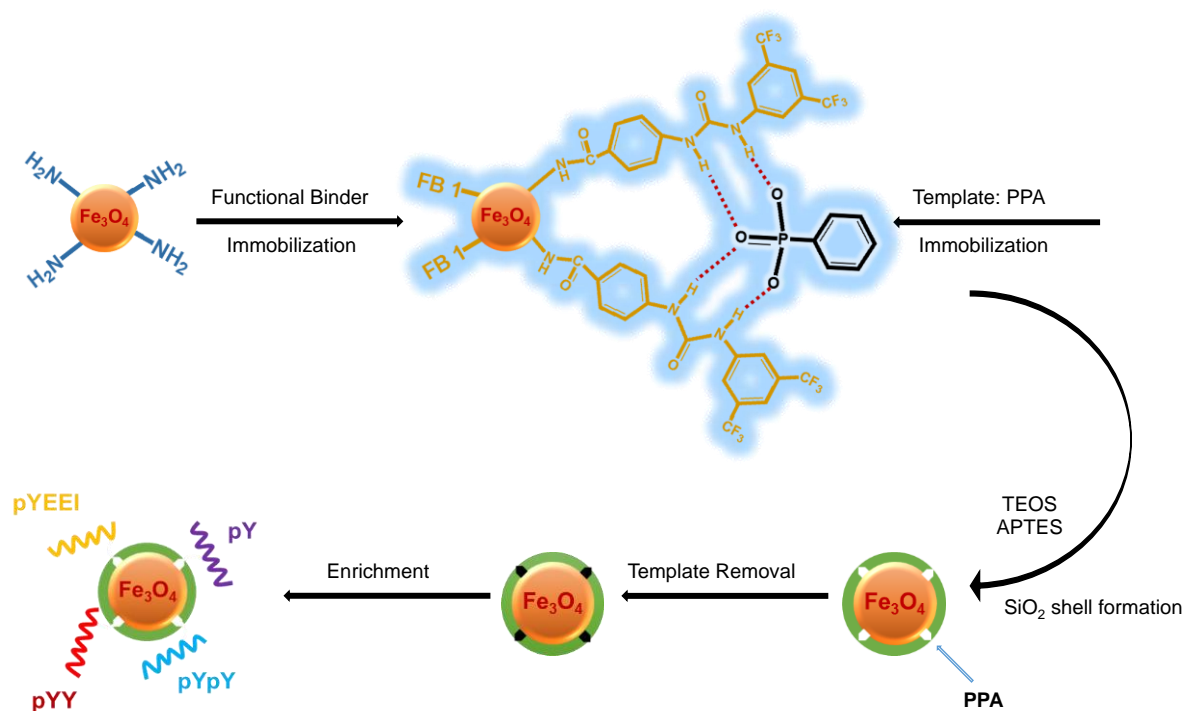


Figure 35 Synthesis of phosphate-imprinted magnetic nanoparticles ($\text{Fe}_3\text{O}_4@FB1@PPA$)

The material was analyzed using a scanning electron microscope (SEM). The size distribution was 40-60 nm.

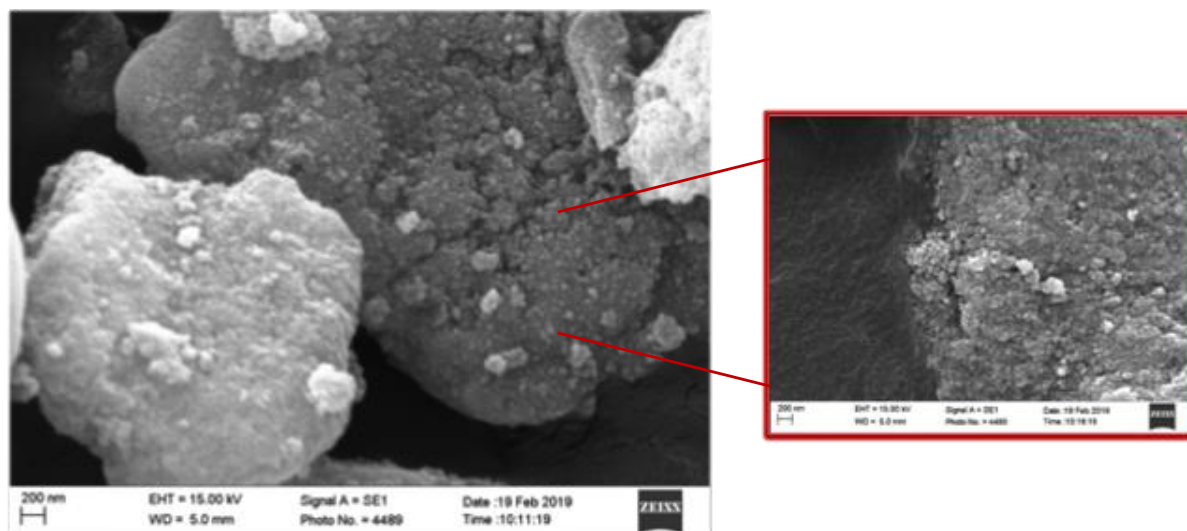


Figure 36 SEM image of phosphate-imprinted magnetic nanoparticles ($\text{Fe}_3\text{O}_4\text{@FB1@PPA}$)

5.2.2 Data analysis

MALDI MS was performed using an Ultra-flextreme mass spectrometer and processed with Flex- analysis software (Bruker Daltonics, Bremen, Germany). The MALDI analysis made it possible to carry out fast analyzes to assess the enrichment performance of the developed MIP material both for simple and complex mixtures. To test the binding of the MIP material, a mixture of 8 phosphorylated and non-phosphorylated synthetic peptides and a complex mixture consisting of a tryptic digest of casein and bovine serum albumin (BSA) were used. For more precise studies, nano-HPLC coupled with high resolution mass spectrometry was also used.

NanoHPLC-MS/MS analysis and peptide identification were carried out as follows: a Dionex Ultimate 3000 was coupled to a Orbitrap Elite hybrid ion trap-Orbitrap mass spectrometer (Thermo Scientific). Samples were online preconcentrated on a μ -precolumn (Dionex, 300 μm i.d. \times 5 mm Acclaim PepMap 100 C18, 5 μm particle size, 100 \AA pore size), employing a premixed mobile phase $\text{H}_2\text{O}/\text{ACN}$ 98:2 (v/v) containing 0.1% (v/v) TFA at a flow-rate of 10 $\mu\text{L min}^{-1}$. RP separation was performed on an EASY-Spray column (50 cm \times 75 μm i.d. PepMap C18, 2 μm particles, 100 \AA pore size, Thermo Scientific) operated at 200 nL min^{-1} and at 40 $^\circ\text{C}$. A 280 min long multistep gradient was employed to separate peptides, using H_2O with 0.1% (v/v) FA as phase A and ACN with 0.1% (v/v) FA as phase B. Starting from 1%

phase B, such composition was maintained for 5 min, and then phase B was linearly increased to 5% within 2 min; afterward, phase B was first increased to 30% within 187 min and then to 50% within the following 13 min and 80% in 5 min. Phase B was maintained at 80% for 20 min to rinse the column and finally lowered to 1% within 1 min. The column was then equilibrated at this percentage for 44 min. Full scan and MS/MS analysis of eluting peptides were performed in the m/z range of 400–1800 and 60,000 (Full Width Half Maximum at m/z 400) resolution for the full scan. A data dependent mode acquisition was enabled, in top 20 mode, rejecting +1 and unassigned charge states, using a normalized collision energy of 35% and an isolation window of 2 m/z . Ion trap and Orbitrap maximum ion injection times were set to 100 and 200 ms, respectively. Automatic gain control was used to prevent overfilling of the ion traps and was set to 1×10^6 for full FTMS scan and 1×10^4 ions in MS/MS mode for the linear ion trap. To minimize redundant spectral acquisitions, dynamic exclusion was enabled with a repeat count of 1 and a repeat duration of 30 s with exclusion duration of 70 s. For each sample, three technical replicates were performed. Identification for the acquired raw MS/MS data files from Xcalibur software (version 2.2 SP1.48, Thermo FisherScientific) was performed searching the Uniprot database with Proteome Discoverer software (version 1.3, Thermo Scientific) and the Mascot (v.2.3.2, Matrix Science) search engine, using *S. cerevisiae* taxonomy (7803 entries) for yeast samples.

5.3 Application

The material was initially tested with a mixture of 8 peptides (phosphorylated or not) to test the selectivity. The mixture was constituted as listed below:

PEPTIDE SEQUENCE	ABBREVIATION	[M+H] ⁺
DRVPSIHPF	DF-8-pS	1050.47
DRVPYIHPF	DF-8-pY	1126.51
GADDSYPYTAAR	ZAP70-YpY	1198.44
GADDSPPYPTAR	ZAP70-pYpY	1278.41
GADDSYYTAR	ZAP70-YY	1118.10
DRVYIHPF	DF-8-Y	1046.54
AC-PYEEI	SH2 domain-pYEEI	1473.50

The procedure for the enrichment was very simple and fast due to the magnetic properties of the MIP material, which allowed to enrich phosphopeptides directly in the bulk solution by dispersion and retrieve the MIP by magnetic decantation with the aid of an external permanent magnet.

For each enrichment experiment, MIP was weighed and then sequentially washed with 500 μL of MeOH/H₂O, 80:20 (v/v) with 0.1% (v/v) TFA and 500 μL of MeOH with 0.1% (v/v) TFA, each time with slight agitation for 2 min. A 1-min centrifugation (2300 \times g) procedure was performed at every step to sediment the entire solution before recovery of the magnetic phase and discarding of the supernatant; then the phase was conditioned with the loading buffer (ACN/H₂O, 95:5 (v/v) with 0.1% (v/v) TFA) as previously described. After this step, the material was put in contact with the mix containing the 8 peptides dissolved in the loading buffer, and the suspension was stirred for 60 min for binding. After centrifugation and magnetic recovery of the loaded Fe₃O₄@FB1@PPA, the supernatant was discarded, and the phase was washed once with the loading buffer and twice with 500 μL of MeOH/H₂O, 80:20 (v/v) with 0.1% (v/v) TFA. At beginning a first elution was made 500 μL of MeOH with 0.1% (v/v) TFA. A second elution was performed with 500 μL of elution buffer (5% NH₃ (aq)). The eluates were acidified with TFA to pH 2.5, desalted, dried down in a Speed-Vac SC250 Express (Thermo Savant, Holbrook, NY, USA), and resuspended with 100 μL of 0.1% FA. Acidification is an important step in the enrichment procedure because phosphorylations are not stable in a basic environment over long times. Desalting the samples is also essential because TFA, which is added to neutralize the eluent, after evaporation forms the ammonium salt and causes suppression during MS ionization with subsequent reduction of the number of peptide identifications.

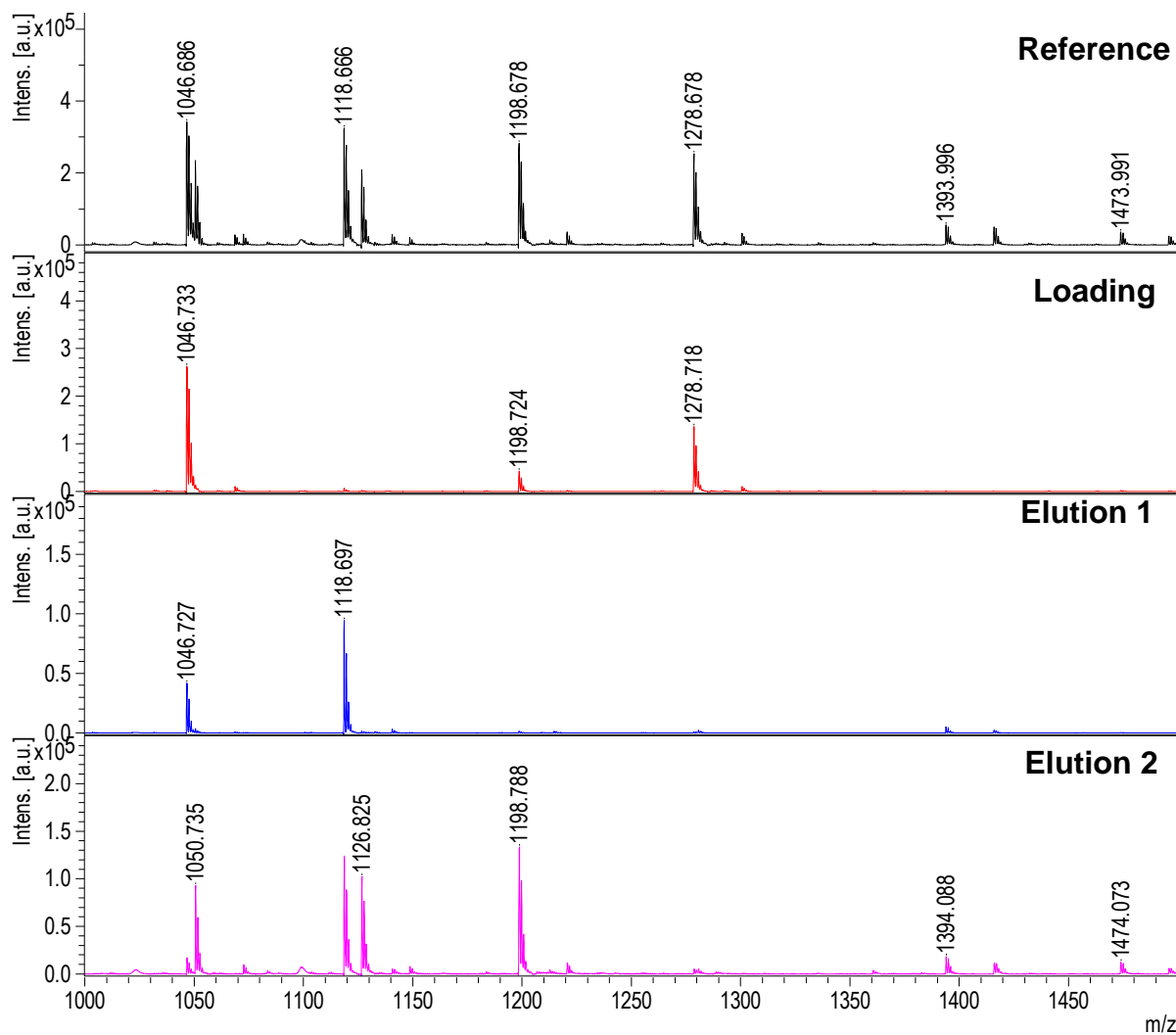


Figure 37 MALDI MS spectrum of the standard peptide mixture (reference) for each step of the enrichment process (loading and elution) with reference solution

Initially the performance of the MIP for phosphopeptides enrichment was tested using a simple mixture of tryptic peptides containing regular (non-phosphorylated) peptides and a series of phosphorylated peptides, to test the experimental workflow (Fig. 37). These experiments indicated that the material had a good affinity for pTyr peptides and a potential in enriching pTyr peptides, which are the lower abundant (<1%) than pSer (90%) and pThr (10%) in most eukaryote cells.

After the initial tests, the material was employed to enrich the standard phosphopeptides from tryptic digests of casein and bovine serum albumin (BSA). The samples were analyzed by MALDI MS (Fig. 38). The MIP sample processing protocol reduced the complexity of the MALDI mass spectrum, i.e. less ionic signals were observed compared to the control sample.

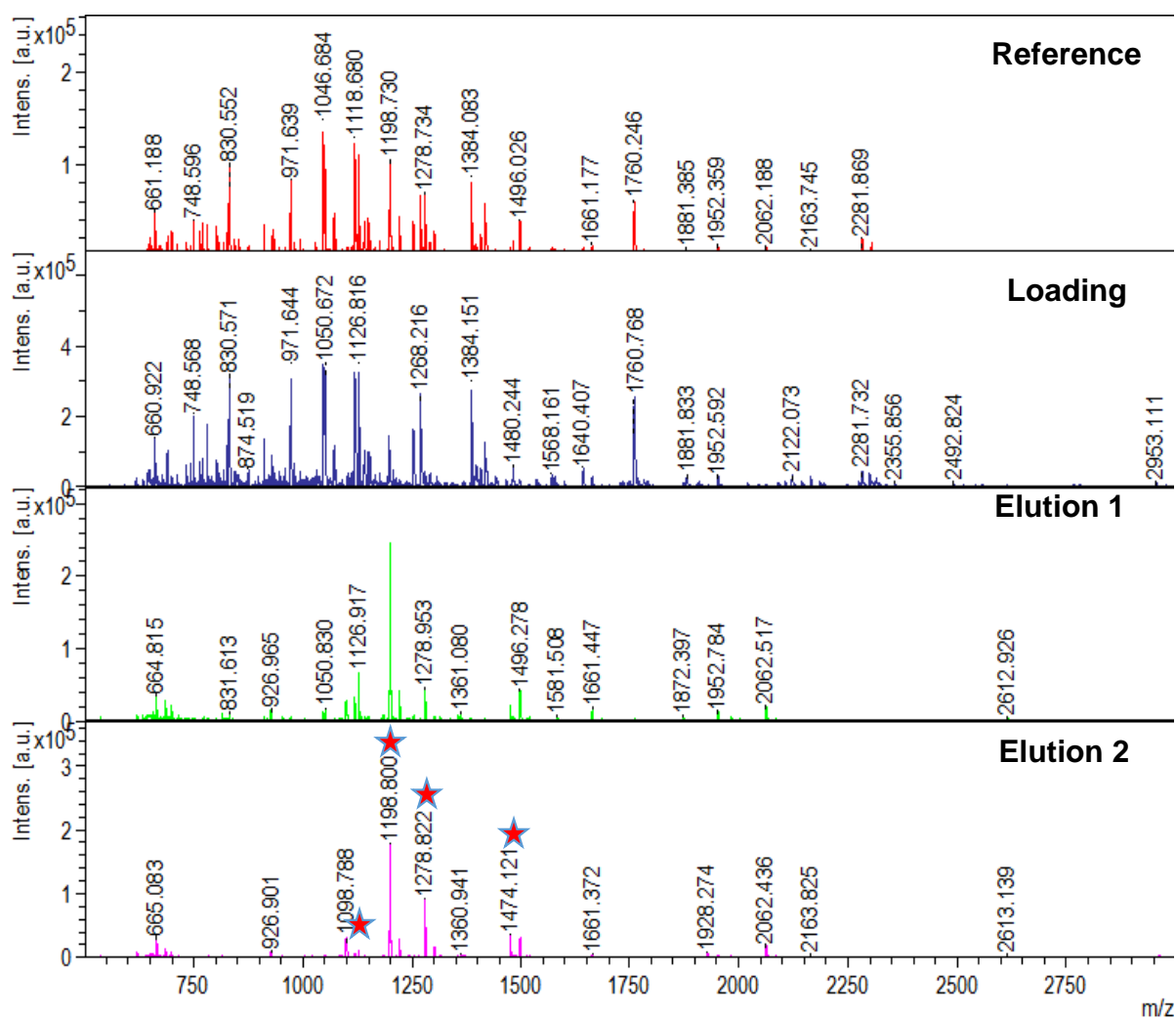


Figure 38 MALDI MS spectrum of each fraction from the enrichment of standard phosphopeptides from a mixture of casein and BSA digests; the reference is a tryptic digest of casein and BSA spiked with the 8 standard phosphopeptides. Stars label pTyr peptides

In Fig. 38 it is possible to evaluate the efficiency of the enrichment: most non-phosphorylated peptide signals are clearly visible in the reference and loading fraction, whereas the spectrum of the elution 2 fraction is very simplified, with the most intense signals belonging to pTyr peptides (signals marked with stars).

After the positive results obtained from the enrichment of pTyr phosphopeptides in BSA:casein, 100:1 digests (in Sweden), further experiments were planned (in Rome). In fact, in most of the works in which new phases are proposed for application to phosphopeptide

enrichment, the developed materials are tested on simulated mixtures, as the BSA:casein mixture, and results are monitored mainly by MALDI MS, directly without any separation. This approach, together with application on a real sample of small complexity, is the standard approach in method development for new materials. In most cases, MALDI MS is employed for enrichment testing; however, such an approach is limited for final real-world applications from very complex samples, such as tissue and cell extracts. Such samples need more high-throughput and comprehensive techniques for appropriate analysis, thus shotgun proteomics workflows based on HPLC separation coupled to tandem high resolution MS are needed. For this reason, further experiments were devised, in order to apply the composite to a yeast extract for phosphopeptide enrichment and comparison to commercial TiO₂ spin columns. Yeast was preferred over standard cell lines because it is cheap and readily commercially available, and it does not need any specific biological equipment for production, as opposed to the case of cell lines. At the same time, yeast is a complex matrix for which up to 3477 phosphoproteins were identified. This makes yeast extracts a convenient matrix to better test the enrichment efficiency of new materials for phosphoproteomics applications.

A tryptic yeast digest was then prepared as follows. One g of yeast from *Saccharomyces cerevisiae* (Type II) (YSC2 Sigma-Aldrich) was dissolved in 4 mL of milliQ water and rehydrated overnight at 30 °C (for reactivation). Then the yeast was centrifuged at 8000 × g for 10 min at room temperature, and the supernatant was discarded. 300 mg of glass beads, acid-washed and 200 mg of the yeast was added with 1 mL of cold lysis buffer (8 mol L⁻¹ urea in 50 mmol L⁻¹ Tris-HCl, pH 8, added with MS SAFE protease and inhibitor cocktail) (Sigma-Aldrich)), used according to the manufacturer's instructions. 10 cycles of mechanical agitation and freezing for one minute each were performed. Then samples were centrifuged at 9400 × g at 4 °C for 10 min to sediment cell debris, and finally transferred into a new tube. Protein concentration was determined by the Bradford assay. For digestion, 1 mg of protein was diluted to 1 µg µL⁻¹ with 8 mol L⁻¹ urea in Tris- HCl buffer and then treated with 200 mmol L⁻¹ dithiothreitol (DTT) in Tris-HCl buffer and 200 mmol L⁻¹ iodoacetamide (IAA) in Tris-HCl as described for BSA and casein samples. Digestion was performed with Trypsin/Lys-C Mix (enzyme to protein ratio, 1:25), allowing Lys-C digestion for 4 h at 37 °C and then diluting the urea concentration to 1 mol L⁻¹ for tryptic overnight digestion. Digestion was terminated with TFA, and then samples were desalted and dried.

Table 10. Percentage of enrichment for different experiments ^a Enrichment (%) = [phosphopeptides/total peptides × 100] ^bthe protocol included and additional washing step with H₂O with 0.1% (v/v) TFA (experiment D)

		Total peptides	phosphopeptides	E ^a %
A	1mg MIP 1mg of digest	3915	102	2.60
B	5mg MIP 1mg of digest	2152	4	0.18
C	commercial spin column	849	239	28.15
D	1mg MIP 1mg of digest ^b	2341	78	3.33

The results were not as good as expected from the preliminary tests. The complex mixture showed an unexpected situation. Despite the optimization of the amount of MIP material used for enrichment (several tests have been carried out with 1 mg and 5 mg of material), the selectivity was only modest and several non-phosphorylated peptides were eluted. A wash with H₂O 0.1% (v/v) TFA, performed before elution (experiment D), was also added to eliminate peptides bound by unspecific interactions, but only a small but not substantial improvement was obtained. The problem was attributed to the external silica shell, which allows the non-specific adsorption of peptides; if the hypothesis proves true, then the selectivity can be improved only by changing the design of the material, which should be modified to eliminate the silica shell or replace it with a titanium dioxide shell (work in progress).

Table 11: percentage of phosphopeptide enrichment compared to the total number of identified peptides. ^bthe protocol included and additional washing step with H₂O with 0.1% (v/v) TFA (experiment D)

	PERCENTAGE ENRICHMENT COMPARED TO PHOSPHOPEPTIDES

	pSer	pTyr	pThr
Commercial Spin column	78%	2%	19%
1mg MIP 1mg of digest (b)	72%	3%	25%
1mg MIP 1mg of digest	69%	2%	29%

We concluded that the MIP material alone did not have sufficient capacity and specificity to allow the enrichment of phosphopeptides from very complex peptide mixtures, such as those derived from yeast. Table X shows these results, which are reported as the absolute enrichment percentage for each type of phosphorylation both by the MIP material and a reference material; the abundance of pTyr was comparable with that of titanium dioxide, but the selectivity was low. After suitable modification of the MIP material, we hypothesize that the combination of enrichment by MIP and TiO₂ could provide the capacity, specificity and selectivity for pTyr peptide enrichment in phosphoproteomic experiments (ongoing experiment). This idea is reinforced by the type of interactions that the MIP material establishes with the pTyr phosphopeptides, which include hydrogen bonds, this does not show great selectivity but probably the combination of the two cleaning systems can be very promising.

Appendix 1

1.1 Liquid chromatography

Techniques based on liquid chromatography (LC) are the most suitable for the separation of analytes because it is possible to exploit differences between substances, such as differences in hydrophobicity and charge. LC is the most used technique in all research laboratories. The operating principle of LC is based on the different interaction of the molecules with the stationary phase and the mobile phase. The analytes move through the chromatographic column with a certain mobile phase flow. The column has a stationary phase inside, consisting of polymerized monoliths, or particles with functional groups. If the interaction with the stationary phase is greater than the mobile phase, the compound will be more retained, this translates into a longer retention time; if the compound has no interaction with the stationary phase it will be eluted with the mobile phase. Thus, distinct physical-chemical molecules can be separated in a timely manner by sequential elution from the column. The principles of chromatographic separation are different, based on different interactions (distribution, ion exchange, adsorption, molecular exclusion, affinity or chiral interaction).

Reversed phase (RP) is the most exploited LC mode used in combination with MS due to the compatibility of the volatile components with mass spectrometry. The columns are usually packed with silica microspheres functionalized with hydrophobic C18 alkyl chains. In the RP mode, the elution is based on hydrophobicity and is obtained by increasing the concentrations of the organic modifier (for example ACN) in the mobile phase.

The disadvantages of conventional LC, although very popular for different applications are a massive use of solvents, large amount of sample to be analyzed, and the low sensitivity of detection techniques due to sample dilution in mobile phase. These drawbacks can be solved by chromatographic columns packed with particles of smaller dimensions with a reduced

internal diameter. This mode is known as UHPLC, and has allowed to obtain numerous advantages over conventional HPLC, such as: lower consumption of the sample; lower volumes of the mobile phase, which does not only comply with the principles of the green chemistry, but also reduces sample dilution therefore increasing the overall method sensitivity; greater thermostating capacity, which allows maintaining a constant temperature throughout the column; greater efficiency due to a greater number of theoretical plates and therefore reduction of the peak width; greater permeability obtained with the use of smaller particles. Furthermore, UHPLC chromatography also simplifies the interface of the chromatographic system with the mass spectrometer. The development of UHPLC has greatly modified the classic HPLC instrumentation. The most important change is the construction of systems capable of managing the increase in pressure. The new UHPLC instruments can operate at pressures of 1500 bar, compared to around 200 bar for traditional HPLC. To reduce peak enlargement, it is important to reduce dead volume sites in the system. Even the electronics have been updated to allow a more rapid data collection as the peak widths can be up to 10 times lower than those of traditional HPLC systems, thus requiring a much faster data collection interface.[118,119]

1.2 Ionization source

In the field of peptidomics and small molecule research, two ionization methods are mainly applied because they are "soft ionization" techniques: electrospray ionization (ESI) and matrix-assisted laser desorption/ionization (MALDI). In this thesis work both ionization techniques were used, the ESI source for all the research carried out, the MALDI source was instead used in the period in Sweden, to be able to do fast screening analysis.

1.2.1 ESI

Today there are many ionization sources available, but ESI ionization remains the most used because it allows the ionization of a wider range of molecules. Fig. 39 shows the general scheme of operation.

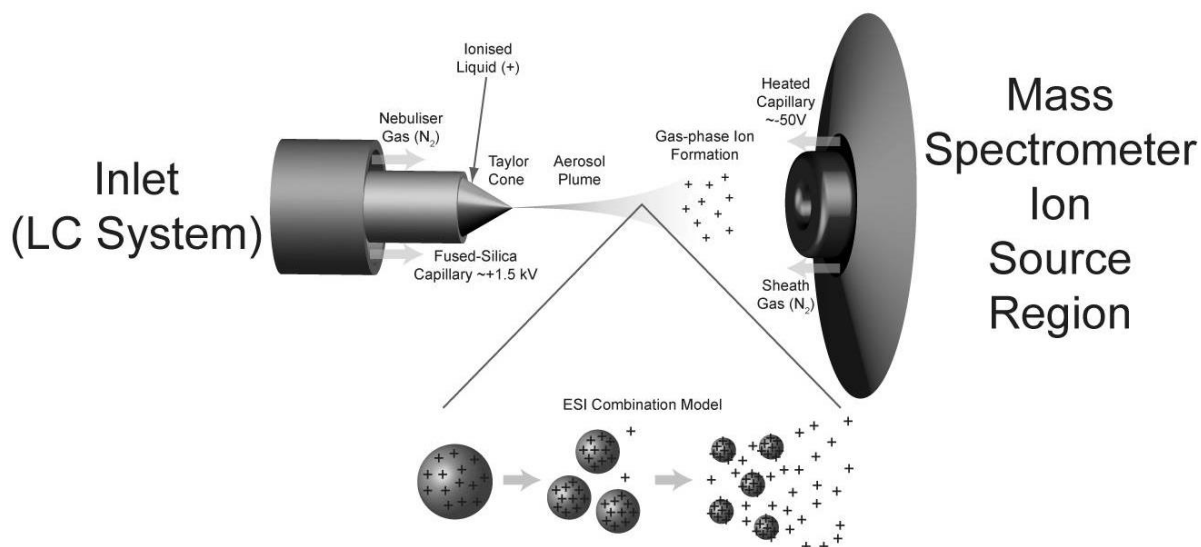


Figure 39. ESI ionization process [120]

ESI ionization is in the liquid phase, it occurs in the solution itself, this represents an advantage because it allows the coupling of liquid chromatography and mass spectrometry. Chromatographic separation is essential to avoid ionic suppression, because when many analytes reach the source at the same time, only the most hydrophobic molecules are ionized.

In the initial phase of the ionization process, the analyte solution passes into a thin conductive capillary to which a voltage of a few kV is applied. The influence of the electric field on the liquid on the tip of the capillary in combination with the surface tension causes the formation of a Taylor cone. Once the electric field is higher than the surface tension, the Taylor cone emits a solvent jet. The jet tip is inherently unstable and collapses into charged droplets. The solvent evaporates from these droplets until the charge density on the surface of the droplets reaches the Rayleigh limit. Once this limit is exceeded, the coulombic repulsion force is greater than the surface tension which causes the droplet to undergo fission in smaller droplets, the so-called coulomb explosion. These highly charged droplets will continue to lose solvent and when the electric field on their surface becomes large enough, desorption of ions from the surface occurs. Since ESI is a soft ionization source, the gaseous ions formed are generally protonated or deprotonated molecules depending on the selected ionization polarization mode [121]. Once ionized, the compounds can be separated based on their m/z ratios in the mass analyzer.

1.2.2 MALDI

The MALDI source produces ions from a solid layer [122]. Before the ionization in the gaseous phase, the analyte must be incorporated in a matrix that absorbs UV rays. The ionization process takes place at the expense of a laser that strikes the matrix, energy is mostly absorbed by the π electrons of the matrix molecules (commonly small aromatic acids) which leads to the desorption of the matrix in combination with the nested analyte molecules in a "soft" phase transfer of solid gas. There is no decomposition of the molecules in the gas phase, since they cool and expand in the vacuum. For this reason, MALDI is suitable for analyzing large molecules or intact proteins. MALDI is commonly used to analyze low complexity samples, in this thesis work it was used in Sweden, to be able to quickly monitor the phosphopeptide binding on the synthesized selective materials.

1.3 Mass analyzers

Mass spectrometry is a highly sensitive detection technique and, when used as a detector, it offers advantages over traditionally used detectors. The greater sensitivity allows the detection of trace compounds, moreover the possibility to determine the mass of the analytes, and their fragmentation model, provides the unequivocal identification of the compounds of interest.

The fundamental role of mass spectrometers is to determine the mass, charge (m/z) ratio of the ions. A mass spectrometer is thus always composed of three main components:

- An ion source to charge the analyte molecules
- The mass analyzer, in which the ions are separated based on their mass-charge ratio (m/z)
- The detector, where the abundance of each m/z value is recorded.

The process that occurs in a mass spectrometer includes three phases (Fig. 40)

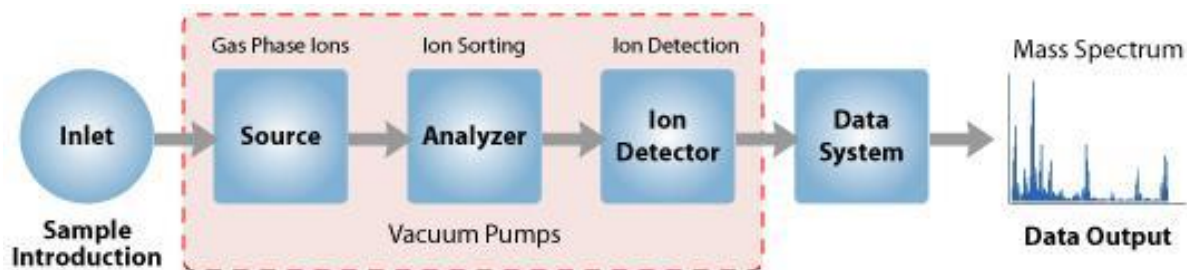


Figure 40 Basic scheme of a mass spectrometer [123]

The analytes from in the ion source are then accelerated by an electric field and separated in the analyzer according to their m/z ratio, and finally detected [124]. Several mass analyzers have been proposed throughout history; each of these shows advantages depending on the required analysis, in this thesis low resolution (triple quadrupole), high resolution mass spectrometers (hybrid Orbitrap systems, and time of flight (TOF)) were used.

1.3.1 Triple quadrupole

Quadrupole analyzers consist of four parallel cylindrical bands that act as electrodes (Fig. 41).

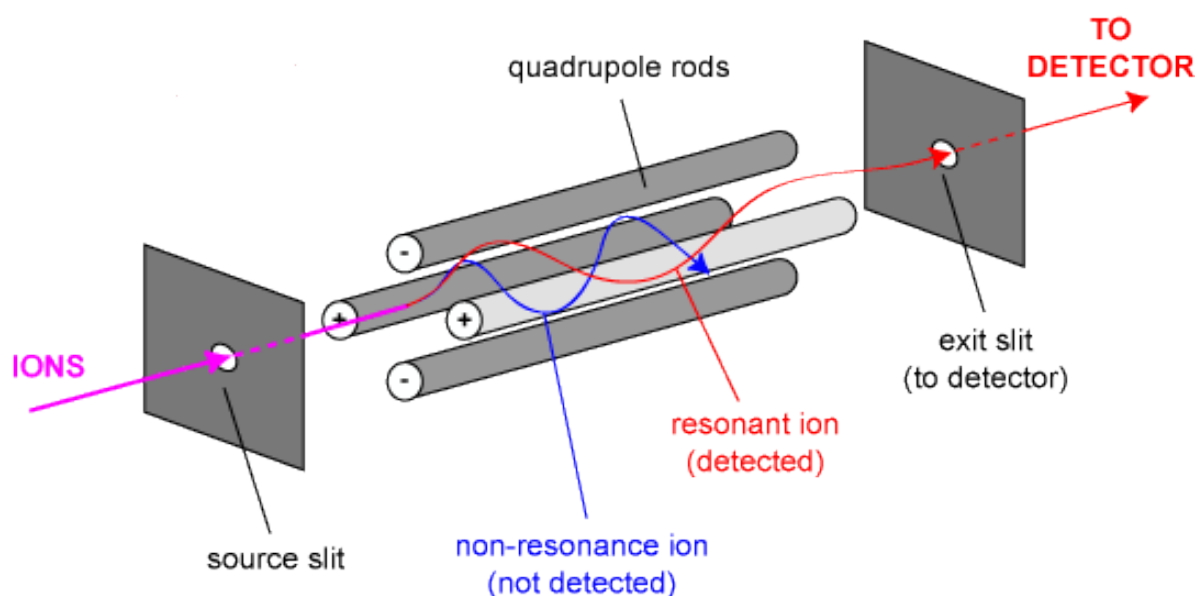


Figure 41 Diagram of a quadrupole

A variable radiofrequency is applied to each pair of bars while a direct current is instead applied to the four bars. Ions are subject to a total electric field consisting of a constant field and a quadrupolar alternative field. The analyzer uses the stability of the ion trajectories in oscillating electric fields to separate the ions based on the different m/z ratios. A positive ion will be attracted towards a negative field. By fixing the potentials of the direct current and those of the variable radiofrequency, only the ions with a specific m/z will be able to pass through the quadrupole without touching the rods and reaching the analyzer [124].

The quadrupole is a low resolution instrument, capable of distinguishing only ions that differ by a unit mass, but it is economical, compact and robust. The sensitivity of this analyzer when so many ions are monitored decreases significantly. When few ions are analyzed, instead, the sensitivity is increased; moreover in the configuration of 3 quadrupoles combined together (QqQ), with the use of MS/MS, the sensitivity increases considerably, also increasing the signal to noise ratio.

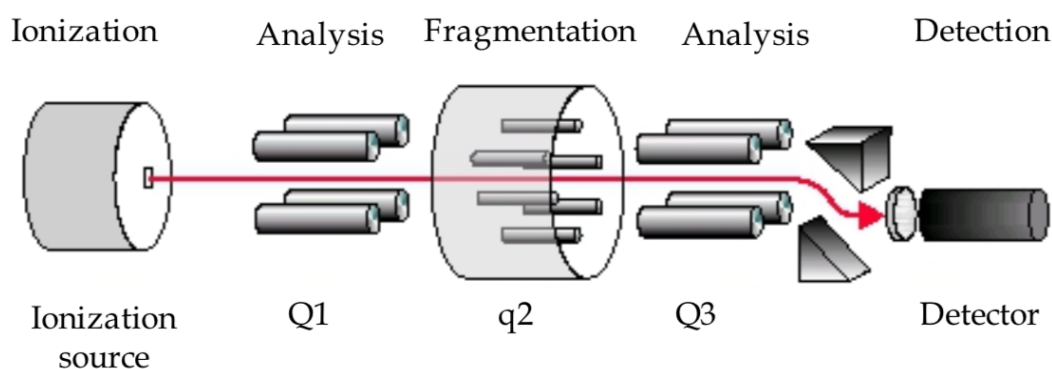


Figure 42 QqQ mass spectrometer

In Fig. 42 the general scheme of the QqQ system is shown, formed by three quadrupoles in series, where two quadrupoles act as analyzers, the second in the center, acts as a collision cell for ion fragmentation. The operation is very simple: the first quadrupole selects a specific ion (precursor ion), this ion is fragmented in the second quadrupole by collision with inert gases, such as He, N₂ or Ar, the fragments generated (product ions) are detected in the third quadrupole, generating a MS/MS spectrum. The main advantage of the MS/MS experiments is the increase in sensitivity, making QqQ, the analyzer of choice for quantitative analysis.

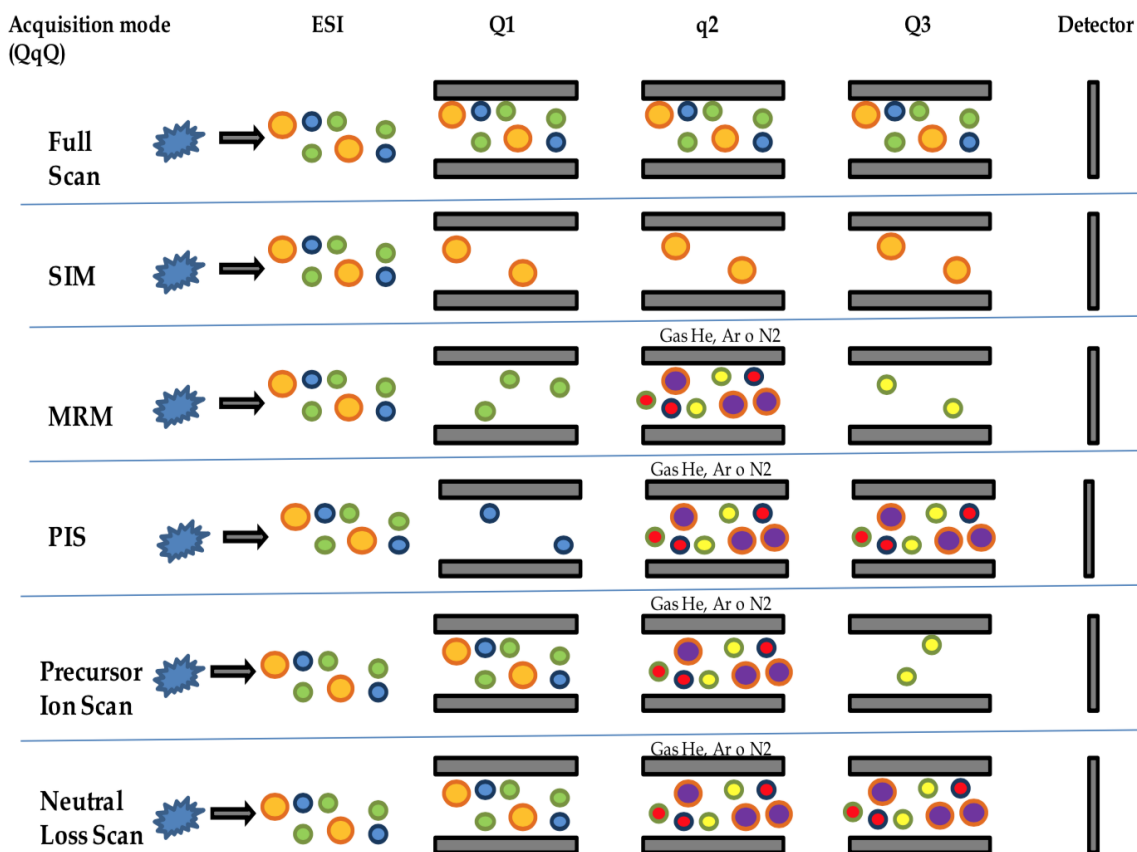


Figure 43 Acquisition modes of a QqQ instrument

The QqQ analyzer offers great versatility in the acquisition modes, as shown in Fig. 43:

- full scan: full scan allows to scan a whole range of m/z values
- Single Ion Monitoring (SIM): this mode allows to select a specific m/z in the first analyzer, which is followed up to the third analyzer; the absence of scanning allows concentrating on the precursor for longer times, obtaining a better sensitivity than the acquisition in full scan.
- Selected Reaction Monitoring (SRM) or Multiple Reaction Monitoring (MRM): select a specific fragmentation reaction. In the first analyzer an ion with a specific m/z will be selected, this is fragmented in the collision cell, only specific fragments will be selected and detected in the third quadrupole. The ions selected in the first analyzer will be detected only if they produce a certain pattern of fragmentation. The absence of scanning allows not only to increase the sensitivity but in this case also selectivity.

- The Product Ion Scan (PIS): this mode selects a product ion and determines the precursor ions. All precursor ions that produce ions with the selected mass by fragmentation are then detected.
- Neutral loss: in this mode a neutral loss (a) is monitored by detecting all the precursors (m) that undergo that neutral loss. In the third quadrupole all the ions with a loss (m-a) will be detected, in this case the first and third quadrupoles are scanned.

The described scanning methods have different characteristics, usable for different purposes depending on the analysis performed. Acquisition in MRM mode is the most used in quantitative analysis, to determine compounds while minimizing the presence of interferences. Furthermore, the robustness of the instrument and the selectivity of this mode make it possible to carry out reproducible analyzes over time

1.3.2 Orbitrap

The Orbitrap mass analyzer consists of an external barrel-shaped electrode and an internal spindle-shaped electrode. The electric field created by both electrodes traps the ions inside the analyzer. The ions oscillate between both electrodes in the three axes. The oscillation around the z axis (Fig. 44) depends on the m/z value of the ion and is recorded as the current of the image. The image current is then transformed into a mass spectrum by the Fourier transform.

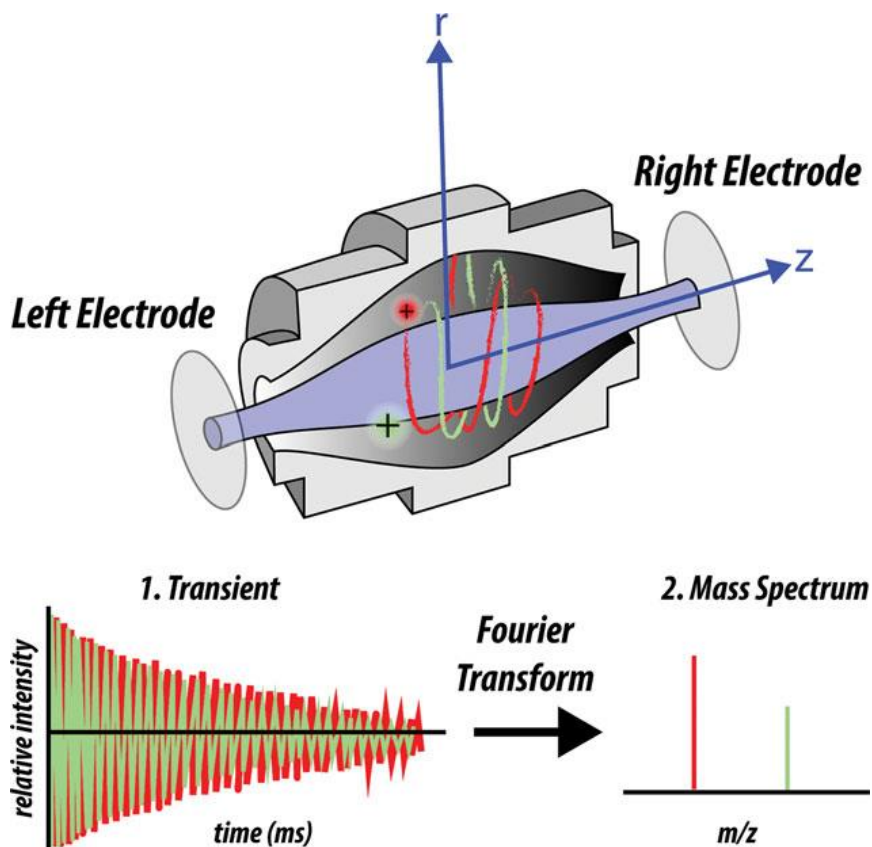


Figure 44 Scheme of Orbitrap analyzer FT mass analyzer [125]

The first Orbitrap instrument was marketed by Thermo Scientific in 2005. Orbitrap instruments are always hybrid mass spectrometers because they have at least one trap, in addition to the Orbitrap itself. The key to the tools (and the most challenging step in the practical implementation of the Orbitrap analyzer) is the external storage device, called the C-trap. The C-trap allows the accumulation of ions, before the injection in the Orbitrap and allows to interface continuous ion sources (such as ESI) with a discontinuous analyzer. In this thesis work different Orbitrap analyzers were used, which are discussed in detail below.

1.3.2.1 LTQ-Orbitrap XL

LTQ Orbitrap, is the first instrument of the Orbitrap family; the high-resolution, accurate mass (HR/AM) detection provided by the Orbitrap, is coupled to a linear ion trap capable of isolating the precursors and fragmenting them. It is precisely the trap that provided speed and sensitivity, indispensable for complete scanning and peptide MS/MS detection. The trap also

allows to isolate the precursor at different levels of MSⁿ fragmentation, by dissociation induced by the collision cell (CID). In Fig. 45 the scheme of the instrument is reported.

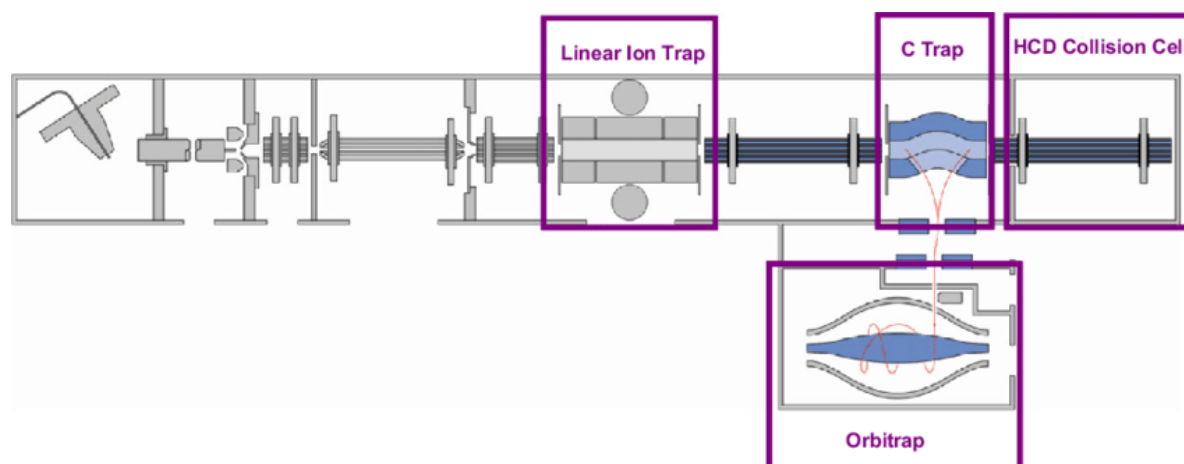


Figure 45 Ion trap/Orbitrap hybrid mass spectrometer architecture

The main advantage of HR/AM systems is to allow the determination of the mass and state of charge of the multiple-charged species; the accurate detection allows a better search in the databases [126].

The LTQ Orbitrap for the detection of the nominal mass can reach a scan rate of 4-5 Hz in MS/MS, while for the accurate mass at 3 Hz in MS/MS. This makes the LTQ Orbitrap a great tool since its introduction. The automatic gain control (AGC) has improved the quantitative phase, through a short pre-scan in the linear trap, which has the objective of always collecting a sufficient quantity of ions to be further analyzed in the successive phases. To further improve sensitivity, a better C-trap has been introduced for LTQ Orbitrap XL: the inserted C-Trap has, in fact, a much higher transmission of ions, leaving the same architecture of the instrument.

1.3.2.2 Orbital Velos and Elite

In 2009 LTQ Orbitrap Velos was introduced, although LTQ Orbitrap XL offers great results, the analysis of really complex matrices requires much more sensitivity and speed. In the LTQ Orbitrap Velos this was achieved through the objective S (S-lens), which replaced the capillary interface and allowed for greater sensitivity (even 10 times in MS/MS mode). Velos has a dual-pressure linear trap analyzer, a high-pressure cell isolates and fragments the ions, a low-pressure cell analyzes the accelerated ions. This configuration allows faster acquisition without affecting the quality of the spectra [127].

A high-energy collisional dissociation cell (HCD) was also inserted, allowing fragmentation in HCD. In 2011 a new geometry for Orbitrap was developed, designed to acquire spectra in less time. The new instrument called Orbitrap Elite, exploited the good enhancement made in the Velos, and added some improvements to the ionic optics, the electrodes and the amplifier. The outline of this tool is provided in Fig. 46

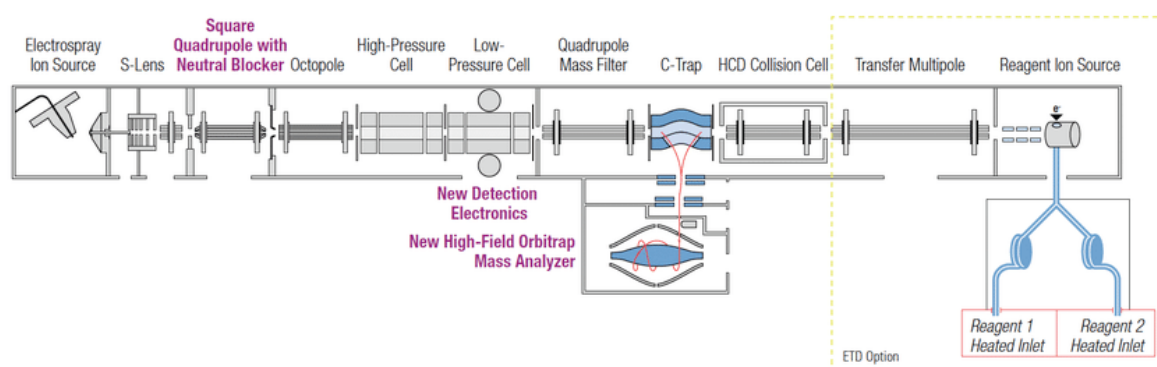


Figure 46 Schematic representation of Orbitrap Elite

In comparison with the first commercial version of Orbitrap, the acquisition frequency was doubled with the Elite [128]. In experiments where the resolution and the number of acquired MS/MS spectra is important, the possibility of performing data-dependent MS/MS analyzes was created. The Orbitrap analyzer acquires high-resolution full scan spectra while MS/MS spectra are acquired in the ion trap, thus reducing acquisition cycles. This tool is now the benchmark in the proteomics market.

1.3.2.3 Q Exactive Orbitrap.

In 2011 the tandem mass spectrometer, Q Exactive, was introduced, which extended the scope of the Orbitrap-based MS for routine analysis in proteomics together with metabolism, food and safety analysis. The Q Exactive mass spectrometer is equipped with an ESI source and includes, a superimposed ring ion guide (objective S) in the source region, a quadrupole mass filter, a C trap, a high energy collisional dissociation (HCD) cell and an Orbitrap mass analyzer, as shown in Fig.47

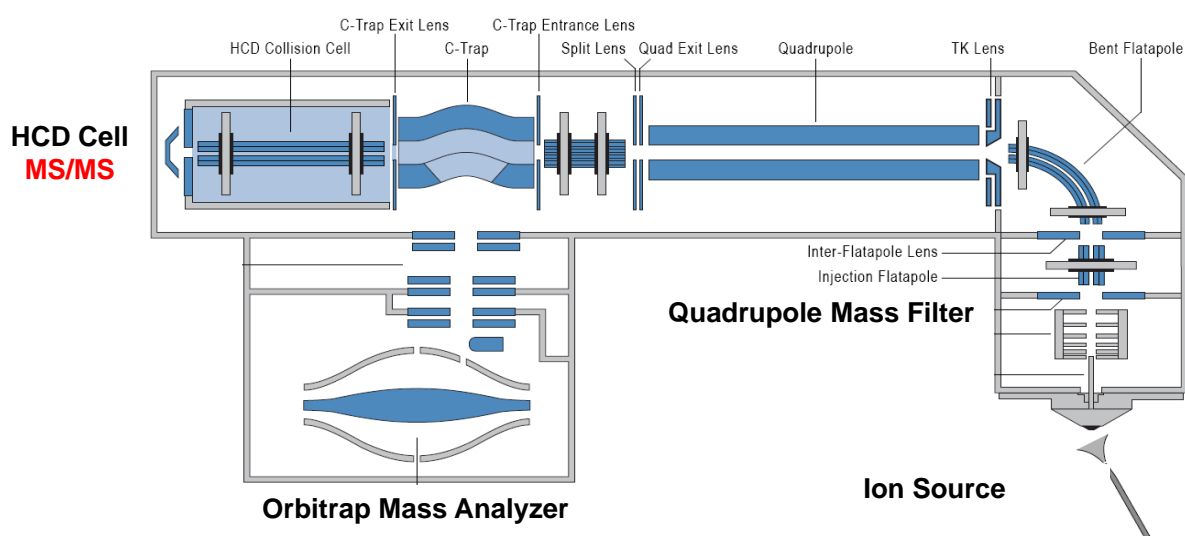


Figure 47 Schematic representation of Orbitrap Q-Exactive

In the Q-Exactive Orbitrap, in addition to the C-trap, the HCD cell, and CID already seen in the previous instruments, there is a hyperbolic quadrupole with the ionic optics through a combination of direct current, radiofrequency voltage and a driving vacuum gradient ions. This is able to isolate the ions up to an isolation width of 0.4 Th at m/z 400.

What differentiates this instrument from the previous ones is the quadrupole. The quadrupole and the Orbitrap are two independent MS detectors. The quadrupole has the function of isolating the ions and sending them to the Orbitrap to be analyzed. However, after the isolation process, the ions can be expelled and analyzed by the Orbitrap or subjected to fragmentation to produce product ions and then expelled and analyzed again by Orbitrap (this allows to analyze both product ions and high resolution fragment ions).

Due to the characteristics of this hybrid mass spectrometer, different acquisition modes are available, such as Full Scan, SIM, Product ion, Neutral Loss, etc. However, two acquisition modes in particular make the difference compared to other tools:

- Data dependent acquisition (DDA): this is the most used mode, initially the instrument performs a complete scan to detect all the ions coming from the source. In the following scan, the most abundant ions (5-20 ions) are selected from the quadrupole, fragmented by the collision cell, and analyzed by the Orbitrap. In order to avoid the resampling of the previously selected precursors, a dynamic exclusion list is used. Furthermore, it is possible to use an inclusion list, which forces the instrument to select a desired peak for fragmentation, regardless of its abundance, to ensure identification, this forcing is done above all for species that are not very abundant; for example, this modality in this thesis work was used for the identification of short peptides.
- Data independent acquisition (DIA) or all ion fragmentation (AIF) has been introduced in recent years. In this case, no selection of precursors is performed, but all the precursors present of a distinct mass window are fragmented.

For target analysis, it is possible to use the MRM mode, the limit of this mode is the optimization of the fragmentation of the compounds before the analysis. DDA has the limit of a stochastic selection of precursors for the fragmentation, compromising the reproducibility (mainly of less abundant ions). This is why the use of DIA is constantly increasing.

The Q-Exactive also is equipped with two collision cells, CID and HCD, and has the possibility of fragmenting in a different way, a very useful precaution for particular classes of molecules [129].

1.3.3 Time of flight (TOF)

The TOF mass analyzer is usually associated with the MALDI source. The ions are accelerated by an electric field and subsequently separated along the flight tube due to different speeds. Ions with a lower m/z have a higher speed, and therefore reach the detector faster than ions with a higher m/z value. The mass range that can be analyzed with TOF, makes it a superior instrument, particularly for soft ionization techniques and for the analysis of whole proteins. Furthermore, another advantage is the transmission efficiency which leads to greater

sensitivity. The disadvantage of the first TOF instruments was the low mass resolution; since ions with the same m/z run the same flight time, one way to improve mass resolution is to use an electrostatic reflector (reflectron). The reflectron corrects the dispersion of kinetic energy of the ions with the same m/z leaving the source. Ions with more kinetic energy and therefore more velocities will penetrate more deeply into the reflectron than the ions with lower kinetic energy. As a result, the fastest ions will spend more time in the reflectron and reach the detector simultaneously than the slower ions with the same m/z [124].

The tool used in this thesis work is a MALDI TOF/TOF, where the ions are desorbed from the microplate and accelerated in the first TOF; within this, collision-induced metastable ions continue to travel with the velocity of the molecular ions from which they are derived. The first TOF ends with a selector. In the second TOF (called LIFT™) only the analytes of the selected mass and the derived fragments can pass, all other ions are rejected. In the second TOF the parent ions and selected fragments are accelerated. Subsequently, these analyte ions are separated in the second TOF (conventional analyzer). This allows a mass analysis of the fragments to be carried out by measuring their arrival time on the detector. The reflectron in the second TOF analyzer is used to improve the resolution of the mass spectrum of the fragments [130]. In Fig. 48 the scheme of the instrumentation.

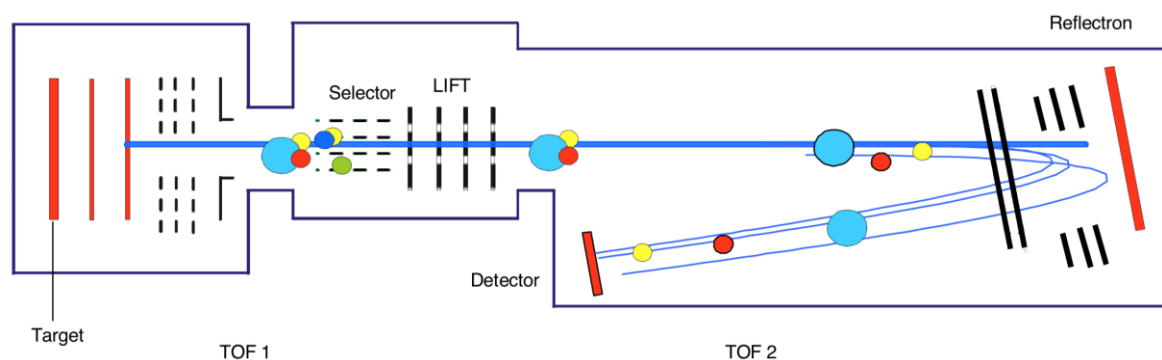


Figure 48 MALDI TOF/TOF instrumentation

Conclusions

During my three-year doctorate I studied bioactive molecules, for valorization of food or waste products. In paper I and paper II, a peptidomic study was performed with determination of bioactive sequences. Bioactive peptides were produced by simulated digestion with alcalase, as this enzyme was low cost compared to trypsin and large-scale implementation is possible. In paper I, bioactive peptides were identified from cauliflower waste, the hydrolyzate obtained from cauliflower waste was fractionated by preparative RP-HPLC in 12 fractions; therefore, each fraction were analyzed for the ABTS and DPPH assay and the ACE inhibitor activity. In particular, compared to trypsin, the use of alcalase improved the antioxidant activity of the hydrolysates maintaining the ACE inhibitor activity. After the bioactivity tests on the 12 fractions, the two most active fractions of each assay were selected and identified using the shotgun peptidomics. PeptideRanker was subsequently used to attribute a possible bioactivity to each peptide and the most likely peptides were synthesized and tested for individual bioactivity. For ACE inhibitor activity, two peptides were synthesized, APYDPDWYYIR and SKGFTSPLF, which provided an EC₅₀ value of 2.59 $\mu\text{mol L}^{-1}$ and 15.26 $\mu\text{mol L}^{-1}$, respectively. For the radical scavenger activity of the ABTS radicals, SKGFTSPLF and LDDPVFRPL were tested and provided an EC₅₀ of 10.35 $\mu\text{mol L}^{-1}$ and 8.29 $\mu\text{mol L}^{-1}$, respectively. For the scavenging activity of the DPPH radicals, SKGFTSPLF and LRAPPGWGR were tested and provided an EC₅₀ of 8.2 $\mu\text{mol L}^{-1}$ and 5.26 $\mu\text{mol L}^{-1}$, respectively.

In paper II, for the first time the antioxidant and ACE inhibitory activity of peptides derived from *Tetrademus obliquus* was reported; the extraction process was first optimized, then the extract was digested, and subjected to purification by 2D LC RP and identification by nanoLC-MS / MS RP. Approximately 500 potential bioactive peptides have been identified. The use of a bioinformatic analysis, which allowed to assign a bioactivity score using an algorithm, allowed to limit the list of potential candidates for chemical synthesis to a number

of 25 amino acid sequences. Of these, four peptides were synthesized and analyzed in vitro. Two new antioxidant and two new ACE inhibitory peptides (WPRGYFL, GPDRPKFLGPF, WYGPDRPKFL, SDWDRF) were then extracted, purified and identified. In papers III and IV, short peptides have been identified; this represents a great analytical novelty, because these peptides are usually lost during the purification of the sample, but they are very important, because they have many biological activities. As far as we know, paper IV is the first work done on short endogenous peptides in cow milk samples. Specifically, UHPLC separation was performed using two different columns, C18 and PGC, which work with a different retention and selectivity mechanism. A suspect screening approach for MS/MS spectra acquisition was used and peptide identification was achieved by matching the experimental fragmentation spectra with those generated in silico. A total of 57 and 41 peptides were identified and validated from the separation on C18 and PGC columns, respectively, with 26 peptides common to both separation strategies. Although C18 provided a greater number of identified peptides, PGC allowed the identification of more hydrophilic peptides, providing complementary information. This combined approach allowed the analysis of a wide range of peptides. Furthermore these peptides are bioactive, so their study is very important to understand the bioactivity of milk and exploit it to prepare ingredients in functional foods and pharmaceutical preparations.

papers V, VI, and VII aimed to identify the seleno-amino acids present in olive oil (papers V and VI) and in wheat bran (paper VII). In paper V a chromatographic separation is described, which allows the complete enantioresolution of three seleno-amino acids using a very polar aqueous mobile phase in less than 15 minutes on a 5 cm long CHIROBIOTIC TAG column. This is the first work that can solve the seleno-cystine stereoisomers, which had never been separated before. To avoid any sample preparation, a direct preconcentration of the target seleno-aminoacids was obtained on the CHIROBIOTIC TAG pre-column under normal phase conditions; the method was validated and allowed to quantify the seleno-amino acids in soybean, sunflower and fish oils, but not in olive oil. In paper VI an enrichment method was optimized for the determination of seleno-amino acids in olive oil. The commercial Oasis MCX cartridge was used for method optimization, for the maximum recovery of seleno-amino acids. Only seleno-methionine was identified in olive oil. Though no D-forms or meso-forms were detected in the analyzed samples, still the developed methods with enantioresolution could be useful for other matrices, where racemization of seleno-amino acids can occur. For this reason

seleno-amino acids were investigated in another matrix, wheat bran, either directly or after protein digestion. The main purpose of paper VII was the development of a method capable of simultaneously extracting both free and conjugated seleno-amino acids. Four protocols were tested and compared based on the quantification of the extracted seleno-amino acids. In this case, stereoisomers different from the common L-forms were identified. The last chapter of this thesis concerns my doctoral period abroad; the objective was to study and synthesize new materials for the selective enrichment of bioactive molecules, specifically a new material was synthesized for the enrichment of phosphopeptides. This part is still work in progress.

Outlooks

During my thesis I faced real problems, I solved analytical challenges, problems in the detection and identification of bioactive compounds. In the future, this goal will continue more and more. My interest will be always focus on compounds that are difficult to detect with common pre-concentration techniques. In particular, after an analytical optimization of enrichment technique for short bioactive peptides in milk samples, applications to biological fluids will be carried out, since short peptides can be considered potential biomarkers in diagnostic field. For this reason, during my time abroad, I have acquired an in-depth understanding of molecularly imprinted polymers for enrichment of PTMs, which can also considered potential biomarkers in clinical application. Further, all my knowledge will be useful for peptidomic and proteomic clinical studies.

Bibliography

- [1] T.M. Gibson, L.M. Ferrucci, J.A. Tangrea, A. Schatzkin, Epidemiological and Clinical Studies of Nutrition, *Semin. Oncol.* 37 (2010) 282–296. doi:10.1053/j.seminoncol.2010.05.011.
- [2] L. Di Renzo, C. Colica, A. Carraro, B. Cenci Goga, L.T. Marsella, R. Botta, M.L. Colombo, S. Gratteri, T.F.M. Chang, M. Droli, F. Sarlo, A. De Lorenzo, Food safety and nutritional quality for the prevention of non communicable diseases: the Nutrient, hazard Analysis and Critical Control Point process (NACCP), *J. Transl. Med.* 13 (2015) 128. doi:10.1186/s12967-015-0484-2.
- [3] A. Cifuentes, Foodomics, John Wiley & Sons, Inc., Hoboken, NJ, USA, 2013. doi:10.1002/9781118537282.
- [4] J. Azmir, I.S.M. Zaidul, M.M. Rahman, K.M. Sharif, A. Mohamed, F. Sahena, M.H.A. Jahurul, K. Ghafoor, N.A.N. Norulaini, A.K.M. Omar, Techniques for extraction of bioactive compounds from plant materials: A review, *J. Food Eng.* 117 (2013) 426–436. doi:10.1016/j.jfoodeng.2013.01.014.
- [5] A. Nzihou, *Toward the Valorization of Waste and Biomass, Waste and Biomass Valorization.* 1 (2010) 3–7. doi:10.1007/s12649-010-9014-x.
- [6] R.E.C. Wildman, R. Wildman, T.C. Wallace, eds., *Handbook of Nutraceuticals and Functional Foods*, CRC Press, 2016. doi:10.1201/9781420006186.
- [7] T. Shibamoto, K. Kanazawa, F. Shahidi, C.-T. Ho, *Functional Food and Health: An Overview*, in: 2008: pp. 1–6. doi:10.1021/bk-2008-0993.ch001.
- [8] D.Z. do Prado, B.L. Capoville, C.H.O. Delgado, J.C.A. Heliodoro, M.R. Pivetta, M.S. Pereira, M.R. Zanutto, P.K. Novelli, V.C.B. Francisco, L.F. Fleuri, *Nutraceutical Food: Composition, Biosynthesis, Therapeutic Properties, and*

Applications, in: *Altern. Replace. Foods*, Elsevier, 2018: pp. 95–140. doi:10.1016/B978-0-12-811446-9.00004-6.

[9] D. Agyei, C.M. Ongkudon, C.Y. Wei, A.S. Chan, M.K. Danquah, Bioprocess challenges to the isolation and purification of bioactive peptides, *Food Bioprod. Process.* 98 (2016) 244–256. doi:10.1016/j.fbp.2016.02.003.

[10] N.R.A. Halim, H.M. Yusof, N.M. Sarbon, Functional and bioactive properties of fish protein hydrolysates and peptides: A comprehensive review, *Trends Food Sci. Technol.* 51 (2016) 24–33. doi:10.1016/j.tifs.2016.02.007.

[11] M. Kussmann, A. Panchaud, M. Affolter, Proteomics in Nutrition: Status Quo and Outlook for Biomarkers and Bioactives, *J. Proteome Res.* 9 (2010) 4876–4887. doi:10.1021/pr1004339.

[12] C. Daskaya-Dikmen, A. Yucetepe, F. Karbancioglu-Guler, H. Daskaya, B. Ozcelik, Angiotensin-I-Converting Enzyme (ACE)-Inhibitory Peptides from Plants, *Nutrients.* 9 (2017) 316. doi:10.3390/nu9040316.

[13] C.G. Rizzello, D. Tagliazucchi, E. Babini, G. Sefora Rutella, D.L. Taneyo Saa, A. Gianotti, Bioactive peptides from vegetable food matrices: Research trends and novel biotechnologies for synthesis and recovery, *J. Funct. Foods.* 27 (2016) 549–569. doi:10.1016/j.jff.2016.09.023.

[14] R. Zenezini Chiozzi, A.L. Capriotti, C. Cavaliere, G. La Barbera, S. Piovesana, R. Samperi, A. Laganà, Purification and identification of endogenous antioxidant and ACE-inhibitory peptides from donkey milk by multidimensional liquid chromatography and nanoHPLC-high resolution mass spectrometry, *Anal. Bioanal. Chem.* 408 (2016) 5657–5666. doi:10.1007/s00216-016-9672-z.

[15] A.L. Capriotti, C. Cavaliere, S. Piovesana, R. Samperi, A. Laganà, Recent trends in the analysis of bioactive peptides in milk and dairy products, *Anal. Bioanal. Chem.* 408 (2016) 2677–2685. doi:10.1007/s00216-016-9303-8.

[16] S. Piovesana, A.L. Capriotti, C. Cavaliere, G. La Barbera, R. Samperi, R. Zenezini Chiozzi, A. Laganà, Peptidome characterization and bioactivity analysis of donkey milk, *J. Proteomics.* 119 (2015) 21–29. doi:10.1016/j.jprot.2015.01.020.

[17] Z. Yu, Y. Yin, W. Zhao, F. Chen, J. Liu, Application and bioactive properties of proteins and peptides derived from hen eggs: opportunities and challenges, *J. Sci. Food Agric.* 94 (2014) 2839–2845. doi:10.1002/jsfa.6670.

[18] T. Lafarga, M. Hayes, Bioactive peptides from meat muscle and by-products: generation, functionality and application as functional ingredients, *Meat Sci.* 98 (2014) 227–239. doi:10.1016/j.meatsci.2014.05.036.

[19] B.T. Meneguetti, L. dos S. Machado, K.G.N. Oshiro, M.L. Nogueira, C.M.E. Carvalho, O.L. Franco, Antimicrobial Peptides from Fruits and Their Potential Use as Biotechnological Tools—A Review and Outlook, *Front. Microbiol.* 7 (2017). doi:10.3389/fmicb.2016.02136.

[20] R. Hartmann, H. Meisel, Food-derived peptides with biological activity: from research to food applications, *Curr. Opin. Biotechnol.* 18 (2007) 163–169. doi:10.1016/j.copbio.2007.01.013.

[21] A.G. Atanasov, B. Waltenberger, E.-M. Pferschy-Wenzig, T. Linder, C. Wawrosch, P. Uhrin, V. Temml, L. Wang, S. Schwaiger, E.H. Heiss, J.M. Rollinger, D. Schuster, J.M. Breuss, V. Bochkov, M.D. Mihovilovic, B. Kopp, R. Bauer, V.M. Dirsch, H. Stuppner, Discovery and resupply of pharmacologically active plant-derived natural products: A review, *Biotechnol. Adv.* 33 (2015) 1582–1614. doi:10.1016/j.biotechadv.2015.08.001.

[22] S. Piovesana, A.L. Capriotti, C. Cavaliere, G. La Barbera, C.M. Montone, R. Zenezini Chiozzi, A. Laganà, Recent trends and analytical challenges in plant bioactive peptide separation, identification and validation, *Anal. Bioanal. Chem.* 410 (2018) 3425–3444. doi:10.1007/s00216-018-0852-x.

[23] J.L. Lau, M.K. Dunn, Therapeutic peptides: Historical perspectives, current development trends, and future directions, *Bioorg. Med. Chem.* 26 (2018) 2700–2707. doi:10.1016/j.bmc.2017.06.052.

[24] M. Bosso, L. Ständker, F. Kirchhoff, J. Münch, Exploiting the human peptidome for novel antimicrobial and anticancer agents, *Bioorg. Med. Chem.* 26 (2018) 2719–2726. doi:10.1016/j.bmc.2017.10.038.

[25] Sotirios Koutsopoulos, Peptide Applications in Biomedicine,

Biotechnology and Bioengineering, Elsevier, 2018. doi:10.1016/C2015-0-02002-0.

[26] K. Sato, Structure, Content, and Bioactivity of Food-Derived Peptides in the Body, *J. Agric. Food Chem.* 66 (2018) 3082–3085. doi:10.1021/acs.jafc.8b00390.

[27] S. Ward, N.T. Powles, M.I. Page, Peptide biomarkers for identifying the species origin of gelatin using coupled UPLC-MS/MS, *J. Food Compos. Anal.* 73 (2018) 83–90. doi:10.1016/j.jfca.2018.08.002.

[28] F. Piguet, H. Ouldali, M. Pastoriza-Gallego, P. Manivet, J. Pelta, A. Oukhaled, Identification of single amino acid differences in uniformly charged homopolymeric peptides with aerolysin nanopore, *Nat. Commun.* 9 (2018) 966. doi:10.1038/s41467-018-03418-2.

[29] E.T. Chin, D.I. Papac, The Use of a Porous Graphitic Carbon Column for Desalting Hydrophilic Peptides prior to Matrix-Assisted Laser Desorption/Ionization Time-of-Flight Mass Spectrometry, *Anal. Biochem.* 273 (1999) 179–185. doi:10.1006/abio.1999.4242.

[30] O.I. Obolensky, W.W. Wu, R.-F. Shen, Y.-K. Yu, Using dissociation energies to predict observability of b- and y-peaks in mass spectra of short peptides. II. Results for hexapeptides with non-polar side chains, *Rapid Commun. Mass Spectrom.* 27 (2013) 152–156. doi:10.1002/rcm.6451.

[31] L. Ou, M.J. Przybilla, C.B. Whitley, Metabolomics profiling reveals profound metabolic impairments in mice and patients with Sandhoff disease, *Mol. Genet. Metab.* 126 (2019) 151–156. doi:10.1016/j.ymgme.2018.09.005.

[32] A. McMillan, A.E. Orimadegun, M.W. Sumarah, J. Renaud, M.M. da Encarnacao, G.B. Gloor, O.O. Akinyinka, G. Reid, S.J. Allen, Metabolic derangements identified through untargeted metabolomics in a cross-sectional study of Nigerian children with severe acute malnutrition, *Metabolomics.* 13 (2017) 13. doi:10.1007/s11306-016-1150-2.

[33] V.R. Koskinen, P.A. Emery, D.M. Creasy, J.S. Cottrell, Hierarchical Clustering of Shotgun Proteomics Data, *Mol. Cell. Proteomics.* 10 (2011) M110.003822. doi:10.1074/mcp.M110.003822.

- [34] A.B. Nongonierma, R.J. FitzGerald, Strategies for the discovery and identification of food protein-derived biologically active peptides, *Trends Food Sci. Technol.* (2017). doi:10.1016/j.tifs.2017.03.003.
- [35] S. Le Maux, A.B. Nongonierma, R.J. FitzGerald, Improved short peptide identification using HILIC–MS/MS: Retention time prediction model based on the impact of amino acid position in the peptide sequence, *Food Chem.* 173 (2015) 847–854. doi:10.1016/j.foodchem.2014.10.104.
- [36] U. Tinggi, Selenium: its role as antioxidant in human health, *Environ. Health Prev. Med.* 13 (2008) 102–108. doi:10.1007/s12199-007-0019-4.
- [37] P.O. Amoako, P.C. Uden, J.F. Tyson, Speciation of selenium dietary supplements; formation of S-(methylseleno)cysteine and other selenium compounds, *Anal. Chim. Acta.* 652 (2009) 315–323. doi:10.1016/j.aca.2009.08.013.
- [38] R. Jagtap, W. Maher, F. Krikowa, M.J. Ellwood, S. Foster, Measurement of selenomethionine and selenocysteine in fish tissues using HPLC-ICP-MS, *Microchem. J.* 128 (2016) 248–257. doi:10.1016/j.microc.2016.04.021.
- [39] R. Stoffaneller, N.L. Morse, A review of dietary selenium intake and selenium status in Europe and the Middle East, *Nutrients.* 7 (2015) 1494–1537. doi:10.3390/nu7031494.
- [40] M.P. Rayman, Selenium and human health, *Lancet.* 379 (2012) 1256–1268. doi:10.1016/S0140-6736(11)61452-9.
- [41] NIH, Selenium — Health Professional Fact Sheet, *Natl. Inst. Heal.* (2018). doi:10.1093/bmb/ldg009.
- [42] H. El-Ramady, N. Abdalla, H.S. Taha, T. Alshaal, A. El-Henawy, S.E.D.A. Faizy, M.S. Shams, S.M. Youssef, T. Shalaby, Y. Bayoumi, N. Elhawat, S. Shehata, A. Sztrik, J. Prokisch, M. Fári, É. Domokos-Szabolcsy, E.A. Pilon-Smits, D. Selmar, S. Haneklaus, E. Schnug, Selenium and nano-selenium in plant nutrition, *Environ. Chem. Lett.* 14 (2016) 123–147. doi:10.1007/s10311-015-0535-1.
- [43] A. Rusczyńska, A. Konopka, E. Kurek, J.C. Torres Elguera, E. Bulska, Investigation of biotransformation of selenium in plants using spectrometric methods,

Spectrochim. Acta - Part B At. Spectrosc. 130 (2017) 7–16.
doi:10.1016/j.sab.2017.02.004.

[44] M. Schiavon, E.A.H. Pilon-Smits, The fascinating facets of plant selenium accumulation – biochemistry, physiology, evolution and ecology, *New Phytol.* 213 (2017) 1582–1596. doi:10.1111/nph.14378.

[45] M.P. Rayman, H.G. Infante, M. Sargent, Food-chain selenium and human health: Spotlight on speciation, *Br. J. Nutr.* 100 (2008) 238–253. doi:10.1017/S0007114508922522.

[46] S. Oguri, M. Kumazaki, R. Kitou, H. Nonoyama, N. Tooda, Elucidation of intestinal absorption of d,l-amino acid enantiomers and aging in rats, *Biochim. Biophys. Acta - Gen. Subj.* 1472 (1999) 107–114. doi:10.1016/S0304-4165(99)00110-5.

[47] M. Friedman, C.E. Levin, Nutritional and medicinal aspects of d-amino acids, *Amino Acids.* 42 (2012) 1553–1582. doi:10.1007/s00726-011-0915-1.

[48] J.A. Ubersax, J.E. Ferrell Jr, Mechanisms of specificity in protein phosphorylation, *Nat. Rev. Mol. Cell Biol.* 8 (2007) 530–541. doi:10.1038/nrm2203.

[49] L.-R. Yu, T. Veenstra, Phosphopeptide Enrichment Using Offline Titanium Dioxide Columns for Phosphoproteomics, in: 2013: pp. 93–103. doi:10.1007/978-1-62703-360-2_8.

[50] C. Sun, R. Bernards, Feedback and redundancy in receptor tyrosine kinase signaling: relevance to cancer therapies, *Trends Biochem. Sci.* 39 (2014) 465–474. doi:10.1016/j.tibs.2014.08.010.

[51] M. Steger, F. Tonelli, G. Ito, P. Davies, M. Trost, M. Vetter, S. Wachter, E. Lorentzen, G. Duddy, S. Wilson, M.A. Baptista, B.K. Fiske, M.J. Fell, J.A. Morrow, A.D. Reith, D.R. Alessi, M. Mann, Phosphoproteomics reveals that Parkinson's disease kinase LRRK2 regulates a subset of Rab GTPases, *Elife.* 5 (2016). doi:10.7554/eLife.12813.

[52] S. Hartmann, A.J. Ridley, S. Lutz, The Function of Rho-Associated Kinases ROCK1 and ROCK2 in the Pathogenesis of Cardiovascular Disease, *Front.*

Pharmacol. 6 (2015). doi:10.3389/fphar.2015.00276.

[53] R. Kumar, V.P. Singh, K.M. Baker, Kinase inhibitors for cardiovascular disease, *J. Mol. Cell. Cardiol.* 42 (2007) 1–11. doi:10.1016/j.yjmcc.2006.09.005.

[54] J.D. Clark, M.E. Flanagan, J.-B. Telliez, Discovery and Development of Janus Kinase (JAK) Inhibitors for Inflammatory Diseases, *J. Med. Chem.* 57 (2014) 5023–5038. doi:10.1021/jm401490p.

[55] R. Galien, Janus kinases in inflammatory bowel disease: Four kinases for multiple purposes, *Pharmacol. Reports.* 68 (2016) 789–796. doi:10.1016/j.pharep.2016.04.001.

[56] A.S. Banks, F.E. McAllister, J.P.G. Camporez, P.-J.H. Zushin, M.J. Jurczak, D. Laznik-Bogoslavski, G.I. Shulman, S.P. Gygi, B.M. Spiegelman, An ERK/Cdk5 axis controls the diabetogenic actions of PPAR γ , *Nature.* 517 (2015) 391–395. doi:10.1038/nature13887.

[57] B. Ruprecht, S. Lemeer, Proteomic analysis of phosphorylation in cancer, *Expert Rev. Proteomics.* 11 (2014) 259–267. doi:10.1586/14789450.2014.901156.

[58] X.-S. Li, B.-F. Yuan, Y.-Q. Feng, Recent advances in phosphopeptide enrichment: Strategies and techniques, *TrAC Trends Anal. Chem.* 78 (2016) 70–83. doi:10.1016/j.trac.2015.11.001.

[59] G.R. Blacken, M. Sadílek, F. Tureček, Gallium metal affinity capture tandem mass spectrometry for the selective detection of phosphopeptides in complex mixtures, *J. Mass Spectrom.* 43 (2008) 1072–1080. doi:10.1002/jms.1387.

[60] H. Zhou, M. Ye, J. Dong, E. Corradini, A. Cristobal, A.J.R. Heck, H. Zou, S. Mohammed, Robust phosphoproteome enrichment using monodisperse microsphere-based immobilized titanium (IV) ion affinity chromatography, *Nat. Protoc.* 8 (2013) 461–480. doi:10.1038/nprot.2013.010.

[61] S. Feng, M. Ye, H. Zhou, X. Jiang, X. Jiang, H. Zou, B. Gong, Immobilized Zirconium Ion Affinity Chromatography for Specific Enrichment of Phosphopeptides in Phosphoproteome Analysis, *Mol. Cell. Proteomics.* 6 (2007) 1656–

1665. doi:10.1074/mcp.T600071-MCP200.

[62] C.A. Nelson, J.R. Szczech, Q. Xu, M.J. Lawrence, S. Jin, Y. Ge, Mesoporous zirconium oxide nanomaterials effectively enrich phosphopeptides for mass spectrometry-based phosphoproteomics, *Chem. Commun.* (2009) 6607. doi:10.1039/b908788e.

[63] M. Emgenbroich, C. Borrelli, S. Shinde, I. Lazraq, F. Vilela, A.J. Hall, J. Oxelbark, E. De Lorenzi, J. Courtois, A. Simanova, J. Verhage, K. Irgum, K. Karim, B. Sellergren, A Phosphotyrosine-Imprinted Polymer Receptor for the Recognition of Tyrosine Phosphorylated Peptides, *Chem. - A Eur. J.* 14 (2008) 9516–9529. doi:10.1002/chem.200801046.

[64] D.-Y. Li, Y.-P. Qin, H.-Y. Li, X.-W. He, W.-Y. Li, Y.-K. Zhang, A “turn-on” fluorescent receptor for detecting tyrosine phosphopeptide using the surface imprinting procedure and the epitope approach, *Biosens. Bioelectron.* 66 (2015) 224–230. doi:10.1016/j.bios.2014.11.023.

[65] M. Mann, S.-E. Ong, M. Grønberg, H. Steen, O.N. Jensen, A. Pandey, Analysis of protein phosphorylation using mass spectrometry: deciphering the phosphoproteome, *Trends Biotechnol.* 20 (2002) 261–268. doi:10.1016/S0167-7799(02)01944-3.

[66] L. Chen, X. Wang, W. Lu, X. Wu, J. Li, Molecular imprinting: perspectives and applications, *Chem. Soc. Rev.* 45 (2016) 2137–2211. doi:10.1039/C6CS00061D.

[67] A.B. Nongonierma, R.J. FitzGerald, Strategies for the discovery and identification of food protein-derived biologically active peptides, *Trends Food Sci. Technol.* 69 (2017) 289–305. doi:10.1016/j.tifs.2017.03.003.

[68] I.S. Sheoran, A.R.S. Ross, D.J.H. Olson, V.K. Sawhney, Compatibility of plant protein extraction methods with mass spectrometry for proteome analysis, *Plant Sci.* 176 (2009) 99–104. doi:10.1016/j.plantsci.2008.09.015.

[69] W. Wang, F. Tai, S. Chen, Optimizing protein extraction from plant tissues for enhanced proteomics analysis, *J. Sep. Sci.* 31 (2008) 2032–2039. doi:10.1002/jssc.200800087.

[70] T. Kleffmann, D. Russenberger, A. von Zychlinski, W. Christopher, K. Sjölander, W. Gruissem, S. Baginsky, The Arabidopsis thaliana Chloroplast Proteome Reveals Pathway Abundance and Novel Protein Functions, *Curr. Biol.* 14 (2004) 354–362. doi:10.1016/j.cub.2004.02.039.

[71] A. Jakubczyk, M. Karas, U. Zlotek, U. Szymanowska, Identification of potential inhibitory peptides of enzymes involved in the metabolic syndrome obtained by simulated gastrointestinal digestion of fermented bean (*Phaseolus vulgaris* L.) seeds, *Food Res. Int.* 100 (2017) 489–496. doi:10.1016/j.foodres.2017.07.046.

[72] M.L. Fournier, J.M. Gilmore, S.A. Martin-Brown, M.P. Washburn, Multidimensional Separations-Based Shotgun Proteomics, *Chem. Rev.* 107 (2007) 3654–3686. doi:10.1021/cr068279a.

[73] E. Sommella, G. Pepe, G. Ventre, F. Pagano, M. Manfra, G. Pierri, O. Ismail, A. Ciogli, P. Campiglia, Evaluation of two sub-2 μ m stationary phases, core-shell and totally porous monodisperse, in the second dimension of on-line comprehensive two dimensional liquid chromatography, a case study: Separation of milk peptides after expiration date, *J. Chromatogr. A.* 1375 (2015) 54–61. doi:10.1016/j.chroma.2014.11.072.

[74] L. Sánchez-Rivera, D. Martínez-Maqueda, E. Cruz-Huerta, B. Miralles, I. Recio, Peptidomics for discovery, bioavailability and monitoring of dairy bioactive peptides, *Food Res. Int.* 63 (2014) 170–181. doi:10.1016/j.foodres.2014.01.069.

[75] M. Björkman, I. Klingen, A.N.E. Birch, A.M. Bones, T.J.A. Bruce, T.J. Johansen, R. Meadow, J. Mølmann, R. Seljåsen, L.E. Smart, D. Stewart, Phytochemicals of Brassicaceae in plant protection and human health – Influences of climate, environment and agronomic practice, *Phytochemistry.* 72 (2011) 538–556. doi:10.1016/j.phytochem.2011.01.014.

[76] R. Zenezini Chiozzi, A.L. Capriotti, C. Cavaliere, G. La Barbera, S. Piovesana, A. Laganà, Identification of three novel angiotensin-converting enzyme inhibitory peptides derived from cauliflower by-products by multidimensional liquid chromatography and bioinformatics, *J. Funct. Foods.* 27 (2016) 262–273. doi:10.1016/j.jff.2016.09.010.

[77] C. Mooney, N.J. Haslam, G. Pollastri, D.C. Shields, Towards the Improved Discovery and Design of Functional Peptides: Common Features of Diverse Classes Permit Generalized Prediction of Bioactivity, *PLoS One*. 7 (2012). doi:10.1371/journal.pone.0045012.

[78] M.M. Bradford, A rapid and sensitive method for the quantitation of microgram quantities of protein utilizing the principle of protein-dye binding, *Anal. Biochem.* 72 (1976) 248–254. doi:10.1016/0003-2697(76)90527-3.

[79] G.L. Peterson, Review of the folin phenol protein quantitation method of lowry, rosebrough, farr and randall, *Anal. Biochem.* 100 (1979) 201–220. doi:10.1016/0003-2697(79)90222-7.

[80] C.V. González López, M. del C.C. García, F.G.A. Fernández, C.S. Bustos, Y. Chisti, J.M.F. Sevilla, Protein measurements of microalgal and cyanobacterial biomass, *Bioresour. Technol.* 101 (2010) 7587–7591. doi:10.1016/j.biortech.2010.04.077.

[81] I.-C. Sheih, T.-K. Wu, T.J. Fang, Antioxidant properties of a new antioxidative peptide from algae protein waste hydrolysate in different oxidation systems, *Bioresour. Technol.* 100 (2009) 3419–3425. doi:10.1016/j.biortech.2009.02.014.

[82] O.S. Nimmi, P. George, Evaluation of the antioxidant potential of a newly developed polyherbal formulation for antiobesity, 2012.

[83] Q. Wang, Preparation of Functional Peanut Oligopeptide and Its Biological Activity, in: *Peanut Process. Charact. Qual. Eval.*, Springer Singapore, Singapore, 2018: pp. 461–537. doi:10.1007/978-981-10-6175-2_9.

[84] C. West, C. Elfakir, M. Lafosse, Porous graphitic carbon: A versatile stationary phase for liquid chromatography, *J. Chromatogr. A*. 1217 (2010) 3201–3216. doi:10.1016/j.chroma.2009.09.052.

[85] J.H. Knox, P. Ross, *Carbon-Based Packing Materials for Liquid Chromatography: Structure, Performance, and Retention Mechanisms*, 1997.

[86] J.-P. Mercier, P. Morin, M. Dreux, A. Tambuté, *Liquid chromatography*

analysis of phosphonic acids on porous graphitic carbon stationary phase with evaporative light-scattering and mass spectrometry detection, *J. Chromatogr. A.* 849 (1999) 197–207. doi:10.1016/S0021-9673(99)00556-7.

[87] G. Gu, C.K. Lim, Separation of anionic and cationic compounds of biomedical interest by high-performance liquid chromatography on porous graphitic carbon, *J. Chromatogr. A.* 515 (1990) 183–192. doi:10.1016/S0021-9673(01)89312-2.

[88] M. Nshanian, R. Lakshmanan, H. Chen, R.R.O. Loo, J.A. Loo, Enhancing sensitivity of liquid chromatography–mass spectrometry of peptides and proteins using supercharging agents, *Int. J. Mass Spectrom.* 427 (2018) 157–164. doi:10.1016/j.ijms.2017.12.006.

[89] Y. Xiao, M.M. Vecchi, D. Wen, Distinguishing between Leucine and Isoleucine by Integrated LC–MS Analysis Using an Orbitrap Fusion Mass Spectrometer, *Anal. Chem.* 88 (2016) 10757–10766. doi:10.1021/acs.analchem.6b03409.

[90] H.J. Issaq, K.C. Chan, J. Blonder, X. Ye, T.D. Veenstra, Separation, detection and quantitation of peptides by liquid chromatography and capillary electrochromatography, *J. Chromatogr. A.* 1216 (2009) 1825–1837. doi:10.1016/j.chroma.2008.12.052.

[91] H. Kataoka, New trends in sample preparation for clinical and pharmaceutical analysis, *TrAC Trends Anal. Chem.* 22 (2003) 232–244. doi:10.1016/S0165-9936(03)00402-3.

[92] B. Buszewski, M. Szultka, Past, Present, and Future of Solid Phase Extraction: A Review, *Crit. Rev. Anal. Chem.* 42 (2012) 198–213. doi:10.1080/07373937.2011.645413.

[93] B. Levine, *Principles of forensic toxicology*, 2003.

[94] R. Guedes-Alonso, Z. Sosa-Ferrera, J.J. Santana-Rodríguez, An on-line solid phase extraction method coupled with UHPLC-MS/MS for the determination of steroid hormone compounds in treated water samples from waste water treatment plants, *Anal. Methods.* 7 (2015) 5996–6005. doi:10.1039/C5AY00807G.

[95] J.L. Gómez-Ariza, V. Bernal-Daza, M.J. Villegas-Portero, First

approach of a methodological set-up for selenomethionine chiral speciation in breast and formula milk using high-performance liquid chromatography coupled to atomic fluorescence spectroscopy, *Appl. Organomet. Chem.* 21 (2007) 434–440. doi:10.1002/aoc.1239.

[96] S. Torres, R. Gil, M.F. Silva, P. Pacheco, Determination of seleno-amino acids bound to proteins in extra virgin olive oils, *Food Chem.* 197 (2016) 400–405. doi:10.1016/j.foodchem.2015.10.008.

[97] M. Tie, J. Sun, Y. Gao, Y. Yao, T. Wang, H. Zhong, H. Li, Identification and quantitation of seleno-amino acids in mung bean sprouts by high-performance liquid chromatography coupled with mass spectrometry (HPLC–MS), *Eur. Food Res. Technol.* 244 (2018) 491–500. doi:10.1007/s00217-017-2967-2.

[98] M. Montes-Bayón, E.G. Yanes, C.P. De León, K. Jayasimhulu, A. Stalcup, J. Shann, J.A. Caruso, Initial studies of selenium speciation in *Brassica juncea* by LC with ICPMS and ES-MS detection: An approach for phytoremediation studies, *Anal. Chem.* 74 (2002) 107–113. doi:10.1021/ac0106804.

[99] F. Garousi, É. Domokos-Szabolcsy, M. Jánószky, A.B. Kovács, S. Veres, Á. Soós, B. Kovács, Selenoamino Acid-Enriched Green Pea as a Value-Added Plant Protein Source for Humans and Livestock, *Plant Foods Hum. Nutr.* 72 (2017) 168–175. doi:10.1007/s11130-017-0606-5.

[100] R. Jagtap, W. Maher, Determination of selenium species in biota with an emphasis on animal tissues by HPLC-ICP-MS, *Microchem. J.* 124 (2016) 422–529. doi:10.1016/j.microc.2015.07.014.

[101] A. Berthod, X. Chen, J.P. Kullman, D.W. Armstrong, F. Gasparrini, I. D'Acquarica, C. Villani, A. Carotti, Role of the carbohydrate moieties in chiral recognition on teicoplanin- based LC stationary phases, *Anal. Chem.* 72 (2000) 1767–1780. doi:10.1021/ac991004t.

[102] S.P. Méndez, E.B. González, A.S. Medel, Chiral speciation and determination of selenomethionine enantiomers in selenized yeast by HPLC-ICP-MS using a teicoplanin-based chiral stationary phase, *J. Anal. At. Spectrom.* (2000). doi:10.1039/b001579m.

[103] S. Torres, S. Cerutti, J. Raba, P. Pacheco, M.F. Silva, Preconcentration of seleno-amino acids on a XAD resin and determination in regional olive oils by SPE UPLC-ESI-MS/MS, *Food Chem.* 159 (2014) 407–413. doi:10.1016/j.foodchem.2014.03.045.

[104] G. Cao, D. Ruan, Z. Chen, Y. Hong, Z. Cai, Recent developments and applications of mass spectrometry for the quality and safety assessment of cooking oil, *TrAC Trends Anal. Chem.* 96 (2017) 201–211. doi:10.1016/j.trac.2017.07.015.

[105] I. López-García, Y. Vicente-Martínez, M. Hernández-Córdoba, Nonchromatographic speciation of selenium in edible oils using dispersive liquid-liquid microextraction and electrothermal atomic absorption spectrometry, *J. Agric. Food Chem.* 61 (2013) 9356–9361. doi:10.1021/jf4027537.

[106] B.K. Matuszewski, M.L. Constanzer, C.M. Chavez-Eng, Strategies for the assessment of matrix effect in quantitative bioanalytical methods based on HPLC-MS/MS, *Anal. Chem.* 75 (2003) 3019–3030. doi:10.1021/ac020361s.

[107] C.-Y. TSAI, S.-J. JIANG, Microwave-assisted Extraction and Ion Chromatography Dynamic Reaction Cell Inductively Coupled Plasma Mass Spectrometry for the Speciation Analysis of Arsenic and Selenium in Cereals, *Anal. Sci.* (2011). doi:10.2116/analsci.27.271.

[108] S.M. Bird, P.C. Uden, J.F. Tyson, E. Block, E. Denoyer, Speciation of Selenoamino Acids and Organoselenium Compounds in Selenium-enriched Yeast Using High-performance Liquid Chromatography?Inductively Coupled Plasma Mass Spectrometry, *J. Anal. At. Spectrom.* 12 (1997) 785–788. doi:10.1039/a701429e.

[109] J. Zembrzuska, H. Matusiewicz, H. Polkowska-Motrenko, E. Chajduk, Simultaneous quantitation and identification of organic and inorganic selenium in diet supplements by liquid chromatography with tandem mass spectrometry, *Food Chem.* 142 (2014) 178–187. doi:10.1016/j.foodchem.2013.05.004.

[110] B. Chen, M. He, C. Zhong, B. Hu, Chiral speciation of selenoamino acids in biological samples, *J. Chromatogr. A.* 1363 (2014) 62–70. doi:10.1016/j.chroma.2014.07.098.

[111] C.R. DeCou, T.T. Cole, S.M. Lynch, M.M. Wong, K.C. Matthews,

Assault-related shame mediates the association between negative social reactions to disclosure of sexual assault and psychological distress., *Psychol. Trauma Theory, Res. Pract. Policy.* 9 (2017) 166–172. doi:10.1037/tra0000186.

[112] K. Mosbach, O. Ramström, The Emerging Technique of Molecular Imprinting and Its Future Impact on Biotechnology, *Nat. Biotechnol.* 14 (1996) 163–170. doi:10.1038/nbt0296-163.

[113] B. Sellergren, Enantiomer Separations Using Designed Imprinted Chiral Phases, in: *Chiral Sep. Tech.*, Wiley-VCH Verlag GmbH, Weinheim, FRG, n.d.: pp. 151–184. doi:10.1002/3527600361.ch6.

[114] K. Haupt, K. Mosbach, Molecularly Imprinted Polymers and Their Use in Biomimetic Sensors, *Chem. Rev.* 100 (2000) 2495–2504. doi:10.1021/cr990099w.

[115] D. CUNLIFFE, A. KIRBY, C. ALEXANDER, Molecularly imprinted drug delivery systems, *Adv. Drug Deliv. Rev.* (2005). doi:10.1016/j.addr.2005.07.015.

[116] N.W. Turner, C.W. Jeans, K.R. Brain, C.J. Allender, V. Hlady, D.W. Britt, From 3D to 2D: A Review of the Molecular Imprinting of Proteins, *Biotechnol. Prog.* 22 (2006) 1474–1489. doi:10.1021/bp060122g.

[117] A. Rachkov, N. Minoura, Recognition of oxytocin and oxytocin-related peptides in aqueous media using a molecularly imprinted polymer synthesized by the epitope approach, *J. Chromatogr. A.* 889 (2000) 111–118. doi:10.1016/S0021-9673(00)00568-9.

[118] *Handbook of Instrumental Techniques for Analytical Chemistry*, *J. Liq. Chromatogr. Relat. Technol.* 21 (1998) 3072–3076. doi:10.1080/10826079808006889.

[119] T. McCreedy, High performance liquid chromatography fundamental principles and practice, *Anal. Chim. Acta.* (1997). doi:10.1016/s0003-2670(97)81192-0.

[120] A.M. Siouffi, High performance liquid chromatography, in: *Handb. Food Sci. Technol. Eng.* - 4 Vol. Set, 2005.

[121] S.J. Gaskell, *Electrospray: Principles and Practice*, *J. Mass Spectrom.* 32 (1997) 677–688. doi:10.1002/(SICI)1096-9888(199707)32:7<677::AID-

JMS536>3.0.CO;2-G.

[122] M. Karas, F. Hillenkamp, Laser desorption ionization of proteins with molecular masses exceeding 10,000 daltons, *Anal. Chem.* 60 (1988) 2299–2301. doi:10.1021/ac00171a028.

[123] Biosoft, *Mass Spectrometry: Introduction, Principle of Mass Spectrometry, Components of Mass Spectrometer, Applications*, Prem. Biosoft. (2015).

[124] E. de. Hoffmann, V. Stroobant, *Mass Analyzers*, in: *Mass Spectrom. Princ. Appl.*, 2007.

[125] J.P. Savaryn, T.K. Toby, N.L. Kelleher, A researcher's guide to mass spectrometry-based proteomics, *Proteomics*. (2016). doi:10.1002/pmic.201600113.

[126] K.R. Clauser, P. Baker, A.L. Burlingame, Role of Accurate Mass Measurement (± 10 ppm) in Protein Identification Strategies Employing MS or MS/MS and Database Searching, *Anal. Chem.* 71 (1999) 2871–2882. doi:10.1021/ac9810516.

[127] T. Pekar Second, J.D. Blethrow, J.C. Schwartz, G.E. Merrihew, M.J. MacCoss, D.L. Swaney, J.D. Russell, J.J. Coon, V. Zabrouskov, Dual-Pressure Linear Ion Trap Mass Spectrometer Improving the Analysis of Complex Protein Mixtures, *Anal. Chem.* 81 (2009) 7757–7765. doi:10.1021/ac901278y.

[128] S. Eliuk, A. Makarov, Evolution of Orbitrap Mass Spectrometry Instrumentation, *Annu. Rev. Anal. Chem.* 8 (2015) 61–80. doi:10.1146/annurev-anchem-071114-040325.

[129] A. Michalski, E. Damoc, J.-P. Hauschild, O. Lange, A. Wiegand, A. Makarov, N. Nagaraj, J. Cox, M. Mann, S. Horning, Mass Spectrometry-based Proteomics Using Q Exactive, a High-performance Benchtop Quadrupole Orbitrap Mass Spectrometer, *Mol. Cell. Proteomics*. 10 (2011) M111.011015. doi:10.1074/mcp.M111.011015.

[130] W. Pusch, M.T. Flocco, S.-M. Leung, H. Thiele, M. Kostrzewa, Mass spectrometry-based clinical proteomics, *Pharmacogenomics*. 4 (2003) 463–476. doi:10.1517/phgs.4.4.463.22753.



Characterization of antioxidant and angiotensin-converting enzyme inhibitory peptides derived from cauliflower by-products by multidimensional liquid chromatography and bioinformatics



Carmela Maria Montone, Anna Laura Capriotti, Chiara Cavaliere, Giorgia La Barbera, Susy Piovesana, Riccardo Zenezini Chiozzi*, Aldo Laganà

Dipartimento di Chimica, Sapienza Università di Roma, Piazzale Aldo Moro 5, 00185 Rome, Italy

ARTICLE INFO

Keywords:

Peptidomics
Cauliflower waste
Antioxidant peptides
ACE-inhibitory peptides

ABSTRACT

In the present paper, bioactive peptides from cauliflower by-products (leaves and stems) were investigated. Alcalase® protein hydrolysis time and pH conditions were optimized, then the hydrolysates were fractionated by preparative RP-HPLC into 12 fractions. Each fraction was tested for the ABTS (2,2'-Azino-bis(3-ethylbenzothiazoline-6-sulfonic acid)), and DPPH (2,2-diphenyl-1-picrylhydrazyl) radical scavenging activity and for ACE (angiotensin-converting enzyme) inhibitor activity. The peptides in the most active fractions were identified by peptidomics technologies and screened for bioactivity by the use of bioinformatics. For ACE-inhibitor activity, two peptides were synthesized, APYDPDWYYIR and SKGFTSPLF, which provided an EC₅₀ value of 2.59 μmol L⁻¹ and 15.26 μmol L⁻¹, respectively. For the ABTS radical scavenging activity, SKGFTSPLF and LDDPVFRPL were tested, and provided an EC₅₀ of 10.35 μmol L⁻¹ and 8.29 μmol L⁻¹, respectively. For the DPPH radical scavenging activity, SKGFTSPLF and LRAPPGWGTGR were tested and provided an EC₅₀ of 8.2 μmol L⁻¹ and 5.26 μmol L⁻¹, respectively.

1. Introduction

A significant amount of waste and secondary products are furnished by agriculture; the disposal of such products could represent an economic and environmental problem. In the last few years, a great social and scientific interest has arisen for reusing by-products in an efficient manner, since these residues are often rich in bioactive compounds, such as antioxidants, carotenoids, sterols, bioactive peptides, that can be employed, depending on their activity, for disease treatment and prevention, as cosmetic ingredients, as active agents for intelligent packaging, as ingredients in conventional food products or as functional ingredients for nutraceutical products. The identification and the recovery of such compounds would transform waste products in valuable material, enhancing the ecological sustainability of agriculture and reducing the waste disposal (Herrero, Sánchez-Camargo, Cifuentes, & Ibáñez, 2015; Kumar, Yadav, Kumar, Vyas, & Dhaliwal, 2017).

Brassica crops, a huge vegetable family mainly constituted by cauliflower and broccoli, have a world production of about 71.8 million

tons (data of 2014 taken from <http://www.fao.org/faostat/en/>). As a consequence of this intensive production, every year tons of cauliflower by-products are generated, which are mainly made up of leaves (50% of the total) and stems which are often neglected and discarded. For this reason, the recovery and identification of bioactive compounds coming from *Brassica* crop wastes is an important challenge, nowadays. While in the past, many studies were focused on edible parts of cauliflowers, containing antioxidant (AO) and anti-carcinogenic compounds (Ahmed & Ali, 2013; Hwang & Lim, 2015), more recently the scientific attention was drawn to the re-use of food industry-related by-products to obtain bioactive compounds, such as glycosylated flavonoids (Gonzales et al., 2014; Llorach, Gil-Izquierdo, Ferreres, & Tomás-Barberán, 2003), phenolic and sulfuraphane compounds (Hwang & Lim, 2015) and bioactive peptides (Lee, Bae, Lee, & Yang, 2006; Xu et al., 2016, 2017; Zenezini Chiozzi et al., 2016)

The interest for bioactive peptides has considerably increased in the last 10 years mainly due to the many biological activities that can be exerted. If on the one hand fish (Capriotti et al., 2015; Villamil,

Abbreviations: ABTS, 2,2'-azino-bis(3-ethylbenzothiazoline-6-sulfonic acid); ACE, angiotensin-converting enzyme; AO, antioxidant; DPPH, 2,2-diphenyl-1-picrylhydrazyl; DTT, dithiothreitol; EDTA, ethylenediaminetetraacetic acid; HHL, N-hippuryl-L-histidyl-L-leucine; SDS, sodium dodecyl sulphate; SPE, solid phase extraction; TCA, trichloroacetic acid; TFA, trifluoroacetic acid

* Corresponding author at: Dipartimento di Chimica, Sapienza Università di Roma, Box no 34 – Roma 62, Piazzale Aldo Moro 5, 00185 Rome, Italy.

E-mail addresses: carmelamaria.montone@uniroma1.it (C.M. Montone), annalaura.capriotti@uniroma1.it (A.L. Capriotti), chiara.cavaliere@uniroma1.it (C. Cavaliere), giorgia.labarbera@uniroma1.it (G. La Barbera), susy.piovesana@uniroma1.it (S. Piovesana), riccardo.zenezini@uniroma1.it (R. Zenezini Chiozzi), aldo.lagana@uniroma1.it (A. Laganà).

<https://doi.org/10.1016/j.jff.2018.02.022>

Received 18 December 2017; Received in revised form 14 February 2018; Accepted 18 February 2018

Available online 23 March 2018

1756-4646/ © 2018 Elsevier Ltd. All rights reserved.

Vázquez, & Solanilla, 2017), meat (Lafarga & Hayes, 2014) and milk by-products derived bioactive peptides (Capriotti, Cavaliere, Piovesana, Samperi, & Laganà, 2016; Ortega-Requena & Rebouillat, 2015) have been extensively investigated, bioactive peptides from fruit and vegetables by-products are less investigated (Banerjee et al., 2017). However, plants can provide a very wide variety of bioactive compounds and, therefore, offer great promise for the study of bioactive peptides. In fact, since plants need to constantly defend themselves from numerous environmental offenders (i.e. insects, fungi and bacteria), they produce a great amount of secondary metabolites in response to such attacks, such as phenols, oxygen-substituted derivatives, terpenoids, quinines, tannins, (La Barbera et al., 2017) and bioactive peptides (Piovesana et al., 2018).

For these reason, there is a need to develop a semi-industrial scale up strategy in order to treat larger sample quantities. The steps for bioactive peptide production required on an industrial-scale differ from the laboratory-scale as hydrolysis, separation and purification need to be adapted to a large scale while controlling the cost of the entire process to produce goods which are economically advantageous.

In view of the above, the goal of this work was the characterization of cauliflower by-products AO and angiotensin-converting enzyme (ACE)-inhibitory bioactive peptides by the development of a feasible and economic semi-industrial method. With respect to our first study, carried out on the same matrix, we decided to set up a procedure compatible with a scale up of bioactive peptide production from cauliflower. The extraction included a common detergent, sodium dodecyl sulphate (SDS), and was followed by an *in vitro* digestion by Alcalase®, an economic enzyme much suitable for large scale production of bioactive peptides. We also optimized the hydrolysis conditions, such as pH and hydrolysis incubation time. The purification of peptides was carried out by preparative liquid chromatography; the resulting fractions were tested for antihypertensive and AO activities. The most active fractions were characterized by nano-liquid chromatography-tandem mass spectrometry and identified by database search. The identified peptides were further mined by *in silico* analysis using PeptideRanker to ascribe a bioactivity rank to each peptide. The sequences with the highest probability of being bioactive were synthesized and tested to calculate EC₅₀ values.

2. Materials and methods

2.1. Chemicals and standards

Alcalase® enzyme from *Bacillus licheniformis*, 2,2-Diphenyl-1-picrylhydrazyl (DPPH), 2,2'-Azino-bis(3-ethylbenzothiazoline-6-sulfonic acid) (ABTS), Angiotensin Converting Enzyme (ACE) from rabbit lung, N-hippuryl-L-histidyl-L-leucine (HHL) hippuric acid, Tris (hydroxymethyl) aminomethane (Tris-HCl), trifluoroacetic acid (TFA) and all other chemicals and solvents, of the highest grade available, were purchased from Sigma Aldrich (St. Louis, MO, USA), unless otherwise stated. Pierce BCA Protein Assay Kit was bought from Thermo Fisher Scientific. Ultrapure water (resistivity 18.2 MV cm) was obtained by an Arium 611 VF system from Sartorius (Göttingen, Germany). Solid phase extraction (SPE) C18 cartridges were Bond Elut (Varian, Palo Alto, CA, USA).

2.2. Plant material, protein extraction and precipitation

The cauliflower (*Brassica oleracea L. var. botrytis*) was provided by local farmers. Cauliflower by-products consisting of leaves and stem have been isolated, chopped with a sharp stainless steel knife into small pieces, lyophilized and finally ground to a fine powder with liquid nitrogen. Protein extraction and precipitation were chosen according to the best protocol employed in our first work (Zenezini Chiozzi et al., 2016). The protocol was carried out as previously described, starting from 50 g of cauliflower by-products. Briefly, samples were extracted

with 500 mL of a buffer consisting of 50 mmol L⁻¹ Tris-HCl (pH 8.8), 15 mmol L⁻¹ KCl, 20 mmol L⁻¹ dithiothreitol (DTT), and 1% (w/v) SDS. Briefly, the samples were incubated on ice for 1 h with intermittent vortexing (1 min every 15 min), followed by 1 h of sonication; the two steps were repeated twice. Finally, the insoluble material was removed by centrifugation at 4 °C for 15 min at 11,000g. The supernatants containing proteins were transferred into new centrifuge tubes and subjected to protein precipitation procedure, adding four volumes of cold acetone. The precipitation was carried out overnight at -20 °C. The obtained pellets were collected by centrifugation (4000g for 15 min at 4 °C), washed three times with ice-cold acetone, air-dried, and dissolved in 50 mL of 8 mol L⁻¹ urea. Proteins samples were quantified by the BCA assay, using bovine serum albumin (BSA) as standard and stored at -80 °C until digestion.

2.3. Protein digestion

After quantification, the cauliflower by-product protein pellet was hydrolyzed by Alcalase®. An optimization of the hydrolysis conditions was performed, changing buffer pH and hydrolysis time. In the optimized conditions, 100 mg protein aliquot was diluted with 50 mmol L⁻¹ Tris-HCl pH 8 to obtain a final urea concentration of 0.8 mol L⁻¹. Alcalase was added (1:10, enzyme: protein ratio) and the samples were incubated at 60 °C for 4 h. Enzymatic hydrolysis was quenched by decreasing the pH to 2 with TFA. The resulting peptide mixture was stored at -20 °C until analysis.

2.4. Peptide solid phase extraction

Digested samples were purified by SPE on C18 cartridges, containing 1 g C18, previously conditioned with acetonitrile (ACN): the maximal amount of peptides which could be purified was 4% of the sorbent weight (data not shown). After loading, peptides were rinsed with 0.1% trifluoroacetic (TFA) aqueous solution and then eluted with ACN/ddH₂O (70/30, v/v) with 0.1% TFA, and dried in the Speed-Vac. Samples were reconstituted with 5 mL of 0.1% TFA aqueous solution for subsequent chromatographic purification.

2.5. Purification of the cauliflower waste hydrolysate by RP-HPLC

Hydrolyzed peptides, using Alcalase®, were purified using an Xbridge BEH preparative C18 5 µm OBD 19 × 250 mm (Waters) connected to Shimadzu Prominence LC-20A system, including a CBM-20A controller, two LC-20 AP preparative pumps, a DGU-20A3R online degasser. A SPD-20A UV with a preparative cell (0.5 mm) was used as detector. As autocollector a FRC-10A Shimadzu was employed. Data acquisition was performed by the LabSolution version 5.53 software (Shimadzu, Kyoto, Japan). The detector was set at 214 nm.

The sample was eluted with a flow rate of 17 mL min⁻¹ using ddH₂O/TFA (99.9/0.1, v/v) as mobile phase A and MeOH/TFA (99.9/0.1, v/v) as mobile phase B. The gradient started from 25% B, was kept for 1 min and then increased to 50% in 19 min; finally, B was increased to 95% and maintained constant for 5 min. The column was re-equilibrated for 6 min. Twelve fractions were collected every 2 min (except for fraction 1 and 12, as it possible to see in Fig. 1). Collected peptide fractions (F1-12) were subjected to bioactivity tests to identify the most active ones.

2.6. Peptide quantitation

All peptide fractions were solubilized in 1 mL of phosphate-buffered saline buffer 0.1 mol L⁻¹ at pH 7.4. Then, 1 µL of the solution was analyzed in the NanoDrop 2000c (Thermo Fischer Scientific Inc., Massachusetts) at 280 nm reading wavelength. The measurement was done in triplicate.

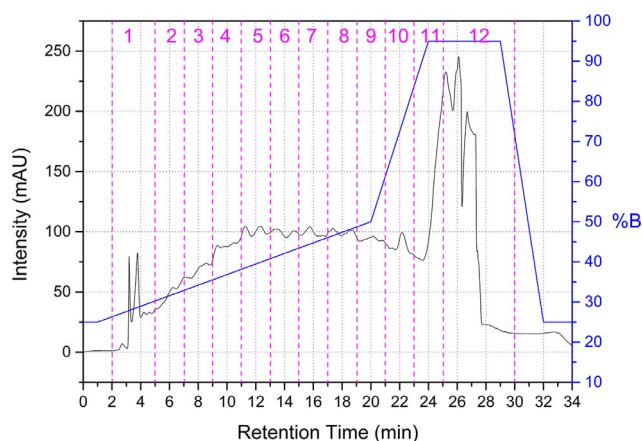


Fig. 1. Fractionation scheme adopted for preparative RP-HPLC of cauliflower waste hydrolysates.

2.7. Bioactivity assay

The total hydrolysates and the obtained fractions coming from RP-HPLC were tested for the ACE-inhibitory and AO activities, in particular for the AO activity two different tests were carried out, namely the DPPH and the ABTS radical scavenging activity assays. ACE-inhibitory and DPPH assays were carried out as described previously in our work (Zenezini Chiozzi et al., 2016).

Briefly, the ACE inhibitor assay was performed in Tris buffer (50 mmol L⁻¹, pH 8.3) containing 300 mmol L⁻¹ NaCl. Fifty µL of N-Hippuryl-L-histidyl-L-leucine (5 mmol L⁻¹), 50 µL of ACE solution containing 1 mU of declared enzyme activity and 50 µL of sample were employed for the assay. After incubation at 37 °C for 90 min, the reaction was quenched by adding 250 µL of 1 mol L⁻¹ HCl. Then hippuric acid was extracted with 1.5 mL of ethyl acetate, centrifuged for 15 min at 2500g and 25 °C. One mL of the organic layer was dried down and redissolved in 100 µL of ddH₂O/HCOOH (99.9%/0.1%) and analyzed by HPLC-UV (SpectraSystem P4000 with UV1000, Thermo Scientific). The separation was performed on a PLRP-S column (4.6 × 250 mm, 5 µm, Agilent Technologies Santa Clara, CA, USA) equipped with PLRP-S guard cartridge (5 × 3 mm, Agilent Technologies Santa Clara, CA, USA) at 1.5 mL min⁻¹, monitoring at 228 nm. The sample was eluted by ddH₂O/HCOOH (99.9:0.1, v/v) as mobile phase A, and ACN/HCOOH (99.9:0.1, v/v) as mobile phase B in a 15 min run.

The inhibition activity (IA) was calculated as:

$$IA(\%) = \frac{A_{Blank} - A_{Peptide}}{A_{Blank}} \times 100$$

A_{Blank} is the area of the peak of hippuric acid in the control sample (Tris buffer), A_{peptide} is the area of hippuric acid in the peptide sample.

DPPH AO assays were performed using a 2.5 mmol L⁻¹ solution of DPPH diluted with methanol to obtain a final 0.125 mmol L⁻¹ concentration. Peptide samples were reconstituted with 2 mL ddH₂O and mixed with 2 mL 0.125 mmol L⁻¹ DPPH solution. The absorbance was determined at 517 nm at t = 0 min and after 60 min. A methanol/ddH₂O, 50/50 (v/v) solution was used as a blank. The AO activity (AA) was calculated according to the following equation:

$$AA(\%) = \frac{\Delta A_{Blank} - \Delta A_{Peptide}}{\Delta A_{Blank}} \times 100$$

where ΔA_{peptide} is the absorbance of the peptide sample (calculated as the difference between measurements at t = 0 min e t = 60 min) and ΔA_{Blank} is the absorbance of the blank sample (calculated as the difference between t = 0 min and t = 60 min).

ABTS assays were performed following the procedure reported in (Re et al., 1999) with some modifications. ABTS was dissolved in water to obtain a final concentration of 7 mmol L⁻¹. ABTS radical cation was

produced by reacting ABTS stock solution with 2.45 mmol L⁻¹ potassium persulfate (final concentration) and allowing the mixture to stand in the dark at room temperature for 12–16 h. The solution was diluted 1:20 (v/v) before use. One mg of peptides was solubilized in 2 mL of ddH₂O and added to 1 mL of ABTS solution. The absorbance was read at 745 nm.

2.8. NanoHPLC-MS/MS analysis

The most active fractions, namely F2, F7, F9 and F11, were analyzed by nanoHPLC coupled to MS/MS on a Dionex Ultimate 3000 (Dionex Corporation Sunnyvale, CA, USA) directly connected to a LTQ-Orbitrap XL mass spectrometer (Thermo Scientific, Bremen, Germany) by a nano-electrospray ion source. Then, peptide mixtures were separated by RP chromatography and spectra acquired as previously described (Zenezini Chiozzi et al., 2016).

2.9. Database search and peptide identification

All raw files from Xcalibur software (version 2.2 SP1.48, Thermo Fisher Scientific) were submitted to Proteome Discoverer software (version 1.3, Thermo Scientific) with the Mascot search engine (v.2.3, Matrix Science) for peptide/protein identification. The searches were performed against the proteome of *Brassica oleracea* species from Uniprot (<http://www.uniprot.org/>), as previously described (Zenezini Chiozzi et al., 2016), but setting no enzyme specificity. The potential bioactive peptides were subsequently filtered using three parameters: a Mascot-score larger than 30, an area of the integrated peak larger than 5E7 and the score of PeptideRanker (Mooney, Haslam, Pollastri, & Shields, 2012) larger than 0.7. The potential peptide candidates were searched against the BIOPEP database (<http://www.uwm.edu.pl/biochemia/index.php/en/biopep>) and PepBank (<http://pepbank.mgh.harvard.edu/>) to determine their novelty.

2.10. Peptide synthesis and individual bioactivity assays

The selected peptide sequences (SKGFTSPLF, APYDPDWYYIR, LRAPPGWTR, LDDPVFRPL) were synthesized by Life Technologies Europe (Thermo Scientific, Bremen, Germany) at the highest available purity (> 90%). Peptide standards were reconstituted in the bioassay specific buffer and tested to calculate EC₅₀ values; all fitting calculations were done using Origin 9.0.

3. Results and discussion

3.1. Optimization of protein hydrolysis

Trypsin enzyme, formerly used to digest extracted proteins from cauliflower wastes, was substituted in this work by the use of Alcalase®. Among the different approaches for protein digestion which are compatible with a large scale production, the use of enzymes still represents a reliable system. Enzymatic hydrolysis can be controlled choosing the experimental conditions under which the experiment is performed, to provide a very reproducible hydrolysate in terms of molecular weight distribution and peptide composition. Additionally, the process is faster than, for instance, fermentation by microorganisms. Thus, enzymatic hydrolysis is very suited for the production of peptides with a target functionality. Trypsin is a classical enzyme, largely employed in proteomics studies, the specificity of which allows to simplify the identification process of peptides, as the cleavage rule is known. However, the enzyme is also expensive and this does not comply with requirements for large scale production of bioactive peptides. Alcalase® is a valuable alternative, which has been widely employed in studies for the production of bioactive peptides, also from wastes, and it has been used widely to generate peptide hydrolysates on a commercial basis (Rizzello et al., 2016). Additionally, recent reports improved Alcalase® digestion

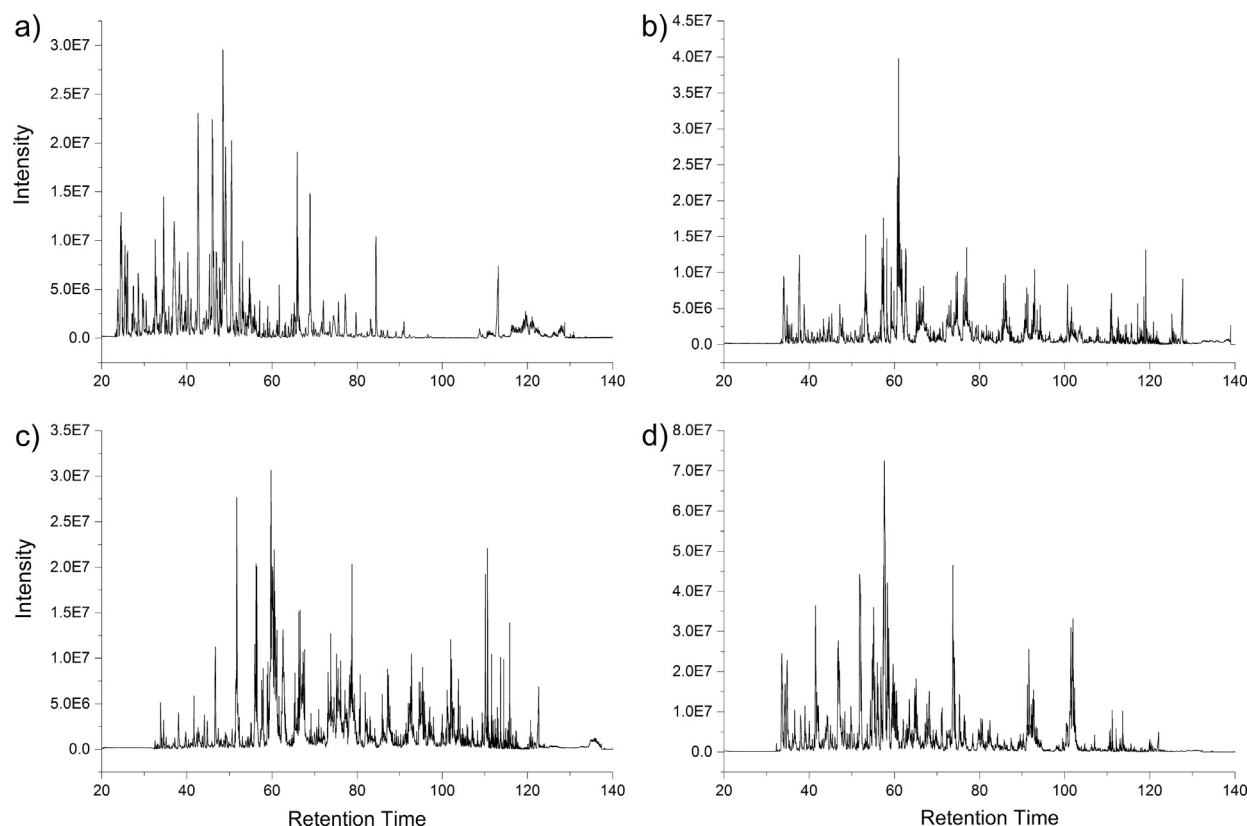


Fig. 2. Chromatograms related to the optimization of cauliflower waste proteins digestion by Alcalase® at pH 7 for 2 h (a), pH 7 for 4 h (b), pH 8 for 2 h (c) or pH 8 for 4 h (d).

shortening time by the use of hydrostatic pressure for improving the < 3 kDa AO peptide fraction in sweet potato hydrolysates (Zhang & Mu, 2017), making the Alcalase® hydrolysis an ideal process for peptide production on a large scale.

To identify the best conditions under which protein hydrolysis could be maximized, two pH conditions (7 and 8) and two hydrolysis times (2h and 4 h) were tested starting from the same protein extract (Fig. 2 and Table 1). Results were compared with the classical trypsin digestion. To monitor the efficiency of digestion, the same amount of sample was analyzed by nanoHPLC-MS/MS and the spectra analyzed. The number of MS/MS spectra was considered a surrogate of peptide species on the assumption that peptide identification is strictly related to the number of acquired MS/MS spectra (Kalli, Smith, Sweredoski, & Hess, 2013). The RawMeat software (Vast Scientific, version 2.0, <http://vastsci.com/rawmeat/>) was employed to extract the number of MS/MS spectra, along with additional information, such as the average intensity and the charge distribution of acquired ions. In both conditions, the number of MS/MS spectra increased over hydrolysis time and was largest for the digestion at pH 8 (Table 1). The charge distribution supported the good hydrolysis of precursor proteins, as the acquired ion signals were mainly +2 and +3 charged. Thus, hydrolysis at pH 8 for 4 h was selected for further experiments.

The use of Alcalase® provided protein hydrolysates more bioactive

than the hydrolysates provided by trypsin, which was used in the previous work (Zenezini Chiozzi et al., 2016); in the present work the ACE-inhibitor activity was maintained (90.5% for trypsin vs 92.6% for Alcalase®), while significantly increasing the AO activity, at least for the DPPH assay (7.4% for trypsin vs 38.6% for Alcalase®). A direct comparison indicated an improved bioactivity for Alcalase® hydrolysates than trypsin hydrolysates, as the above mentioned results are normalized on the same amount of precursor proteins, 1 mg in both experiments.

3.2. Peptide fractionation and bioactivity assessment

A multidimensional fractionation strategy was chosen to characterize the bioactive peptides isolated from cauliflower wastes after Alcalase® digestion under the most efficient conditions. Such an approach proved useful when working with trypsin, as it helps reducing the number of peptide candidates responsible for the observed bioactivity. In the case of Alcalase® hydrolysis the use of a multidimensional approach which reduces the number of peptide sequences in each fraction is essential, as the enzyme is unspecific. The direct consequence is not simply longer computational time for spectra identification, but also lower identification scores and loss of possible identifications when searching a too large space. For the present paper, the first dimension is

Table 1

MS/MS spectra of chromatograms obtained from 5 µg cauliflower waste digest by Alcalase® at two pH conditions (pH 7 and 8) and two hydrolyzing times (2h and 4 h). The last row provides MS/MS spectra for the same sample digested by trypsin.

Digestion conditions	Average intensity ± SD	Full scan spectra ± SD	MS/MS spectra ± SD
pH7_2h	4656121 ± 235462	9423 ± 198	16039 ± 330
pH7_4h	4705293 ± 250381	9541 ± 219	16581 ± 325
pH8_2h	5265321 ± 300654	9221 ± 175	17012 ± 381
pH8_4h	8523595 ± 441680	8247 ± 164	21807 ± 463
trypsin	8125511 ± 425945	7569 ± 151	28623 ± 570

Table 2

Peptide quantification in the fractions from the preparative C18 fractionation of cauliflower waste proteins hydrolyzed by Alcalase®.

Peptide fractions	Peptide concentration \pm SD ($\mu\text{g } \mu\text{L}^{-1}$)
Fraction 1	10.6 \pm 0.4
Fraction 2	10.2 \pm 0.2
Fraction 3	12.3 \pm 0.5
Fraction 4	18.9 \pm 0.1
Fraction 5	19.6 \pm 0.7
Fraction 6	22.1 \pm 0.5
Fraction 7	22.9 \pm 0.6
Fraction 8	20.4 \pm 0.9
Fraction 9	17.3 \pm 0.3
Fraction 10	19.6 \pm 0.8
Fraction 11	16.4 \pm 0.3
Fraction 12	12.2 \pm 0.5

a preparative one by C18 RP-chromatography. This is a traditional and mature technique, which is scalable and eventually suitable for plant production, thus appeared an ideal system for peptide fractionation on a preparative scale.

To assess the efficiency of fractionation by this approach, the peptide amounts recovered from each fraction were calculated using the NanoDrop technology (Table 2). The results indicated a good separation of the cauliflower waste hydrolysates, as the hydrolysate amount originally injected was distributed nearly equally among all recovered fractions. In particular, only the initial three fractions and the last fraction displayed a lower amount of peptides (10.2–12.3 $\mu\text{g } \mu\text{L}^{-1}$) whereas all other fractions had an average amount of 16.4–22.9 $\mu\text{g } \mu\text{L}^{-1}$. From the shotgun peptidomics analysis, the distribution of the molecular weights in the identified fractions did not show a specific trend as a function of C18 fractionation (Supplementary Material A, Fig. S1). The same applied to the isoelectric point distribution (Supplementary Material A, Fig. S2), as the only dependence was observed as function of peptide hydrophobicity (calculated as the grand average of hydropathy, GRAVY), which ranged between -2 and -1.5 for fraction 2, -1 and -0.5 for fraction 7, -1 and 0 for fraction 9 and -0.5 and 0.5 for fraction 11 (Supplementary Material A, Fig. S3).

After collection, each fraction was tested for the investigated bioactivities. The results from peptide quantification by NanoDrop were employed to normalize bioactivity assays measurements on peptide amounts in each fraction, to obtain values which could be directly compared to one another. For the AO bioactivity, both assays provided a similar distribution with the exception of fraction 7, where the DPPH assay provided a significant higher activity than the ABTS assay (37% vs 13%) (Fig. 3, Supplementary Material B). For both assays, later eluting fractions showed a higher activity. In particular, fraction 11 showed the highest ABTS radical scavenging activity (34%) and DPPH radical scavenging activity (46%), followed by fraction 9 for the ABTS assay (30%) and fraction 7 for DPPH (37%). On a general basis, the AO activity of extracts was not very high, values did not exceed 46% for the DPPH and 34% for the ABTS assay. Nevertheless, the result is valuable, as no significant AO activity was observed from cauliflower waste protein hydrolysis by trypsin. Thus the use of Alcalase® allowed to increase the bioactivity of the produced hydrolysates with an additional moderate AO bioactivity.

For ACE-inhibitor activity, the bioactivity was much higher than the AO activity generally for all fractions (Fig. 4). Only fraction 12 and 4 were below 40% ACE-inhibition. The most potent fraction reached 82% (fraction 2) and 94% (fraction 11) ACE-inhibition.

3.3. Identification of AO and ACE-inhibitory peptides by MS/MS and *in vitro* assays on chemically synthesized peptides

Two most active fraction for each investigated test were selected for further characterization by shotgun peptidomics. Fraction 2 was

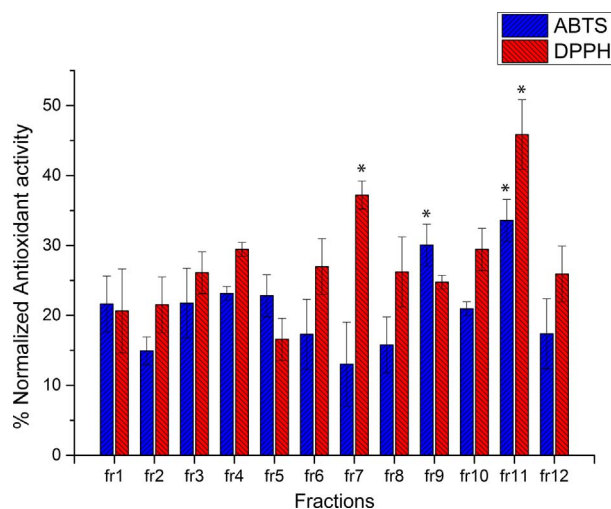


Fig. 3. Results of AO activity assays on the 12 peptide fractions obtained by the preparative system. Results are reported as mean \pm SD (n = 3). Student's *t*-test was also calculated and indicated with * when the *p* < 0.05.

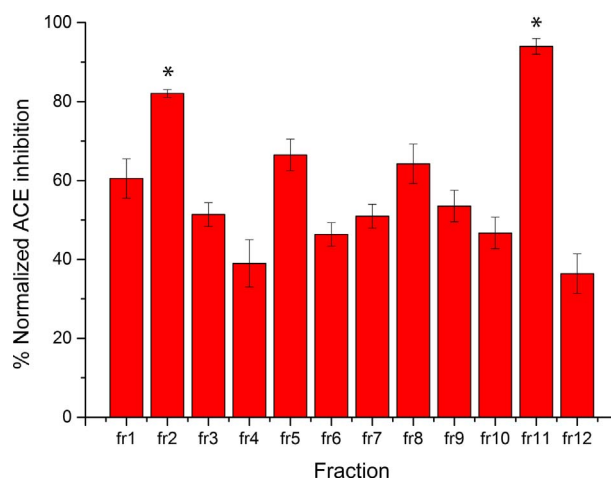


Fig. 4. Results of ACE-inhibitor tests on the 12 peptide fractions obtained by the preparative system. Results are reported as mean \pm SD (n = 3). Student's *t*-test was also calculated and indicated with * when the *p* < 0.05.

selected for ACE-inhibitor activity, fraction 7 for DPPH radical scavenging activity, fraction 9 for ABTS radical scavenging activity and fraction 11 for all tested activities. From this identification, a total number of 461 peptides were identified and distributed as follows: 128 peptides were found in fraction 2, 114 in fraction 7, 76 in fraction 9 and 72 in fraction 11. Even if partial, the obtained results demonstrate that a simple one-dimensional fractionation as the one described in this paper is enough to reduce the complexity of Alcalase® hydrolysates from cauliflower wastes. The relatively limited number of peptide identifications in each fraction can be attributed to the efficiency of the preparative fractionation but one must also take into consideration that Alcalase® is a very efficient enzyme and most peptides are +2 and +3 charged. This implies that peptides can also be very small, which would cause them to be in the initial part of the chromatographic separation; indeed, fraction 2 was the richest among the identified ones.

To shed light on the possible bioactivity associated with the identified peptide sequences, PeptideRanker (Mooney et al., 2012) was used to assign a bioactivity probability to each sequence. The software uses a built-in N-to-1 neural network to predict the bioactivity according to typical features of bioactive peptides (the complete list of probability scores assigned to each identified peptide is reported in the Supplementary Material B). To identify possible candidates for

Table 3

Sequence of peptides with the best score from PeptideRanker and related bioactivity, mass and original fraction from which they were identified. Color scale: in blue are marked the hydrophobic residues, in green are marked the negatively charged residues and in red are marked the positively charged residues. The EC₅₀ values obtained from in vitro assays of each peptide standard are also reported.

Sequence	Fraction	Mass	PeptideRanker score	Potential bioactivity	EC ₅₀ [$\mu\text{mol L}^{-1}$] \pm SD
SKGFTSPLF	11	983.12	0.85	AO DPPH ACE-inhibitor AO ABTS	8.20 \pm 0.95 15.26 \pm 1.60 10.35 \pm 1.21
APYDPDWYYIR	2	1458.58	0.84	ACE-inhibitor	2.59 \pm 0.29
LRAPPGWTGR	7	1110.27	0.82	AO DPPH	5.26 \pm 0.33
LDDPVFRPL	9	1071.23	0.81	AO ABTS	8.29 \pm 1.38

individual in vitro test, a higher threshold than the default one was applied, and candidates were selected among the peptides with the presumed higher activity (Table 3, Supplementary Material B and Supplementary Material A Tables S1–S4).

The typical features of AO and ACE-inhibitor peptides include quite short chains, 3–6 amino acid long for the AO peptides and 2–12 amino acid long for ACE-inhibitor peptides, even though for ACE-inhibitor peptides longer chains have been reported to be active as well (Chen & Li, 2012; Daskaya-Dikmen, Yucetepe, Karbancioglu-Guler, Daskaya, & Ozcelik, 2017). The selected candidates do not completely match this requirement, as they are 9–11 amino acid long, thus suit better for ACE-inhibitor typical candidate than for the AO peptide candidate. Nevertheless, they have other remarkable features of AO activity. Hydrophobic amino acid residues are typical of AO peptides, in particular His, Trp, Phe, Pro, Gly, Lys, Ile and Val, which are abundant in the selected peptide candidates (Table 3, residues marked in blue). Negatively charged residues Glu and Asp also contribute to the AO activity (Zou, He, Li, Tang, & Xia, 2016) and are part of sequences of two peptide candidates (Table 3, residues marked in green).

As far as the ACE-inhibitor activity was concerned, the most important contribution to the bioactivity is usually related to the C-terminal residues. In particular, ACE-inhibitor peptides typically display highly acidic amino acids (Asp and Glu), positively charged amino acids (in particular, Arg at the C-terminus) and hydrophobic amino acids (especially ACE-inhibitor dipeptides). The selected candidates all contain a large number of hydrophobic residues, and two of them displayed the charged C-terminal residues as well (Table 3, residues marked in red) (Daskaya-Dikmen et al., 2017).

At first sight, the overall scores provided by PeptideRanker for the peptides generated by Alcalase® hydrolysis were lower than the ones obtained from experiments on trypsin hydrolysates, which for the synthesized targets exceeded 0.90. Nevertheless, the four most probable sequences were synthesized to assess the bioactivity of each individual peptide. The results of bioactivity tests are reported in Table 3 and Fig. 5. The four peptide candidates displayed EC₅₀ values in the μmolar range. As far as the ACE-inhibitor activity was concerned, two peptides were tested, APYDPDWYYIR and SKGFTSPLF, which provided an EC₅₀ value of 2.59 and 15.26 $\mu\text{mol L}^{-1}$, respectively. This result was comparable to values obtained in the previous work on cauliflower bioactive peptide identification by trypsin hydrolysis, where the three most ACE-inhibitor peptides had an EC₅₀ value of 17.76, 12.81 and 0.46 $\mu\text{mol L}^{-1}$ (Zenezini Chiozzi et al., 2016), demonstrating that the change in enzyme did not significantly affect the ACE-inhibitor potential of cauliflower hydrolysates, a result which agreed with values obtained for the whole hydrolysate. These values indicated an ACE-inhibitor activity lower than the reference drug captopril (EC₅₀ of $0.021 \pm 0.013 \mu\text{mol L}^{-1}$). Peptide SKGFTSPLF was identified in fraction 11, a fraction which was highest for all tested bioactivities. However, this EC₅₀ value was higher than that of APYDPDWYYIR from fraction 2, for which the ACE-inhibitor assay provided a lower degree of inhibition than fraction 11. This demonstrates that the ACE-inhibitor potential of this peptide is not enough to explain the potential of the entire fraction 11, which was the highest, and a synergistic effect was

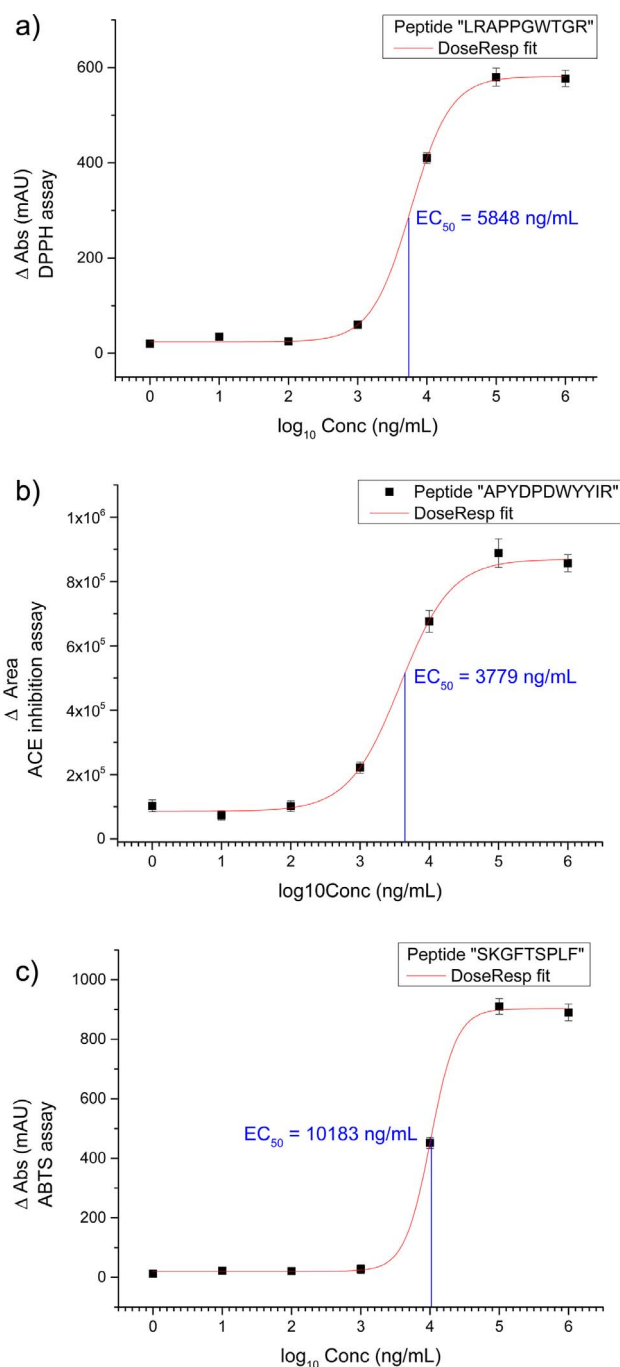


Fig. 5. Graphs related to the bioactivity test on the most active peptides: LRAPPGWTGR (for DPPH radical scavenging activity, (a)), APYDPDWYYIR (for ACE-inhibitor activity, (b)) and SKGFTSPLF (for ABTS radical scavenging activity, (c)). Graphs related to the other peptide standards are reported in Supplementary material, Figs. S4–S6.

operating in the peptide mixture. This phenomenon is sometimes reported for other matrices as well (Mäkinen, Streng, Larsen, Laine, & Pihlanto, 2016; Vásquez-Villanueva, Marina, & García, 2016) and can nevertheless be exploited to prepare bioactive fractions rather than a single peptide.

As far as the AO EC₅₀ values of the peptide candidates was concerned, they were generally lower for the DPPH test than for the ABTS test. In this regard, even if higher than the peptide LRAPPGWTR, SKGFTSPLF displayed low EC₅₀ values for both AO tests. Compared to the reference standard trolox, the EC₅₀ values of the identified bioactive peptides were generally larger for both AO assays. In fact, for trolox we experimentally calculated a EC₅₀ value of 1.56 μmol L⁻¹ for the ABTS assay (Supplementary Material A Fig. S7), and 0.86 μmol L⁻¹ for the DPPH assay (Supplementary Material A Fig. S8).

4. Conclusions

The work describes the scale up of bioactive peptide production from cauliflower wastes. Cauliflower waste proteins were extracted by SDS and purified by precipitation. Differently from previous reports on cauliflower waste bioactive peptide characterization, in this work Alcalase® was chosen for hydrolysis, due to the low cost of this enzyme compared to trypsin and the possible implementation on a large scale. The most suited hydrolysis conditions were determined comparing two pH values and two hydrolysis times, from which the best condition was identified in pH 8 and 4 h hydrolysis. After setting up the best hydrolyzing conditions, the obtained hydrolysates were fractionated by preparative RP-HPLC into 12 fractions; then, each fraction was assayed for the ABTS and DPPH radical scavenging activity and the ACE-inhibitor activity. Notably, compared to trypsin, the use of Alcalase® improved the AO activity of hydrolysates while maintaining the ACE-inhibitor activity. After bioactivity assays on the 12 fractions, the two most active fractions from each assay were selected and identified using shotgun peptidomics. PeptideRanker was later used to ascribe a possible bioactivity to each peptide and the most probable peptides were synthesized and tested for individual bioactivity. From the results, a synergistic effect was observed for ACE-inhibitor activity and DPPH radical scavenging activity, as the lowest EC₅₀ was found for the second most active fraction in all assays, except the ABTS radical scavenging activity. The obtained values, nevertheless, demonstrate the suitability of the preparation process for bioactive hydrolysates from low cost cauliflower wastes. The impact of digestion and of the intestinal absorption on the identified peptides still needs to be evaluated and will be necessary for future nutraceutical applications.

Acknowledgements

This work has been carried out within the framework of the Research Project “PRIN 2015”: securing and ensuring sustainable use of agriculture waste, co- and by-products: an integrated analytical approach combining mass spectrometry with health effect-based biosensing, supported by the Italian Ministry of University and Scientific Research, no. B86J16002440001. The authors wish to thank Prof. Roda and his research group for measurements of peptide concentration using NanoDrop technology.

Compliance with Ethical Standards

The authors declare no conflict of interest.

Appendix A. Supplementary material

Supplementary data associated with this article can be found, in the online version, at <http://dx.doi.org/10.1016/j.jff.2018.02.022>.

References

- Ahmed, F. A., & Ali, R. F. M. (2013). Bioactive compounds and antioxidant activity of fresh and processed white cauliflower. *BioMed Research International*, 2013, 1–9. <http://dx.doi.org/10.1155/2013/367819>.
- Banerjee, J., Singh, R., Vijayaraghavan, R., MacFarlane, D., Patti, A. F., & Arora, A. (2017). Bioactives from fruit processing wastes: Green approaches to valuable chemicals. *Food Chemistry*, 225, 10–22. <http://dx.doi.org/10.1016/j.foodchem.2016.12.093>.
- Capriotti, A. L., Cavaliere, C., Foglia, P., Piovesana, S., Samperi, R., Zenezini Chiozzi, R., & Laganà, A. (2015). Development of an analytical strategy for the identification of potential bioactive peptides generated by in vitro tryptic digestion of fish muscle proteins. *Analytical and Bioanalytical Chemistry*, 407(3), 845–854. <http://dx.doi.org/10.1007/s00216-014-8094-z>.
- Capriotti, A. L., Cavaliere, C., Piovesana, S., Samperi, R., & Laganà, A. (2016). Recent trends in the analysis of bioactive peptides in milk and dairy products. *Analytical and Bioanalytical Chemistry*, 408(11), 2677–2685. <http://dx.doi.org/10.1007/s00216-016-9303-8>.
- Chen, M., & Li, B. (2012). The effect of molecular weights on the survivability of casein-derived antioxidant peptides after the simulated gastrointestinal digestion. *Innovative Food Science and Emerging Technologies*, 16, 341–348. <http://dx.doi.org/10.1016/j.ifset.2012.07.009>.
- Daskaya-Dikmen, C., Yucetepe, A., Karbancioglu-Guler, F., Daskaya, H., & Ozcelik, B. (2017). Angiotensin-I-converting enzyme (ACE)-inhibitory peptides from plants. *Nutrients*, 9(4), 1–19. <http://dx.doi.org/10.3390/nu9040316>.
- Gonzales, G. B., Raes, K., Coelus, S., Struijs, K., Smaghe, G., & Van Camp, J. (2014). Ultra (high)-pressure liquid chromatography–electrospray ionization–time-of-flight–ion mobility–high definition mass spectrometry for the rapid identification and structural characterization of flavonoid glycosides from cauliflower waste. *Journal of Chromatography A*, 1323, 39–48. <http://dx.doi.org/10.1016/j.chroma.2013.10.077>.
- Herrero, M., Sánchez-Camargo, A. del P., Cifuentes, A., & Ibáñez, E. (2015). Plants, seaweeds, microalgae and food by-products as natural sources of functional ingredients obtained using pressurized liquid extraction and supercritical fluid extraction. *TrAC Trends in Analytical Chemistry*, 71, 26–38. <http://dx.doi.org/10.1016/j.trac.2015.01.018>.
- Hwang, J.-H., & Lim, S.-B. (2015). Antioxidant and anticancer activities of broccoli by-products from different cultivars and maturity stages at harvest. *Preventive Nutrition and Food Science*, 20(1), 8–14. <http://dx.doi.org/10.3746/pnf.2015.20.1.8>.
- Kalli, A., Smith, G. T., Sweredoski, M. J., & Hess, S. (2013). Evaluation and optimization of mass spectrometric settings during data-dependent acquisition mode: focus on LTQ-orbitrap mass analyzers. *Journal of Proteome Research*, 12(7), 3071–3086. <http://dx.doi.org/10.1021/pr3011588>.
- Kumar, K., Yadav, A. N., Kumar, V., Vyas, P., & Dhaliwal, H. S. (2017). Food waste: a potential bioresource for extraction of nutraceuticals and bioactive compounds. *Bioresources and Bioprocessing*, 4(1), 18. <http://dx.doi.org/10.1186/s40643-017-0148-6>.
- La Barbera, G., Capriotti, A. L., Cavaliere, C., Montone, C. M., Piovesana, S., Samperi, R., ... Laganà, A. (2017). Liquid chromatography–high resolution mass spectrometry for the analysis of phytochemicals in vegetal-derived food and beverages. *Food Research International*, 100, 28–52. <http://dx.doi.org/10.1016/j.foodres.2017.07.080>.
- Lafarga, T., & Hayes, M. (2014). Bioactive peptides from meat muscle and by-products: Generation, functionality and application as functional ingredients. *Meat Science*, 98(2), 227–239. <http://dx.doi.org/10.1016/j.meatsci.2014.05.036>.
- Lee, J.-E., Bae, I. Y., Lee, H. G., & Yang, C.-B. (2006). Tyr-Pro-Lys, an angiotensin I-converting enzyme inhibitory peptide derived from broccoli (*Brassica oleracea* Italica). *Food Chemistry*, 99(1), 143–148. <http://dx.doi.org/10.1016/j.foodchem.2005.06.050>.
- Llorach, R., Gil-Izquierdo, A., Ferreres, F., & Tomás-Barberán, F. A. (2003). HPLC-DAD-MS/MS ESI characterization of unusual highly glycosylated acylated flavonoids from cauliflower (*Brassica oleracea* L. v. ar. botrytis) Agroindustrial Byproducts. *Journal of Agricultural and Food Chemistry*, 51(13), 3895–3899. <http://dx.doi.org/10.1021/jf030077h>.
- Mäkinen, S., Streng, T., Larsen, L. B., Laine, A., & Pihlanto, A. (2016). Angiotensin I-converting enzyme inhibitory and antihypertensive properties of potato and rapeseed protein-derived peptides. *Journal of Functional Foods*, 25, 160–173. <http://dx.doi.org/10.1016/j.jff.2016.05.016>.
- Mooney, C., Haslam, N. J., Pollastri, G., & Shields, D. C. (2012). Towards the improved discovery and design of functional peptides: common features of diverse classes permit generalized prediction of bioactivity. *PLoS ONE*, 7(10), e45012. <http://dx.doi.org/10.1371/journal.pone.0045012>.
- Ortega-Requena, S., & Rebouillat, S. (2015). Retracted Article: Bigger data open innovation: Potential applications of value-added products from milk and sustainable valorization of by-products from the dairy industry. *Green Chemistry*, 17(12), 5100–5113. <http://dx.doi.org/10.1039/C5GC01428J>.
- Piovesana, S., Capriotti, A. L., Cavaliere, C., la Barbera, G., Montone, C. M., Zenezini Chiozzi, R., & Laganà, A. (2018). Recent trends and analytical challenges in plant bioactive peptide separation, identification and validation. *Analytical and Bioanalytical Chemistry*. <http://dx.doi.org/10.1007/s00216-018-0852-x>.
- Re, R., Pellegrini, N., Proteggente, A., Pannala, A., Yang, M., & Rice-Evans, C. (1999). Antioxidant activity applying an improved ABTS radical cation decolorization assay. *Free Radical Biology and Medicine*, 26(9–10), 1231–1237. [http://dx.doi.org/10.1016/S0891-5849\(98\)00315-3](http://dx.doi.org/10.1016/S0891-5849(98)00315-3).
- Rizzello, C. G., Tagliacozzi, D., Babini, E., Sefora Rutella, G., Taneyo Saa, D. L., & Gianotti, A. (2016). Bioactive peptides from vegetable food matrices: Research trends and novel biotechnologies for synthesis and recovery. *Journal of Functional Foods*, 27,

- 549–569. <http://dx.doi.org/10.1016/j.jff.2016.09.023>.
- Vásquez-Villanueva, R., Marina, M. L., & García, M. C. (2016). Identification by hydrophilic interaction and reversed-phase liquid chromatography-tandem mass spectrometry of peptides with antioxidant capacity in food residues. *Journal of Chromatography A*, 1428, 185–192. <http://dx.doi.org/10.1016/j.chroma.2015.07.032>.
- Villamil, O., Váquiro, H., & Solanilla, J. F. (2017). Fish viscera protein hydrolysates: Production, potential applications and functional and bioactive properties. *Food Chemistry*, 224, 160–171. <http://dx.doi.org/10.1016/j.foodchem.2016.12.057>.
- Xu, Y., Bao, T., Han, W., Chen, W., Zheng, X., & Wang, J. (2016). Purification and identification of an angiotensin I-converting enzyme inhibitory peptide from cauliflower by-products protein hydrolysate. *Process Biochemistry*, 51(9), 1299–1305. <http://dx.doi.org/10.1016/j.procbio.2016.05.023>.
- Xu, Y., Li, Y., Bao, T., Zheng, X., Chen, W., & Wang, J. (2017). A recyclable protein resource derived from cauliflower by-products: Potential biological activities of protein hydrolysates. *Food Chemistry*, 221, 114–122. <http://dx.doi.org/10.1016/j.foodchem.2016.10.053>.
- Zenezini Chiozzi, R., Capirotti, A. L., Cavaliere, C., La Barbera, G., Piovesana, S., & Laganà, A. (2016). Identification of three novel angiotensin-converting enzyme inhibitory peptides derived from cauliflower by-products by multidimensional liquid chromatography and bioinformatics. *Journal of Functional Foods*, 27, 262–273. <http://dx.doi.org/10.1016/j.jff.2016.09.010>.
- Zenezini Chiozzi, R., Capirotti, A. L., Cavaliere, C., La Barbera, G., Piovesana, S., Samperi, R., & Laganà, A. (2016). Purification and identification of endogenous antioxidant and ACE-inhibitory peptides from donkey milk by multidimensional liquid chromatography and nanoHPLC-high resolution mass spectrometry. *Analytical and Bioanalytical Chemistry*, 408(20), 5657–5666. <http://dx.doi.org/10.1007/s00216-016-9672-z>.
- Zhang, M., & Mu, T.-H. (2017). Identification and characterization of antioxidant peptides from sweet potato protein hydrolysates by Alcalase under high hydrostatic pressure. *Innovative Food Science and Emerging Technologies*, 43, 92–101. <http://dx.doi.org/10.1016/j.ifset.2017.08.001>.
- Zou, T. Bin, He, T. P., Li, H. Bin, Tang, H. W., & Xia, E. Q. (2016). The structure-activity relationship of the antioxidant peptides from natural proteins. *Molecules*, 21(1), 72. <http://dx.doi.org/10.3390/molecules21010072>.



Peptidomic strategy for purification and identification of potential ACE-inhibitory and antioxidant peptides in *Tetradesmus obliquus* microalgae

Carmela Maria Montone¹ · Anna Laura Capriotti¹ · Chiara Cavaliere¹ · Giorgia La Barbera¹ · Susy Piovesana¹ · Riccardo Zenezini Chiozzi¹ · Aldo Laganà¹

Received: 4 December 2017 / Revised: 15 January 2018 / Accepted: 29 January 2018 / Published online: 23 February 2018

© Springer-Verlag GmbH Germany, part of Springer Nature 2018

Abstract

Microalgae are unicellular marine organisms that have promoted complex biochemical pathways to survive in greatly competitive marine environments. They could contain significant amounts of high-quality proteins which, because of their structural diversity, contain a range of yet undiscovered novel bioactive peptides. In this work, a peptidomic platform was developed for the separation and identification of bioactive peptides in protein hydrolysates. In this work, a peptidomic platform was developed for the extraction, separation, and identification of bioactive peptides in protein hydrolysates. Indeed, extraction of proteins from recalcitrant tissues is still a challenge due to their strong cell walls and high levels of non-protein interfering compounds. Therefore, seven different protein extraction protocols, based on mechanical and chemical methods, were tested in order to produce high-quality protein extracts. Proteins obtained by means of the best protocol, consisting of milling the recalcitrant tissue with glass beads, were subjected to enzymatic digestion with Alcalase® and subsequently the hydrolysate was purified by two-dimensional semi-preparative reversed phase liquid chromatography. Fractions were assayed for antioxidant and antihypertensive activities and only the most active ones were finally analyzed by RP nanoHPLC-MS/MS. Around 500 peptide sequences were identified in these fractions. The identified peptides were subjected to an in silico analysis by PeptideRanker algorithm in order to assign a score of bioactivity probability. Twenty-five sequenced peptides were found with potential antioxidant and angiotensin-converting-enzyme-inhibitory activities. Four of these peptides, WPRGYFL, GPDRPKFLGPF, WYGPDRPKFL, SDWDRF, were selected for synthesis and in vitro tested for specific bioactivity, exhibiting good values of antioxidant and ACE-inhibitory activity.

Keywords Protein extraction methods · Peptidomics · Microalgae · Antioxidant peptides · ACE-inhibitory peptides · Off-line two-dimensional chromatography · High resolution mass spectrometry

Introduction

The research in the field of food bioactive peptides has greatly increased in the last decades, due to peptide health benefits

Published in the topical collection *Discovery of Bioactive Compounds* with guest editors Aldo Laganà, Anna Laura Capriotti and Chiara Cavaliere.

Electronic supplementary material The online version of this article (<https://doi.org/10.1007/s00216-018-0925-x>) contains supplementary material, which is available to authorized users.

✉ Anna Laura Capriotti
annalaura.capriotti@uniroma1.it

¹ Department of Chemistry, Sapienza Università di Roma, Piazzale Aldo Moro 5, 00185 Rome, Italy

and functional and bioactive properties [1–4]. Many matrices have been widely studied, such as fish [5, 6], milk [1, 2, 7], meat [4], and soybean [8]. However, more recently, particular attention is being paid to microalgae, which are one of the most promising sources for new food and functional food products, as the quantity and quality of microalgae proteins can compete favorably with conventional food proteins, such as soybeans, eggs, and fish [9, 10].

A peculiar characteristic of microalgae is their chemical composition, which varies according to the variation of a wide range of environmental factors, such as temperature, salinity, illumination, pH value, mineral content, CO₂ supply, population density, growth phase, and physiological status; for this reason, the environmental growing conditions could be optimized to maximize the production of a specific class of chemical compounds. Moreover, due to their rapid adaptation to the

new environmental conditions, they produce a variety of biologically active compounds, which usually cannot be found in other organisms. Generally, microalgae contain 40–70% proteins, 12–30% carbohydrates, 4–20% lipids, 8–14% carotene, and substantial amounts of vitamins B₁, B₂, B₃, B₆, B₁₂, E, K, and D [9, 10]. While in the past, microalgae have been extensively used to produce biofuel and biodiesel [11, 12] and to biofix CO₂ in a sustainable way to mitigate coal gas emissions [13], nowadays there has been a growing demand to isolate novel bioactive peptides from the marine microalgae [14, 15]. Despite this, a few studies have investigated the bioactive peptides from marine microalgae and none of these were meticulously performed as required in a peptidomic experiment; bioactive peptide studies are in fact more focused on the bioactivity investigation rather on the analytical method employed to prepare peptide samples [10, 16–18]. In fact, just few studies have identified the amino acid sequence of the microalgal peptides; moreover, in all the described approaches, peptide separation was not achieved and simple filtration of protein hydrolysates was performed, instead. When mass spectrometry is used to identify peptide sequences, matrix-assisted laser desorption ionization MS is frequently employed without a real separation or upstream fractionation. For instance, it is common to identify only the most abundant ions in a complex permeate, assuming that the observed bioactivity can be ascribed to such peptides. Moreover, none of the above-mentioned papers validated the aminoacidic identified sequence, as is the case of some recent works performed on macroalgae [19], fish [20], milk [7], and cauliflower by-products [21].

For these reasons, we decided to characterize *Tetradesmus obliquus*, a green microalga which, to the best of our knowledge, has never been investigated in terms of bioactive peptides but already exploited for other active metabolites extraction, such as essential lipids, astaxanthin, and phycobiliproteins [22].

In particular, in this study, we compared seven different extraction methods in order to choose the best extraction protocol able to furnish the maximum protein yield. Proteins extracted by the best protocol were *in vitro* digested by Alcalase®, after optimization of the hydrolysis conditions, such as pH and hydrolyzing time. The hydrolysates were tested for the antihypertensive and antioxidant (AO) activity. The obtained peptides were subsequently purified by two-dimensional liquid chromatography in order to simplify the complexity of the mixtures and the most active fractions were further analyzed by nanoHPLC coupled to high resolution mass spectrometry with an Orbitrap mass spectrometer for peptide sequencing. After a database search, the identified peptides were analyzed by a software, PeptideRanker, which provided a bioactivity score based on structural characteristic of the peptides. Four peptides, namely those with the greatest score of bioactivity, were chemically synthesized and their AO and angiotensin converting enzyme-inhibitory (ACE-

inhibitory) activities were determined by *in vitro* bioassays on the individual peptide standards.

Materials and methods

Chemicals and standards

All chemicals, reagents, and organic solvents of the highest grade available were purchased from Sigma-Aldrich (St. Louis, MO, USA) unless otherwise stated. Alcalase Enzyme from *Bacillus licheniformis*, 2,2-diphenyl-1-picrylhydrazyl (DPPH), 2,2'-azino-bis(3-ethylbenzothiazoline-6-sulfonic acid (ABTS), angiotensin converting enzyme (ACE) from rabbit lung, N-hippuryl-L-histidyl-L-leucine (HHL), hippuric acid, trifluoroacetic acid (TFA), Tris (hydroxymethyl) aminomethane (Tris), 1,4-dithiothreitol (DTT), potassium chloride, hydrochloric acid, sodium dodecyl sulfate (SDS), sodium chloride, acetone, methanol, hexane, ethanol, methyl tert-butyl ether (MTBE), and glass beads (acid-washed 425–600 μm) were purchased from Sigma-Aldrich (St. Louis, MO, USA). Pierce Bicinchoninic acid (BCA) Protein Assay Kit was purchased from Thermo Fisher Scientific. Ultrapure water (resistivity 18.2 MΩ cm) was obtained by an Arium water purification system (Sartorius, Gottingen, Germany).

Microalgae culturing

A strain of *Tetradesmus obliquus* (generally known as *Scenedesmus*) was selected in Siracusa (Sicily, Italy) and cultivated in a photoautotrophic pilot plant (21 L tubular photobioreactors) located in Rome, as previously described [23]. Briefly, an aliquot was taken from the pilot plant and used as inoculum for laboratory cultivation operated in this experimentation. In the laboratory, microalgae were centrifuged at 3500 rpm and the collected pellet was inoculated in 4 L tubular photobioreactor at an initial biomass concentration of $0.46 \pm 0.03 \text{ g L}^{-1}$. The reactor was maintained at room temperature ($27 \pm 3 \text{ }^\circ\text{C}$) under magnetic agitation, constant light illumination of $80 \pm 10 \text{ } \mu\text{E m}^{-2} \text{ s}^{-1}$, and constant air feeding (0.5 L min^{-1}). Cultivation was carried out in a modified BG11 containing a reduced NaNO₃ concentration of 0.3 g L^{-1} . Biomass concentration was determined as dry weight by filtering 10 mL of the suspension on glass microfiber filters (0.7 μm) previously dried at 105 °C. The filters were again dried after filtration at 105 °C until reaching constant weight. The measurement was performed in duplicate.

Protein extraction

The biomass was decanted overnight; then, the supernatant was discarded and the solide residue was harvested via centrifugation at 25 °C for 10 min at 3000×g. Pellets

were lyophilized and then ground to a fine powder with liquid nitrogen. Twenty-five milligrams of raw material was extracted evaluating seven different extraction protocols. Every extraction was performed in triplicate. Extraction typically involves disrupting the cells by physical or chemical means. In Table 1, the seven protocols employed for protein extraction are summarized.

In *protocol I*, lyophilized microalgae were solubilized with 1 mL of extraction buffer prepared as previously described [24] and consisting of 50 mmol L⁻¹ Tris (pH 8.8), 15 mmol L⁻¹ KCl, 20 mmol L⁻¹ DTT, and 1% (w/v) SDS. Then, samples were incubated on ice for 1 h with intermittent vortexing (1 min) every 15 min, and finally the insoluble material was removed by centrifugation at 4 °C for 15 min at 11,000×g. The supernatant was collected and subsequently proteins therein present were precipitated.

In *protocol II*, lyophilized microalgae protein extracts were prepared by glass beads lysis method [25]. Briefly, 25 mg of lyophilized microalgae was added to 150 mg of acid-washed glass beads and 1 mL of lysis buffer (60 mmol L⁻¹ Tris pH 9, 15 mmol L⁻¹ KCl, 20 mmol L⁻¹ DTT, 2% (w/v) SDS). The samples were placed in an ultrasonic bath for 4 h with intermittent vortexing (1 h) every 30 min, then they were incubated for 30 min at 100 °C and finally the insoluble material was removed by centrifugation at 4 °C for 15 min at 11,000×g. The supernatant coming from experiment was transferred into a new centrifuge tube and subjected to protein precipitation.

Protocol III was carried out adapting the methodology of Munoz and coworkers with some modifications [26]. The microalgae biomass was suspended in 1 mL of distilled water and subsequently 2 mol L⁻¹ of NaOH was added to water solution to adjust the sample pH at 11 and protein extraction was carried out under continuous stirring for 15 min and at room temperature (RT). The resulting mixture was centrifuged 15 min at 11,000×g and the pellet was discarded. The supernatant pH was adjusted at 3.3 by 1 mol L⁻¹ HCl and centrifuged at 11,000×g for 15 min to obtain a precipitate of microalgal protein fraction.

Protocol IV was based on HCl-Bligh and Dyer method with slight modifications [27]. Sample was heated in a water bath with 1 mL of 3 mol L⁻¹ HCl for 1 h at

80 °C. After cooling, 1 mL of chloroform and 1.5 mL of methanol were added. Sample was vortexed for 15 min, and then 2 mL of chloroform and 1 mL of water were added. The sample was centrifuged for 15 min at 11,000×g. After centrifugation, the upper layer containing methanol and water was removed and protein pellet was recovered by centrifugation for 15 min at 11,000×g.

In *protocol V*, lyophilized microalgae were mixed with 5 mL of hexane/ethanol (1/1, v/v) in a conical flask and sonicated at 38 kHz for 20 min in an ice-bath for disrupting the cell walls. Protein extraction was carried out by magnetic stirring at 180 rpm for 60 min at 25 °C. The resulted mixture was centrifuged for 10 min at 11,000×g and the upper phase containing hexane was discarded. The extraction process was repeated twice on the residual lower phase. The ethanolic phase was subjected to protein precipitation [28].

In *protocol VI*, 1.5 mL of methanol was added to 25 mg sample aliquot, which was placed into a tube and vortexed. Then, 5 mL of MTBE was added and the mixture was incubated for 1 h at room temperature in a shaker. Phase separation was induced by adding 1.25 mL of water. After 10 min of incubation at RT, the sample was centrifuged at 11,000×g for 10 min. The upper organic phase was discarded, the protocol was repeated once again. The aqueous phase was transferred into a new centrifuge tube and subjected to protein precipitation [29].

In *protocol VII*, the strength of osmotic shock was adjusted by dissolving 0.3 g of NaCl in 5 mL of microalgae culture. Five milliliters of a mixture of methanol and hexane 7:3 (v/v) was added. Then, the vials were gently shaken at 20 °C for 1 day to separate the protein component from cell debris. The lower phase of water-methanol contained solubilized proteins. After centrifugation at 4 °C for 15 min at 11,000×g, the supernatant was separated from cell debris and subjected to protein precipitation [30].

Protein precipitation and quantification

Protein precipitation was carried out for all extraction protocols, except for *protocols III* and *VI*.

Table 1 Summary of the seven protocols employed for protein extraction

Protocol name	Protocol description	Type of method
Protocol I	Suspension in lysis buffer and sonication using a commercial sonic bath	Chemical method
Protocol II	Milling in presence of glass beads	Mechanical method
Protocol III	Alkaline process	Chemical method
Protocol IV	HCl-Bligh and Dyer method (MeOH/CH ₂ Cl ₂ /H ₂ O)	Chemical method using organic solvent
Protocol V	Hexane/ethanol	Chemical method using organic solvent
Protocol VI	MTBE	Chemical method using green organic solvent
Protocol VII	Osmotic shock	Mechanical method

Precipitation was performed using a solution consisting in 10% (w/v) trichloroacetic acid in ice-cold acetone. Four volumes of this solution were added to the supernatants. The tubes were vortexed and incubated overnight at $-20\text{ }^{\circ}\text{C}$. The obtained pellets were collected by centrifugation ($18,400\times g$ for 15 min at $4\text{ }^{\circ}\text{C}$), washed three times with ice-cold acetone, air-dried, and dissolved in 2 mL of 8 mol L^{-1} urea (pH 8.8) in Tris-HCl 60 mmol L^{-1} . All proteins samples were quantified by the BCA assay using bovine serum albumin (BSA) as standard and stored at $-80\text{ }^{\circ}\text{C}$ until digestion (Table 2).

Protein digestion

The extracted and quantified microalgae proteins coming from the best extraction protocol (*Protocol II*) were hydrolyzed by Alcalase®. After optimization of hydrolysis pH and time, 150 mg protein aliquot was digested under the best condition. Proteins were solubilized in 8 mol L^{-1} urea for 1 h at $37\text{ }^{\circ}\text{C}$ and diluted with 60 mmol L^{-1} Tris-HCl to obtain a final urea concentration of 0.8 mol L^{-1} before adding Alcalase®. The enzyme was added in 1:10, enzyme/protein ratio and the samples were incubated at pH 8 at $60\text{ }^{\circ}\text{C}$ for 4 h. Enzymatic hydrolysis was stopped by decreasing the pH to 2 with TFA. The resulting peptide mixture was stored at $-20\text{ }^{\circ}\text{C}$ until analysis.

Peptide solid phase extraction

Digested samples were purified by solid phase extraction (SPE) on C18 cartridges (Bond Elut C18 1 g 6 mL, Agilent Technologies), previously conditioned with 15 mL of acetonitrile (ACN). After loading, peptides were rinsed with 15 mL of 0.1% TFA aqueous solution and then eluted with ACN/ddH₂O (70/30, v/v) with 0.1% TFA, and dried in the Speed-Vac. Maximum loading capacity of the cartridges was calculated as 4% (w/w) of the adsorbing material, after some testing (data not shown). Samples were reconstituted with 5 mL of 0.1% TFA aqueous solution for subsequent chromatographic purification.

Table 2 Quantification results from BCA assay for the seven extraction protocols. Data are reported in microgram per microliter \pm standard deviation and in percentage of protein yield for each experimental replicate

Exp. replicates	R1	R2	R3	% protein (average)
Protocol I	0.22 \pm 0.01	0.22 \pm 0.02	0.18 \pm 0.01	1.7 \pm 0.2
Protocol II	1.63 \pm 0.01	1.62 \pm 0.03	1.52 \pm 0.01	12.7 \pm 0.6
Protocol III	0.15 \pm 0.01	0.14 \pm 0.05	0.06 \pm 0.01	0.4 \pm 0.1
Protocol IV	0.47 \pm 0.01	0.52 \pm 0.02	0.50 \pm 0.01	3.9 \pm 0.5
Protocol V	1.55 \pm 0.01	1.27 \pm 0.03	1.24 \pm 0.03	10.9 \pm 1.5
Protocol VI	0.74 \pm 0.01	0.83 \pm 0.03	0.82 \pm 0.03	6.4 \pm 0.6
Protocol VII	1.54 \pm 0.01	1.43 \pm 0.02	1.41 \pm 0.01	11.6 \pm 0.2

Bioactivity assays

The whole hydrolysates were tested for ACE-inhibitory and AO activities, in particular for the AO activity two different tests were carried out (DPPH and ABTS). The same assays were carried out again on fractions obtained by the first and second chromatographic dimensions. Only the fractions with the most intense bioactivity were further fractionated and assayed once again.

For ACE-inhibition and DPPH AO activities, the same protocol employed in our previous work [21] was followed. For ABTS AO assay, the protocol from Re and coworkers [31] was carried out with some modifications. ABTS was dissolved in water to a 7 mmol L^{-1} concentration. ABTS radical cation was produced by reacting ABTS stock solution with 2.45 mmol L^{-1} potassium persulfate (final concentration) and allowing the mixture to stand in the dark at RT for 12–16 h. The solution was diluted 1:20 (v/v) before use. One milligram of peptides was solubilized in 2 mL of water and added to 1 mL of ABTS solution. The absorbance was measured at 745 nm.

Purification of antioxidant and ACE-inhibitory peptides from microalgae

Hydrolyzed peptides were purified by two-dimensional chromatography using the Xbridge BEH C18 OBD Prep column $19\times 250\text{ mm}$ ($5\text{ }\mu\text{m}$ particle size, Waters) in the first dimension, and the Xbridge BEH C18 OBD Prep Column $10\times 250\text{ mm}$ ($5\text{ }\mu\text{m}$ particle size, Waters) for the second one. Columns were connected to the Shimadzu Prominence LC-20A system, including a CBM-20A controller, two LC-20 AP preparative pumps, and a DGU-20A3R online degasser. As detectors, a SPD-20A UV detector with a preparative cell (0.5 mm) and a SPD-M20A UV detector were used. The autocollector FRC-10A (Shimadzu) was employed. Data acquisition was performed by the LabSolution version 5.53 software (Shimadzu, Kyoto, Japan). The detector was set at 214 nm.

In the first dimension, the sample was eluted at a flow rate of 17 mL min^{-1} using ddH₂O/TFA (99.9/0.1, v/v) as mobile phase A and MeOH/TFA (99.9/0.1, v/v) as mobile phase B. In

the gradient, phase B started from 25% and was kept constant for 1 min, then increased to 50% in 19 min; finally, B was increased to 95% and maintained constant for 5 min. The column was re-equilibrated for 6 min. Twelve fractions were collected every 2 min (except for fractions 1 and 12, as it possible to see in Fig. 2). Each collected peptide fraction (F1–12) was subjected to bioactivity tests to identify the most active ones. The most active fractions (F5, F6, F9, and F10) were again fractionated by the instrumental setup previously described, at a flow rate of 7 mL min⁻¹. To obtain a good degree of orthogonality to the first dimension, the separation in the second dimension employed ddH₂O with 10 mmol L⁻¹ ammonium formate at pH 10 as phase A and MeOH/ddH₂O (90/10, v/v, with 10 mmol L⁻¹ ammonium formate, pH 10) as the phase B. This gradient started from 25% of B, increased to 40% in 20 min; then, B was increased to 100% and maintained constant for 2 min and the column equilibrated for 10 min.

NanoHPLC-MS/MS analysis

The most active fractions coming from the second chromatographic dimension (see Fig. 4) were analyzed by nanoHPLC coupled to MS/MS. The analysis was performed on a Dionex Ultimate 3000 (Dionex Corporation, Sunnyvale, CA, USA) directly connected to a hybrid linear ion trap-Orbitrap mass spectrometer (Orbitrap Elite; Thermo Scientific, Bremen, Germany). Peptide mixtures were enriched on a 300 µm ID × 5 mm Acclaim PepMap 100 C18 precolumn (Dionex Corporation Sunnyvale, CA, USA), employing ddH₂O containing 0.1% (v/v) TFA, at a flow rate of 10 µL min⁻¹. Then, peptide mixtures were separated on an Easy-Spray column (500 mm × 75 µm, 2 µm particle size, Thermo Scientific) at 40 °C and 200 µL min⁻¹ using ddH₂O/HCOOH (99.9:0.1, v/v) as mobile phase A and ACN/HCOOH (99.9:0.1, v/v) as mobile phase B. MS spectra of eluting peptides were recorded in the *m/z* range of 300–1400, using a resolution setting of 60,000 (FWHM at *m/z* 400). The HCD fragmentation spectra were collected for the 10 most abundant ions at normalized energy of 35% in data-dependent mode. For all the details, we refer the reader to a previous article [25].

Database search and peptide identification

All raw files from Xcalibur software (version 2.2 SP1.48; Thermo Fisher Scientific) were submitted to Proteome Discoverer software (version 1.3; Thermo Scientific) with the Mascot search engine (v.2.3; Matrix Science) for peptide/protein identification. The searches were performed against the proteome of *Sphaeropleales* downloaded from Uniprot (<http://www.uniprot.org/>) on 27-07-2017 (19040 sequences). Unspecific digestion was chosen and neither fixed nor variable modifications were set. The precursor mass tolerance was set at 10 ppm and the fragment mass tolerance was

set at 0.05 Da. Peptide-spectrum match identifications were filtered using the mascot score: peptide identifications with a score below 25 were eliminated. The potential bioactive peptides were subsequently filtered using PeptideRanker at a threshold of 0.7 [32]. The potential peptide candidates were also searched against the BIOPEP database (<http://www.uwm.edu.pl/biochemia/index.php/en/biopep>) and PepBank (<http://pepbank.mgh.harvard.edu/>) to determine their novelty.

Peptide synthesis and individual bioactivity assays

The selected peptide sequences (WPRGYFL, GPDRPKFLGPF, WYGPDRPKFL, SDWDRF) were synthesized by Life Technologies Europe (Thermo Scientific, Bremen, Germany) at the highest available purity (>90%). Peptide standards were reconstituted in the bioassay specific buffer and tested to calculate EC₅₀; all fitting calculations were done using Origin 9.0.

For the ease of the reader, Fig. S1 in the Electronic Supplementary Material (ESM) shows a diagram summarizing the entire peptidomic analytical procedure.

Results and discussion

Comparison of protein extraction and protein quantification

Protein extraction is a crucial challenge, mostly in recalcitrant tissues where it is not possible to provide a universal and simple sample preparation method. The critical phase of the extraction procedure is the breaking of the cell wall. For these reasons, in this work seven different extraction protocols, based on mechanical methods and chemical methods with or without the using of organic solvent, were compared in order to select the best extraction protocol for the subsequent peptidomic experiment. The effectiveness of the cell disruption methods was determined using protein yield percentages. Quantitative analysis of the protein extracted by each extraction protocol was carried out by BCA assay. Results are shown in Fig. 1 and Table 2.

The extraction methods based on *protocols II* and *VII* were the most reliable with a comparable percentage of protein yield, namely 12.7 and 11.6%, respectively, because both involved the disrupting of the cell wall by physical means. In particular, in *protocol II*, a cell slurry was obtained using glass beads that are, as it is well known, one of the most effective system for the releasing of intracellular proteins from recalcitrant samples [33]. In *protocol VII*, a different physical procedure based on osmotic shock was employed. The subsequent choice to carry out all peptidomic experiments using *protocol II* rather than *protocol VII* was basically ascribed to the fact that *protocol VII* was a laborious and time-consuming method

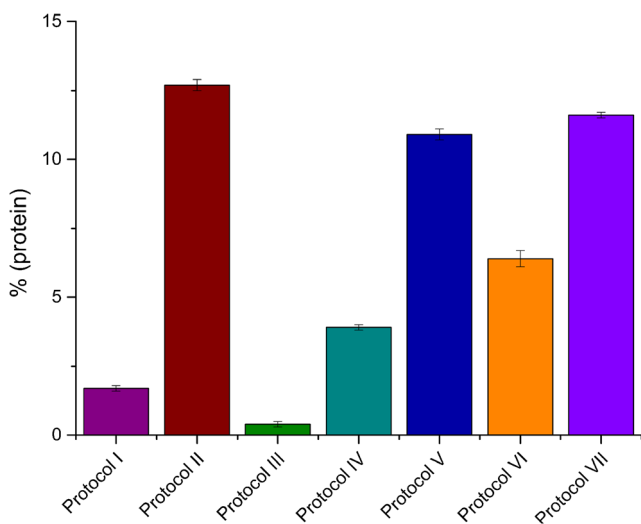


Fig. 1 Effect of different cell disruption methods for protein extraction from *Tetradesmus obliquus*. Average protein extraction of each protocol was reported as percentage of total extracted proteins

and it furnished a slightly lower protein recovery. Protocol VII would, however, be suitable in case of a possible scale up of the methodology. Chemical processes, using organic solvents, have also been employed (*protocols IV and V*) as alternatives to mechanical techniques, but the obtained results were for *protocol IV* much lower, with a percentage of protein recovery of 3.9, while for *protocol V* quite lower with respect to *protocols II and VII* with a percentage of yield of 10.9%; moreover, the process-scale application is a crucial limitation in this case for the high toxicity of hexane and chloroform. For this reason, in *protocol VI*, these toxic organic solvents were replaced with a green one, namely MTBE, but the protein recovery was quite low with a percentage of yield of 6.4%. Regarding *protocols I and III*, based on chemical process, the results were the worst, with a protein recovery of 1.7 and 0.4%, respectively (results are shown in Table 2 and Fig. 1). The explanation of a very low protein yield for *protocol III* lies in the fact that the extracted proteins were precipitated adjusting pH at 3.3 with HCl; the pI of most proteins is usually in the pH range of 4 to 7. At pH 3.3, only the proteins that possess an isoelectric point around 3 were precipitated, most likely our analyzed microalga did not possess proteins with this specific isoelectric point. Another possible explanation should be that the acids tend to denature the protein.

At first glance, it seems also unusual that *protocol I* led to a protein recovery of barely 1.7% even though the lysis extraction buffer used was the same as in *protocol II*. A possible explanation for the very low release of proteins in *protocol I* lies in the fact that bead milling along with vortexing, sonication, and incubation at 100 °C greatly help in obtaining a more efficient break of the cell wall. Microalgae, as well as all green plants, are recalcitrant tissues, for this reason common extraction methods using just organic solvent and denaturing buffers are not enough to obtain a high recovery of protein. Milling

the biomass with glass beads was, therefore, essential for completely releasing of the intracellular proteins. Results obtained from one species cannot be generalized to all other species but cell disruption could depend on microalgae species, age of the culture, and composition of cell wall.

Another important issue to underline was about the high levels of interfering compounds in green microalgae, especially viscous polysaccharides, such as alginic acid or fucoidan [34] which could be co-extracted together with proteins and could interfere with protein quantification, misrepresenting the data. To overcome this problem and concentrate and purify proteins in the lysis solution extract, a protein precipitation with cold acetone and trichloroacetic acid was performed in all protocols, with exception of *protocols III and IV*, where the precipitation was already driven by methanol and HCl, respectively.

BCA assay is one of the most accurate spectrophotometric method to measure the protein content of the pre-treated biomass along with Bradford [35] and Lowry [36] methods. If the protein content is determined by one of the above-mentioned methods, following the manufacturer's instructions, the precipitation step is necessary. González López et al. [37] reported that *Scenedesmus* protein content, obtained milling the biomass with ceramic particles, by Lowry method, was about 40%, but the precipitation step was neglected. The value could be over-estimated by the presence of non-protein compounds that could absorb to the same wavelength. Many works, reported in a recent review article [38], stated that microalgae species that are currently being industrially produced exhibit a relatively high protein content ranging from 30 to 70% but none of these papers carried out a protein precipitation step before quantification. Our best extraction protocol combined to a protein precipitation by cold acetone led to obtain a protein percentage of about 12%. At first glance, this result may seem lower than the data reported in literature [38]; for this reason alongside the precipitation step, we carried out a different experiment in which the protein quantification by BCA assay was performed without any precipitation step. We carried out this experiment employing our best extraction protocol (*Protocol II*). By this method, the protein content of the biomass was about 47% of dry weight and the result was in line with those reported by many authors highlighting that precipitation is clearly needed to remove contaminants and to have a reliable result of the protein content. To give weight to the argument, Kouhei Nagai and his coworkers [34] developed a chemical extraction method based on the use of organic solvent in combination with a precipitation step and their data showed that the recovery percentage of protein was lower in comparison with the above-mentioned papers and more similar to the data obtained following our best protocol in which a precipitation step was performed. Such low protein recovery could be ascribed to the fact that organic solvent methods are not enough to disrupt the cell wall in a very efficient way, but

at the same time the protocol is also affected by an under-estimation of proteins, due to possible absorption phenomena during non-protein compounds elimination. Obviously, one has to take into account the microalgae growth conditions, as they widely affect the protein content.

Optimization of Alcalase® hydrolysis of bioactive peptides

Digestion of proteins obtained by means of *protocol II* were carried out with Alcalase®. The choice of this enzyme was related to its low cost and the possibility to use it also in a possible scale up; moreover, this enzyme produced peptides from plum products with the highest AO capacity, reducing power and potential antihypertensive capacity [39].

Digestion parameters, including time of incubation with Alcalase® and pH, were closely monitored for the purpose of understanding how they affect rate and completeness of digestion. Previous studies [40, 41] on other substrates have shown Alcalase® to have activity within the alkaline pH range, for this reason we decided to test two pH values, namely 7 and 8. For each pH value, three hydrolysis times were investigated (1, 2, and 4 h). Results of digestion in terms of the effect of pH and hydrolysis time are shown in Table 3 and Fig. S2 (see ESM), where we reported the chromatograms showing the separation of an identical protein mixture hydrolyzed under different conditions.

The RawMeat software (Vast Scientific, version 2.0, <http://vastsci.com/rawmeat/>) was employed to understand which conditions were the best for microalgae protein digestion. It has been shown that the number of MS/MS scans significantly affects the proteome coverage and, most importantly for the aim of this work, the number of peptide identification, which strongly depends on the availability of MS/MS spectra [42]. Thus, the number of MS/MS spectra were the first parameter which was considered for comparison. For digestion at pH 7, there was no significant dependence on the hydrolysis time, as the MS/MS spectra, as well as the average intensity and full scan spectra, remain practically unaffected. A different situation was observed for digestion at pH 8. If, on the one hand, no chromatographic peak was observed carrying out the digestion at pH 8 for just 1 h (Table 3, ESM Fig. S2), on the other hand increasing the digestion time to 4 h provided the best

condition for hydrolysis. In fact, the largest number of MS/MS spectra was obtained for the digestion at pH 8 and for 4 h. This indicated that better peptide identifications could be accomplished under these conditions. As far as the other parameters reported in Table 3 is concerned, if the number of full scan spectra did not differ too much among the different conditions, the average intensity of detected species was highest for the pH 8 and 4 h digestion. This latter value is related to MS/MS spectra, as higher intensities increase the number of fragmentation events by guaranteeing the minimum threshold for MS/MS event triggering.

Fractionation and purification of AO and ACE-inhibitory peptides from microalgae

Protein hydrolysates were subjected to two-dimensional LC in order to purify and simplify the sample complexity and decrease under-sampling during the subsequent LC-MS/MS analysis. In peptide separation, the most commonly used chromatography techniques coupled to RP chromatography are strong cation-exchange chromatography (SCX) or, as a good alternative, hydrophilic interaction liquid chromatography (HILIC). Both techniques can achieve an orthogonal separation but both of them suffer from some limitations, namely low separation efficiency, poor resolution. Additionally, a desalting step is needed for SCX, while HILIC suffers from an ambiguous separation mechanism and poor solubility of peptides in solvents with high organic content. Recently, two-dimensional chromatography using RP columns in both dimensions was very promising since RPLC provides significantly greater peak capacity than other LC techniques and because it has been demonstrated that significant differences in mobile phase pH between the two dimensions can lead separations with a high degree of orthogonality [43]. For these reasons, in the present paper the orthogonality was achieved employing two C18 columns using pH 2 in the first and pH 10 in the second LC dimension. Twelve fractions (F1–F12) were obtained from the first dimension (Fig. 2A) and their AO and ACE-inhibitory activity were assayed in all fractions. Fractions F5, F6, F9, and F10, the most active ones, were further purified on a RP column and fractionated into other 10 fractions (Fig. 2B–E). At the end of the second fractionation process, the collected fractions were tested again for

Table 3 Average intensity, full scan, and MS/MS spectra obtained from Alcalase® at two pH conditions (pH 7 and 8) and three hydrolyzing times (1, 2, and 4 h)

Digestion conditions	Average intensity ± SD	Full scan spectra ± SD	MS/MS spectra ± SD
pH7_1h	462,204 ± 55,646	9423 ± 471	16,819 ± 673
pH7_2h	208,222 ± 27,693	9155 ± 366	16,504 ± 825
pH7_4h	470,529 ± 51,758	9720 ± 583	16,722 ± 502
pH8_1h	There are no peaks in the chromatogram		
pH8_2h	508,605 ± 55,946	9900 ± 495	16,289 ± 489
pH8_4h	852,359 ± 93,759	9047 ± 362	17,717 ± 709

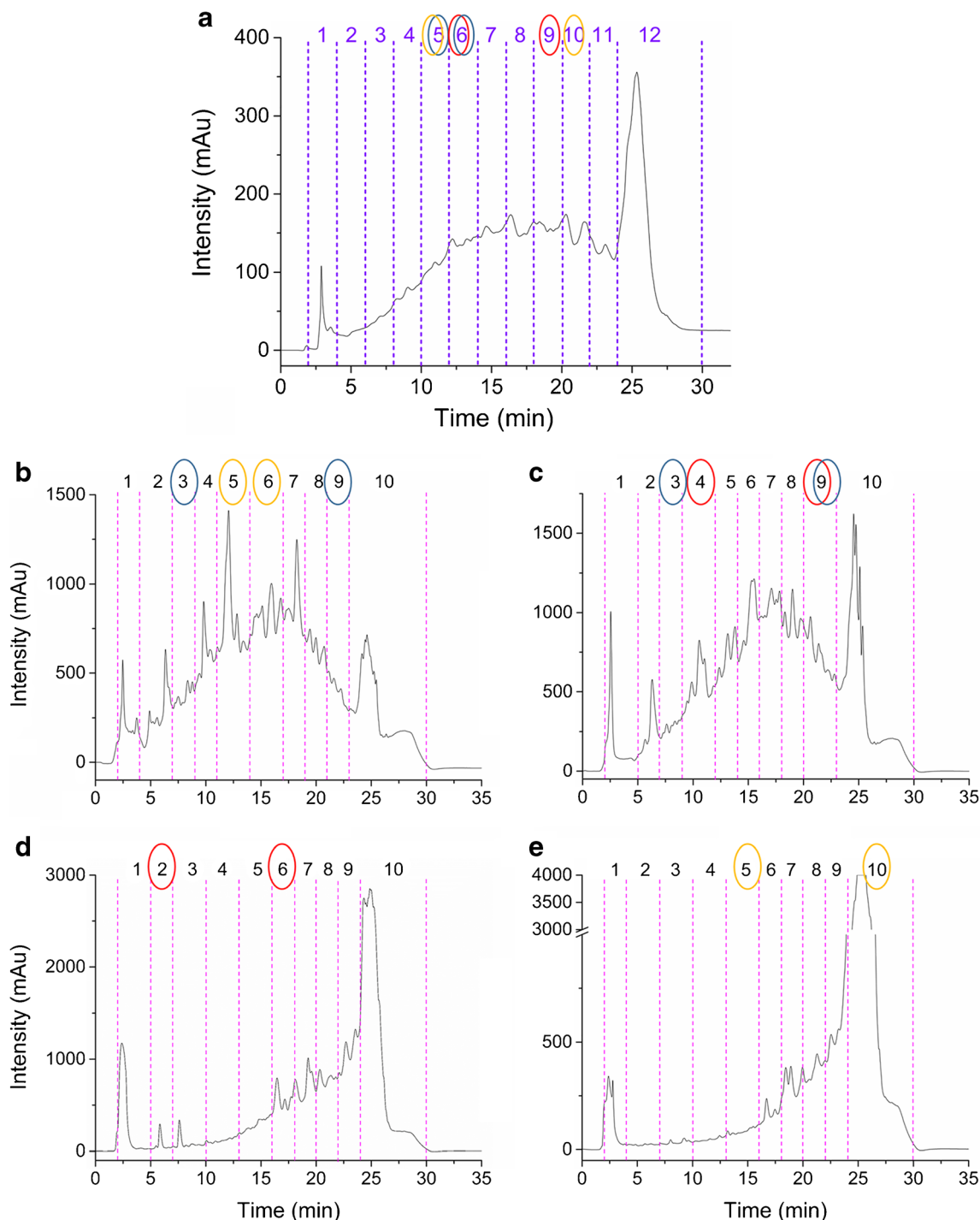


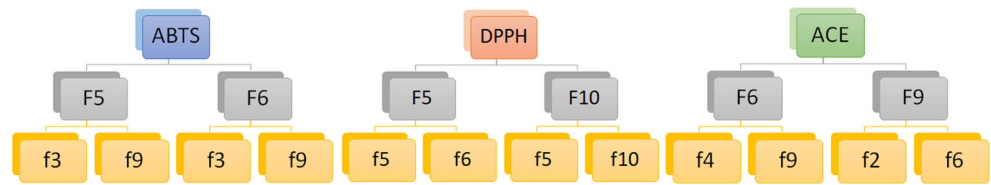
Fig. 2 Chromatograms for the first fractionation of hydrolyzed peptides in microalgae (A), and for the second dimension of fractions F5, F6, F9, and F10 (B–E, respectively)

bioactivity. For the ease of the reader, the entire scheme of fractionation is shown in Fig. 3.

The complete absorbance measurements and calculated activities for each fraction coming from first and second chromatographic dimension are reported in the ESM (see ESM_S1.xlsx) and in Fig. 4. Fractions F5 and F10 were the most active for the DPPH radical scavenging assay, which showed an AO activity

of 56 and 60%, respectively; fractions F5 and F6 were the most active for the ABTS assay, with 50 and 60%, respectively (Fig. 4A); fractions F6 and F9 were found to exhibit the highest ACE-inhibitory activity, with 82.5 and 80.8%, respectively (Fig. 4C). All the other fractions showed high percentage of activities, but being the values quite lower than the previously discussed fractions they were not further processed (Fig. 4A, C).

Fig. 3 Fractionation scheme for the purification of peptides from microalgae by two-dimensional RPLC



The most active fractions for DPPH radical scavenging activity were F5f5 and F5f6, with 56 and 70% of activity, respectively, and F10f5 and F10f10, with 50 and 56%, respectively; for ABTS activity, the most active fractions were F5f3 and F5f9, with 86 and 80%, respectively, and F6f3 and F6f9, with 85 and 80%, respectively (Fig. 4B); fractions F6f4, F6f9, F9f2, and F9f6 showed the highest ACE-inhibitory activities, with 78.7, 76.4, 91.2, and 80% activity, respectively (Fig. 4D).

Identification of AO and ACE-inhibitory peptides by MS/MS and in vitro assays on chemically synthesized peptides

In order to carry out the identification of peptides in the hydrolyzed protein extracts from microalgae, they were analyzed

by nanoHPLC-MS/MS method. Then, the obtained MS/MS raw files were searched by the Proteome Discoverer software to obtain peptide sequences. The complete list of identified peptides coming from the 11 most active fractions from the second chromatographic dimension, with sequence and related data, is reported in the ESM (see ESM_S1.xlsx). A total of 522 peptides were identified. This number is very high with respect to other papers carried out on microalgae samples where MS analysis is frequently employed without any real separation or upstream fractionation [44]. For instance, it is common to identify only the most abundant ions in a complex permeate, assuming that the observed bioactivity can be ascribed to such peptides.

Bioactive peptides usually show short amino acid sequence (2–20 amino acids units). Therefore, taking into

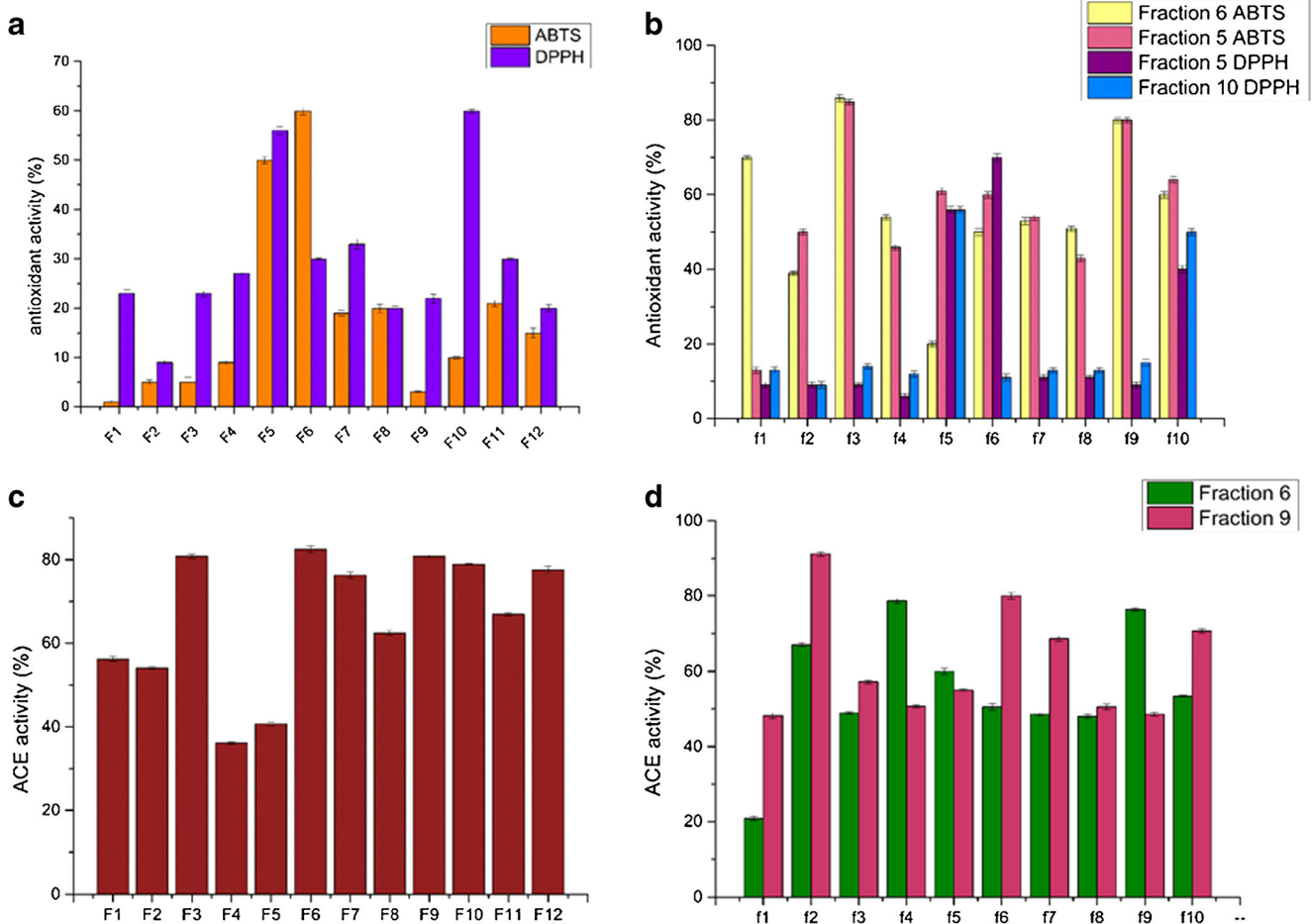


Fig. 4 Graph displaying the results of AO activity assays (DPPH and ABTS) on first and second dimension fractions (A, B) and the results of ACE-inhibitory activity on first and second dimension fractions (C, D)

account that the identified peptides in this work had molecular weights ranging between 488 and 1782 Da, they could potentially include bioactive properties. The identified peptide sequences were subjected to a BLAST (Basic Local Alignment Search Tool) search against the BIOPEP and PepBank databases, which include known and validated bioactive peptides. This alignment was carried out in order to find out if any already established bioactive peptide was to be found among the selected candidates for synthesis. The search did not provide any positive hit.

After that, an in silico analysis using PeptideRanker [32] was carried out to further mine data. In this way, each peptide was assigned a score based on the probability of being bioactive, probability that the built-in N-to-1 neural network computed on the basis of the peptide primary sequence (the complete list of

probability scores assigned to each identified peptide is reported in S2). Such algorithm is capable of predicting the bioactivity of peptides because of the general features that different bioactive peptide functional classes have in common; therefore, PeptideRanker represented a useful tool to select the most probable bioactive peptides. Since the software labeled as “bioactive” any peptide possessing a score above the 0.5 threshold, we applied a higher 0.8 threshold in order to reduce the number of false positive hits. After such filtering of peptide scores, most peptide sequences were rejected.

In Table 4 are shown the 25 potentially bioactive amino acid sequences.

Of the 25 potential bioactive peptides originating from microalgal proteins, six peptides were homologous to protein sequences from *Monoraphidium neglectum* species;

Table 4 Sequences of the 25 potentially bioactive peptides obtained by means of PeptideRanker algorithm

Parent protein (organism)	Peptide sequence	PeptideRanker score	Potential bioactivity	1st dimension fraction
Signal peptide peptidase-like 2B (<i>Monoraphidium neglectum</i>) A0A0D2MLL4	WPRGYFL	0.97	AO	F5
Chlorophyll a-b binding protein, chloroplastic (<i>Tetrademus obliquus</i>) A2SY33	GPDRPKFLGPF	0.96	ACE-inhibitory	F9
Chlorophyll a-b binding protein, chloroplastic (<i>Tetrademus obliquus</i>) A2SY33	WYGPDRPKFL	0.92	ACE-inhibitory	F9
–	SDWDRF	0.92	AO	F11
–	KDPFAPL	0.86	ACE-inhibitory	F9
–	GAGFVYPL	0.86	ACE-inhibitory	F9
–	NDPAGF	0.84	AO	F5
Uncharacterized protein (<i>Monoraphidium neglectum</i>) A0A0D2K3E1	GAGGGALGAGGGVL	0.82	AO	F5
Chlorophyll a-b binding protein, chloroplastic (<i>Tetrademus obliquus</i>) A2SY33	IEWYGPDRPKFL	0.81	ACE-inhibitory	F9
Uncharacterized protein (<i>Monoraphidium neglectum</i>) A0A0D2L6W6	SAAPAGLRPAL	0.8	ACE-inhibitory	F9
–	KPCDVIF	0.8	ACE-inhibitory	F9
–	RFIGPI	0.78	ACE-inhibitory	F9
–	GRSPLLL	0.78	ACE-inhibitory	F9
–	ADVPRF	0.78	AO/ACE-inhibitory	F6
–	SGSWDGTLR	0.77	AO/ACE-inhibitory	F6
–	SDPWVR	0.77	AO	F5
Uncharacterized protein (<i>Monoraphidium neglectum</i>) A0A0D2K8V1	AAAALVCGPLR	0.77	AO	F5
–	GPKDDPAAW	0.76	AO/ACE-inhibitory	F6
–	AQCGELALGWADAP	0.76	AO	F11
Uncharacterized protein (<i>Monoraphidium neglectum</i>) A0A0D2LVM0	SWDGTLR	0.75	AO/ACE-inhibitory	F6
Phosphoglycerate kinase (<i>Monoraphidium neglectum</i>) A0A0D2MS42	SGPEDKFRLTPVAPRL	0.75	ACE-inhibitory	F9
–	QFPVGR	0.75	AO	F5
Photosystem I P700 chlorophyll a apoprotein (<i>Neochloris aquatica</i>) A2A0A140H9L5	QWGADPIHVRPI	0.74	ACE-inhibitory	F9
–	SWIAR	0.73	AO/ACE-inhibitory	F6
–	REPFGR	0.72	AO	F5

– no homology with algal protein sequences

three of these peptides were originated from protein chlorophyll a-b binding protein chloroplastic, a protein belonging to the *Tetrademus obliquus*, and one was homologous to Photosystem I P700 chlorophyll a apoprotein A2 from *Neochloris aquatic*. For the other 15 peptides, no homology with algal protein sequences was found. The reason could be ascribed to two facts: microalgae are non-sequenced organisms and mostly, when non-specific enzymes are used for hydrolysis of precursor proteins, the cleavage rule of peptide production is either missing or not known. This implies different data management workflows for peptide identification, where database search is performed without enzyme specificity [45].

Four peptides, having the greatest score assigned by PeptideRanker, were chemically synthesized to assess their ascribed bioactivity by in vitro assays. The MS/MS spectra of the four identified and synthesized peptides are shown in Fig. S3 (see ESM).

WPRGYFL and SDWDRF were assayed for AO activity taking into account that they came from F5f9 and F10f10 fractions, which gave higher values of ABTS and DPPH radical scavenging activity, respectively. Moreover, also the

characteristic of amino acidic composition and molecular weight of the peptides can greatly affect the biological activity; usually AO peptides are associated with 5–11 amino acid residues. It is well known that the amino acid composition is related to a certain biological activity, for instance a peptide sequence with high amounts of hydrophobic residues at the N-terminal position and aromatic, amphiphilic, and polar amino acid residues at C terminal is likely to influence the AO properties [46]. In fact, the two considered peptides possessed a large number of aromatic residues, two of which were also hydrophobic and they had a low molecular weight of 937 and 824 Da, respectively. The aromatic amino acids (Y, F, and W) could make active oxygen stable through direct electron transfer and hydrophobic amino acids might increase the affinity and reactivity to the cell membrane in the living cells [46]. Results of bioassays are displayed in Fig. 5A, B. As shown in Fig. 5A, B, ABTS radical scavenging activity of peptide WPRGYFL gave a value of EC_{50} of 4405 ng mL^{-1} ($4.70 \text{ } \mu\text{mol L}^{-1}$), while the DPPH radical scavenging activity of SDWDRF peptide was $11,532 \text{ ng mL}^{-1}$ ($13.97 \text{ } \mu\text{mol L}^{-1}$). The obtained results are significantly higher than the AO standard trolox (EC_{50} value $1 \text{ } \mu\text{mol L}^{-1}$) [47], but with respect to

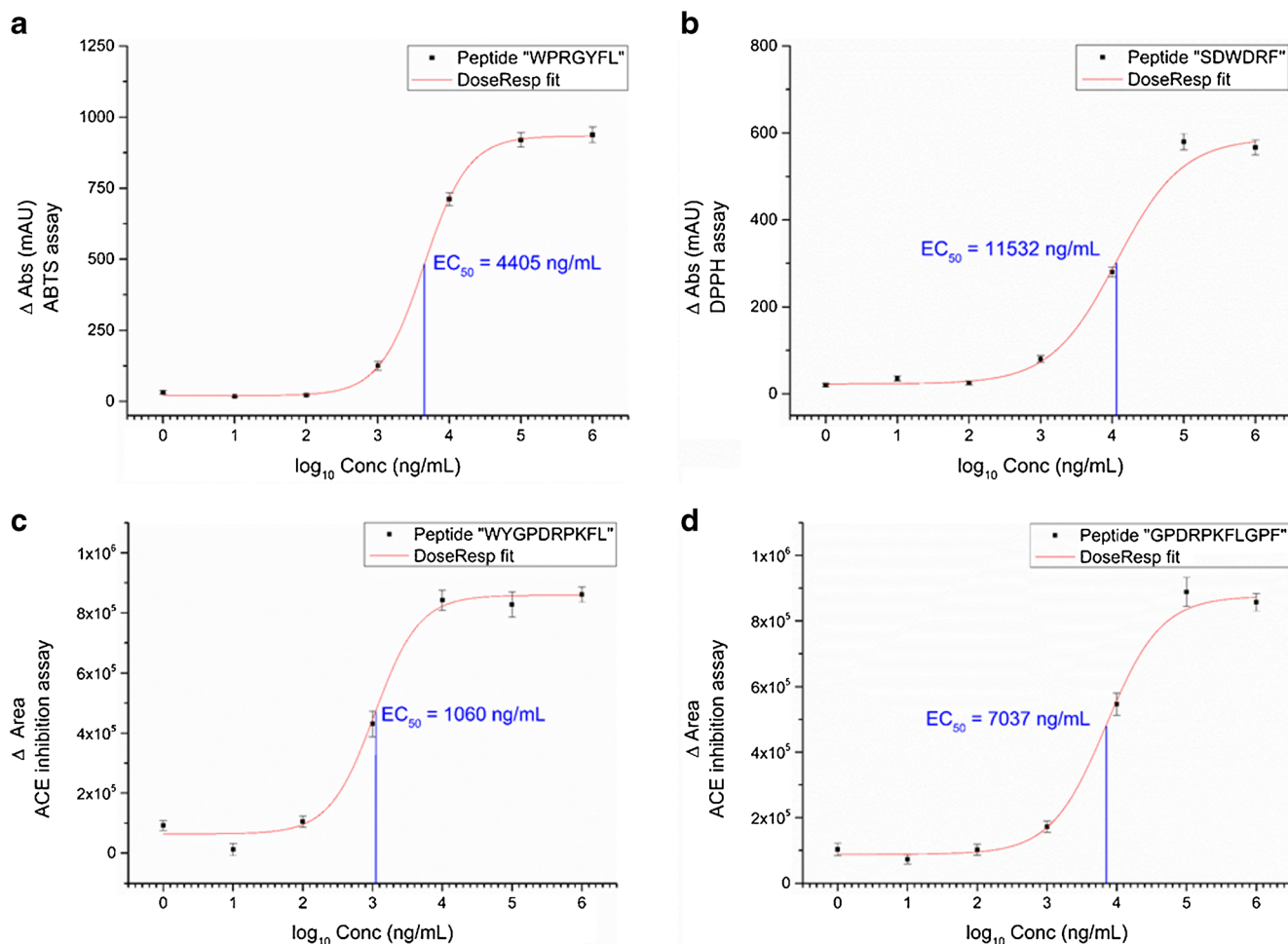


Fig. 5 Graphs reporting the EC_{50} values of the in vitro bioassays for the DPPH and ABTS radical scavenging (A, B) and ACE-inhibitory (C, D) activity

other results obtained for *Chlorella vulgaris* [48], our values for ABTS and DPPH radical scavenging were quite lower. Thus, the AO peptides identified in this study are not as active as the reference drug, but still they are more AO than other peptides isolated from different microalgae species.

Regarding the other two peptides, both GPDRPKFLGPF and WYGPDRPKFL came from F9f6 fraction, which had a percentage of ACE-inhibitory activity of 80%. Usually, a strong antihypertensive activity is related to the presence of hydrophobic and aromatic residues at N and C terminal [49]; the two peptides presented a large number of these kinds of residues (Table 3). In fact, they showed a potent activity, with EC₅₀ values of 5.73 and 0.82 $\mu\text{mol L}^{-1}$, respectively (Fig. 5C, D where the data are reported in ng mL^{-1}). Such results were better than the results obtained for *Chlorella vulgaris*, *Chlorella ellipsoidea*, *Spirulina platensis*, and *Nannochloropsis oculata*, where the lowest IC₅₀ value was around 11 $\mu\text{mol L}^{-1}$ and the highest value was around 300 $\mu\text{mol L}^{-1}$ as reported in a recent review article [10]. With respect to captopril, the most widely used antihypertensive drug, which has an approximate IC₅₀ of 0.0071 $\mu\text{mol L}^{-1}$ [50], GPDRPKFLGPF and WYGPDRPKFL have shown a significantly higher value, indicating that their antihypertensive power is quite lower. The four peptides are, nevertheless, great candidates as functional ingredients in nutraceutical and cosmeceutical fields.

Conclusions

In this study, for the first time the AO and ACE-inhibitory activity of peptides derived from *Tetrademus obliquus* hydrolysates was reported. Some studies presented in literature have investigated the bioactive peptides from marine microalgae but none of these were meticulously performed as required in a peptidomic experiment, probably due to the cultural background of bioactivity studies which is much bioactivity-centered than analytical-centered. In particular, seven extraction protocols were compared in order to choose the best protocol in terms of protein recovery and ease of use from green microalgae, which is a recalcitrant tissue. The mechanical method using glass beads provided high-quality protein extracts and was applied to the entire peptidomic experiments. The paper also highlighted the importance of a precipitation step after extraction for the removal of non-protein interfering compounds, which could lead to an over-estimation of results in terms of protein concentration. After extraction and precipitation, microalgae were subjected to purification and identification by two-dimensional RP-liquid chromatography and RP nanoLC-MS/MS. Around 500 potential bioactive peptides were identified.

The combination with bioinformatics analysis, availed of an algorithm able to assign a score of probability that a peptide

could be bioactive, has allowed to restrict the list of potential candidates for chemical synthesis to a number of 25 amino acidic sequences. Among these, four peptides were synthesized and in vitro assayed. Two novel AO and two novel ACE-inhibitory peptides were then extracted, purified, and identified. Given the good values of biological activity, they appear suitable candidates for future application in the nutraceutical field. Moreover, the use of this modern analytical platform, which greatly excel in sensitivity, resolution, and throughput over those available to the traditional pharmaceutical industry, can be extended to other food matrices, facilitate the discovery and identification of a wealth of novel peptides with nutraceutical potential.

Acknowledgements This work has been carried out within the framework of the Research Project “Microalgae as a source of bioactive compounds: chromatographic fractionation of peptides and lipids and their mass spectrometric characterization,” supported by Sapienza, no. RM11715C82118E74.

Moreover, the authors wish to thank Prof. Francesca Pagnanelli for providing the microalgae samples.

Compliance with ethical standards

Conflict of interest The authors declare that they have no conflict of interest

References

1. Capriotti AL, Cavaliere C, Piovesana S, Samperi R, Laganà A. Recent trends in the analysis of bioactive peptides in milk and dairy products. *Anal Bioanal Chem*. 2016;408:2677–85. <https://doi.org/10.1007/s00216-016-9303-8>.
2. Piovesana S, Capriotti ALAL, Cavaliere C, La Barbera G, Samperi R, Zenezini Chiozzi R, et al. Peptidome characterization and bioactivity analysis of donkey milk. *J Proteome*. 2015;119:21–9. <https://doi.org/10.1016/j.jprot.2015.01.020>.
3. Yu Z, Yin Y, Zhao W, Chen F, Liu J. Application and bioactive properties of proteins and peptides derived from hen eggs: opportunities and challenges. *J Sci Food Agric*. 2014;94:2839–45. <https://doi.org/10.1002/jsfa.6670>.
4. Lafarga T, Hayes M. Bioactive peptides from meat muscle and by-products: generation, functionality and application as functional ingredients. *Meat Sci*. 2014;98:227–39. <https://doi.org/10.1016/j.meatsci.2014.05.036>.
5. Capriotti AL, Cavaliere C, Foglia P, Piovesana S, Samperi R, Zenezini Chiozzi R, Laganà A. Development of an analytical strategy for the identification of potential bioactive peptides generated by in vitro tryptic digestion of fish muscle proteins. *Anal Bioanal Chem* 2015;407. doi: <https://doi.org/10.1007/s00216-014-8094-z>.
6. Halim NRA, Yusof HM, Sarbon NM. Functional and bioactive properties of fish protein hydrolysates and peptides: a comprehensive review. *Trends Food Sci Technol*. 2016;51:24–33. <https://doi.org/10.1016/j.tifs.2016.02.007>.
7. Zenezini Chiozzi R, Capriotti AL, Cavaliere C, La Barbera G, Piovesana S, Samperi R, et al. Purification and identification of endogenous antioxidant and ACE-inhibitory peptides from donkey milk by multidimensional liquid chromatography and nanoHPLC-high resolution mass spectrometry. *Anal Bioanal Chem*. 2016;408:5657–66. <https://doi.org/10.1007/s00216-016-9672-z>.

8. Capriotti AL, Caruso G, Cavaliere C, Samperi R, Ventura S, Zenezini Chiozzi R, et al. Identification of potential bioactive peptides generated by simulated gastrointestinal digestion of soybean seeds and soy milk proteins. *J Food Compos Anal.* 2015;44:205–13. <https://doi.org/10.1016/j.jfca.2015.08.007>.
9. Batista AP, Gouveia L, Bandarra NM, Franco JM, Raymundo A. Comparison of microalgal biomass profiles as novel functional ingredient for food products. *Algal Res.* 2013;2:164–73. <https://doi.org/10.1016/j.algal.2013.01.004>.
10. Ejike CECC, Collins SA, Balasuriya N, Swanson AK, Mason B, Udenigwe CC. Prospects of microalgae proteins in producing peptide-based functional foods for promoting cardiovascular health. *Trends Food Sci Technol.* 2017;59:30–6. <https://doi.org/10.1016/j.tifs.2016.10.026>.
11. Hallenbeck PC, Grogger M, Mraz M, Veverka D. Solar biofuels production with microalgae. *Appl Energy.* 2016;179:136–45. <https://doi.org/10.1016/J.APENERGY.2016.06.024>.
12. Faried M, Samer M, Abdelsalam E, Yousef RS, Attia YA, Ali AS. Biodiesel production from microalgae: processes, technologies and recent advancements. *Renew Sust Energ Rev.* 2017;79:893–913. <https://doi.org/10.1016/J.RSER.2017.05.199>.
13. Duarte JH, Fanka LS, Costa JAV. Utilization of simulated flue gas containing CO₂, SO₂, NO and ash for *Chlorella fusca* cultivation. *Bioresour Technol.* 2016;214:159–65. <https://doi.org/10.1016/J.BIORTECH.2016.04.078>.
14. Kim S-K, Chojnacka K. Marine algae extracts. Weinheim: Wiley-VCH Verlag GmbH & Co. KGaA; 2015.
15. Admassu H, Gasmalla MAA, Yang R, Zhao W. Bioactive peptides derived from seaweed protein and their health benefits: antihypertensive, antioxidant, and antidiabetic properties. *J Food Sci.* 2018;83:6–16. <https://doi.org/10.1111/1750-3841.14011>.
16. Alzahrani MAJ, Perera CO, Hemar Y. Production of bioactive proteins and peptides from the diatom *Nitzschia laevis* and comparison of their in vitro antioxidant activities with those from *Spirulina platensis* and *Chlorella vulgaris*. *Int J Food Sci Technol.* 2017; <https://doi.org/10.1111/ijfs.13642>.
17. Ochoa-Méndez CE, Lara-Hernández I, González LM, Aguirre-Bañuelos P, Ibarra-Barajas M, Castro-Moreno P, et al. Bioactivity of an antihypertensive peptide expressed in *Chlamydomonas reinhardtii*. *J Biotechnol.* 2016;240:76–84. <https://doi.org/10.1016/j.jbiotec.2016.11.001>.
18. Piovesana S, Capriotti AL, Cavaliere C, La Barbera G, Montone CM, Zenezini Chiozzi R, Laganà A. Recent trends and analytical challenges in plant bioactive peptide separation, identification and validation. *Anal Bioanal Chem* 2018; 852. <https://doi.org/10.1007/s00216-018-0852-x>.
19. Harnedy PA, O’Keeffe MB, FitzGerald RJ. Fractionation and identification of antioxidant peptides from an enzymatically hydrolysed *Palmaria palmata* protein isolate. *Food Res Int.* 2017;100:416–22. <https://doi.org/10.1016/J.FOODRES.2017.07.037>.
20. Neves AC, Harnedy PA, O’Keeffe MB, FitzGerald RJ. Bioactive peptides from Atlantic salmon (*Salmo salar*) with angiotensin converting enzyme and dipeptidyl peptidase IV inhibitory, and antioxidant activities. *Food Chem.* 2017;218:396–405. <https://doi.org/10.1016/j.foodchem.2016.09.053>.
21. Zenezini Chiozzi R, Capriotti AL, Cavaliere C, La Barbera G, Piovesana S, Laganà A. Identification of three novel angiotensin-converting enzyme inhibitory peptides derived from cauliflower by-products by multidimensional liquid chromatography and bioinformatics. *J Funct Foods.* 2016;27:262–73. <https://doi.org/10.1016/j.jff.2016.09.010>.
22. Cuellar-Bermudez SP, Aguilar-Hernandez I, Cardenas-Chavez DL, Omelas-Soto N, Romero-Ogawa MA, Parra-Saldivar R. Extraction and purification of high-value metabolites from microalgae: essential lipids, astaxanthin and phycobiliproteins. *Microb Biotechnol.* 2015;8:190–209. <https://doi.org/10.1111/1751-7915.12167>.
23. Di Caprio F, Visca A, Altamari P, Toro L, Iaquaniello G, Pagnanelli F. Two stage process of microalgae cultivation for starch and carotenoid production. *Chem Eng Trans.* 2016;49:415–20. <https://doi.org/10.3303/CET1649070>.
24. Capriotti AL, Cavaliere C, Piovesana S, Stampachiachiere S, Ventura S, Zenezini Chiozzi R, et al. Characterization of quinoa seed proteome combining different protein precipitation techniques: improvement of knowledge of nonmodel plant proteomics. *J Sep Sci.* 2015;38:1017–25. <https://doi.org/10.1002/jssc.201401319>.
25. Capriotti AL, Cavaliere C, Ferraris F, Gianotti V, Laus M, Piovesana S, et al. New Ti-IMAC magnetic polymeric nanoparticles for phosphopeptide enrichment from complex real samples. *Talanta.* 2018;178:274–81. <https://doi.org/10.1016/j.talanta.2017.09.010>.
26. Muñoz R, Navia R, Ciudad G, Tessini C, Jeison D, Mella R, et al. Preliminary biorefinery process proposal for protein and biofuels recovery from microalgae. *Fuel.* 2015;150:425–33. <https://doi.org/10.1016/J.FUEL.2015.02.004>.
27. Jensen SK. Improved Bligh and Dyer extraction procedure. *Lipid Technol.* 2008;20:280–1. <https://doi.org/10.1002/lite.200800074>.
28. Abedini Najafabadi H, Pazuki G, Vossoughi M. Experimental study and thermodynamic modeling for purification of extracted algal lipids using an organic/aqueous two-phase system. *RSC Adv.* 2015;5:1153–60. <https://doi.org/10.1039/C4RA11914B>.
29. Matyash V, Liebisch G, Kurzchalia TV, Shevchenko A, Schwudke D. Lipid extraction by methyl-tert-butyl ether for high-throughput lipidomics. *J Lipid Res.* 2008;49:1137–46. <https://doi.org/10.1194/jlr.D700041-JLR200>.
30. Yoo G, Park W-K, Kim CW, Choi Y-E, Yang J-W. Direct lipid extraction from wet *Chlamydomonas reinhardtii* biomass using osmotic shock. *Bioresour Technol.* 2012;123:717–22. <https://doi.org/10.1016/J.BIORTECH.2012.07.102>.
31. Re R, Pellegrini N, Proteggente A, Pannala A, Yang M, Rice-Evans C. Antioxidant activity applying an improved ABTS radical cation decolorization assay. *Free Radic Biol Med.* 1999;26:1231–7. [https://doi.org/10.1016/S0891-5849\(98\)00315-3](https://doi.org/10.1016/S0891-5849(98)00315-3).
32. Mooney C, Haslam NJ, Pollastri G, Shields DC. Towards the improved discovery and design of functional peptides: common features of diverse classes permit generalized prediction of bioactivity. *PLoS One.* 2012;7:e45012. <https://doi.org/10.1371/journal.pone.0045012>.
33. Klimek-Ochab M, Brzezińska-Rodak M, Zymańczyk-Duda E, Lejczak B, Kafarski P. Comparative study of fungal cell disruption—scope and limitations of the methods. *Folia Microbiol (Praha).* 2011;56:469–75. <https://doi.org/10.1007/s12223-011-0069-2>.
34. Nagai K, Yotsukura N, Ikegami H, Kimura H, Morimoto K. Protein extraction for 2-DE from the lamina of *Ecklonia kurome* (laminariales): recalcitrant tissue containing high levels of viscous polysaccharides. *Electrophoresis.* 2008;29:672–81. <https://doi.org/10.1002/elps.200700461>.
35. Bradford MM. A rapid and sensitive method for the quantitation of microgram quantities of protein using the principle of protein dye binding. *Anal Biochem.* 1976;72:248–54. [https://doi.org/10.1016/0003-2697\(76\)90527-3](https://doi.org/10.1016/0003-2697(76)90527-3).
36. Peterson GL. Review of the Folin phenol protein quantitation method of Lowry, Rosebrough, Farr and Randall. *Anal Biochem.* 1979;100:201–20. [https://doi.org/10.1016/0003-2697\(79\)90222-7](https://doi.org/10.1016/0003-2697(79)90222-7).
37. González López CV, del Carmen Cerón García M, Fernández FGA, Bustos CS, Chisti Y, Sevilla JMF. Protein measurements of microalgal and cyanobacterial biomass. *Bioresour Technol.* 2010;101:7587–91. <https://doi.org/10.1016/j.biortech.2010.04.077>.
38. Barka A, Blecker C. Microalgae as a potential source of single-cell proteins. A review. *Biotechnol Agron Soc Environ.* 2016;20:427–36.

39. González-García E, Marina ML, García MC. Plum (*Prunus domestica* L.) by-product as a new and cheap source of bioactive peptides: extraction method and peptides characterization. *J Funct Foods*. 2014;11:428–37. <https://doi.org/10.1016/J.JFF.2014.10.020>.
40. Awuor OL, Edward Kirwa M, Betty M, Jackim MF (2017) Optimization of Alcalase hydrolysis conditions for production of Dagaa (*Rastrineobola argentea*) protein hydrolysate with antioxidative properties. *Ind Chem*; 3. <https://doi.org/10.4172/2469-9764.1000122>.
41. Jeong H-S, Kim H-Y, Ahn SH, Oh SC, Yang I, Choi I-G. Optimization of enzymatic hydrolysis conditions for extraction of pectin from rapeseed cake (*Brassica napus* L.) using commercial enzymes. *Food Chem*. 2014;157:332–8. <https://doi.org/10.1016/j.foodchem.2014.02.040>.
42. Kalli A, Smith GT, Sweredoski MJ, Hess S. Evaluation and optimization of mass spectrometric settings during data-dependent acquisition mode: focus on LTQ-Orbitrap mass analyzers. *J Proteome Res*. 2013;12:3071–86. <https://doi.org/10.1021/pr3011588>.
43. Gilar M, Olivova P, Daly AE, Gebler JC. Two-dimensional separation of peptides using RP-RP-HPLC system with different pH in first and second separation dimensions. *J Sep Sci*. 2005;28:1694–703. <https://doi.org/10.1002/jssc.200500116>.
44. Furuta T, Miyabe Y, Yasui H, Kinoshita Y, Kishimura H. Angiotensin I converting enzyme inhibitory peptides derived from phycobiliproteins of dulce *Palmaria palmata*. *Mar Drugs*. 2016;14:32. <https://doi.org/10.3390/md14020032>.
45. Connolly A, O’Keeffe MB, Piggott CO, Nongonierma AB, FitzGerald RJ. Generation and identification of angiotensin converting enzyme (ACE) inhibitory peptides from a brewers’ spent grain protein isolate. *Food Chem*. 2015;176:64–71. <https://doi.org/10.1016/j.foodchem.2014.12.027>.
46. Sheih I-CC, Wu T-KK, Fang TJ. Antioxidant properties of a new antioxidative peptide from algae protein waste hydrolysate in different oxidation systems. *Bioresour Technol*. 2009;100:3419–25. <https://doi.org/10.1016/j.biortech.2009.02.014>.
47. Nimmi OS, George P. Evaluation of the antioxidant potential of a newly developed polyherbal formulation for antiobesity. *Int J Pharm Pharm Sci*. 2012;4:505–10.
48. Brahmachari G. Chemistry and pharmacology of naturally occurring bioactive compounds. 1st ed. Boca Raton: CRC Press; 2013.
49. Wang Q. Preparation of functional peanut oligopeptide and its biological activity. In: Peanut processing characteristics and quality evaluation. Singapore: Springer Singapore; 2018. p. 461–537.
50. Tsai J-S, Chen T-J, Pan BS, Gong S-D, Chung M-Y. Antihypertensive effect of bioactive peptides produced by protease-facilitated lactic acid fermentation of milk. *Food Chem*. 2008;106:552–8. <https://doi.org/10.1016/J.FOODCHEM.2007.06.039>.



Sensitive untargeted identification of short hydrophilic peptides by high performance liquid chromatography on porous graphitic carbon coupled to high resolution mass spectrometry

Susy Piovesana^a, Carmela Maria Montone^a, Chiara Cavaliere^{a,*}, Carlo Crescenzi^b,
Giorgia La Barbera^a, Aldo Laganà^a, Anna Laura Capriotti^a

^a Department of Chemistry, Università di Roma "La Sapienza", Piazzale Aldo Moro 5, 00185 Rome, Italy

^b Department of Pharmacy, University of Salerno, Via Giovanni Paolo II, 132, I-84084 Fisciano, SA, Italy

ARTICLE INFO

Article history:

Received 26 September 2018

Received in revised form

14 December 2018

Accepted 30 December 2018

Available online 31 December 2018

Keywords:

Short peptides

Porous graphitic carbon

Supercharging agents

Mass spectrometry

Serum

Bioactive peptides

ABSTRACT

The combination of an efficient chromatographic separation with post-column addition of a supercharging agent was evaluated for the determination of small peptides. The procedure takes advantage of porous graphitic carbon (PGC) ability in retaining very polar and ionic molecules to overstep the poor retention of small peptides on conventional reversed phase (RP) columns. The method was developed specifically for the most hydrophilic di-, tri- and tetrapeptides, which are not identified in ordinary peptidomics experiments. In addition to retention mechanisms acting on conventional RP, the method exploited the charge induced interactions generated by the charges on the peptides with the polarizable surface of PGC. This results in efficient retention of very short and highly polar peptides using classical RP mobile phases. The effects of varying mobile phase composition (organic solvent and ion-pairing additives) as well as column temperature have been thoroughly investigated using short peptide standards. Under optimized conditions (water and acetonitrile/tetrahydrofuran 99:1 (v/v), both with 0.15% trifluoroacetic acid, as phase A and B, respectively, 0.5 mL min⁻¹ flowrate at 50 °C) the effect of post-column addition of 3-nitrobenzyl alcohol was also investigated allowing effective coupling of the chromatographic system with high resolution mass spectrometry. Finally, an untargeted approach for peptide identification was pursued, based on precursor identification in database with all possible combinations of the 20 natural amino acids and fragmentation spectra matching to *in silico* generated spectra. The method was then applied to investigation of the short endogenous peptides in human serum from healthy individuals resulting in the identification of 30 short peptides.

© 2019 Elsevier B.V. All rights reserved.

1. Introduction

The identification of peptides has been growing an importance of its own, becoming an independent field in the omics approaches usually referred to as peptidomics [1]. The interest in this field is boosted by well-established potential of peptides in diagnostic and therapeutic use. In fact, there are accumulating evidences that certain endogenous peptides in biofluids, for long time considered as waste products, mediate specific functions, for instance, in modulating cancer cells aggressiveness [2] or may serve as biomarkers for diseases [3]. In this context, endogenous peptides can be investigated in biofluids and tissues [4]. Another important application field is the search for short bioactive peptides in food or derived with health-promoting activities, such as antioxidant, antihyper-

tensive and antimicrobial properties [5–8]. Currently, the market for peptide and protein drugs accounts for more than 10% of the pharmaceutical market and this sector is growing much faster than that of small molecules drugs [9]. According to US-FDA, "peptide" is any alpha amino acid polymer with specific defined sequence that is 40 amino acids or less in size [10]. Among the over 100 approved peptide-based therapeutics on the market, the majority is smaller than 20 amino acids [11].

In either field, the use of advanced analytical techniques for separation and identification of peptides is mandatory. More specifically, challenges still exist for the low molecular weight window of the peptidome, especially shorter peptide sequences (< 5 amino acid long), which remains under-investigated. Even in this limited field, physicochemical properties of small peptides span over "small molecule" and "large molecule" classification and over a very broad range of polarity, from charged molecules to more lipophilic ones. Direct MS/MS-based approaches for identification of short, non-

* Corresponding author.

E-mail address: chiara.cavaliere@uniroma1.it (C. Cavaliere).

tryptic peptides without prior derivatization are limited and mainly restricted to the analysis of food protein hydrolysates [12–14].

There are three main problems with the analysis of very short peptide sequences. The first one is related to the wide range of polarity of such peptides, which makes the typical C18 reversed phase (RP) separation unsuitable for separation of very hydrophilic peptides. Moreover, very hydrophilic peptides can be lost during the common desalting step [15] or during analysis if the chromatographic method comprises an on-line precolumn enrichment. The use of different separation strategies can help in retaining such short sequences, as recently described for short angiotensin-converting-enzyme inhibitor peptides in Tilapia [16]. Hydrophilic interaction chromatography has also been suggested for separation of short peptide sequences [12] and combination with reversed phase for separation of short isobaric peptides [17].

The second problem with short peptide sequences analysis is related to spectra bioinformatic interpretation. The ordinary shotgun proteomics database search usually cannot identify sequences shorter than 5 amino acids. Search engine scores are usually low for short sequences [18], and different short peptide sequences can be isobaric. Some approaches have been suggested to solve this problem: 1) target MS analysis using standard compounds for which retention time (t_R) and mass data are recorded; 2) *de novo* sequence identification [14]; 3) retention time prediction [12].

The third problem is connected to MS detection. Short peptides do not easily become at least doubly positively charged, a limitation which reduces the information acquired by MS/MS experiments as background noise is increased and fragmentation of the backbone is reduced [13]. A different MS approach needs to be pursued, and fragmentation energy becomes a fundamental parameter to be evaluated to optimize fragmentation and peptide identification [13,19].

In this context, porous graphitic carbon (PGC) can be a suitable system for separation of short peptides sequences, as multiple retention mechanisms can be exploited. Its ability in retaining very polar and ionic molecules [20,21] was previously employed for fractionating short peptides and phosphopeptides in wine [22], desalting flow-through fractions from a C18 column [15] or separation of underivatized di-, tri-, tetrapeptides using nonafluoropentanoic acid as an ion pair reagent and evaporative light scattering detection [23] but never in direct coupling with MS detection.

In the present paper, a strategy for underivatized short peptide identification in complex samples is provided. Firstly, the chromatographic issues were solved using PGC as stationary phase for separation of di-, tri- and tetra-peptides. The chromatographic conditions (mobile phase composition, ion-pairing modifiers, column temperature) were optimized to improve peak shape and resolution under MS compatible conditions. Secondly, separation of small peptides on PGC was coupled with high resolution (HR)MS and ionization improved by post-column addition of 3-nitrobenzyl alcohol (3-NBA) to boost sensitivity. High resolution tandem MS using data dependent mode was used for spectra acquisition. Thirdly, an untargeted investigation based on suspect screening is provided for short peptide identification. A database with all possible combinations of the 20 natural amino acids within di-, tri- and tetrapeptides was compiled with both precursor and fragment exact masses and used for searching of experimental spectra. Finally, the developed method was applied for characterization of di-, tri- and tetrapeptides in human serum.

2. Materials and methods

2.1. Materials

Optima® LC–MS grade water, acetonitrile (ACN) and methanol (MeOH) were purchased from Thermo Fisher Scientific (Waltham,

Massachusetts, USA). Trifluoroacetic acid (TFA) and tetrahydrofuran (THF) were supplied by Romil Ltd (Cambridge). Formic acid and 3-NBA were purchased from Sigma-Aldrich (Germany). Synthetic peptides Gly-Asp-Leu-Glu (GDLE), Leu-Pro-Leu (LPL), Ile-Pro-Pro-Leu (IPPL), Lys-His (KH), Pro-Ile (PI), Arg-Phe (RF), Ser-His (SH), Val-Glu-Pro (VEP), Val-Arg-Gly-Pro (VRGP), Arg-Lys-Lys-His (RKKH), Pro-Leu (PL), Ile-Pro-Ile (IPI), Leu-Pro (LP), Lys-His-Lys (KHK) were also purchased from Thermo Fisher Scientific (Ulm, Germany). Peptides stock solutions were prepared at 1 mg mL⁻¹ concentration in H₂O/TFA, 99:1 (v/v); two working solutions were prepared by dilution of stock solutions at 1 ng μL⁻¹.

2.2. Ultra-high performance liquid chromatography-HRMS analysis

The ultra-high performance liquid chromatography system was a Vanquish binary pump H (Thermo Fisher Scientific, Bremen, Germany), equipped with a thermostated auto-sampler and a thermostated column compartment. The separation was carried out at 0.5 mL min⁻¹ flow rate. Ten μL of each sample were injected onto a Hypercarb™ Porous Graphitic Carbon LC Column (50 × 2.1 mm, 3 μm particle size). We strongly recommend to properly connect the PGC column to the grounding systems, typically included in standard modern ESI interfaces for safety reason, in order to avoid the potential oxidation of the PGC stationary phase [24]. In the best conditions, the column was maintained at 50 °C using the still air option. Peptides were eluted using H₂O (phase A) and ACN with 1% THF (v/v) (phase B) both with 0.15% of TFA (v/v), with post-column addition of ACN with 1.2% 3-NBA at 0.1 mL min⁻¹. The chromatographic gradient was the following: 0% B for 2 min, 0–35% B in 15 min, 35–90% B in 8 min; at the end of the gradient, a washing step was inserted at 90% B for 3 min and a re-equilibration step at 0% B for 7 min. The chromatographic system was coupled to a hybrid quadrupole-Orbitrap mass spectrometer Q Exactive (Thermo Fisher Scientific) using a heated electrospray ionization (ESI) source. The ESI source was operated in positive mode under the following conditions: 220 °C capillary temperature, 50 (arbitrary units) sheath gas, 25 (arbitrary units) auxiliary gas, 0 (arbitrary units) sweep gas, 3200 V spray voltage, 280 °C auxiliary gas heater temperature, 50 (%) S-Lens RF level. For all the investigated chromatographic conditions, the detection was conducted in HRMS top five data dependent acquisition mode in the range m/z 150–2000 with a resolution (full width at half maximum, FWHM, m/z 200) of 70,000. Automatic gain control (AGC) target value was 500,000 in full scan, with a max ion injection time set of 100 ms. Isolation window width was 2 m/z . Higher-energy collisional dissociation (HCD) fragmentation was performed at 40% normalized collision energy at resolution (FWHM, @ m/z 200) of 140,000. AGC target value was 10,000. Dynamic exclusion was set to 3 s. An exclusion list containing the most abundant ions commonly detected in the blank was set. Three blank samples were acquired and used to create an exclusion list with masses therein present. The new method with exclusion list was used for final acquisition of peptide samples in triplicate analysis.

2.3. Data analysis and peptide identification

Matlab R2018a was used to generate all possible amino acid combinations in di- tri- and tetrapeptides, which resulted in 168,400 combinations. Duplicate masses were removed and database reduced to 18,533 combinations. The sequences database was completed with exact m/z values for singly charged precursor ions, doubly charged precursor ions (only for tri- and tetrapeptides), triply charged ions (tetrapeptides only) and quadruply charged ions (tetrapeptides only). The freeware MZmine 2 (v2.26, <http://mzmine.sourceforge.net/>) [25] was used to search the

database thus created for precursors in the acquired HRMS spectra. Briefly, data were imported, and a list of ions for each scan was generated using a mass detection module (Exact mass algorithm with noise 1E4). A filter was applied to correct the false signals around m/z peaks, called shoulder peaks that are residues of the Fourier Transform function (Gaussian peak model function). Then, mass lists generated and filtered for each MS scan were used to build a chromatogram for each mass that could be detected continuously over the scans by means of the chromatogram builder tool (minimum time span 0.5 min; minimum height 5E4; m/z tolerance 0.001 or 5 ppm). Later, the deconvolution module deconvoluted these chromatograms into individual peaks (local minimum search algorithm with chromatographic threshold 30; minimum t_R range 0.05 min); minimum relative height 0%; minimum absolute height 5E4; minimum top/edge 1.5; peak duration 5 min). With the isotopic peak grouper algorithms, the isotopic peaks were removed from the peak list keeping only the highest peak (m/z tolerance 0.001 or 5 ppm; t_R tolerance 0; maximum charge 4; most intense representative isotope). The peak lists obtained for samples and the blanks were aligned with the Join alignment module (m/z tolerance 0.001 or 5 ppm; t_R tolerance 0.1 min; weight for m/z 70; weight for t_R 30). Peaks coming from the blank were subtracted. Only repeatable features (peaks common to all three replicates) were considered for further analysis.

mMass [26] was then used to generate and match fragment ion spectra for identification. The following parameters were selected from the software interface: S/N threshold = 1.0, apply baseline and smoothing; the sequence editor section was set as follows: regular amino acid sequence type, max charge = 2, product ion types = M, im, a, b, c, x, y, z, inta, intb, Nladder, Cladder, $-H_2O$, $-NH_3$, tolerance = 0.01 Da. Each spectral matching was finally manually checked.

Clarity (Antec Scientific) was used to calculate the following chromatographic parameters: peak area, peak height, W_{05} (min), skew, asymmetry, efficiency [theoretical plates], Eff/I [t.pl/m], peak capacity and used for optimization of the chromatographic conditions (Table S-1 summarises all data calculated as mean with standard deviation from the three runs per condition).

Partial least squares (PLS) model was calculated using NIPALS algorithm as implemented in The Unscrambler® X version 10.5 by CAMO Software AS (Oslo Science Park, NORWAY).

2.4. Serum sample preparation

Commercial serum (1 mL, Sigma-Aldrich) was centrifuged at 4 °C, at 18,000 × g for 30 min, then 4 mL of cold acetone was added, following a previously reported procedure with some modification [27]. The precipitation was carried out overnight at –20 °C. The sample was centrifuged (4000 × g for 15 min at 4 °C), then the pellet was washed 3 times with cold acetone; the supernatants were pooled and evaporated under gentle nitrogen flow. The residue was reconstituted with 200 μL of H_2O with 0.1% HCOOH. Ten μL of each sample were injected and analyzed as previously described. Experiments were performed in triplicate.

3. Results and discussion

3.1. Chromatographic separation of short peptides on PGC

In the first step of the study, a set of 14 short peptide standards was exploited to optimize an efficient chromatographic separation for small peptides suitable for coupling with sensitive ESI-MS detection. For this purpose, a PGC column was evaluated in combination with different organic solvents and additives as shown in Table 1. As the PGC surface retention mechanism is consistently

Table 1 Summary of the experimental conditions tested for peptide standards separation and related advantages and disadvantages.

	Mobile phase A	Mobile phase B	Mobile phases additives	Temp (°C)	post-column addition	Peptide identifications	Pros	Cons	Further evaluation
1	H ₂ O	ACN	–	40	–	10/14	–	Broad peaks	–
2	H ₂ O	ACN/THF (99:1, v/v)	FA (0.1, 0.5 or 1%)	40	–	14/14	–	4 peptides elute with the dead volume RKKH not detected	–
5	H ₂ O	ACN/THF (99:1, v/v)	0.1% TFA	40	–	13/14	Good peak height and area; LP/PI separated	–	–
6	H ₂ O	ACN/THF (99:1, v/v)	0.1% TFA	50	–	13/14	Good peak shape, efficiency, peak capacity; LP/PI separated	RKKH not detected	TFA % (0.05% and 0.15%)
7	H ₂ O	ACN/THF (99:1, v/v)	0.1% TFA	60	–	13/14	–	LP/PI not separated; peaks too sharp	–
8	H ₂ O	ACN/THF (99:1, v/v)	0.05% TFA	50	–	12/14	–	LP/PI not separated	–
9	H ₂ O	ACN/THF (99:1, v/v)	0.15% TFA	50	–	14/14	RKKH detected	LP/PI not completely resolved	NBA
10	H ₂ O	MeOH/THF (99:1, v/v)	0.1% TFA	40	–	–	–	Pressure too high	–
11	H ₂ O	MeOH/THF (99:1, v/v)	0.1% TFA	50	–	13/14	–	–	TFA % (0.05% and 0.15%)
12	H ₂ O	MeOH/THF (99:1, v/v)	0.1% TFA	60	–	13/14	–	LP/PI not separated	–
13	H ₂ O	MeOH/THF (99:1, v/v)	0.05% TFA	50	–	12/14	–	–	–
14	H ₂ O	MeOH/THF (99:1, v/v)	0.15% TFA	50	–	13/14	–	RKKH not detected	–
15	H ₂ O	ACN/THF (99:1, v/v)	0.15% FA	50	ACN with 1.2% NBA	14/14	RKKH detected; doubly charged ions preferred; increase in signal intensity	LP/PI not completely resolved	Selected for real sample analysis

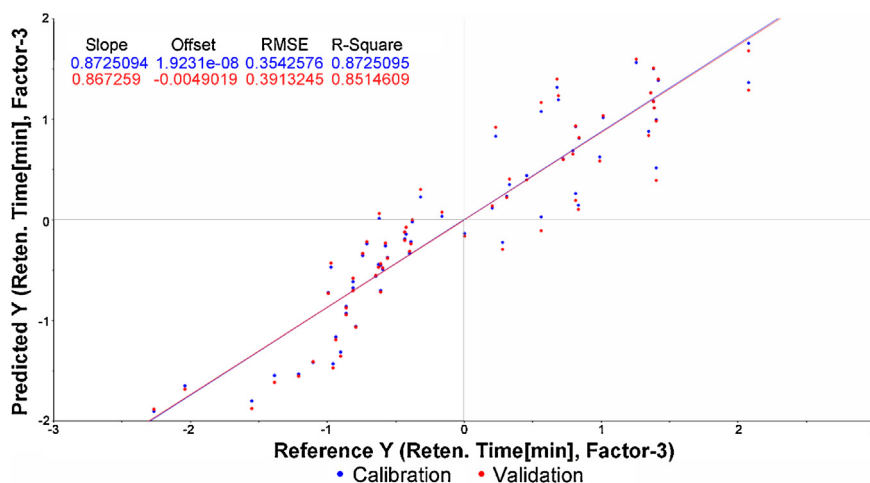


Fig. 1. PLS response plot: cross-validation predicted vs reference value for regression coefficients, root mean square error and coefficients of determination.

affected by previously injected samples unless a proper “maintenance step” is optimized [28], in our study 1% of THF was added in mobile phase B in order to assure complete restoration of the original conditions and to prevent contamination by peptides with aromatic side chains [23].

Initially, unbuffered mobile phase in a simple gradient of ACN in water was used for short peptide separation. Some peaks exhibited poor peak shape (they were broad more than a minute) and some standards were not eluted at all (KH, GDLE, RKKH, KHK). Therefore, different acidic additives were exploited to investigate the balance between the two retention mechanisms expected to be involved in the retention of peptides, i.e. RP and electronic interaction [29]. In fact, according to the general retention model for very polar molecules on PGC as described by Knox and Ross [30], this sorbent is not a “pure carbon reversed phase”, as it demonstrated a surprising ability in retaining even ions via charge-induced interactions with the graphitic surface. Electronic interaction was also extended to organic anions [31,32]. While anions were retained by electronic interaction with the PGC surface and their retention was reduced by addition TFA (used as competitor), cations were poorly retained or not retained depending on charge distribution and their retention could be increased with TFA (this time used as ion pairing reagent) [32]. In the case of peptides, their zwitterionic nature will make their retention be dependent on their charge states and mobile phase composition (for details on the physico-chemical features of standard peptides see Table S-2).

3.1.1. Effect of organic modifier and acidic additives

In our experiments, regardless of formic acid concentration, retention times were reduced for all the analytes compared to the separation using unbuffered mobile phase, with some peptides being eluted with the dead volume (KH, RKKH, KHK and SH). Such behaviour can be ascribed to formic acid insufficient hydrophobicity as ion-pairing agent while competing for the polar interactions of carboxyl side chains with the PGC surface.

On the contrary, the use of TFA in water/ACN gradients improved analyte retention in all cases (Table S-1, Figure S-1). Experiments with TFA indicated that an increase of phase acidity positively impacted on peak areas and height, which were generally increased under these conditions, probably due to an improved ionisation of the investigated peptides. Also, peak shapes were generally improved (W_{05} and asymmetry), as well as efficiency and peak capacity. As far as identification was concerned, at 0.05% TFA 12 peptides out of 14 could be detected, within t_R 1.66–9.69 min. KHK and RKKH could not be detected. Increasing the percent of

TFA to 0.1% and 0.15% increased t_R for all peptides (Figure S-1), to 4.24–10.67 min and 4.91–12.28 min, respectively, while allowing detection of 13 peptides out of 14: RKKH was not detected at 0.1% TFA and PI and LP isobars could not be completely resolved at 0.15% TFA. Despite the decreased selectivity for separation of peptide isomers, 0.15% TFA was selected as RKKH could be identified while remained undetected under all other tested conditions.

A PLS model was used to interpret these behaviours using non-linear iterative partial least squares (NIPALS) algorithm based on grand average of hydrophathy (GRAVY), molecular weight and isoelectric point as reported in Table S-2. These factors were analysed toward the retention time (t_R) at three TFA concentration levels and three different temperatures. When using ACN as organic modifier, the regression model (Fig. 1) could explain more than 85% of the contribute to the t_R variance (Figure S-5). In particular, 80% of the variance was explained by factor 1, which mainly depended on analyte polarity (it increases with the increase in molecular weight and decreases with decreasing GRAVY value, Figure S-6, S-7). Experimentally, analyte t_R was shown to increase with the increase of the concentration of TFA, which allowed to infer that the prevailing mechanism was similar to ion pair chromatography. Consequently, the high value of the coefficient of determination and a similar value obtained in cross validation indicated that the model had adequate predictive ability.

A significant difference is observed when MeOH is used as organic modifier (Figure S-2). In this case, the increase of TFA from 0.05% to 0.15% also generally increased analyte retention, but some exceptions were observed, for SH and VEP, for which a U-shaped trend could be observed: retention decreased from 0.05% to 0.1% TFA but increased again at 0.15% TFA (Figure S-2). This behaviour was likely due to role of the hydrogen-bond in both retention and solvation attributed to the multiple retention mechanisms of PGC. In this case, the same PLS model explained approximately 50% of the retention time variance. This observation suggested the presence of an additional relevant interaction, such as the hydrogen bond.

3.1.2. Effect of temperature

Temperature effect was investigated at three levels (40 °C, 50 °C, 60 °C) and 0.1% TFA concentration (for MeOH, 40 °C could not be investigated due to a backpressure exceeding the maximum one for the column in use). Increase of temperature resulted in faster elution and narrower peaks. In ACN, extremely sharp peaks were obtained at 60 °C even causing problems in proper peak acquisition. At this temperature the two isobaric compounds LP and PI coeluted

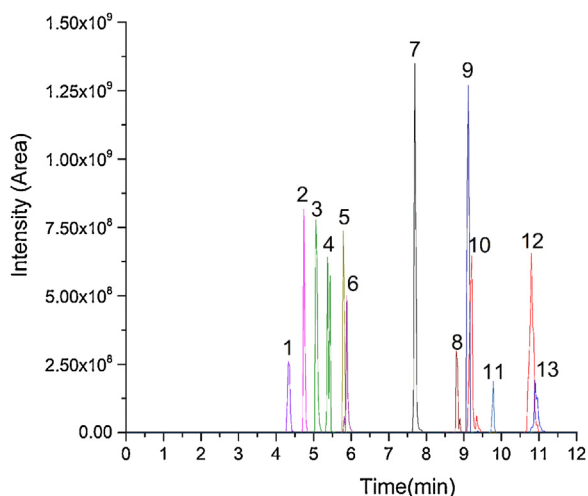


Fig. 2. Extracted ion chromatogram of the short peptide mixture under the final chromatographic conditions (10 μL injected volume, 1 $\mu\text{g } \mu\text{L}^{-1}$ concentration). Analyte order: SH (1), KH (2), PL (3), LP and PI (4), KHK (5), VEP (6), GDLE (7), VRGP (8), RF (9), LPL (10), RKKH (11), IPI (12), IPPL (13).

(Table S-1, Figure S-3). Peak area and height were better for 40 °C runs, whereas shape (W_{05} , skew, asymmetry) was better for 50 °C runs as well as efficiency and peak capacity.

Compared to ACN, when using MeOH as organic modifier the increase in temperature resulted in a more consistent decrease of the retention (Table S-1, Figure S-4). As well as in the previous separation using ACN, the decreased retention caused PI and LP to coelute at 60 °C. The best performance was found at 50 °C for both organic solvents.

3.1.3. Post-column addition of 3-NBA

After comparison between results with 0.15% TFA in ACN and MeOH, the latter was rejected and no longer optimized, as RKKH was detected only in ACN mobile phase. ACN with 0.15% TFA was finally tested with signal enhancing agent 3-NBA (Fig. 2).

Despite the general observation of suppression of ESI signal by TFA, such phenomenon was not observed in the optimization of short peptide separation, as peak areas were larger and peak intensities higher by increasing TFA up to 0.15%. Still, short peptides pose problems with ESI and ionize as singly charged species, which in turn affects subsequent data dependent ion fragmentation and decreases analyte detection due to the large abundance of singly charged contaminants and high background noise. 3-NBA, as supercharging agent [33], was therefore post-column added in order to improve ESI detection without affecting the chromatographic separation. 3-NBA generated a consistent increase of the signal for all the analyte up to 18-fold (Fig. 3, Table S-1).

3.2. Untargeted identification of short peptides and application to serum samples

For identification of short peptide in complex samples, in this work an untargeted analysis by suspect screening investigation was performed. Untargeted analysis by suspect screening is much more used in environmental analysis and in investigation of structurally related compounds [34–36]. The advantage of this approach is that it can be employed when there are no reference standards but a list of possible target compounds is available, which can be used to create a database with compound-specific information, in particular molecular formula, isotopic pattern, structure and mass spectra, if available. Such database is then used to search the experimental HRMS spectra for tentative compounds identification. Given that for the 20 natural amino acids the number of combinations making

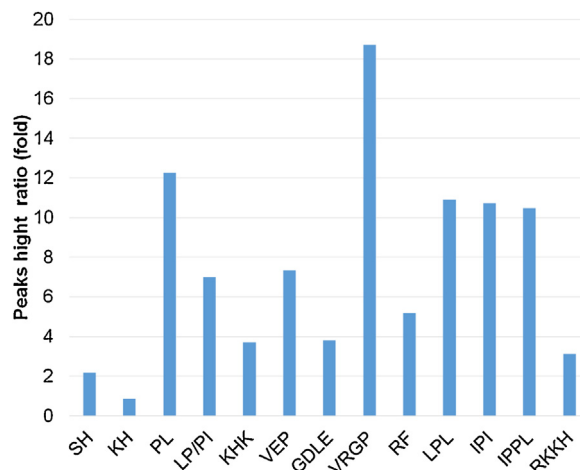


Fig. 3. Signal increase obtained by post-column addition of 3-NBA. For details, see Table S-1.

up di-, tri- and tetra-peptides is limited, all possible combinations were computed with exact masses and used to extract precursor masses from the experimental spectra. The product ions list from the experimental fragmentation spectra was used for matching to the in silico generated product ions list associated with the probable peptide sequences matching the exact precursor mass. The matching is reported both as table and visual identification of matched product ions between the in silico and the experimental product ions lists. Peptides were identified by matching different product ions, in particular *a*, *b* and *y* fragments, as well as immonium ions arising from internal fragmentation. If more than one peptide candidate was present, selection was based on the total number of matched product ions and on matching of the most intense signals. The peptide with the largest number of matching product ions, especially the most intense ones, was selected as identified.

Compared to the targeted analysis, the developed approach has the advantage of much larger search space for peptide identification than the employ of a database of literature sequences [16] and allows to match not only precursor exact masses, but also the fragmentation pattern, which is fundamental for confident identification also of isomers [19,37,38].

In comparison to t_R prediction, the developed method provides some advantages. Retention time prediction technique requires large numbers of synthetic peptides to establish a reliable model, is limited to the selected chromatographic conditions, and is not suited for identification of unknown sequences but can prove useful when MS/MS fragmentation data are insufficient to distinguish between isobaric peptides [12]. The approach described in this paper is independent from the chromatographic separation which is exploited and can potentially be automated for matching of precursor and fragment spectra to the resulting comprehensive database. Finally, the building of a database with all possible combinations making up the target short peptides allows to bypass the limits of ordinary database search used in peptidomics and proteomics investigations, as no match is performed against a protein sequence database and the number of multiple ambiguous matches is thus reduced. Even if suspect screening can be grouped within metabolomics approaches, and short peptides can be identified within metabolomics investigations [39], it differs from pure untargeted metabolomics as metabolites databases do contain short peptide data but they are not comprehensive enough for large scale short peptide identification.

To test the suitability for real sample application, human serum was analysed. Some short peptides have been identified in serum within metabolomics studies [40], as they cannot be identified by

Table 2
Short peptides identified in 1 mL human serum.

Sequence	m/z	t _R	Peak height	Peak area
PP	213.1234	1.89	4.78E+06	8.57E+07
LP	229.1546	5.31	1.08E+08	1.99E+09
LI	245.1859	1.64	5.83E+06	1.80E+08
MM	281.0995	7.54	1.35E+07	1.32E+08
GRS	319.1726	8.59	1.18E+08	5.66E+08
HGN	327.1414	13.47	3.11E+07	2.36E+08
HAN	341.1570	10.84	6.67E+07	6.61E+08
KGH	341.1934	12.33	1.10E+07	1.19E+08
SSR	349.1831	8.24	1.24E+07	8.00E+07
RSS	349.1831	8.46	1.85E+08	9.43E+08
RST	363.1988	9.89	1.48E+08	7.97E+08
HGP	381.1883	13.98	1.61E+07	6.96E+07
TQH	385.1832	13.09	4.39E+07	7.77E+08
PDR	387.1989	10.62	4.81E+07	6.61E+08
GHSP	397.1833	14.52	1.87E+07	1.83E+08
ASSH	401.1782	16.65	1.90E+07	3.20E+08
PWK	430.2437	10.52	7.10E+07	4.04E+08
DWI	433.2082	11.73	1.26E+07	1.41E+08
PAQQ	443.2251	17.18	1.96E+07	5.69E+08
HTAE	457.2043	19.98	1.92E+07	1.21E+08
PHTI	467.2616	20.93	1.31E+07	2.88E+08
IQQP	485.2721	19.15	1.09E+07	1.19E+08
IDHI	497.2722	20.58	1.79E+07	2.21E+08
QHE	499.2514	20.64	1.31E+07	2.31E+08
PEQK	501.2670	19.37	1.17E+07	1.48E+08
KPKF	519.33	22.29	1.70E+07	9.18E+07
PF	263.1389	9.97	7.29E+06	3.77E+07
FR	322.1872	8.90	1.74E+07	1.05E+08
IWL	430.2433	11.09	3.57E+07	2.19E+08
PW	352.1652	19.43	2.70E+07	1.47E+08

usual peptidomics approaches [41]. For this reason, serum was chosen as test matrix for characterization of endogenous short peptides by the developed method. The method allowed to identify 30 short peptide sequences. The list of the identified peptides is reported in Table 2, and the extracted ions chromatogram is reported in Figure S-8.

A short survey to investigate any bioactivity previously reported for the identified peptides searching the BIOPEP database [42] indicated 7 peptides, mainly with dipeptidyl peptidase IV inhibitor (PP, LP, LI, MM, PF, FR, PW) but also with angiotensin-converting enzyme inhibitors (PP, MM, FR), antioxidative activity (MM, PW) and glucose uptake stimulating peptide (LI). The result is particularly interesting, as the complexity of the human peptidome has not been functionally characterized yet, suggesting that many more endogenous peptides remain to be discovered and they are potentially relevant for new bioactive peptides identification [3,43].

4. Conclusion

PGC has a unique retention mechanism comprising a combination of hydrophobic interactions, polar interaction of polarizable or polarized groups and electronic interactions. Such variety of interactions can be exploited to tailor a chromatographic separation of isobar species, which is particularly advantageous for short peptide separation. The use of 3-NBA as supercharging agent allows to improve ionization and increase higher charge states, which allows an efficient coupling with HRMS. Finally, an untargeted approach for peptide identification by suspect screening with a comprehensive database for precursor identification and confirmation by in silico MS/MS spectra matching completes the developed method for discrimination of short peptide isobars. The approach was developed on peptides standards and applied for identification of endogenous short peptides in serum, with final identification of 30 short peptides. Besides many analytical problems have been overstepped by the spectacular advances in mass spectrometry and bioinformatics, still there is a need for efficient separative

techniques, especially for preparative purposes. The approach presented in this study provides an efficient tool for the analysis of very polar small peptides or, for a wider range of peptide polarity, can serve as orthogonal condition in combination with conventional RP in 2D chromatographic systems.

Appendix A. Supplementary data

Supplementary material related to this article can be found, in the online version, at doi:<https://doi.org/10.1016/j.chroma.2018.12.066>.

References

- [1] D.C. Dallas, A. Guerrero, E.A. Parker, R.C. Robinson, J. Gan, J.B. German, D. Barile, C.B. Lebrilla, Current peptidomics: applications, purification, identification, quantification, and functional analysis, *Proteomics* 15 (2015) 1026–1038, <http://dx.doi.org/10.1002/pmic.201400310>.
- [2] F. Piguet, H. Ouldali, M. Pastoriza-Gallego, P. Manivet, J. Pelta, A. Oukhaled, Identification of single amino acid differences in uniformly charged homopolymeric peptides with aerolysin nanopore, *Nat. Commun.* 9 (2018), <http://dx.doi.org/10.1038/s41467-018-03418-2>, Article number 966.
- [3] M. Bosso, L. Ständker, F. Kirchhoff, J. Münch, Exploiting the human peptidome for novel antimicrobial and anticancer agents, *Bioorg. Med. Chem.* 26 (2018) 2719–2726, <http://dx.doi.org/10.1016/j.bmc.2017.10.038>.
- [4] A. Secher, C.D. Kelstrup, K.W. Conde-Frieboes, C. Pyke, K. Raun, B.S. Wulff, J.V. Olsen, Analytic framework for peptidomics applied to large-scale neuropeptide identification, *Nat. Commun.* 7 (2016), <http://dx.doi.org/10.1038/ncomms11436>, Article number 11436.
- [5] K. Sato, Structure, Content, and Bioactivity of Food-Derived Peptides in the Body, *J. Agric. Food Chem.* 66 (2018) 3082–3085, <http://dx.doi.org/10.1021/acs.jafc.8b00390>.
- [6] S. Piovesana, A.L. Capriotti, C. Cavaliere, G. La Barbera, R. Samperi, R. Zenezini Chiozzi, A. Laganà, Peptidome characterization and bioactivity analysis of donkey milk, *J. Proteomics* 119 (2015) 21–29, <http://dx.doi.org/10.1016/j.jprot.2015.01.020>.
- [7] R. Zenezini Chiozzi, A.L. Capriotti, C. Cavaliere, G. La Barbera, S. Piovesana, R. Samperi, A. Laganà, Purification and identification of endogenous antioxidant and ACE-inhibitory peptides from donkey milk by multidimensional liquid chromatography and nanoHPLC-high resolution mass spectrometry, *Anal. Bioanal. Chem.* 408 (2016) 5657–5666, <http://dx.doi.org/10.1007/s00216-016-9672-z>.
- [8] S. Piovesana, A.L. Capriotti, C. Cavaliere, G. La Barbera, C.M. Montone, R. Zenezini Chiozzi, A. Laganà, Recent trends and analytical challenges in plant bioactive peptide separation, identification and validation, *Anal. Bioanal. Chem.* 410 (2018) 3425–3444, <http://dx.doi.org/10.1007/s00216-018-0852-x>.
- [9] A. Henninot, J.C. Collins, J.M. Nuss, The Current State of Peptide Drug Discovery: Back to the Future? *J. Med. Chem.* 61 (2018) 1382–1414, <http://dx.doi.org/10.1021/acs.jmedchem.7b00318>.
- [10] FDA, DRAFT guidance for industry from FDA: quality considerations in demonstrating biosimilarity to a reference protein product, *Biotechnol. Law Rep.* 31 (2012) 185–195, <http://dx.doi.org/10.1089/blr.2012.9939>.
- [11] D.J. Craik, D.P. Fairlie, S. Liras, D. Price, The future of peptide-based drugs, *Chem. Biol. Drug Des.* 81 (2013) 136–147, <http://dx.doi.org/10.1111/cbdd.12055>.
- [12] S. Le Maux, A.B. Nongonierma, R.J. Fitzgerald, Improved short peptide identification using HILIC-MS/MS: retention time prediction model based on the impact of amino acid position in the peptide sequence, *Food Chem.* 173 (2015) 847–854, <http://dx.doi.org/10.1016/j.foodchem.2014.10.104>.
- [13] M.B. O'Keeffe, R.J. Fitzgerald, Identification of short peptide sequences in complex milk protein hydrolysates, *Food Chem.* 184 (2015) 140–146, <http://dx.doi.org/10.1016/j.foodchem.2015.03.077>.
- [14] A.B. Nongonierma, R.J. Fitzgerald, Strategies for the discovery and identification of food protein-derived biologically active peptides, *Trends Food Sci. Technol.* 69 (2017) 289–305, <http://dx.doi.org/10.1016/j.tifs.2017.03.003>.
- [15] E.T. Chin, D.I. Papac, The use of a porous graphitic carbon column for desalting hydrophilic peptides prior to matrix-assisted laser desorption/ionization time-of-flight mass spectrometry, *Anal. Biochem.* 273 (1999) 179–185, <http://dx.doi.org/10.1006/abio.1999.4242>.
- [16] B.H. Yesmine, B. Antoine, N.G. da Silva Ortência Leocádia, B.W. Rogério, A. Ingrid, B. Nicolas, M. Thierry, J.M. Piot, S. Frédéric, B.J. Stéphanie, Identification of ace inhibitory cryptides in Tilapia protein hydrolysate by UPLC-MS/MS coupled to database analysis, *J. Chromatogr. B Anal. Technol. Biomed. Life Sci.* 1052 (2017) 43–50, <http://dx.doi.org/10.1016/j.jchromb.2017.02.015>.
- [17] S. Le Maux, A.B. Nongonierma, B. Murray, P.M. Kelly, R.J. Fitzgerald, Identification of short peptide sequences in the nanofiltration permeate of a bioactive whey protein hydrolysate, *Food Res. Int.* 77 (2015) 534–539, <http://dx.doi.org/10.1016/j.foodres.2015.09.012>.
- [18] V.R. Koskinen, P.A. Emery, D.M. Creasy, J.S. Cottrell, Hierarchical clustering of shotgun proteomics data, *Mol. Cell Proteomics* 10 (2011), <http://dx.doi.org/10.1074/mcp.M110.003822>, M110.003822.

- [19] O.I. Obolensky, W.W. Wu, R.F. Shen, Y.K. Yu, Using dissociation energies to predict observability of b- and y-peaks in mass spectra of short peptides. II. Results for hexapeptides with non-polar side chains, *Rapid Commun. Mass Spectrom.* 27 (2013) 152–156, <http://dx.doi.org/10.1002/rcm.6451>.
- [20] L. Pereira, Porous graphitic carbon as a stationary phase in HPLC: theory and applications, *J. Liq. Chromatogr. Relat. Technol.* 31 (2008) 1687–1731, <http://dx.doi.org/10.1080/10826070802126429>.
- [21] V. Németh-Kiss, E. Forgács, T. Cserhádi, Anomalous retention behaviour of peptides on porous graphitized carbon column, *J. Chromatogr. A* 776 (1997) 147–152, [http://dx.doi.org/10.1016/S0021-9673\(97\)00269-0](http://dx.doi.org/10.1016/S0021-9673(97)00269-0).
- [22] C. Desportes, M. Charpentier, B. Duteurtre, A. Maujean, F. Duchiron, Liquid chromatographic fractionation of small peptides from wine, *J. Chromatogr. A* 893 (2000) 281–291, [http://dx.doi.org/10.1016/S0021-9673\(00\)00698-1](http://dx.doi.org/10.1016/S0021-9673(00)00698-1).
- [23] A.A. Adoubel, S. Guenu, C. Elfakir, M. Dreux, Separation of underivatized small peptides on a porous graphitic carbon column by ion-pair chromatography and evaporative light scattering detection, *J. Liq. Chromatogr. Relat. Technol.* 23 (2000) 2433–2446, <http://dx.doi.org/10.1081/JLC-100100499>.
- [24] M. Rodriquez, D.S. Cretoso, M.A. Euterpio, P. Russo, C. Crescenzi, R.P. Aquino, Fast determination of underivatized gentamicin C components and impurities by LC-MS using a porous graphitic carbon stationary phase, *Anal. Bioanal. Chem.* (2015), <http://dx.doi.org/10.1007/s00216-015-8933-6>.
- [25] T. Pluskal, S. Castillo, A. Villar-Briones, M. Orešič, MZmine 2: modular framework for processing, visualizing, and analyzing mass spectrometry-based molecular profile data, *BMC Bioinformatics* 11 (2010) 395, <http://dx.doi.org/10.1186/1471-2105-11-395>.
- [26] T.H.J. Niedermeyer, M. Strohal, mMass as a software tool for the annotation of cyclic peptide tandem mass spectra, *PLoS One* 7 (2012), <http://dx.doi.org/10.1371/journal.pone.0044913>, Article number e44913.
- [27] G. La Barbera, A.L. Capriotti, C. Cavaliere, F. Ferraris, M. Laus, S. Piovesana, K. Sparnacci, A. Laganà, Development of an enrichment method for endogenous phosphopeptide characterization in human serum, *Anal. Bioanal. Chem.* 410 (2018) 1177–1185, <http://dx.doi.org/10.1007/s00216-017-0822-8>.
- [28] T.E. Bapiro, F.M. Richards, D.I. Jodrell, Understanding the complexity of porous graphitic carbon (PGC) chromatography: modulation of mobile-stationary phase interactions overcomes loss of retention and reduces variability, *Anal. Chem.* 88 (2016) 6190–6194, <http://dx.doi.org/10.1021/acs.analchem.6b01167>.
- [29] C. West, C. Elfakir, M. Lafosse, Porous graphitic carbon: a versatile stationary phase for liquid chromatography, *J. Chromatogr. A* 1217 (2010) 3201–3216, <http://dx.doi.org/10.1016/j.chroma.2009.09.052>.
- [30] J.H. Knox, P. Ross, Carbon-based packing materials for liquid chromatography: structure, performance, and retention mechanisms, *Adv. Chromatogr.* 37 (1997) 73–119.
- [31] J.P. Mercier, P. Morin, M. Dreux, A. Tambuté, Liquid chromatography analysis of phosphonic acids on porous graphitic carbon stationary phase with evaporative light-scattering and mass spectrometry detection, *J. Chromatogr. A* 849 (1999) 197–207, [http://dx.doi.org/10.1016/S0021-9673\(99\)00556-7](http://dx.doi.org/10.1016/S0021-9673(99)00556-7).
- [32] G. Gu, C.K. Lim, Separation of anionic and cationic compounds of biomedical interest by high-performance liquid chromatography on porous graphitic carbon, *J. Chromatogr. A* 515 (1990) 183–192, [http://dx.doi.org/10.1016/S0021-9673\(01\)89312-2](http://dx.doi.org/10.1016/S0021-9673(01)89312-2).
- [33] M. Nshanian, R. Lakshmanan, H. Chen, R.R.O. Loo, J.A. Loo, Enhancing sensitivity of liquid chromatography–mass spectrometry of peptides and proteins using supercharging agents, *Int. J. Mass Spectrom.* 427 (2018) 157–164, <http://dx.doi.org/10.1016/j.ijms.2017.12.006>.
- [34] G. La Barbera, A.L. Capriotti, C. Cavaliere, S. Piovesana, R. Samperi, R. Zenezini Chiozzi, A. Laganà, Comprehensive polyphenol profiling of a strawberry extract (*Fragaria × ananassa*) by ultra-high-performance liquid chromatography coupled with high-resolution mass spectrometry, *Anal. Bioanal. Chem.* 409 (2017) 2127–2142, <http://dx.doi.org/10.1007/s00216-016-0159-8>.
- [35] A.L. Capriotti, C. Cavaliere, G. La Barbera, C.M. Montone, S. Piovesana, R. Zenezini Chiozzi, A. Laganà, Chromatographic column evaluation for the untargeted profiling of glucosinolates in cauliflower by means of ultra-high performance liquid chromatography coupled to high resolution mass spectrometry, *Talanta* 179 (2018) 792–802, <http://dx.doi.org/10.1016/j.talanta.2017.12.019>.
- [36] R. Zenezini Chiozzi, A.L. Capriotti, C. Cavaliere, F. Ferraris, G. La Barbera, S. Piovesana, A. Laganà, Evaluation of column length and particle size effect on the untargeted profiling of a phytochemical mixture by using UHPLC coupled to high-resolution mass spectrometry, *J. Sep. Sci.* 40 (2017) 2541–2557, <http://dx.doi.org/10.1002/jssc.201700135>.
- [37] S.V. Kovalyov, S.S. Zhokhov, L.V. Onoprienko, B.V. Vaskovsky, A.T. Lebedev, Exploration of doubtful cases of leucine and isoleucine discrimination in mass spectrometric peptide sequencing by electron-transfer and higher-energy collision dissociation-based method, *Eur. J. Mass Spectrom.* (Chichester) 23 (2017) 376–384, <http://dx.doi.org/10.1177/1469066717730705>.
- [38] Y. Xiao, M.M. Vecchi, D. Wen, Distinguishing between leucine and isoleucine by integrated LC-MS analysis using an orbitrap fusion mass spectrometer, *Anal. Chem.* 88 (2016) 10757–10766, <http://dx.doi.org/10.1021/acs.analchem.6b03409>.
- [39] C. Guijas, J.R. Montenegro-Burke, X. Domingo-Almenara, A. Palermo, B. Warth, G. Hermann, G. Koellensperger, T. Huan, W. Uritboonthai, A.E. Aisporna, D.W. Wolan, M.E. Spilker, H.P. Benton, G. Siuzdak, METLIN: a technology platform for identifying knowns and unknowns, *Anal. Chem.* 90 (2018) 3156–3164, <http://dx.doi.org/10.1021/acs.analchem.7b04424>.
- [40] T. Saito, M. Sugimoto, K. Okumoto, H. Haga, T. Katsumi, K. Mizuno, T. Nishina, S. Sato, K. Igarashi, H. Maki, M. Tomita, Y. Ueno, T. Soga, Serum metabolome profiles characterized by patients with hepatocellular carcinoma associated with hepatitis B and C, *World J. Gastroenterol.* 22 (2016) 6224–6234, <http://dx.doi.org/10.3748/wjg.v22.i27.6224>.
- [41] R. Vitorino, Digging deep into peptidomics applied to body fluids, *Proteomics* 18 (2018), <http://dx.doi.org/10.1002/pmic.201700401>, Article number 1700401.
- [42] P. Minkiewicz, J. Dziuba, A. Iwaniak, M. Dziuba, M. Darewicz, BIOPEP database and other programs for processing bioactive peptide sequences, *J. AOAC Int.* 91 (2008) 965–980.
- [43] J. Münch, L. Ständker, W.G. Forssmann, F. Kirchhoff, Discovery of modulators of HIV-1 infection from the human peptidome, *Nat. Rev. Microbiol.* 12 (2014) 715–722, <http://dx.doi.org/10.1038/nrmicro3312>.



Identification of bioactive short peptides in cow milk by high-performance liquid chromatography on C18 and porous graphitic carbon coupled to high-resolution mass spectrometry

Carmela Maria Montone¹ · Anna Laura Capriotti¹ · Andrea Cerrato¹ · Michela Antonelli¹ · Giorgia La Barbera¹ · Susy Piovesana¹ · Aldo Laganà¹ · Chiara Cavaliere¹

Received: 12 February 2019 / Revised: 15 March 2019 / Accepted: 27 March 2019 / Published online: 22 April 2019
© Springer-Verlag GmbH Germany, part of Springer Nature 2019

Abstract

Short peptides are important compounds in a variety of fields, including food and nutraceutical applications, but also biomarker discovery, bioactive peptide discovery and peptide drug separation. Despite the importance of short peptides, they are currently less studied than other peptides because of the lack of dedicated methods for their characterization. The method described in this paper comprises a combination of strategies to tackle the main limitations in short peptide analysis. In particular, in this work an untargeted peptidomic approach based on ultrahigh-performance liquid chromatography coupled to high-resolution mass spectrometry was developed for the identification of short peptides in cow milk samples. After milk defatting and precipitation, the sample was purified by cotton-hydrophilic interaction liquid chromatography (HILIC) micro tip in order to avoid suppression phenomena due to contaminants present in milk, such as carbohydrates. The sample was then separated by means of two chromatographic columns, with a complementary selectivity mechanism, namely reversed-phase C18 column and porous graphitic carbon (PGC). By this approach, the method allowed the separation and characterization of di-, tri- and tetrapeptides. A total of 57 and 41 peptides were identified by using a C18 and a PGC column, respectively; in particular, 31 were exclusively identified by using the C18 column, 15 unique peptides were identified by using the PGC column, while 26 were in common between the two data sets, demonstrating that the two columns have a different selectivity mechanism. The results indicated that an integrated approach may be appropriate to improve the separation of different peptides and increase the number of identifications because of the wide range of polarity of short peptides. The method allowed the untargeted identification of short peptides in milk, a complex matrix chosen as a representative real sample for method application, and provides complementary information to that accessible by ordinary peptidomics.

Keywords Short peptides · Milk · Bioactive peptides · Untargeted peptidomics · Mass spectrometry

Introduction

Milk contains a wide variety of bioactive compounds, such as lipids, vitamins, minerals, immunoglobulins, enzymes,

lactoferrins and bioactive peptides (BPs). In the last two decades, milk from various farm animals, such as cow, goat, sheep, camel and donkey, has been extensively analysed in terms of BPs, which have been proven to have a broad spectrum of bioactivities, including antimicrobial, antihypertensive, antioxidative, anticarcinogenic, immunomodulatory, opioid and mineral-carrying activities [1].

However, although a thorough investigation has been performed on the composition of different types of milk in terms of BPs obtained by digestive enzymes or by lactobacilli during the fermentation of milk, too little attention has been paid to the endogenous BPs that may also be contained in milk used for human consumption and which may play important biological roles [2]. For instance, naturally occurring peptides

Electronic supplementary material The online version of this article (<https://doi.org/10.1007/s00216-019-01815-0>) contains supplementary material, which is available to authorized users.

✉ Anna Laura Capriotti
annalaura.capriotti@uniroma1.it

¹ Department of Chemistry, Sapienza Università di Roma, Piazzale Aldo Moro 5, 00185 Rome, Italy

may exert activities in the upper gastrointestinal tract independent from digestive processes. Additionally, the presence of endogenous physiologically active peptides in milk may render whey, which is an abundant by-product in cheese production, a valuable source of bioactive peptides for hypothetical nutraceutical employment.

While the majority of studies were carried out on the identification of endogenous peptides in human milk [3–5], few studies have so far focused on the endogenous peptidomic profile of milk intended for broad consumption. Baum et al. identified 248 endogenous peptides [6] and 18 putative phosphopeptides [7] in raw cow milk by matrix-assisted laser desorption/ionization time-of-flight mass spectrometry (MS), either directly or after pre-fractionation of milk peptides by reversed-phase high-performance liquid chromatography or OFFGEL fractionation. Dallas and co-workers also investigated naturally occurring peptides in bovine colostrum sweet whey and identified more than 245 endogenous peptides [8]. Subsequently, two other studies focused on the investigation of the endogenous peptides in donkey milk samples [9, 10].

Although these studies showed promising results on the investigation of naturally occurring bioactive peptides in milk samples, they reported amino acid sequences longer than four residues, since the classic database search approach, borrowed from proteomics, was employed. The minimum peptide length in Mascot has a default setting of five residues, and it is difficult to get a significant match to very short peptides [11]. To overcome this issue, *de novo* sequencing is mandatory [12, 13]. To improve the peptide identification confidence, in some recent works by FitzGerald et al. short peptide sequences in milk hydrolysates were determined by *de novo* sequencing and a retention time prediction model [14]. In another study, the use of peptide retention time, multiple reaction monitoring analysis and variation in the collision energy has been adopted for the analysis of 117 di- and tripeptides in a whey protein hydrolysate employing a mixture of synthetic peptides [15].

Identification is not the only problem related to short peptide analysis; in fact, there is a second issue concerning MS detection, since short peptide precursor ions are commonly singly charged. This is a considerable disadvantage for peptide sequencing due to the decrease of fragmentation along the backbone of the amino acid sequence. A different MS approach and a different fragmentation energy should be employed in order to promote peptide fragmentation. Nowadays, ion mobility MS represents the method of choice for the detection of isobaric peptides or peptides presenting similar masses [16].

There is also one last issue related to short peptide analysis, which derives from the wide range of polarity of these biomolecules. Common purification and separation strategies, which are employed in traditional peptidomic analysis, are usually carried out by reversed-phase (RP) chromatography

on C18, which could lead to the loss of the most hydrophilic peptides. Several different separation strategies could help in retaining these short sequences. For example, hydrophilic interaction liquid chromatography (HILIC) either alone [17] or coupled to RP liquid chromatography tandem mass spectrometry (LC–MS/MS) strategies were employed to identify short peptides in a whey protein hydrolysate [18]. Also, an RP C18 HSS T3 column, which is specific for highly hydrophilic compounds, was tested in tilapia samples [19]. In a recent application carried out in our research group, a porous graphitic carbon (PGC) column was employed for separation of short peptide sequences in serum [20].

Short peptide studies require a proper method development in order to obtain a comprehensive peptidomic characterization and to overcome all the issues mentioned above. The optimization of protocols for sample preparation, separation, MS detection and identification is required to achieve a reliable characterization of the analysed samples.

In this work, we present an untargeted peptidomic approach based on ultra-HPLC (UHPLC)–high-resolution (HR) MS for the analysis of the short peptides in cow milk samples. In particular, a purification step based on cotton-HILIC microtips was employed, followed by a UHPLC separation. Two different columns, namely Kinetex C18 and PGC, were employed to exploit the different selectivity mechanisms. The chromatographic separation was coupled to HRMS with the purpose of accomplishing an untargeted investigation based on suspect screening for short peptides in milk. A database with all possible combinations of the 20 natural amino acids within di-, tri- and tetrapeptides was compiled and fragment ions spectra were matched to *in silico* fragmentation spectra to identify the precursor ions. To the best of our knowledge, this is the first investigation of short peptides in cow milk providing a detailed characterization of short peptides.

Materials and methods

Chemicals and reagents

Optima® LC-MS grade water and acetonitrile (ACN) were purchased from Thermo Fisher Scientific (Waltham, Massachusetts, USA). LC-MS grade methanol (MeOH), trifluoroacetic acid (TFA) and tetrahydrofuran (THF) were supplied by Romil (Cambridge, UK). 3-Nitrobenzyl alcohol (3-NBA) was purchased from Sigma-Aldrich (St. Louis, MO, USA). Synthetic peptides Pro-Ile (PI), Pro-Leu (PL), Leu-Pro (LP), Lys-His (KH), Arg-Phe (RF), Ser-His (SH), Leu-Pro-Leu (LPL), Ile-Pro-Ile (IPI), Val-Glu-Pro (VEP), Lys-His-Lys (KHK), Ile-Pro-Pro-Leu (IPPL), Gly-Asp-Leu-Glu (GDLE), Val-Arg-Gly-Pro (VRGP) and Arg-Lys-Lys-His (RKKH) were also purchased from Thermo Fisher

Scientific. Commercial cow milk samples were purchased from a local store (Rome, Italy). Five different whole milk samples, coming from different Italian regions (Lazio, Marche, Basilicata, Lombardy and Sardinia), were purchased from a local supplier. The five samples were pooled before the subsequent analysis. All commercial milk samples were pasteurized by the continuous high-temperature short-time (HTST) method at 72 °C for 15 s.

Cow milk delipidation and protein precipitation

Cow milk samples were centrifuged at 2900×g for 30 min at 4 °C. The upper milk fat layer was discarded and the defatted milk was stored at -80 °C for further processing.

An aliquot of milk sample (2 mL) was added with seven volumes of ACN (14 mL) in an ACN-compatible tube. The tube was vortex shaken and incubated overnight at -20 °C. The precipitated proteins were removed by centrifugation at 9400×g for 15 min at 4 °C, and the supernatant containing the peptides was dried down using a Speed-Vac SC 250 Express (Thermo S164 avant, Holbrook, NY, USA) and reconstituted in 800 µL ACN/H₂O (85:15, v/v) with 0.1% TFA (v/v).

Peptide purification with cotton-HILIC tips

The samples were cleaned up with cotton-HILIC microtips in order to remove the majority of carbohydrates from milk. Hydrophilic cotton wool was purchased from a local store and, according to the manufacturer, it consisted of 100% pure cotton. The purification was carried out as previously described [21]. Approximately 10 mg of cotton wool was packed into a 200-µL microtip using a steel piston. The cotton-HILIC microtip was washed five times with 200 µL of water and conditioned three times with 200 µL ACN/H₂O (85:15, v/v) with 0.1% TFA (v/v). The milk sample was then loaded and the microtip was washed with 200 µL ACN/H₂O (85:15, v/v) with 0.1% TFA (v/v) to collect the flow-through containing the remaining peptides. The loaded sample was dried down by a Speed-Vac and reconstituted with 200 µL of 0.1% TFA aqueous solution for subsequent UHPLC-MS/MS analysis.

UHPLC-MS/MS analysis

UHPLC analysis was accomplished by a Vanquish liquid chromatograph (Thermo Fisher Scientific, Bremen, Germany), equipped with a binary pump H, a thermostated auto-sampler and column compartment. Two different columns were tested, namely a Kinetex XB-C18 (100 × 2.1 mm, 2.6 µm particle size) and a Hypercarb™ PGC column (150 × 2.1 mm, 5 µm particle size). The chromatographic methods were initially optimized by injecting a 1 ng mL⁻¹ standard peptide mixture covering a wide range of grand

average of hydrophathy (GRAVY) index values. In the most satisfactory conditions, the flow rate was set at 0.5 mL min⁻¹ with post-column addition of MeOH with 1.2% 3-NBA (v/v) at 0.1 mL min⁻¹ for both columns runs.

The C18 column was maintained at 40 °C and the elution was carried out with H₂O (phase A) and ACN (phase B) both with 0.1% TFA (v/v). The injection volume was 10 µL and the chromatographic gradient was the following: 1% phase B for 2 min, 1–35% B in 20 min, 35–99% B in 3 min; at the end of the gradient, a washing step at 99% B for 3 min and a re-equilibration step at 1% B for 5 min were performed.

For the Hypercarb column the chromatographic conditions were the same optimized in our previous work with little modification [20]. The Hypercarb column was maintained at 50 °C using the still air option. Twenty microlitres of each sample was eluted with H₂O (phase A) and ACN/THF (99:1, v/v, phase B) both with 0.2% TFA (v/v). The chromatographic gradient was the following: 1% phase B for 2 min, 1–35% B in 15 min, 35–90% B in 8 min; at the end of the gradient, a washing step at 90% B for 3 min and a re-equilibration step at 1% B for 7 min were performed. The chromatographic system was coupled to a hybrid quadrupole-Orbitrap mass spectrometer (Q Exactive, Thermo Fisher Scientific) using a heated electrospray ionization (ESI) source. For all chromatographic conditions, the ESI source was employed in positive mode using the following conditions: 220 °C capillary temperature, 50 (arbitrary units) sheath gas, 25 (arbitrary units) auxiliary gas, 0 (arbitrary units) sweep gas, 3200 V spray voltage, 280 °C auxiliary gas heater, 50% S-Lens RF level. The detection was achieved in top five data-dependent acquisition mode in the range 150–2000 *m/z* with a resolution (full width at half maximum, FWHM) of 70,000 and automatic gain control (AGC) target value set at 5 × 10⁵ in full scan. The max ion injection time was set at 200 ms. Higher-energy collisional dissociation (HCD) was performed at 40 (arbitrary units) normalized collision energy with a resolution of 35,000 (FWHM). The isolation window was set at 2 *m/z*. AGC target value was set at 1 × 10⁴ and the dynamic exclusion was set at 3 s. Both an exclusion and an inclusion list were added to the MS method. The exclusion list was created using the 150 most abundant ions acquired in three blank samples, which consisted of ultra-pure water, while the inclusion list was obtained by generating on Matlab R2018a all possible amino acid combinations in di-, tri- and tetrapeptides. Duplicate masses were then discarded, resulting in 18,533 combinations. The sequences database contained exact *m/z* values for singly charged precursor ions, doubly charged ions (only for tri- and tetrapeptides), triply and quadruply charged ions (tetrapeptides only). The UHPLC-MS/MS method was employed for the acquisition of peptide samples in triplicate analysis. Raw MS/MS data files were acquired by Xcalibur software (version 3.1, Thermo Fisher Scientific).

Data analysis and peptide identification

Xcalibur raw files were processed by the freeware MZmine 2 software (v 2.26, <http://www.mzmine.sourceforge.net>) [22] to search for peptide precursor ions in the database mentioned above with exact m/z values. Data were imported and a list of ions for each scan was generated using a mass detection module (Exact mass algorithm with noise 1E4) and a filter was applied to correct false signals, the so-called shoulder peaks, which derive from the Fourier transform function (Gaussian peak model function). Then, a chromatogram was built from the mass list previously generated (minimum time span 0.5 s, minimum height 5E4 and m/z tolerance 5 ppm). Later, the deconvolution module was employed to deconvolute chromatograms into individual peaks (local minimum search algorithm with chromatographic threshold 30, minimum retention time range 0.05 min) and the isotopic peak grouper module was used to remove isotopic peaks, keeping only the highest peak (m/z tolerance 5 ppm, retention time tolerance 0 and maximum charge 4). The peak list obtained for samples and blank were aligned, using the join alignment module (m/z tolerance 5 ppm, retention time tolerance 0.1 min, weight for m/z 70, weight for retention time 30) and the peaks coming from the blank were removed from the final list. Peaks without MS/MS fragmentation were eventually subtracted before peptides validation. mMass [23] was employed to match fragment ion spectra from the peak list with those generated in silico. The parameters adopted were the following: S/N threshold 1.0, apply baseline and smoothing. Only regular amino acids were considered and fragment ions maximum charge was set at 2. A broad range of product ions was considered (iminium ions, a, b, c, x, y, z, int-a, int-b, N-ladder, C-ladder, M-H₂O, M-NH₃) in order to manually check the precursor ions and find the correct amino acid sequences.

Results and discussion

Experimental set-up

The aim of this study was a comprehensive peptidomic profiling of short peptides in cow milk. The first part of this work was an evaluation and comparison of two different chromatographic systems with different selectivity and retention capability, namely Kinetex C18 and PGC columns; the separation was performed on a mixture of 14 short peptides sequences with a different and wide range of polarity, in order to obtain an efficient and comprehensive chromatographic separation suitable for coupling with sensitive ESI-MS. RP separation is the most widely used chromatography mechanism for the separation of peptides. Hydrophobic interactions are the major drivers for peptides retention, thus small hydrophilic peptides

are not retained and elute in the flow-through fraction. PGC is a viable alternative for the retention of more hydrophilic peptides [24]. As a matter of fact, in RP separation some rather polar standards were eluted with the dead volume (Ser-His, Lys-His, Arg-Lys-Lys-His, Lys-His-Lys) while on PGC all 14 standards were eluted and separated with a good peak shape and resolution, as shown in the Electronic Supplementary Material (ESM) in Figs. S1 and S2 for PGC and C18, respectively. The chromatographic conditions were already optimized in our previous work, carried out on serum endogenous short peptides, in terms of mobile phases, organic modifier and acidic additives, temperature and post-column addition of 3-NBA [20]. A supercharging agent, such as 3-NBA, was used in the chromatographic method to solve the problem of limited ionization of short peptides and to overcome the suppression due to the use of TFA in the mobile phases. TFA was preferred to formic acid owing to the better ion-pair capability, which was necessary for the separation of small ionizable compounds.

After a target analysis of the peptide standard mixtures, an untargeted analysis by suspect screening investigation was performed in cow milk samples.

Short peptide identification and validation

Short peptide identification in cow milk samples was carried out by a suspect screening investigation, as previously described by Piovesana et al. [20]. Suspect screening is a very useful approach when analytical standards are not available but a list of all the possible targets can be compiled. Because the number of amino acid sequences generated by the combination of the 20 natural amino acids is limited, a comprehensive list of the masses of di-, tri- and tetrapeptides was computed and employed to extract precursor masses from the experimental spectra. Sequences matching the exact precursor masses were fragmented in silico to produce a comprehensive list of product ions, such as iminium ions, a, b, c, x, y, z, int-a, int-b, C-ladder, N-ladder, M-H₂O and M-NH₃. Peptides were identified by matching experimental product ions to those generated in silico, focusing on a, b and y fragments. Particular attention was paid to iminium ions, as they can indicate and confirm the presence of some amino acids, such as proline, leucine, isoleucine, valine and phenylalanine. Manual validation of the amino acid sequences was based on the total number of matched ions and the matching of the most intense ones. Compared to other common approaches for peptide identification, such as retention time prediction, suspect screening investigation has the advantage of furnishing fragmentation patterns, which can help in distinguishing between isomers. In fact, studying a, b and y product ions can be highly predictive of the actual amino acid sequence. In particular, 57 tentative amino acid sequences were identified

in C18 separation (Table 1), while 41 amino acid sequences were identified in PGC separation (Table 2).

The MS/MS spectrum reported in Fig. 1 is exemplary of a typical spectrum used for identification and shows the detected diagnostic fragment ions used for identification of a tetrapeptide.

Moreover six representative spectra were reported in the ESM for a dipeptide, a tripeptide and a tetrapeptide, either identified in the C18 (ESM Fig. S3) or the PGC (ESM Fig. S4) separation.

It is worth mentioning that the fragmentation patterns generated by collisional dissociation do not include product ions

Table 1 Short peptides identified in the C18 column separation, reported with the related amino acid sequence, m/z ratio, retention time (t_r) and peak area. Leu and Ile abbreviations have been replaced by Xle abbreviation, according to standard amino acid nomenclature in case leucine and isoleucine are not distinguished

Sequences	m/z	t_r	Peak area
Ser-Pro	175.1077	0.7	8.77E+06
Val-Lys	246.1811	0.7	1.98E+07
Pro-Asp	231.0979	0.9	3.47E+06
Gly-Pro	173.0924	1.0	2.46E+06
Ala-Val	189.1233	1.8	3.66E+07
Tyr-Gln	310.1397	1.9	8.85E+06
Pro-Arg	272.1720	1.9	7.07E+06
Xle-Gln	260.1607	2.1	2.05E+06
Ala-Met	221.0958	2.4	7.65E+06
Val-Val	217.1547	3.6	2.14E+07
Pro-Val	215.1390	4.7	2.80E+07
Ser-Xle	219.1343	4.8	2.60E+06
Gly-Xle	189.1233	5.3	6.29E+06
Phe-Gly	223.1075	5.6	1.09E+07
Phe-Ala	237.1231	5.6	8.66E+06
Val-Tyr	281.1495	5.7	4.90E+07
Met-Pro	247.1108	5.9	7.17E+07
Xle-Val	231.1701	6.2	8.16E+06
Tyr-Pro	279.1338	6.2	4.02E+07
Xle-Gln-Pro	357.2135	6.8	3.71E+06
Xle-Pro	229.1550	6.8	9.74E+07
Pro-Val-Ala	286.1752	7.0	8.32E+06
Xle-Pro	229.1546	7.3	7.56E+07
Val-Xle	231.1701	7.4	3.85E+06
Xle-Tyr	295.1651	8.7	1.48E+08
Val-Xle-Pro	328.2234	8.8	1.69E+07
Zle-Ala-Tyr	366.2020	9.3	3.74E+06
Phe-Pro	263.1388	9.4	8.28E+07
Xle-Pro-Ala-Val	399.2600	9.5	8.00E+06
Pro-Xle-Tyr	392.2177	9.8	6.19E+07
Lys-Xle-Pro-Val	456.3184	10.0	4.32E+06
Xle-Gly-Pro-Val	385.2443	10.1	1.15E+07
Val-Glu-Phe	394.1970	10.3	7.49E+06
Pro-Phe-Pro	360.1914	10.3	3.53E+06
Xle-Pro-Xle-Ser	429.2706	10.3	8.03E+06
Lys-Val-Pro-Val	442.3013	10.6	7.42E+06
Tyr-Pro-Val-Arg	534.3032	11.3	4.65E+06
Xle-Xle-Val	344.2541	11.3	2.25E+08
Val-Xle-Tyr-Pro	491.2861	11.4	1.22E+07
Pro-Phe-Arg	419.2399	11.5	7.58E+07
Arg-Val-Xle-Tyr	550.3346	11.5	1.21E+08
Arg-Tyr-Xle	451.2660	11.5	2.26E+08
Pro-Gly-Phe-Pro	417.2130	11.5	5.24E+07
Xle-Pro-Tyr-Pro	489.2704	11.9	4.85E+06
Xle-Trp	318.1810	12.0	7.98E+07
Xle-Pro-Val-Pro	425.2755	12.1	1.53E+07
Xle-Pro-Xle	342.2386	12.1	6.37E+06
Tyr-Pro-Val-Xle	491.2861	12.9	3.58E+08
Trp-Pro-Lys-Xle	543.3288	13.7	9.24E+06
Trp-Xle	318.1810	13.7	1.04E+07
Pro-Pro-Xle-Xle	439.2911	13.8	1.35E+07
Pro-Phe-Met-Pro	491.2320	14.1	2.49E+08
Pro-Xle-Trp	415.2335	14.3	4.02E+07
Pro-Phe-Xle-Pro	473.2756	14.7	9.52E+06
Xle-Pro-Met-Trp	546.2737	23.6	1.69E+08
Xle-Pro-Phe-Xle	489.3069	16.8	1.58E+07
Lys-Pro-Val-Phe	548.2957	20.0	6.28E+06

Table 2 Short peptides identified in the PGC column separation, reported with the related amino acid sequence, m/z ratio, retention time (t_r) and peak area. Leu and Ile abbreviations have been replaced by Xle abbreviation, according to standard amino acid nomenclature in case leucine and isoleucine are not distinguished

Sequences	m/z	t_r	Peak area
Ala-Val	189.1230	2.1	1.04E+07
Ser-Ser	193.0817	2.2	2.96E+07
Pro-Val	215.1386	2.4	6.60E+06
Val-Xle	231.1592	2.6	5.81E+06
Ser-Pro	175.1074	2.7	3.26E+07
Ala-Asp	205.0818	2.8	4.22E+06
Lys-Thr	235.0920	2.9	6.26E+06
Gln-Lys	276.1550	3.8	6.98E+06
Glu-Thr	249.1093	3.9	2.83E+07
Pro-Asp	231.0971	3.9	2.74E+06
Xle-Ala	203.1387	4.6	2.22E+07
Val-Pro	215.1387	4.7	1.06E+07
Xle-Pro	229.1544	4.7	2.81E+07
Gln-Glu-Lys	404.2134	6.0	9.26E+06
Val-Val	217.1544	6.2	1.75E+07
Xle-Ala-Lys	374.2392	6.2	3.80E+06
Xle-Pro	229.1542	6.7	6.89E+07
Val-Arg	274.1867	7.2	6.48E+06
Pro-Pro	213.1230	7.9	4.25E+06
Xle-Ala-Val	302.2067	8.5	4.56E+06
Val-Xle-Pro	328.2226	8.8	1.30E+07
Xle-Gln-Gln-Gln	517.2615	9.5	4.70E+06
Phe-Ala	237.1229	10.1	8.23E+06
Xle-Pro-Xle	342.2380	10.5	4.20E+06
Xle-Pro-Xle-Ser	429.2703	10.8	4.88E+06
Xle-Pro-Val-Xle	425.2750	11.1	1.51E+07
Xle-Pro-Ala-Val	399.2594	11.1	6.66E+06
Gln-Tyr	310.1392	11.3	1.50E+07
Xle-Xle-Val	344.2537	12.4	1.83E+08
Xle-Tyr	295.1647	14.5	1.30E+08
Pro-Gly-Phe-Pro	417.2125	14.8	3.68E+07
Arg-Val-Xle-Tyr	550.3338	16.0	2.95E+08
Xle-Tyr	295.1647	16.0	3.44E+07
Pro-Xle-Tyr	392.2171	16.2	5.18E+07
Pro-Phe-Met-Pro	491.2314	17.1	1.78E+08
Lys-Trp-Trp	519.2693	18.1	2.24E+07
Tyr-Pro-Val-Xle	491.2854	19.7	3.59E+08
Trp-Pro-Lys-Xle	543.3280	20.1	1.95E+07
Xle-Trp	318.1806	20.5	5.54E+07
Pro-Xle-Trp	415.2333	22.0	1.98E+07

which can discriminate between leucine and isoleucine. A method to distinguish between the two isomers has been reported in the literature [25, 26] but it requires MS³ to be applied. Nevertheless, the MS method used in this work does not include MS³ fragmentation, because the Q-Exactive instrument we employed cannot accomplish further fragmentation than HCD-MS².

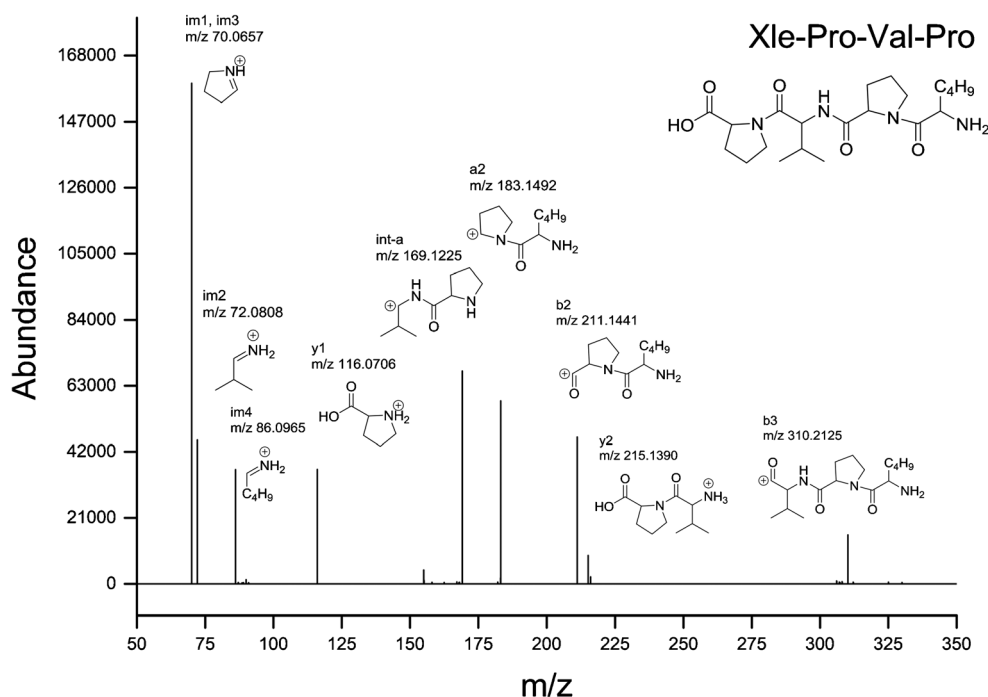
Evaluation of the developed analytical workflow

Two different independent experiments were carried out for peptide identification: in the first one, after milk defatting and protein precipitation, the supernatant, containing peptides, was directly separated by RP and PGC columns coupled to HRMS. Simultaneously, a clean-up strategy was employed in order to remove compounds, such as sugars, that would have interfered with the measurement of the compounds of interest. The clean-up step was performed by homemade cotton-HILIC

microtips. Cotton wool was selected as stationary phase for the removal of sugars from the milk samples because of its wide use in enrichment procedures for glycopeptides and glycans [21, 27]. Carbohydrate-based stationary phases constitute non-ionic HILIC phases in which adsorption is mainly due to hydrogen bonding interactions with glycan moieties, while other polar molecules, such as non-glycosylated peptides, have shown low retention. A procedure employed for glycopeptide and glycan enrichment was adapted to our purposes. The cotton-HILIC extraction was done only to remove sugars and avoid ionic suppression; therefore milk samples were only loaded on the microtip and the elution step was skipped. The loading fractions were recovered to obtain purified short peptides.

The comparison of the two methods, i.e. direct injection versus clean-up step, in terms of the number of identified and validated peptides and peak areas is summarized in the ESM in Tables S1 and S2, for C18 and PGC, respectively. By

Fig. 1 MS/MS spectrum showing diagnostic fragments for the tetrapeptide Xle-Pro-Val-Pro identified in the PGC separation



means of the C18 column, 57 short peptides were detected when the clean-up procedure was employed versus 50 amino acid sequences identified without a purification step; the trend was the same for the PGC column, by means of which we identified 41 and 30 peptides with cotton-HILIC clean-up and direct injection, respectively. A closer look to the peak areas also indicated that the clean-up allowed one to achieve a 54% signal increase in the C18 separation, with 10 peptides identified only by the clean-up procedure. For the PGC separation, the trend was similar, with a 67% signal increase and 13 unique peptides identified when the clean-up procedure was carried out (ESM Tables S1 and S2). These results confirmed that the purification step is useful to obtain a larger number of peptide identifications while avoiding suppression due to the presence of carbohydrates.

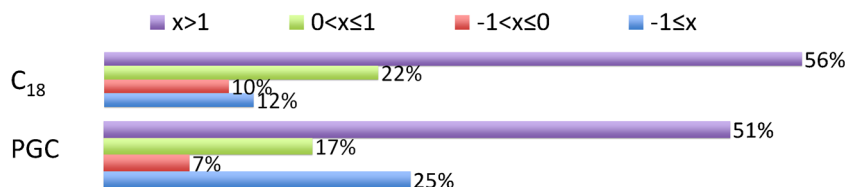
Among the total number of identified short peptides (Tables 1 and 2), 31 were exclusively identified using the C18 column, 15 unique peptides were identified using the PGC column, while 26 were in common between the two data sets.

Finally, the physicochemical properties, in particular the GRAVY index values of the identified peptides, were considered to elucidate any different behaviour between the two columns. The GRAVY value is defined as the sum of hydrophathy values of all amino acids divided by the protein length.

The GRAVY values were calculated using Protein GRAVY-Bioinformatics. The GRAVY values are discussed on the basis of four ranges, depending on the peptide GRAVY value being >1 , $1 \geq x > 0$, $0 \leq x < -1$ or $x \leq -1$ (arbitrary unit). A positive GRAVY value indicates a hydrophobic peptide, whereas a negative GRAVY value is indicative of a hydrophilic peptide. The more positive (or negative) the GRAVY value is, the more hydrophobic (or hydrophilic) the peptide is. The bar chart in Fig. 2 displays the distribution of the short peptides identified in the C18 and PGC experiments as a percentage of peptides over the total for each category.

Some significant differences were observed for the hydrophilicity of the identified peptides for the C18 and PGC separation. When the C18 separation was used, 56% of the peptides had a GRAVY value >1 , and the percentage dropped to 51% for the PGC separation. As far as the highly hydrophilic peptides were concerned, 25% of the peptides retained by the PGC column had a GRAVY value ≤ -1 vs only 12% for the C18 separation. This result agreed with the expected retention behaviours, as PGC can normally retain more hydrophilic peptides. For the other calculated values, the trend seemed to be the same, with 22% and 17% of peptides having a GRAVY value $0 < x \leq 1$ and 10% and 7% having a GRAVY value $-1 < x \leq 0$ for C18 and PGC column, respectively (Fig. 2).

Fig. 2 GRAVY value distribution for the peptides identified in the C18 and PGC separation



The analysis of the GRAVY distribution of the identified peptides demonstrates that the two columns have a different selectivity mechanism confirming that, in order to have a better separation of different peptides and to increase the number of identifications, an integrated approach may be appropriate because of the wide range of polarity of short peptides.

Bioinformatic analysis of the identified peptides

In milk short peptides could be generated by the action of some unspecific and specific milk endogenous proteases, namely plasmin, cathepsins B and D, and elastase. Plasmin usually generates longer peptides, as this enzyme has a specific preference for the carboxyl side of K and R residues. Probably, the presence of short amino acid sequences in cow milk was due to cathepsins B and D and elastase which have a broader cleavage capability (Gly, Ala, Met, Gln, Thr, Val, Leu, Ile, Pro, Phe, Trp, Arg) [28]. Apart from the enzymatic hydrolysis, short peptides could be produced also during the pasteurization process (70 °C, 15 s), as it can induce the proteolysis of casein micelle suspensions in milk. For instance, in work by Gaucheron et al. most peptides came from caseins, i.e. three peptides from κ -casein, two from β -casein and five from α S1-casein [29].

The complete list of validated and identified peptides, with sequence and related data, is reported in Tables 1 and 2 and in the ESM Tables S1 and S2 for C18 and PGC separation, respectively.

The peptide sequences were finally subjected to a BLAST (Basic Local Alignment Search Tool) search against the BIOPEP, a database which includes known and validated bioactive peptides [30]. This alignment was carried out to find out if any already established bioactive peptides had been reported in similar matrices. Some of the identified short peptides in cow milk were found in the BIOPEP database; 24 and 23 peptides, identified in the C18 and PGC separation, respectively, contained complete sequences of previously annotated bioactive peptides. In particular, these peptides showed angiotensin converting enzyme (ACE) inhibitor and dipeptidyl peptidase IV inhibitor activities. The list of peptides with known bioactivity is reported in the ESM Tables S1 and S2.

The BIOPEP database has not been updated in recent years; therefore the bioactivity evaluation of the identified short peptides was complemented by a parallel search carried out on the Milk Bioactive Peptide Database (MBPD), a comprehensive database of functional peptides in milk from mammalian species across the available literature sources. This database contains 944 entries of bioactive peptides [31]. The search results indicated that for the C18 experiments, 12 peptides were previously reported for *Bos taurus* species and one for *Camelus dromedarius*, and were attributed ACE inhibitory (Phe-Ala, Phe-Pro, Gly-Pro, Xle-Pro, Xle-Gln-Pro, Xle-Trp, Pro-Phe-Pro, Val-Xle-Pro, Val-Tyr and Tyr-Pro) and

dipeptidyl peptidase IV inhibitor activities (Xle-Pro, Xle-Pro-Xle, Trp-Xle and Tyr-Pro). As expected, among these peptides the majority derived from casein proteins (α S2-casein and β -casein), lactoferrin and serum albumin. A short survey on the peptides identified by using the PGC column indicated that 10 peptides were previously reported to be bioactive; among them, six peptides mainly displayed ACE inhibitory activity (Xle-Trp, Val-Xle-Pro, Val-Pro, Phe-Ala, Val-Arg and Xle-Tyr), one peptide had ACE and dipeptidyl peptidase IV inhibitor (Xle-Pro), one peptide had ACE inhibitor and antimicrobial activity (Xle-Ala-Lys), and three peptides showed a dipeptidyl peptidase IV inhibitor activity (Xle-Pro-Xle, Xle-Pro and Val-Arg). These peptides derived from α -lactalbumin (Xle-Trp), α S2-casein (Val-Xle-Pro), β -casein (Val-Pro and Phe-Ala), κ -casein (Xle-Pro-Xle and Xle-Ala-Lys), serum albumin (Xle-Pro and Val-Arg) and lactotransferrin (Lys-Arg).

A careful study of the amino acid sequences of peptides, which were not previously attributed with a bioactivity, showed that most peptides could have a great capacity to bind ACE. In fact, some structural characteristics are specific in peptides with ACE inhibitory activity, such as the presence of aromatic residues (Tyr, Phe) or Lys/Arg and Pro at the C-terminal position and hydrophobic branched chains at the N-terminus, namely Leu, Ile and Val [31]. As it is possible to note in the complete list of peptides identified and validated with the C18 and PGC columns (ESM Tables S1 and S2) that many sequences identified in this study fulfilled the aforementioned typical features associated with ACE inhibitory activity, indicating that they could potentially have ACE inhibitory activity.

A large number of peptides identified in this study could also be potential dipeptidyl peptidase IV inhibitors owing to the abundance of Pro in their sequence and some typical structural features, namely Xaa-Pro (Xaa indicates any amino acid), Pro-Xaa and Xaa-Ala [32].

The above discussion of the potential bioactivity associated with the peptides identified in this study and not previously reported for any known bioactivity is not influenced by the inability to discriminate between Leu or Ile under the described experimental conditions, as it is well known that peptide bioactivities are not generally affected by the presence of Leu or Ile in their sequences [33]. As previously discussed, Leu/Ile isomerism does not affect ACE or dipeptidyl peptidase IV inhibitor activities, nor does it affect, for instance, the antioxidant activity, as it is typically attributed to the presence of His, Trp, Cys and Met in the amino acid sequence [1]. Therefore, it is possible to assign bioactivities to amino acid sequences even though it is not possible to discriminate between Leu and Ile. Moreover, such peptides with potential bioactivity should be synthesized for confirmation.

These results are particularly interesting, as the complexity of the milk peptidome has not yet been functionally

characterized, suggesting that many more endogenous peptides remain to be discovered and they are potentially relevant for the identification of new bioactive peptides.

Another important issue pinpointed by the present study is related to the separation conditions, as the C18 column is a good choice for the isolation of ACE inhibitory peptides as they are usually more hydrophobic compared to other short peptides.

Conclusion

In this study, naturally occurring short peptides present in cow milk samples were investigated by a UHPLC-HRMS-based untargeted peptidomics approach. To the best of our knowledge, this is the first work carried out on endogenous short peptides in cow milk samples. Specifically, the UHPLC separation was performed using two different columns with a different selectivity mechanism (C18 and PGC). An untargeted approach for peptide identification by suspect screening was performed comparing the experimental MS/MS spectra with spectra generated *in silico*.

A total of 57 and 41 peptides were identified and validated for the separation by the C18 and PGC columns, respectively, with 26 peptides common to both separation strategies. From the comparison between the C18 and PGC separation of short peptides it could be assessed that the C18 separation provided the larger number of identifications but at the same time the PGC separation is more suitable for hydrophilic peptides and therefore provides complementary information. The approach presented in this study provides an efficient tool for the analysis of small peptides comprising a wide range of polarity. The combination of the information obtained by the two different columns is necessary to have a more comprehensive overview of the short peptide composition of a target matrix. Moreover, the extension of peptidomics investigations to short endogenous peptides may be useful for better understanding of the bioactivity of milk, as many of these amino acid sequences have shown bioactivity and may be suitable candidates for possible ingredients in functional food and pharmaceutical preparations.

Compliance with ethical standards

Conflict of interest The authors declare that they have no conflict of interest.

References

- Park YW, Nam MS. Bioactive peptides in milk and dairy products: a review. *Korean J Food Sci Anim Resour*. 2015;35:831–40. <https://doi.org/10.5851/kosfa.2015.35.6.831>.
- Capriotti AL, Cavaliere C, Piovesana S, Samperi R, Laganà A. Recent trends in the analysis of bioactive peptides in milk and dairy products. *Anal Bioanal Chem*. 2016;408:2677–85. <https://doi.org/10.1007/s00216-016-9303-8>.
- Gan J, Robinson RC, Wang J, Krishnakumar N, Manning CJ, Lor Y, et al. Peptidomic profiling of human milk with LC–MS/MS reveals pH-specific proteolysis of milk proteins. *Food Chem*. 2019;274:766–74. <https://doi.org/10.1016/j.foodchem.2018.09.051>.
- Dingess KA, de Waard M, Boeren S, Vervoort J, Lambers TT, van Goudoever JB, et al. Human milk peptides differentiate between the preterm and term infant and across varying lactational stages. *Food Funct*. 2017;8:3769–82. <https://doi.org/10.1039/C7FO00539C>.
- Su M-Y, Broadhurst M, Liu C-P, Gathercole J, Cheng W-L, Qi X-Y, et al. Comparative analysis of human milk and infant formula derived peptides following *in vitro* digestion. *Food Chem*. 2017;221:1895–903. <https://doi.org/10.1016/j.foodchem.2016.10.041>.
- Baum F, Fedorova M, Ebner J, Hoffmann R, Pischetsrieder M. Analysis of the endogenous peptide profile of milk: identification of 248 mainly casein-derived peptides. *J Proteome Res*. 2013;12:5447–62. <https://doi.org/10.1021/pr4003273>.
- Baum F, Ebner J, Pischetsrieder M. Identification of multiphosphorylated peptides in milk. *J Agric Food Chem*. 2013;61:9110–7. <https://doi.org/10.1021/jf401865q>.
- Dallas DC, Weinborn V, de Moura Bell JMLN, Wang M, Parker EA, Guerrero A, et al. Comprehensive peptidomic and glycomic evaluation reveals that sweet whey permeate from colostrum is a source of milk protein-derived peptides and oligosaccharides. *Food Res Int*. 2014;63:203–9. <https://doi.org/10.1016/j.foodres.2014.03.021>.
- Zenezini Chiozzi R, Capriotti AL, Cavaliere C, La Barbera G, Piovesana S, Samperi R, et al. Purification and identification of endogenous antioxidant and ACE-inhibitory peptides from donkey milk by multidimensional liquid chromatography and nanoHPLC-high resolution mass spectrometry. *Anal Bioanal Chem*. 2016;408:5657–66. <https://doi.org/10.1007/s00216-016-9672-z>.
- Piovesana S, Capriotti AL, Cavaliere C, La Barbera G, Samperi R, Zenezini Chiozzi R, et al. Peptidome characterization and bioactivity analysis of donkey milk. *J Proteome*. 2015;119:21–9. <https://doi.org/10.1016/j.jprot.2015.01.020>.
- Koskinen VR, Emery PA, Creasy DM, Cottrell JS. Hierarchical clustering of shotgun proteomics data. *Mol Cell Proteomics*. 2011;10:M110.003822. <https://doi.org/10.1074/mcp.M110.003822>.
- Frank AM, Savitski MM, Nielsen ML, Zubarev RA, Pevzner PA. De novo peptide sequencing and identification with precision mass spectrometry. *J Proteome Res*. 2007;6:114–23. <https://doi.org/10.1021/pr060271u>.
- Muth T, Renard BY. Evaluating de novo sequencing in proteomics: already an accurate alternative to database-driven peptide identification? *Brief Bioinform*. 2018;19:954–70. <https://doi.org/10.1093/bib/bbx033>.
- O'Keefe MB, FitzGerald RJ. Identification of short peptide sequences in complex milk protein hydrolysates. *Food Chem*. 2015;184:140–6. <https://doi.org/10.1016/j.foodchem.2015.03.077>.
- Lahrichi SL, Affolter M, Zolezzi IS, Panchaud A. Food peptidomics: large scale analysis of small bioactive peptides—a pilot study. *J Proteome*. 2013;88:83–91. <https://doi.org/10.1016/j.jprot.2013.02.018>.
- Nongonierma AB, FitzGerald RJ. Strategies for the discovery and identification of food protein-derived biologically active peptides. *Trends Food Sci Technol*. 2017;69:289–305. <https://doi.org/10.1016/j.tifs.2017.03.003>.
- Le Maux S, Nongonierma AB, FitzGerald RJ. Improved short peptide identification using HILIC–MS/MS: retention time prediction model based on the impact of amino acid position in the peptide sequence. *Food Chem*. 2015;173:847–54. <https://doi.org/10.1016/j.foodchem.2014.10.104>.
- Le Maux S, Nongonierma AB, Murray B, Kelly PM, FitzGerald RJ. Identification of short peptide sequences in the nanofiltration

- permeate of a bioactive whey protein hydrolysate. *Food Res Int*. 2015;77:534–9. <https://doi.org/10.1016/j.foodres.2015.09.012>.
19. Yesmine BH, Antoine B, da Silva Ortência Leocádia NG, Rogério BW, Ingrid A, Nicolas B, et al. Identification of ace inhibitory cryptides in tilapia protein hydrolysate by UPLC–MS/MS coupled to database analysis. *J Chromatogr B*. 2017;1052:43–50. <https://doi.org/10.1016/j.jchromb.2017.02.015>.
 20. Piovesana S, Montone CM, Cavaliere C, Crescenzi C, La Barbera G, Laganà A, et al. Sensitive untargeted identification of short hydrophilic peptides by high performance liquid chromatography on porous graphitic carbon coupled to high resolution mass spectrometry. *J Chromatogr A*. 2018. <https://doi.org/10.1016/j.chroma.2018.12.066>.
 21. Selman MHJ, Hemayatkar M, Deelder AM, Wuhrer M. Cotton HILIC SPE microtips for microscale purification and enrichment of glycans and glycopeptides. *Anal Chem*. 2011;83:2492–9. <https://doi.org/10.1021/ac1027116>.
 22. Pluskal T, Castillo S, Villar-Briones A, Orešič M. MZmine 2: modular framework for processing, visualizing, and analyzing mass spectrometry-based molecular profile data. *BMC Bioinform*. 2010;11:395. <https://doi.org/10.1186/1471-2105-11-395>.
 23. Niedermeyer THJ, Strohalm M. mMass as a software tool for the annotation of cyclic peptide tandem mass spectra. *PLoS One*. 2012;7:e44913. <https://doi.org/10.1371/journal.pone.0044913>.
 24. Issaq HJ, Chan KC, Blonder J, Ye X, Veenstra TD. Separation, detection and quantitation of peptides by liquid chromatography and capillary electrochromatography. *J Chromatogr A*. 2009;1216:1825–37. <https://doi.org/10.1016/j.chroma.2008.12.052>.
 25. Amirotti A, Millo E, Damonte G. How to discriminate between leucine and isoleucine by low energy ESI-TRAP MSⁿ. *J Am Soc Mass Spectrom*. 2007;18:57–63. <https://doi.org/10.1016/j.jasms.2006.08.011>.
 26. Maibom-Thomsen S, Heissel S, Mørtz E, Højrup P, Bunkenborg J. Discrimination of isoleucine and leucine by Dimethylation-assisted MS3. *Anal Chem*. 2018;90:9055–9. <https://doi.org/10.1021/acs.analchem.8b01375>.
 27. Hoffmann M, Pioch M, Pralow A, Hennig R, Kottler R, Reichl U, et al. The fine art of destruction: a guide to in-depth glycoproteomic analyses-exploiting the diagnostic potential of fragment ions. *Proteomics*. 2018;18:1800282. <https://doi.org/10.1002/pmic.201800282>.
 28. Dallas DC, Guerrero A, Parker EA, Garay LA, Bhandari A, Lebrilla CB, et al. Peptidomic profile of milk of Holstein cows at peak lactation. *J Agric Food Chem*. 2014;62:58–65. <https://doi.org/10.1021/jf4040964>.
 29. Gaucheron F, Mollé D, Briard V, Léonil J. Identification of low molar mass peptides released during sterilization of milk. *Int Dairy J*. 1999;9:515–21. [https://doi.org/10.1016/S0958-6946\(99\)00121-1](https://doi.org/10.1016/S0958-6946(99)00121-1).
 30. Perez-Iratxeta C, Andrade-Navarro MA, Wren JD. Evolving research trends in bioinformatics. *Brief Bioinform*. 2006;8:88–95. <https://doi.org/10.1093/bib/bbl035>.
 31. Nielsen SD, Beverly RL, Qu Y, Dallas DC. Milk bioactive peptide database: a comprehensive database of milk protein-derived bioactive peptides and novel visualization. *Food Chem*. 2017;232:673–82. <https://doi.org/10.1016/j.foodchem.2017.04.056>.
 32. Lacroix IME, Li-Chan ECY. Dipeptidyl peptidase-IV inhibitory activity of dairy protein hydrolysates. *Int Dairy J*. 2012;25:97–102. <https://doi.org/10.1016/j.idairyj.2012.01.003>.
 33. Nongonierma AB, FitzGerald RJ. Inhibition of dipeptidyl peptidase IV (DPP-IV) by tryptophan containing dipeptides. *Food Funct*. 2013;4:1843. <https://doi.org/10.1039/c3fo60262a>.
- Publisher's note** Springer Nature remains neutral with regard to jurisdictional claims in published maps and institutional affiliations.

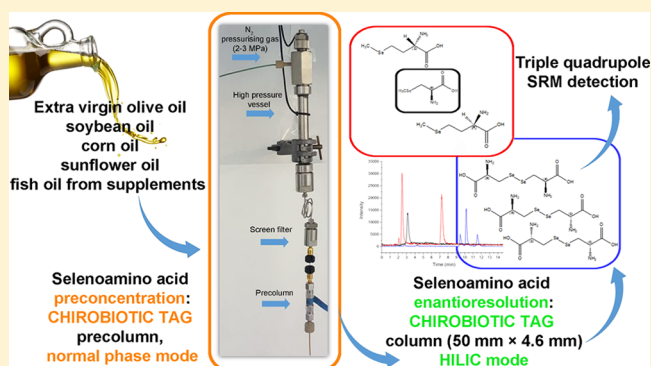
Simultaneous Preconcentration, Identification, and Quantitation of Selenoamino Acids in Oils by Enantioselective High Performance Liquid Chromatography and Mass Spectrometry

Anna Laura Capriotti,[†] Carmela Maria Montone,[†] Michela Antonelli,[†] Chiara Cavaliere,[†] Francesco Gasparrini,[‡] Giorgia La Barbera,[†] Susy Piovesana,^{*,†} and Aldo Laganà[†]

[†]Department of Chemistry and [‡]Department of Drug Chemistry and Technology, Sapienza Università di Roma, Piazzale Aldo Moro 5, 00185 Rome, Italy

S Supporting Information

ABSTRACT: Selenium is an essential micronutrient for humans. In food, selenium can be present in both inorganic and organic forms, the latter mainly being selenomethionine, Se-methyl-selenocysteine, and selenocystine. Selenoamino acid speciation rarely involves the chirality of selenoamino acids. In this work, a 5 cm long CHIROBIOTIC TAG chromatographic column was used for enantioresolution of selenoamino acids (D- and L-selenomethionine, Se-methyl-L-selenocysteine, D-, L- and *meso*-selenocystine); in the optimized conditions, the complete resolution of the analytes was achieved within 15 min by using a very polar aqueous mobile phase (gradient elution by methanol/acetonitrile/H₂O, 45:45:10 (v/v/v) with 10 mmol L⁻¹ of ammonium formate and 0.5% formic acid as the mobile phase A and acetonitrile/H₂O, 20:80 (v/v) with 20 mmol L⁻¹ of ammonium formate at apparent pH 4 as the mobile phase B). The affinity of the teicoplanin aglycone was further exploited to devise a preconcentration method for selenoamino acids in oils. In particular, the CHIROBIOTIC TAG precolumn was used to directly concentrate the selenoamino acids after simple dilution of oil samples with dichloromethane. An optimized procedure for selenoamino acid trapping and preconcentration under normal phase conditions was developed. The enrichment procedure also ensured band focusing during the subsequent separation. The target analytes were finally identified and quantified by triple quadrupole selected reaction monitoring. The method allowed obtention of recovery values up to 73%, with limits of detection between 280 and 750 ng and limits of quantification between 375 and 960 ng for the different selenoamino acids. The method was applied to commercial oil samples, and only L-selenomethionine was detected.



Selenium is an essential micronutrient for human health,¹ the organic forms of which display a higher anticancer activity and lower cytotoxicity.² Most organic selenocompounds are amino acids; thus, chirality is expected to affect their bioactivity.³ Few direct analytical methods that avoid derivatization of selenoamino acids have been described for selenoamino acid enantioseparation, and they exploited CHIROBIOTIC T^{4–8}, chiral ligand-exchange stationary phases,⁹ and chiral crown ether chiral stationary phase (CSP).^{10,11} In more detail, the teicoplanin CHIROBIOTIC T CSP was employed for the enantioresolution of selenomethionine in selenized yeast supplements,⁴ breast milk and infant formulas,^{5,8} and for the enantioresolution of selenomethionine, selenoethionine, and selenocystine in selenized yeast supplements;⁶ the CHIROBIOTIC T column was operated in reversed phase (RP) mode using unbuffered water with or without 2% methanol (MeOH) as an organic modifier, and detection was performed by atomic fluorescence spectrometry or inductively coupled plasma mass spectrometry (ICP-MS). In these works D- and L-selenocystine could not be

resolved.⁶ In comparison to the native teicoplanine CSP, the α values of amino acids on the teicoplanin aglycone CSP were found to be 2–3 times higher under RP mode and polar organic mode (MeOH),¹² even though the sugar could positively improve the resolution of some unusual amino acid analogues.¹³ For the aglycone CSP, recognition occurs for the compounds fitting within the aglycone polypeptidic basket by means of the creation of multiple hydrogen bonds, which mimic the ones with the D-alanine–D-alanine peptide in nature.^{14–19} The enantioselectivity is enhanced when the amino acid carboxylic moiety is close to the stereogenic center.^{19,20} The CHIROBIOTIC TAG CSP was operated in RP mode for the analysis of α -amino acids,²¹ RP, polar organic mode, or polar ionic mode for the enantioresolution of β -amino acids,^{22–26} RP and polar organic mode for different

Received: May 10, 2018

Accepted: June 16, 2018

Published: June 17, 2018

amino acids,^{12,27,28} polar ionic mode, or polar organic mode for the enantioresolution of unusual β 2-²⁹ and β 3-homoamino acids.³⁰

Even though the CHIROBIOTIC TAG CSP was used for enantioresolution of amino acids, no report was ever published on the application to selenoamino acids. In this work, this gap was filled, as the CHIROBIOTIC TAG column was successfully used for the enantioresolution of selenoamino acids, including D-, L- and *meso*-selenocystine. Additionally, the teicoplanin aglycone CSP was exploited to develop a method for the target selenoamino acids' preconcentration from oils. Selenoamino acids are of very low abundance in oil,³¹ and oils are a particularly challenging matrix, as they are a complex mixture of compounds, mainly triacylglycerols, free fatty acids, phenols, sterols, and phospholipids.³² For this reason, selenium determination in oils is particularly difficult, and only a few methods were developed to target selenoamino acids at trace levels in oil, all of them using at least an extraction procedure and none targeting the individual chiral determination of selenoamino acids.^{31,33} Thus, in this work, we also describe a method for the enrichment of the target selenoamino acids directly on the CHIROBIOTIC TAG precolumn after simple dilution of oils with dichloromethane (DCM). The preconcentration was achieved by operating the CHIROBIOTIC TAG precolumn under normal phase (NP) conditions; even if a preconcentration step on a precolumn by NP and separation by a very polar aqueous mobile phase cannot be considered a bidimensional chromatographic system, solvent incompatibility is an important issue for direct coupling, which is not straightforward to solve. Analytes were finally detected by selected reaction monitoring (SRM) tandem mass spectrometry (MS/MS) analysis.

EXPERIMENTAL SECTION

Reagents and Materials. (2*S*)-2-Amino-4-(methylselenanyl)butanoic acid (L-selenomethionine), a racemic mixture of (2*R*)-2-amino-4-(methylselenanyl)butanoic acid (D-selenomethionine) and L-selenomethionine, (R)-2-amino-3-(methylselenanyl)propanoic acid hydrochloride (Se-methyl-L-selenocysteine), a mixture of (2*R*,2'*R*)-3,3'-diselanediybis(2-amino-propanoic acid) (L-selenocystine) with (2*S*,2'*S*)-3,3'-diselanediybis(2-amino-propanoic acid) (D-selenocystine) and (S)-2-amino-3-(((R)-2-amino-2-carboxyethyl)diselanyl)propanoic acid (*meso*-selenocystine) (commercial product containing D-selenocystine/L-selenocystine/*meso*-selenocystine, in a 1:1:2 ratio), a racemic mixture of D- and L-tryptophan, and LC/MS grade organic solvents were purchased from Sigma-Aldrich (St. Louis, MO, USA). The CHIROBIOTIC TAG column (50 × 4.6 mm, L × I.D., 5 μ m particle size) was provided by SUPELCO (Bellefonte, Pennsylvania, USA). The CHIROBIOTIC TAG precolumn was hand-packed with CHIROBIOTIC TAG CSP (5 μ m particle size) into a 20 × 4.6 mm, L × I.D., steel precolumn.

Stock solutions of the selenoamino acids were prepared at 1 mg mL⁻¹ in water, except selenocystine, which was dissolved in 10% (v/v) formic acid. Solutions were kept at -20 °C to avoid degradation. Working mix solutions were prepared weekly by diluting the individual stock solutions.

Selenoamino Acid Trapping on CHIROBIOTIC TAG Precolumn. The apparatus used for preconcentration of the selenoamino acids on the CHIROBIOTIC TAG precolumn is displayed in Figure 1. The stainless steel high pressure vessel (15 × 1 cm) was connected to a nitrogen cylinder by a three-

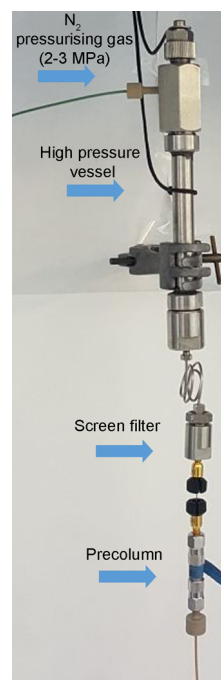


Figure 1. Picture of the trapping system.

way valve. Nitrogen was used as a pressurizing gas at 2–3 MPa to push sample and solvents down the high pressure vessel and through the precolumn. In the final procedure, the high pressure vessel was preliminary washed twice with 6 mL of water, then with 6 mL of ethanol, and finally with 6 mL of DCM. Afterward, the high pressure vessel was connected to the stainless steel filter (0.45 μ m porosity, the filter was previously passivated with HNO₃ to avoid analyte adsorption) and to the precolumn by a virtually zero-dead-volume ultra high performance liquid chromatography (UHPLC) fingertight Viper fitting (50 × 0.1 mm, Thermo Scientific, Figure 1). The precolumn was conditioned with 4 mL of ethanol and 4 mL of DCM (each step to dryness) and was finally equilibrated with 6 mL of hexane. Oil samples (500 mg) were dissolved into 9 mL of DCM and loaded. Then, the precolumn was washed with 3 mL of DCM and finally dried for 15 min by flushing nitrogen.

Chromatographic Separation and MS/MS Analysis. The precolumn was connected to the column by the virtually zero-dead-volume UHPLC fingertight Viper fitting and to an Ultimate 3000 LC system (Thermo Fisher Scientific, Bremen, Germany) into the thermostated column compartment at 50 °C. In the final conditions, samples were eluted at 0.5 mL min⁻¹ using MeOH/ACN/H₂O, 45:45:10 (v/v/v) with 10 mmol L⁻¹ of ammonium formate and 0.5% formic acid as the mobile phase A and ACN/H₂O, 20:80 (v/v) with 20 mmol L⁻¹ of ammonium formate at apparent pH 4 as the mobile phase B (see Supporting Information for details). The optimized gradient elution was the following: 2 min isocratic step at 0% B and then B was increased to 15% in 2 min and to 100% in 10 min. The column was then washed for 5 min at 100% B and equilibrated for 5 min at 0% B.

The UHPLC system was coupled to a TSQ Vantage triple-stage quadrupole mass spectrometer (Thermo Fisher Scientific) via a heated electrospray interface (ESI) for SRM detection of the target compounds. ESI was operated in positive ionization mode (see Supporting Information for

details). The two most abundant Se isotopes for each compound were detected (corresponding to Se^{78} and Se^{80}), using at least two product ions for confirmation for each isotope (Table S2 summarizes all detected ions and related instrumental parameters).

Responses for the direct injection were recorded by injecting 10 μL of composite working solutions in the concentration range 0.094–0.500 $\text{ng } \mu\text{L}^{-1}$ (Table S1). For high pressure vessel preconcentration experiments, the sample was already loaded on the precolumn; thus, 0.1 μL of MeOH was injected by the autosampler just to allow the automatic management of chromatographic runs and data acquisition by Xcalibur (v.2.1, Thermo Fisher Scientific).

Calibration Curves and Application to Real Samples.

The optimized procedure was employed to construct calibration curves from standard solutions and from spiked extra virgin olive oil analyte-free samples; each point of the calibration curves was prepared in triplicate and injected twice at concentrations reported in Table S1. The combined ion current profile for the selected transitions was extracted from the SRM raw files. Unweighted regression lines were calculated (Figures S2–S7). As recovery (R) could not be calculated following reference criteria,³⁴ it was estimated according to the formula: $R\% = (\text{area standard high pressure vessel}/\text{area direct injection}) \times 100$. Similarly, the matrix effect (ME) was estimated according to the formula: $\text{ME}\% = (\text{area oil high pressure vessel}/\text{area standard high pressure vessel}) \times 100$; the process efficiency (PE) was estimated according to the formula: $\text{PE}\% = (\text{area oil high pressure vessel}/\text{area direct injection}) \times 100$. Limits of determination (LODs) and limits of quantification (LOQs) were calculated as signal-to-noise ratio (S/N) = 3 for the second most intense transition and S/N = 10 for the sum of the two most intense transitions, respectively.

The protocol was applied to commercial oil samples bought in a local supermarket: extra virgin olive oil, cold pressed unrefined maize, soy, and sunflower oils, and fish oil from commercial omega-3 supplements.

RESULTS AND DISCUSSION

Selenoamino Acid Enantioresolution on CHIROBIOTIC TAG. The CHIROBIOTIC TAG was considered superior for several aspects to the phases already employed for separation of selenoamino acids.^{35–37} The CHIROBIOTIC TAG consists of teicoplanin aglycone molecules, each of which provides seven polar hydroxyl groups (among which six are phenols), free carboxylic moieties, six polar amide bonds, and seven benzene rings.¹² Such a number of interactions could significantly improve retention of analytes without any need for derivatization or the use of pairing reagents, which in turn increase analysis times and potentially interfere with ionization and MS detection. For the chromatographic separation by CHIROBIOTIC TAG column, the investigated selenoamino acids were eluted using a very polar aqueous mobile phase. The chromatographic retention and enantioselectivity were studied as a function of the buffer composition and chromatographic conditions (gradient and temperature). Different gradient elutions were tested in order to optimize the separation. From this optimization, a generally good retention was achieved, with a significant influence of the water percent in the phase B composition and of the pH of both phase A and B. The water % in phase B was increased from 80 to 85% and to 95%, showing that retention was impaired, and at 95% water, no

separation was any longer observed. The decreased retention agreed with previous reports on amino acid separation on CHIROBIOTIC T CSP.³⁸ The high percent of water in the mobile phase also affected the selectivity for the selenocystine stereoisomers, as all three forms eluted together, indicating that the electrostatic interactions needed for chiral recognition were totally impaired in water when using the CHIROBIOTIC TAG column. As stated before, the retention depends on multiple hydrogen bonds between the aglycone basket and the carboxylate moiety of selenoamino acids; such hydrogen bonds are disrupted in the presence of water, and recognition is no longer possible, as the interaction between the selenoamino acid and the chiral selector is weakened. The optimized conditions developed for selenoamino acid enantioresolution on the CHIROBIOTIC TAG greatly differed from the ones employed on the CHIROBIOTIC T column, as in the latter case, RP conditions were employed,^{4–8} and the enantioresolution of selenomethionine was achieved over 0–40% (v/v) MeOH in water.⁶ The increased retention observed for selenoamino acids on the CHIROBIOTIC TAG under the tested experimental conditions agreed with previous reports, as with the teicoplanin aglycone as selector, the retention factor in most cases increased at high organic modifier content in the mobile phase.³⁰

The pH strongly affected bandwidth: larger bands were obtained without an acid modifier; lowering the pH of phase B to 4 and adding 0.5% formic acid to phase A significantly improved the separation and allowed the separation of D-, L- and *meso*-selenocystine forms. This result did not agree with previous reports on the enantioresolution of selenomethionine on the CHIROBIOTIC T column.⁶ In this case, the retention times and resolution were not affected over the pH range of 4–7. This discrepancy can be attributed to the complementarity of CHIROBIOTIC T and TAG columns, as it was observed for the polar organic and RP modes.^{12,13}

The effect of temperature was also tested, and selenoamino acids were separated at 37 and 50 °C. The increase in temperature improved bandwidth and peak symmetry, especially for selenomethionine and selenocystine stereoisomers, while decreasing retention, as previously observed for amino acids.³⁰

To improve separation between Se-methyl-L-selenocysteine and L-selenomethionine, a ternary solvent mixture was used in phase A: ethanol, isopropanol, and MeOH were tested, and the two compounds were completely separated only using MeOH. Separation was achieved both at high analyte concentration (Figure S1a) and at low analyte concentration (Figure S1b).

Under the optimized conditions, the complete resolution of the analytes, and related isomers when present, was achieved within 15 min (Figure S1, Table 1). The high chromatographic, diastereo-, and enantioselectivity were achieved by the use of a very short, 5 cm long column. Noticeably, on the CHIROBIOTIC TAG, the complete separation of D-, L-, and *meso*-selenocystine was achieved (Table 1) using a very polar aqueous mobile phase, whereas such separation could not be achieved using the CHIROBIOTIC T column.⁶

In the investigated range (0.094–0.500 $\text{ng } \mu\text{L}^{-1}$) the linearity was excellent for all tested compounds, as the R^2 values were above 0.99 in all cases (Figures S1–6).

Optimization of Selenoamino Acid Trapping and Focusing under Normal Phase Conditions. The CHIROBIOTIC TAG CSP is a multimodal CSP; thus, it appeared to be the ideal phase to set up an enrichment system for the target

Table 1. Retention Time (t_R), Apparent Retention Factor (k'_{app}), and Resolution (R_s) for the Chromatographic Separation of the Target Selenoamino Acids^a

selenoamino acid	t_R (min)	k'_{app}	R_s
L-selenomethionine (peak 1)	4.91	1.74	
Se-methyl-L-selenocysteine (peak 2)	5.46	2.05	1.44
D-selenomethionine (peak 3)	7.90	3.41	6.11
L-selenocysteine (peak 4)	9.58	4.35	5.07
meso-selenocysteine (peak 5)	10.37	4.79	2.38
D-selenocysteine (peak 6)	11.96	5.68	3.90

^aChromatographic conditions: 0.5 mL min⁻¹, 50 °C; mobile phase A: MeOH/ACN/H₂O, 45:45:10 (v/v/v) with 10 mmol L⁻¹ of ammonium formate and 0.5% formic acid; mobile phase B: ACN/H₂O, 20:80 (v/v) with 20 mmol L⁻¹ of ammonium formate at apparent pH 4 by formic acid; linear gradient separation: 0% B (0–2 min), 15% B (2–4 min), 100% (4–14 min); 5 min column washing at 100% B, equilibration at 0% B for 5 min; SRM detection.

analytes in oil without sample pretreatment by direct analyte loading on the precolumn. In comparison to the conventional solid phase extraction, such an approach is much easier and faster and does not require any concentration step prior to injection, which is particularly convenient for easily degradable analytes at low concentration, such as selenoamino acids. Additionally, the approach is potentially suitable for stationary phases, which are not available in packed cartridges or are too expensive to be employed in disposable devices.

Trapping conditions were optimized using tryptophan as a surrogate analyte (see [Supporting Information](#) for experimental details), as the elution could be easily monitored by UV–vis detection, and because L-tryptophan had a retention time close to the less retained analyte (L-selenomethionine). DCM was first tested for oil dilution. In order to ensure compatibility between the previously described chromatographic separation and the NP trapping procedure, the precolumn conditioning was performed using miscible solvents with decreasing polarity. The same approach could not be exploited for the washing step after loading, as the use of polar organic solvents would trigger elution. In order to remove oil traces and avoid elution of the target analytes, DCM was used for washing and dried to ensure compatibility between the NP trapping and the elution conditions. In this way, phase miscibility issues were bypassed while avoiding analyte loss or band diffusion. Tryptophan recovery was 60% ([Figure S9](#)). To check if any solubility issue could affect compound recovery during loading, DCM mixtures with polar organic solvents were also tested for oil dilution (DCM/ACN or DCM/isopropanol, 80/20 (v/v)), but no issue was observed. The final procedure was used to trap the target selenoamino acids ([Figure 2](#)).

In comparison to the direct injection, the pre-concentration on the precolumn affected the retention times of the earlier eluting analytes, with a shift up to 2.5 min earlier for L-selenomethionine, as such analytes begin to elute at 0% B. Regardless of time shifts, the enantioresolution of selenoamino acids was not affected.

Method Validation and Application to Commercial Oil Samples. The use of NP conditions for polar compounds, such as amino acids, is not straightforward, and in this case, it is possible as such compounds are present at very low concentration in oil; thus, a compromise between low abundance and compound solubility can be achieved without impairing analyte recovery. Additionally, trapping under NP

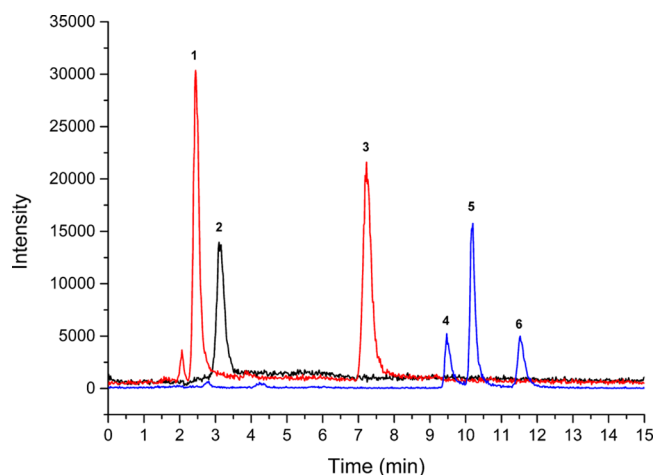


Figure 2. High pressure vessel pre-concentration on the precolumn and enantioresolution of selenoamino acids under the optimized trapping conditions. L-Selenomethionine (peak 1), D-selenomethionine (peak 3), Se-methyl-L-selenocysteine (peak 2), L-selenocysteine (peak 4), D-selenocysteine (peak 6), and meso-selenocysteine (peak 5); chromatographic conditions: 0.5 mL min⁻¹, 50 °C; mobile phase A: MeOH/ACN/H₂O, 45:45:10 (v/v/v) with 10 mmol L⁻¹ of ammonium formate and 0.5% formic acid; mobile phase B: ACN/H₂O, 20:80 (v/v) with 20 mmol L⁻¹ of ammonium formate at apparent pH 4 by formic acid; linear gradient separation: 0% B (0–2 min), 15% B (2–4 min), 100% (4–14 min); 5 min column washing at 100% B, equilibration at 0% B for 5 min; SRM detection.

has the advantage of removing interfering compounds, which are mainly hydrophobic species, an improvement of which can be evaluated by the measured matrix effect. Thus, method validation was performed, and the recovery, matrix effect, and process efficiency values were calculated ([Table S3](#)). Recoveries were in the range of 62–73%, the matrix effect was in the range of 74–115% and the process efficiency was in the range of 48–84% ([Table S3](#)). Such values were not affected by the selenoamino acid spiking level. Despite the use of a procedure where oil was simply diluted and compounds pre-concentrated on the precolumn, the matrix effect was within $\pm 25\%$ for all compounds, and LODs and LOQs were at ng absolute amounts ([Table S4](#)).

After validation, the method was applied to commercial oil samples, where only L-selenomethionine was detected in soybean, sunflower, and fish oils from omega-3 supplements ([Figure S10](#)). In particular, 2 ng of L-selenomethionine was found in 500 mg of sunflower oil (4 ng g⁻¹) and 1.8 ng of L-selenomethionine was found in the fish oil from supplements (3.6 ng g⁻¹). Soybean oil was the most naturally rich with L-selenomethionine; thus, the oil amount employed for pre-concentration was reduced 10-fold, to fit within the calibration curve. In this way, 3.1 ng of L-selenomethionine was quantified in 50 mg of soybean oil (62 ng g⁻¹).

CONCLUSION

The paper describes the complete enantioresolution of three selenoamino acids using a very polar aqueous mobile phase in less than 15 min on a 5 cm long CHIROBIOTIC TAG column. Selenocysteine stereoisomers, which were never resolved before, could be efficiently separated. The separation was performed without need of any derivatization, and it was coupled to a triple quadrupole SRM detection. Additionally, the affinity of CHIROBIOTIC TAG CSP was exploited to

preconcentrate the target selenoamino acids in edible oils. To avoid any sample preparation, a direct preconcentration of the target selenoamino acids was achieved on the CHIROBIOTIC TAG precolumn under NP conditions. Nitrogen was used to dry the precolumn and ensure compatibility between the NP trapping and the subsequent separation. The system was developed for selenoamino acids in oil, but the described enrichment is potentially applicable to other classes of polar analytes in oils. Additionally, the concept can be extended to precolumns packed with different stationary phases or coupled with nonenantioselective analyte separations. Finally, in this work, NP was coupled with a very polar aqueous mobile phase separation, but the method can also be adapted to the coupling of NP with other water-based separation mechanisms, such as with hydrophilic interaction liquid chromatography or RP.

■ ASSOCIATED CONTENT

Supporting Information

The Supporting Information is available free of charge on the ACS Publications website at DOI: [10.1021/acs.analchem.8b02089](https://doi.org/10.1021/acs.analchem.8b02089).

List of standard concentrations, SRM transitions, tables for method validation in extra virgin olive oil, results of selenoamino acid quantification in commercial oil sample (PDF)

■ AUTHOR INFORMATION

Corresponding Author

*E-mail: susy.piovesana@uniroma1.it.

ORCID

Anna Laura Capriotti: 0000-0003-1017-9625

Francesco Gasparrini: 0000-0003-0970-2917

Susy Piovesana: 0000-0001-7134-7421

Author Contributions

The manuscript was written through contributions of all authors. All authors have given approval to the final version of the manuscript.

Notes

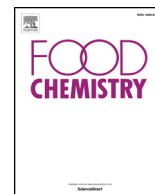
The authors declare no competing financial interest.

■ ACKNOWLEDGMENTS

The project was funded by the Cariplo Foundation within the “Agroalimentare e Ricerca” (AGER) program. Project AGER2-Rif.2016-0169, “Valorization of Italian OLIVE products through INnovative analytical tools—VIOLIN”

■ REFERENCES

- (1) Rayman, M. P. *Lancet* **2012**, 379 (9822), 1256–1268.
- (2) Deng, S.; Zeng, D.; Luo, Y.; Zhao, J.; Li, X.; Zhao, Z.; Chen, T. *RSC Adv.* **2017**, 7 (27), 16721–16729.
- (3) Oguri, S.; Kumazaki, M.; Kitou, R.; Nonoyama, H.; Tooda, N. *Biochim. Biophys. Acta, Gen. Subj.* **1999**, 1472 (1–2), 107–114.
- (4) Méndez, S. P.; González, E. B.; Sanz-Medel, A. *Biomed. Chromatogr.* **2001**, 15 (3), 181–188.
- (5) Gómez-Ariza, J. L.; Bernal-Daza, V.; Villegas-Portero, M. J. *Anal. Chim. Acta* **2004**, 520 (1–2), 229–235.
- (6) Pérez Méndez, S.; Blanco González, E.; Sanz Medel, A. *J. Anal. At. Spectrom.* **2000**, 15 (9), 1109–1114.
- (7) Ilisz, I.; Berkecz, R.; Péter, A. *J. Sep. Sci.* **2006**, 29 (10), 1305–1321.
- (8) Gómez-Ariza, J. L.; Bernal-Daza, V.; Villegas-Portero, M. J. *Appl. Organomet. Chem.* **2007**, 21 (6), 434–440.
- (9) Huang, X.; Wang, J.; Wang, Q.; Huang, B. *Anal. Sci.* **2005**, 21 (3), 253–257.
- (10) Sutton, K. L.; Ponce de Leon, C. A.; Ackley, K. L.; Sutton, R. M. C.; Stalcup, A. M.; Caruso, J. A. *Analyst* **2000**, 125 (2), 281–286.
- (11) Ponce de Leon, C. A.; Sutton, K. L.; Caruso, J. A.; Uden, P. C. *J. Anal. At. Spectrom.* **2000**, 15 (9), 1103–1107.
- (12) Berthod, A.; Chen, X.; Kullman, J. P.; Armstrong, D. W.; Gasparrini, F.; D’Acquaric, I.; Villani, C.; Carotti, A. *Anal. Chem.* **2000**, 72 (8), 1767–1780.
- (13) Péter, A.; Árki, A.; Tourwé, D.; Forró, E.; Fülöp, F.; Armstrong, D. W. *J. Chromatogr. A* **2004**, 1031 (1–2), 159–170.
- (14) Cavazzini, A.; Nadalini, G.; Dondi, F.; Gasparrini, F.; Ciogli, A.; Villani, C. *J. Chromatogr. A* **2004**, 1031 (1–2), 143–158.
- (15) Bois-Choussy, M.; Neuville, L.; Beugelmans, R.; Zhu, J. *J. Org. Chem.* **1996**, 61 (26), 9309–9322.
- (16) Economou, N. J.; Zentner, I. J.; Lazo, E.; Jakoncic, J.; Stojanoff, V.; Weeks, S. D.; Grasty, K. C.; Cocklin, S.; Loll, P. J. *Acta Crystallogr., Sect. D: Biol. Crystallogr.* **2013**, 69 (4), 520–533.
- (17) Han, S.; Le, B. V.; Hajare, H. S.; Baxter, R. H. G.; Miller, S. J. *J. Org. Chem.* **2014**, 79 (18), 8550–8556.
- (18) Ciogli, A.; Kotoni, D.; Gasparrini, F.; Pierini, M.; Villani, C. *Top. Curr. Chem.* **2013**, 340, 73–105.
- (19) Ismail, O. H.; Ciogli, A.; Villani, C.; De Martino, M.; Pierini, M.; Cavazzini, A.; Bell, D. S.; Gasparrini, F. *J. Chromatogr. A* **2016**, 1427, 55–68.
- (20) D’Acquarica, I.; Gasparrini, F.; Misiti, D.; Pierini, M.; Villani, C. *Adv. Chromatogr.* **2007**, 46, 109–173.
- (21) Barbaro, E.; Zangrando, R.; Vecchiato, M.; Turetta, C.; Barbante, C.; Gambaro, A. *Anal. Bioanal. Chem.* **2014**, 406 (22), 5259–5270.
- (22) Sztojokov-Ivanov, A.; Lázár, L.; Fülöp, F.; Armstrong, D. W.; Péter, A. *Chromatographia* **2006**, 64 (1–2), 89–94.
- (23) Berkecz, R.; Török, R.; Ilisz, I.; Forró, E.; Fülöp, F.; Armstrong, D. W.; Péter, A. *Chromatographia* **2006**, 63, S37–S43.
- (24) Árki, A.; Tourwé, D.; Solymár, M.; Fülöp, F.; Armstrong, D. W. *Chromatographia* **2004**, 60, S43–S54.
- (25) Péter, A.; Lázár, L.; Fülöp, F.; Armstrong, D. W. *J. Chromatogr. A* **2001**, 926 (2), 229–238.
- (26) Péter, A.; Árki, A.; Vékes, E.; Tourwé, D.; Lázár, L.; Fülöp, F.; Armstrong, D. W. *J. Chromatogr. A* **2004**, 1031 (1–2), 171–178.
- (27) Xiao, T. L.; Tesarova, E.; Anderson, J. L.; Egger, M.; Armstrong, D. W. *J. Sep. Sci.* **2006**, 29 (3), 429–445.
- (28) Péter, A.; Török, R.; Armstrong, D. W. *J. Chromatogr. A* **2004**, 1057 (1–2), 229–235.
- (29) Pataj, Z.; Berkecz, R.; Ilisz, I.; Misicka, A.; Tymecka, D.; Fülöp, F.; Armstrong, D. W.; Péter, A. *Chirality* **2009**, 21 (9), 787–798.
- (30) Pataj, Z.; Ilisz, I.; Berkecz, R.; Misicka, A.; Tymecka, D.; Fülöp, F.; Armstrong, D. W.; Péter, A. *J. Sep. Sci.* **2008**, 31 (21), 3688–3697.
- (31) Torres, S.; Cerutti, S.; Raba, J.; Pacheco, P.; Silva, M. F. *Food Chem.* **2014**, 159, 407–413.
- (32) Cao, G.; Ruan, D.; Chen, Z.; Hong, Y.; Cai, Z. *TrAC, Trends Anal. Chem.* **2017**, 96, 201–211.
- (33) López-García, I.; Vicente-Martínez, Y.; Hernández-Córdoba, M. J. *Agric. Food Chem.* **2013**, 61 (39), 9356–9361.
- (34) Matuszewski, B. K.; Constanzer, M. L.; Chavez-Eng, C. M. *Anal. Chem.* **2003**, 75 (13), 3019–3030.
- (35) Garousi, F.; Domokos-Szabolcsy, É.; Jánószky, M.; Kovács, A. B.; Veres, S.; Soós, Á.; Kovács, B. *Plant Foods Hum. Nutr.* **2017**, 72 (2), 168–175.
- (36) Ruszczynska, A.; Konopka, A.; Kurek, E.; Torres Elguera, J. C.; Bulska, E. *Spectrochim. Acta, Part B* **2017**, 130, 7–16.
- (37) Jagtap, R.; Maher, W. *Microchem. J.* **2016**, 124, 422–529.
- (38) Berthod, A.; Liu, Y.; Bagwill, C.; Armstrong, D. W. *J. Chromatogr. A* **1996**, 731 (1–2), 123–137.



Investigation of free seleno-amino acids in extra-virgin olive oil by mixed mode solid phase extraction cleanup and enantioselective hydrophilic interaction liquid chromatography-tandem mass spectrometry

Susy Piovesana, Carmela Maria Montone, Michela Antonelli, Chiara Cavaliere*,
Giorgia La Barbera, Silvia Canepari, Roberto Samperi, Aldo Laganà, Anna Laura Capriotti

Department of Chemistry, University of Rome "La Sapienza", Piazzale Aldo Moro 5, Rome, Italy

ARTICLE INFO

Keywords:

Seleno-amino acids
Total Selenium
Extra virgin olive oil
Enantioselective high performance liquid chromatography (eHPLC)
Mass spectrometry

ABSTRACT

An analytical method for determining seleno-methionine (SeMet), methyl-seleno-cysteine and seleno-cystine in extra-virgin olive oil (EVOO) was developed and validated. EVOO sample (15 g) was diluted with hexane, extracted with methanol/water 80:20 (v/v), and cleaned up by a reversed phase/strong cation exchange solid phase extraction. Analysis was performed by chiral hydrophilic interaction liquid chromatography-tandem mass spectrometry. Process efficiency ranged between 49 and 97% and trueness between 87 and 126%, with intermediate precision, expressed as standard deviation, lower than 10%. Method detection limits (MDLs) and method quantification limits (MQLs) were lower than $1 \mu\text{g kg}^{-1}$.

Thirty-two EVOO samples from different Italian regions were analyzed for both total Se and single seleno-amino acids determination. Only L-SeMet was found at level MQL ($0.2 \mu\text{g kg}^{-1}$)- $1.42 \mu\text{g kg}^{-1}$ in ten samples, while total Se was in the range of MDL- $9.1 \mu\text{g kg}^{-1}$. Concentration of L-SeMet (5–6% of total Se) and total Se correlated very well to each other ($R^2 = 0.995$).

1. Introduction

Selenium (Se) is one of the most important microelements and its influence on human health is increasingly apparent. Because Se is both essential and toxic for humans, with a narrow window between essentiality and toxicity compared with other trace elements, it has been extensively measured in food, diet supplements, as well as biological fluids (Amoako, Uden, & Tyson, 2009; Jagtap, Maher, Krikowa, Ellwood, & Foster, 2016; Stoffaneller & Morse, 2015). Se plays an important biochemical role in selenoproteins synthesis (25 in humans), which typically have redox functions and are involved in scavenging free radicals, immune function, thyroid function, spermatogenesis, cancer prevention, and pathogen resistance (Rayman, 2012).

The recommended Se daily intake varies between the U.S. National Institutes of Health (NIH, <https://ods.od.nih.gov/factsheets/Selenium-HealthProfessional/#h2>) and the European Food Safety Authority (EFSA, <http://onlinelibrary.wiley.com/doi/10.2903/j.efsa.2014.3846/epdf>). For the NIH, the recommended Se daily intake is in the

range of $55\text{--}70 \mu\text{g day}^{-1}$ for adults and $15\text{--}40 \mu\text{g day}^{-1}$ for children, while the highest intake level that does not cause adverse effects in adults has been set at $400 \mu\text{g day}^{-1}$.

Se intake in mammalian occurs by diet. Animal-derived foods are a richer dietary source of Se than plants. Nevertheless, Se in plants becomes important in vegetarian and vegan diets, as they depend only on food of plant origin for Se demand. Plants assimilate and metabolize Se (VI) by sulfur uptake and biochemical pathways (El-Ramady et al., 2016; Ruszczyńska, Konopka, Kurek, Torres Elguera, & Bulska, 2017). Selenate anion (SeO_4^{2-}) is firstly reduced to selenite (SeO_3^{2-}), then to selenide (Se^{2-}) and finally metabolized to organic forms, which are mainly seleno-amino acids, i.e. Se-cysteine (SeCys), Se-methionine (SeMet), methyl-Se-cysteine (MeSeCys), Se-cystine (SeCys₂) and sometime other more complex Se organic forms (Schiavon & Pilon-Smits, 2017).

The determination of the total Se content of a given food is an unreliable information because the bioavailability of this nutrient depends on the form in which it is present, being Se better assimilated by

* Corresponding author at: Department of Chemistry, Università di Roma "La Sapienza", Piazzale Aldo Moro 5, 00185 Rome, Italy.

E-mail addresses: susy.piovesana@uniroma1.it (S. Piovesana), carmelamaria.montone@uniroma1.it (C.M. Montone), michela.antonelli@uniroma1.it (M. Antonelli), chiara.cavaliere@uniroma1.it (C. Cavaliere), giorgia.labarbera@uniroma1.it (G. La Barbera), silvia.canepari@uniroma1.it (S. Canepari), roberto.samperi@uniroma1.it (R. Samperi), aldo.lagana@uniroma1.it (A. Laganà), annalaura.capriotti@uniroma1.it (A.L. Capriotti).

<https://doi.org/10.1016/j.foodchem.2018.11.053>

Received 17 July 2018; Received in revised form 5 November 2018; Accepted 9 November 2018

Available online 10 November 2018

0308-8146/© 2018 Elsevier Ltd. All rights reserved.

humans as organic species (Rayman, Infante, & Sargent, 2008). Although other techniques, such as high performance liquid chromatography (HPLC) coupled to atomic fluorescence spectrometry (Sanchez-Rodas, Mellano, Morales, & Giraldez, 2013) and synchrotron-based ones (Lombi & Susini, 2009) have been proposed, the HPLC-inductively coupled plasma (ICP) mass spectrometry (MS) (B'Hymer & Caruso, 2006; Gammelgaard, Jackson, & Gabel-Jensen, 2011; Jagtap & Maher, 2016; Jagtap et al., 2016; Ruszczyńska et al., 2017; Stoffaneller & Morse, 2015) and HPLC-MS/MS (Gammelgaard et al., 2011; Stoffaneller & Morse, 2015) are the most widely used techniques for Se speciation studies. In this context, the information obtainable by electrospray ionization-tandem mass spectrometry (ESI-MS/MS) is surely more reliable, as co-eluting species can be differentiated. Hydrophilic Interaction Liquid Chromatography (HILIC) is a potent LC technique for separation of polar compounds, which are poorly retained and/or resolved by reversed phase (RP) HPLC. Besides, HILIC mobile phases match very well the requirement for a sensitive ESI-MS detection and has been extensively used for polar compounds analysis in food (Bernal, Ares, Pól, & Wiedmer, 2011; Marrubini, Appelblad, Maietta, & Papetti, 2018) and as a complementary separation technique for selenomics of very rich Se sources, such as Se enriched yeast (Arnaudguilhem et al., 2012).

The chirality of seleno-amino acids is only rarely considered. Se- α -amino acids have a single asymmetric carbon atom thus exist as a couple of enantiomers. Se-Cys₂ consists of two Se-Cys molecules bridged by a Se-Se bond, thus it can exist as a couple of enantiomers and a D-L (meso) form. As for ordinary amino acids, chirality can have an important impact on the biodistribution. Amino acids found in proteins are L-amino acids and it has been reported that D- and L-amino acids have different intestinal absorption and metabolic pathways; more specifically, the absorption rate of D-isomers is slower than L-isomers (Oguri, Kumazaki, Kitou, Nonoyama, & Tooda, 1999), which results in L-Se-amino acids being more toxic than the D-forms (Gómez-Ariza, Bernal-Daza, & Villegas-Portero, 2007). Moreover, D-isomers also need conversion into L-isomers before incorporation into proteins, even if this conversion has not been described for all amino acids (Friedman & Levin, 2012). Two chiral stationary phases have been employed for underivatized Se-amino acid separation, such as the Crownpak CR(+) in the anion exchange mode (Sutton et al., 2000) and the Chirobiotic T in the RP mode (Gómez-Jacinto, García-Barrera, Garbayo, Vélchez, & Gómez-Ariza, 2012).

The purpose of this work was to investigate the concentration levels of both total Se and seleno-amino acids that could be present in extra virgin olive oil (EVOO), an important component of the Mediterranean diet. EVOO is usually considered a source of important phytochemicals (Capriotti, Cavaliere, Foglia, Piovesana, & Ventura, 2015; La Barbera et al., 2017), in particular polyphenols (Capriotti et al., 2014), nevertheless minor compounds can be important as well, such as Se content and seleno-amino acids, as these parameters might be correlated with quality or origin of the product. Until now, only one investigation has been published on this topic (Torres, Cerutti, Raba, Pacheco, & Silva, 2014), concerning EVOO from Argentina, a country which accounts for about 6% of worldwide production. With respect of that paper, a new method for the determination of seleno-amino acids, based on liquid-liquid extraction (LLE), mixed mode (RP and strong cation exchanger) cleanup and chiral HILIC chromatographic separation followed by selected reaction monitoring (SRM) MS/MS detection, was developed and validated. Then, 32 samples of EVOO from various geographic proveniences in Italy were analyzed for both total Se and selected seleno-amino acids, and finally data were correlated.

2. Materials and methods

2.1. Chemicals and reagents

Standards of (2S)-2-amino-4-(methylselenanyl)butanoic acid (L-

SeMet) ($\geq 98\%$), racemic SeMet ($\geq 99\%$), (R)-2-amino-3-(methylselenanyl)propanoic acid hydrochloride (L-MeSeCys hydrochloride, $\geq 95\%$), L-SeMet (methyl-¹³C) (≥ 99 atom ¹³C %) internal standard (IS) and 3,3'-diselanediybis(2-aminopropanoic acid) (SeCys₂) (95%) were obtained by Sigma Aldrich, now Merck (Darmstadt, Germany). Once analyzed using a chiral stationary phase (see later), SeCys₂ was resolved into three peaks with the area ratio $\sim 1:2:1$, which were attributed to L-, meso-, and D-SeCys₂ forms, respectively.

Reagent grade methanol (MeOH), hexane, HCl (37%, w/w), NH₃ (28–30%, w/w) were from Sigma Aldrich.

Ultrapure water (resistivity 18.2 M Ω cm) was obtained by an Arium water purification system (Sartorius, Florence, Italy). LC-MS grade water was purchased from Fisher Scientific (Rodano, Italy). LC-MS grade acetonitrile (ACN) was purchased from VWR International (Milan, Italy). Other chemicals used for total Se determination were of the highest grade from various sources.

Oasis HLB™ (200 mg) and Oasis MCX™ (150 mg) cartridges were from Waters (Milford, MA, USA).

The Astec CHIROBIOTIC™ TAG column (50 mm \times 4.6 mm I.D., 5 μ m particle size) was provided by Sigma-Aldrich.

2.2. Standard solutions

Stock solutions of L-SeMet, racemic SeMet and L-MeSeCys hydrochloride were prepared at 1000 μ g mL⁻¹ in water. SeCys₂ was prepared in 10% (v/v) HCOOH at the same concentration. A composite standard stock solution was prepared by combining aliquots of each individual standard solution and diluting with water to the final concentration of 100 μ g mL⁻¹. The IS stock solution was prepared at 100 μ g mL⁻¹ in water. Based on a previous report (Muñoz Olivas, Quevauviller, & Donard, 1998), all the stock solutions were subdivided into aliquots, stored at -20°C in amber glass vials, and brought to room temperature just before use. Working standard solutions were prepared from stock standards by suitable dilution with water, stored at 4°C when not in use and renewed weekly.

2.3. Total Se measurement

Total Se content was measured by hydride generation atomic fluorescence spectroscopy (HG-AFS) following a slightly modified procedure reported elsewhere (Di Dato et al., 2017) on about 1 g of each oil sample in duplicate (for details, see the supplementary material).

Fig. S1 displays a map with the EVOO sample territorial origin correlated with the available data of Se mean concentration in Italian soils, divided by provincial districts (Spadoni et al., 2007).

2.4. Sample preparation for LC-MS/MS analysis

Thirty-two Italian EVOO samples from the 2016 harvest campaign were analyzed in this study (see Table S1 for details on EVOO samples).

Fifteen g of EVOO samples were weighed into a 50 mL polyethylene falcon tube; then, 100 μ L of the IS solution (0.1 ng μ L⁻¹) and 15 mL of hexane were added, and the mixture manually shaken for ca 30 s. Ten mL of MeOH:H₂O (80:20, v/v) were added and the mixture was vortexed for 20 min, then centrifuged for 10 min at 3000g at 15°C . The oil/hexane supernatant was discarded and the lower layer transferred to a clean 15 mL polyethylene tube, 20 μ L of 6 mol mL⁻¹ HCl was added and the mixture vortexed for 30 s. The acidified extract was loaded by gravity on the Oasis MCX™ SPE cartridge, after activation with 5 mL of MeOH and 5 mL of 10 mmol L⁻¹ HCl solution. The cartridge was washed with 2 mL ultrapure water followed by 5 mL MeOH (by gravity) then, the analytes were eluted with 2 mL of MeOH with 3% NH₃ (v/v) into a clean vial. The solvent was evaporated down to ca. 150 μ L at 25°C in a Speed-Vac SC 250 Express (Thermo, Holbrook, NY, USA); finally, 100 μ L of ACN containing 0.5% HCOOH (v/v) were added, the obtained solution was forced through a PTFE syringe filter and 200 μ L

were transferred to the autosampler vial.

2.5. LC-MS/MS analysis

Samples were analyzed by an Ultimate 3000 ultra-HPLC (UHPLC) system connected via a heated ESI source to a TSQ Vantage™ triple-stage quadrupole mass spectrometer (Thermo Fisher Scientific, Bremen, Germany). The UHPLC system consisted of a binary pump equipped with a degasser, a thermostated microwell plate autosampler, set at 14 °C and a thermostated column oven.

The Astec CHIROBIOTIC™ TAG analytical column (50 mm × 4.6 mm I.D., 5 μm particle size) was thermostated at 50 °C, and operated as previously reported with some modifications (Capriotti et al., 2018). Mobile phase A was MeOH:ACN:H₂O, 45:45:10 (v/v/v), 10 mmol L⁻¹ ammonium formate and 0.5% HCOOH; mobile phase B was ACN:H₂O, 20:80 (v/v), 20 mmol L⁻¹ ammonium formate at pH 4 by HCOOH. Gradient elution started with a 2 min isocratic step at 0% B. Then, B was linearly increased to 15% in 2 min, from 15% to 100% in 10 min and kept constant for 5 min. Finally, B was decreased linearly to 0% in 0.5 min and kept constant for 5 min to equilibrate the column. The flow rate was set at 0.5 mL min⁻¹ and 10 μL of the final extract was injected.

The ESI source was operated in positive ionization with the following settings: spray voltage 3.0 kV, vaporizer temperature 280 °C, and the capillary (ion-transfer tube) temperature 280 °C. Sheath gas pressure, ion sweep gas pressure, and auxiliary gas pressures were set to 40, 0, and 20 (arbitrary units), respectively. Source conditions, lens parameters and analyte transitions were optimized by infusing standard solutions at 10 ng μL⁻¹ in mobile phase A at 10 μL min⁻¹. The [M + H]⁺ ions were selected by the first quadrupole and fragmented in the collision cell with the optimized collision energy. The two transitions showing the highest signal-to-noise ratio (S/N) were selected for SRM setting (see Table 1). The UHPLC-MS system was managed by Xcalibur software (v.2.1, Thermo Fisher Scientific).

2.6. Method validation

The method was validated following the guidelines in the

Table 1

Precursor ion and product ions monitored for the investigated seleno-amino acids. S-lens values for each precursor ion and collision energy for each transition are also reported. Scan width was kept at 0.5 m/z for all the transitions.

Compound (isotope)	Precursor ion (m/z)	Product ion (m/z) ^a	Collision energy (V)	S- lens (V)
⁷⁸ Se-Methyl-seleno-cysteine	182.1	121.0	20	40
		165.0	6	
		123.0	19	
⁸⁰ Se-Methyl-seleno-cysteine	184.1	167.0	6	64
		56.0	20	
		107.1	22	
⁷⁸ Se-methionine	196.1	179.0	9	80
		56.0	20	
		109.1	22	
⁸⁰ Se-methionine	198.1	181.0	9	64
		70.0	46	
		74.0	28	
⁷⁸ Se-cystine	335.0	88.0	33	80
		246.0	33	
		70.0	46	
⁸⁰ Se-cystine	337.0	74.0	28	80
		88.0	33	
		248.0	18	
¹³ C-Se-methionine	199.1	110.1	22	64

^a For each compound, product ions used for quantitation and confirmation transitions are reported in bold and in italic, respectively.

Commission Decision 2002/657/EC (Decision 2002/657/CE, 2002).

2.6.1. Calibration curves

Instrumental linearity range was evaluated in a separate experiment. Six standard solutions were prepared in ACN:H₂O, 1:1 (v/v) with 0.5% HCOOH (v/v) in the range 100–2500 ng mL⁻¹ and 10 μL were injected twice.

Three sets of seven-points calibration graphs were prepared. They were named standard in solvent (SS), matrix matched (MM), and matrix assisted (MA), following the definitions by (Nathanail et al., 2015). These graphs were constructed at seven concentration levels (i.e. 0.5, 1.0, 1.5, 2.5, 5.0, 7.5, and 10 μg kg⁻¹).

The SS curves were constructed by diluting the appropriate volumes of the composite working standard solution in ACN:H₂O, 1:1 (v/v) with 0.5% HCOOH (v/v). For MM and MA calibration graphs, EVOO pools, obtained pooling six analyte-free samples, were employed and extracted as reported in Section 2.4. For the MM curves, 15 mL of EVOO were first extracted, then spiked at the concentrations mentioned above. For the MA calibration curves, 15 mL of EVOO were first spiked, then extracted. The IS was added only to the MA samples before extraction. The actual volume of the final extracts was measured with a 500-μL syringe to make correction when necessary. Each concentration point was prepared in duplicate and injected twice, starting from the lowest up to the highest concentration level; finally, the results were averaged to give rise to a single calibration graph for each seleno-amino acid. For each analyte, the combined ion current profile for the selected transitions was extracted from the LC-MRM chromatogram and used to measure the areas. The areas of the analyte were plotted versus the analyte concentration to build the graphs. The unweighted regression lines were calculated using Excel software.

2.6.2. Process efficiency

Process efficiency (PE), as well as extraction recovery (RE) and matrix effect (ME), were assessed in accordance with what is defined elsewhere (Matuszewski, Constanzer, & Chavez-Eng, 2003; Piovesana et al., 2017). Given the general equation $y = ax + b$ for the linear regression in the SS, MM and MA graphs, RE, ME and PE were calculated using the calibration graphs ratios.

RE% was assessed as follows:

$$RE (\%) = (a_{MA}/a_{MM}) \times 100$$

by the ratio of the slope of MA to MM calibration graphs × 100;

ME% was assessed as follows:

$$ME (\%) = (a_{MM}/a_{SS}) \times 100$$

by the ratio of the slope of MM to SS calibration graphs × 100;

finally, PE% was assessed as follows:

$$PE (\%) = (a_{MA}/a_{SS}) \times 100$$

by the ratio of the slope of MA to SS calibration graphs × 100. For these calculations, MM calibration graphs were constructed without normalization to IS.

2.6.3. Trueness, precision, method detection limit, and method quantification limit

Trueness and intermediate precision were calculated as apparent recovery and the relative standard deviation (RSD, %) at two concentration levels, i.e., 2 and 10 μg kg⁻¹. Fifteen g of EVOO samples, not containing detectable amount of the analytes, were spiked at the two above mentioned concentration levels either before extraction (set 1) or after extraction (set 2). Apparent recoveries were calculated as follows:

$$\text{Apparent RE} (\%) = [(Area_{Analyte, set1} / Area_{IS, set1}) / (Area_{Analyte, set2} / Area_{IS, set2})] \times 100$$

For both concentration levels, five replicated samples were extracted and analyzed in five different days. The mean concentrations

obtained were compared with the values expected from the MA calibration lines which were normalized with respect to the IS and expressed as apparent recovery.

MDLs and MQLs were extrapolated from the lowest point of the MA calibration line corresponding to $0.5 \mu\text{g kg}^{-1}$. The actual S/N values were calculated. Then, the SRM transition giving the best S/N value was selected and MQL was estimated as the analyte concentration corresponding to $S/N = 10$, while MDL was estimated as the concentration giving a $S/N = 3$ for the second most favorable SRM transition. As the noise for all three SeCys₂ isomers was very low, a ten time less concentrated sample was prepared and processed to verify the extrapolated values.

2.6.4. Quality control

Although the seleno-amino acids did not show problems of carry-over or background contamination, a procedural blank was analyzed every day. Moreover, an analyte-free sample spiked at $5 \mu\text{g kg}^{-1}$ was analyzed for every experimental set.

3. Results and discussion

3.1. Chromatography

Underivatized amino acids are well retained and have been successfully separated by HILIC before ESI-MS/MS analysis by amide columns (Langrock, Czihal, & Hoffmann, 2006; Prinsen et al., 2016).

In several studies, RP chromatography was performed for separation of seleno-amino acids before ESI-MS/MS (Torres et al., 2014; Zembrzaska, Matusiewicz, Polkowska-Motrenko, & Chajduk, 2014). Some tests were performed under these conditions. In particular, a CORTECS UPLC C18 + column ($2.1 \times 100 \text{ mm}$, $1.6 \mu\text{m}$, Waters) was used for separation. However, all the analytes were poorly retained and eluted practically with the dead volume, within 2 min (Fig. S2a). The poor retention does not impair standard analytes separation but it does hinder the analysis of seleno-amino acids in oil extracts. In fact, when an oil extract was analyzed, an intense signal overlapped to all the transitions selectable for the analytes (Fig. S2b), due to the presence of interfering compounds responding to the transitions of the target analytes though lacking Se isotopic pattern. The poor retention did not allow to separate the target analytes from the interfering compounds, thus a different approach was necessary.

CHIROBIOTIC TAG is a chiral stationary phase (CSP) consisting of teicoplanin aglycone bonded to silica, which provides polar hydroxyl groups, carboxylic moieties, amide bonds and benzene rings (Berthod et al., 2000). Such a number of interactions enables this CSP to work in RP, normal phase as well as HILIC mode. The CHIROBIOTIC TAG is a CSP, thus it allows the enantioresolution of chiral compounds and determination of unexpected non-natural D- and meso-isomers. In addition, the CHIROBIOTIC TAG is very stable to solvent and buffer change and re-equilibration is fast. The chromatographic conditions reported in the experimental section were optimized with respect to separation, peak symmetry and molar response to ESI⁺ ionization. A column as short as 5 cm also allows the separation of the three forms of Se-Cys₂; in addition, the relatively mobile phase linear velocity, which corresponds to the Height Equivalent to the Theoretical Plate (HETP) minimum value, as well as the high organic solvent percentage, also allows better sensitivity if compared with the RP mode. A single column was used for the experiments reported in this paper; to maintain the performances of the column unchanged, the only precaution taken was a monthly wash of the column by sequentially flushing polar and -non polar-polar solvents. Fig. 1A shows the chromatogram of the separation of the seleno-amino acids standard solution. MeSeCys standard was a pure L-form; the D form was not readily commercially available as it was produced only on request. On the other hand, its t_R window is easily predictable and, in case of doubt, it can be confirmed by high resolution MS/MS.

3.2. Mass spectrometry

Table 1 shows all the most intense transitions recorded in the SRM mode at the beginning of this study (H_2O loss was excluded *a priori*), while in bold there are reported the product ions used for quantitation and in italic those used for confirmation, respectively. Selenium possesses a very typical isotopic pattern, which could be very useful for Se-containing compound identification and/or confirmation. The most abundant of these isotopes are ⁷⁸Se (23.6%) and ⁸⁰Se (49.9%), their ratio is about 1:2 and the choice of the most intense transition of the two isotopic compounds appears desirable. However, in light of what was observed by analyzing the EVOO sample extracts, this was not possible. Some transitions showed interferences, while others were too noisy. Finally, only the selected transitions were incorporated in the SRM acquisition method. The ion at m/z 56.0 should have the structure $[\text{NH}_3^+ - \text{CH} = \text{C} = \text{O}]$, which is common to some α -amino acids, but the precursor ion ensures a good specificity.

Isotopic ISs are available only for L-SeMet, namely ¹³C(Me)-L-SeMet, D₃(Me)-L-SeMet and ¹³CD₃(Me)-L-SeMet. Due to the isotopic distribution of Se, none of these compounds is free of reciprocal interference with the non-labeled L-SeMet (Table S2). The most abundant Se isotopes (⁷⁸Se and ⁸⁰Se) were considered for L-SeMet revelation, but only precursor at m/z 198.1 was used for quantitation and confirmation (Table 1). Precursor at m/z 198.1 provides one more transition, which originates the fragment $[\text{CH}_3\text{-Se-CH}_2]^+$, i.e., transition $198.1 \rightarrow 109.1$; such transition was not selected neither for quantitation or confirmation of SeMet; the equivalent transition from the three labeled standards could be employed and monitored, therefore any of the isotopologues was suitable as IS. However, the ¹³C(Me)-L-SeMet (transition $199.1 \rightarrow 110.1$) was selected as IS for this study, as it was the less expensive among the possible candidates.

3.3. Sample preparation

Seleno-amino acids are zwitterionic compounds showing pK_{a1} about 1.5, pK_{a2} about 8.5–9.5 and very low hydrophobicity. This means that at $\text{pH} < 3$ the amine moieties are completely protonated, but carboxylate moieties are not, as they need a $\text{pH} < 1$ to be protonated; in addition, the contribution of hydrophobic interactions to the retention should be low when carboxylate is deprotonated, while a high concentration of hydrogen ions may displace the compounds from the ion exchange sites. This scenario could become even more complex in aqueous-organic solvents and in presence of positively charged compounds coming from the matrix. The first experiment was performed without oil sample on spiked water, following the protocol suggested by the manufacturer, i.e., loading: 5 mL water at $\text{pH} 2$ by HCl; first washing: 5 mL at $\text{pH} 2$ by HCl; second washing: 5 mL MeOH; elution: 2 mL MeOH, 3% NH_3 . Under these conditions, recoveries ranged between 85% (MeSeCys) to 103% (meso-SeCys₂); however, the recoveries decreased drastically when the procedure was applied to 30 mg EVOO sample, diluted with hexane and extracted with 10 mL MeOH:H₂O, 80:20 (v/v); all other conditions were kept constant (Fig. 2, Table 2, condition a). A remarkable improvement was obtained by using only 15 mg EVOO sample (Fig. 2, Table 2, condition b), but for SeMet and MeSeCys the recovery remained unsatisfactory and decreased further by increasing the acidity (Fig. 2, Table 2, condition c), as well as decreasing it (Fig. 2, Table 2, condition d). At this point, the first washing step was substituted by 2 mL H₂O, with a significant improvement of analyte recoveries (Fig. 2, Table 2, condition e).

Literature data on the total Se content in *Olea Europea* fruit was only determined recently in biofortified plants (D'Amato et al., 2018) while no data is available on Se speciation; therefore, the Se content data available for non-accumulating plants (tens of mg kg^{-1}) and $\log K_{ow}$ of seleno-amino acids (< -3) were considered to estimate a concentration for the single non-bound compound, which may be expected in the low $\mu\text{g kg}^{-1}$ range. This hypothesis is substantiated by the data

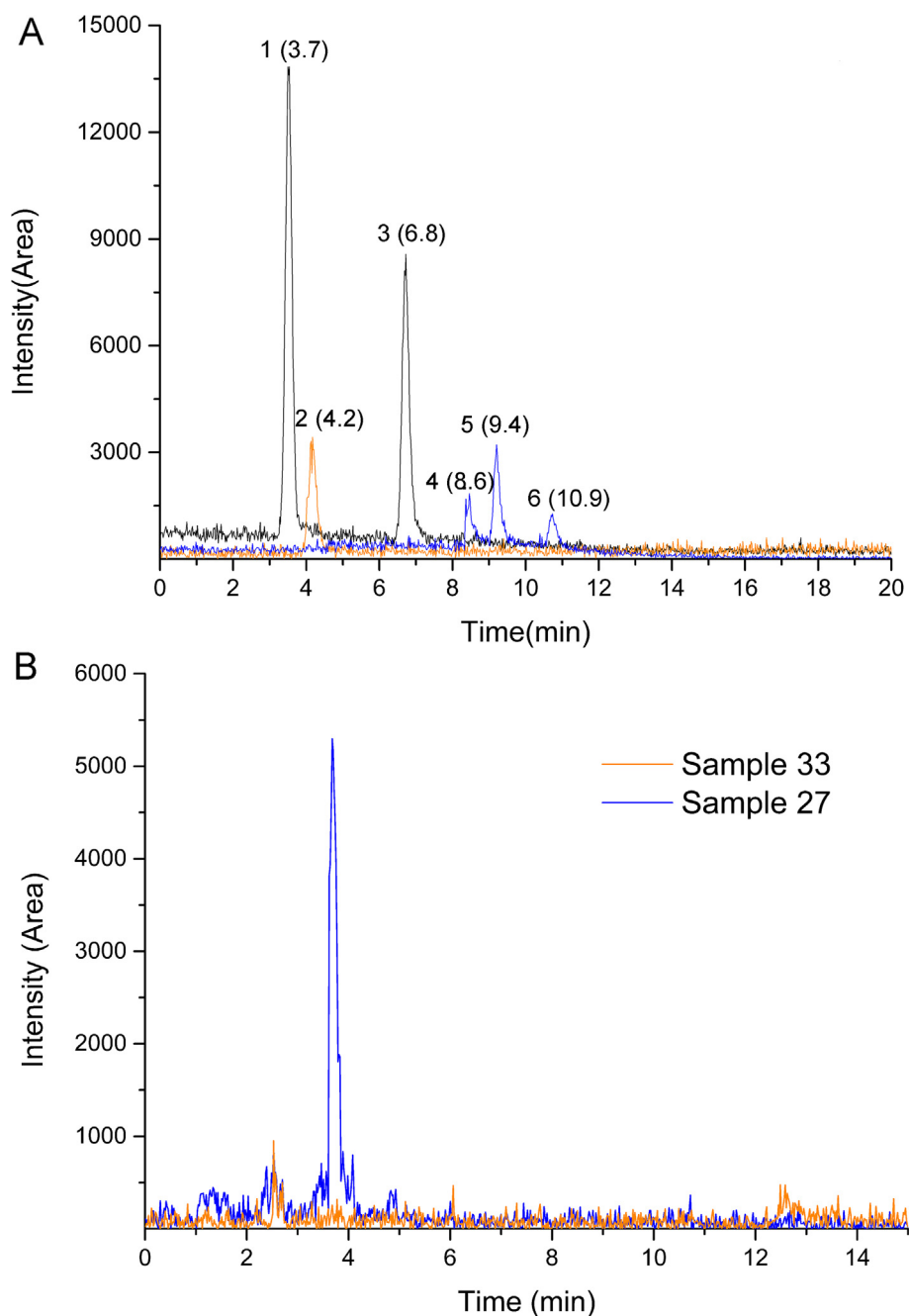


Fig. 1. A: Enantioresolution of the target seleno-amino acids (0.4 ng injected of each standard) on the CHIROBIOTIG TAG. See test for conditions. Sum of SRM. Numbers indicate the peak and the related retention time (in brackets). Elution order: L-SeMet (1), L-MeSeCys (2), D-SeMet (3), L-SeCys₂ (4), meso-SeCys₂ (5), D-SeCys₂ (6). B: Mass chromatograms of two representative EVOO samples, one containing 0.72 $\mu\text{g kg}^{-1}$ L-SeMet (sample 27) and an apparently blank sample (sample 33). SRM m/z 196 \rightarrow 56 was used for quantification.

reported in a previous work (Torres et al., 2014) therefore, to comply with the low abundance of the target seleno-amino acids, the sample preparation methods required not only the extraction from a relatively high amount of a fatty matrix, but also a concentration/cleanup step before HPLC analysis.

In these initial experiments, samples were extracted by LLE with 10 mL MeOH:H₂O, 80:20 (v/v). For comparison, SPE by both OASIS HLB and OASIS MCX was considered, and in the case of OASIS HLB a concentration of the extract was necessary, to reduce the content in MeOH. Therefore, the stability of the investigated seleno-amino acids was checked for solvent removal conditions, although such an investigation was outside the purpose of this work. In this context, while the stability to oxidation of SeCys and SeMet incorporated into proteins

has been largely studied, and the addition of dithiothreitol (DTT) to buffers seems to prevent oxidation, the stability of free seleno-amino acids has never been studied systematically. Free seleno-amino acid stability was checked also after elution, as evaporation increased method sensitivity. The eluent volume was fixed at 2 mL MeOH, to ensure a quantitative elution after SPE. Therefore, 10 mL MeOH:H₂O, 80:20 (v/v) and 2 mL of MeOH were tested for evaporation under neutral, acidic (0.01 mol L⁻¹ HCl) and basic (3% NH₃) conditions, either with or without addition of 1% (w/v) DTT. Solvent evaporation was performed at 25 °C in a Speed-Vac to ensure equal condition for all samples. For the 10 mL MeOH:H₂O, 80:20 (v/v) extract evaporation, the worst results were obtained with DTT addition, as all SeMet and most of the other two analytes disappeared before evaporation of 50% of the

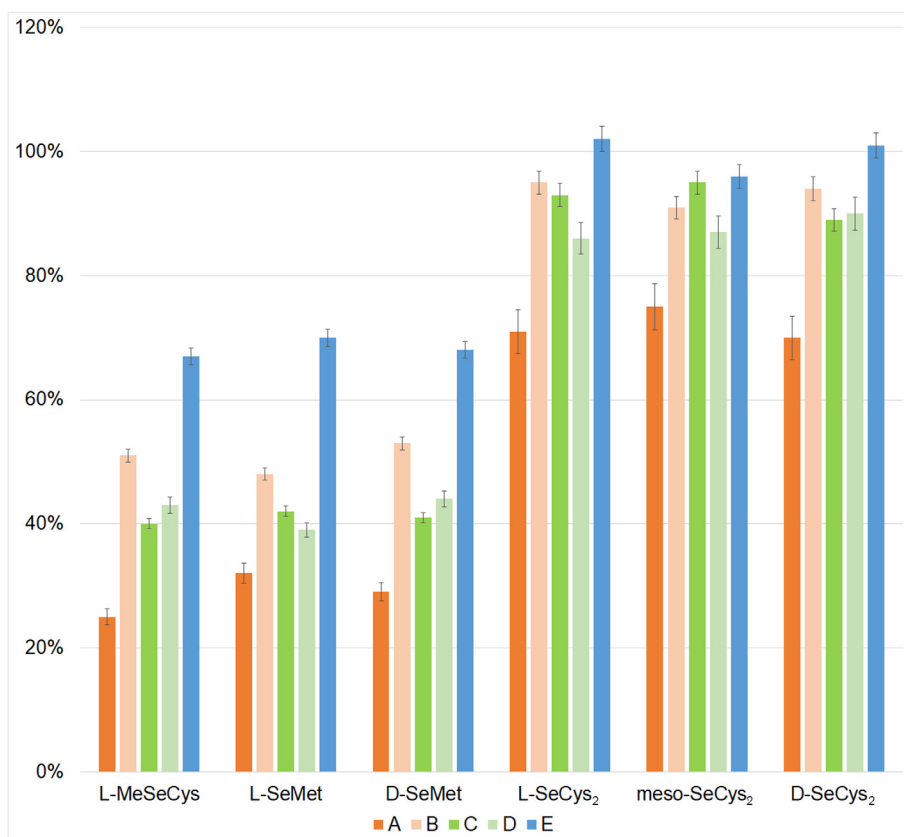


Fig. 2. Recovery (%) for different loaded sample and cleanup conditions (a–e) for the OASIS MCX (150 mg) cartridge. Experiments were performed from 10 mL sample extract in MeOH:H₂O, 80:20 (v/v). The second washing was 5 mL MeOH in all experiments. Data from three experimental replicates and two technical replicates. Conditions: A) 30 g EVOO sample, first washing with 5 mL 0.01 mol L⁻¹ HCl; B) 15 g EVOO sample, first washing with 5 mL 0.01 mol L⁻¹ HCl; C) 15 g EVOO sample, first washing with 5 mL 0.050 mol L⁻¹ HCl; D) 15 g EVOO sample, first washing with 5 mL 0.005 mol L⁻¹ HCl; E) 15 g EVOO sample and W1^a with 2 mL H₂O.

initial volume, whatever the pH was. For samples without DTT addition, in neutral solution, the SeMet loss was less dramatic, but still substantial, time depending and not reproducible (30–40% at half solvent removal). Analytes were much more stable to evaporation under acidic and basic conditions, as no loss was detected for 50% solvent removal, and SeMet slightly decreased only for further evaporation. For eluate evaporation, analytes were stable without DTT addition under both acidic and basic conditions, provided the samples were not evaporated to dryness. From a practical point of view, this means that: i) the acidified extract can be evaporated down to 5 mL before OASIS HLB cleanup and ii) a basified eluate from the cleanup cartridge can be evaporated to μ Ls level without analytes degradation. For eluates, evaporation was stopped at 150 μ L residual volume, considered as a safe security limit. Although up to 20 μ L can be directly injected without peak broadening, in the final procedure samples were diluted with ACN to assure the compatibility with HPLC mobile phase; 10 μ L were injected from the resulting solution, as no improvement was obtained in the S/N ratio by doubling the injection volume.

After establishing the possibility of analyte concentration, two SPE strategies were pursued. Initially, the OASIS HLB was used for sample cleanup, maintaining the extraction procedure from EVOO reported in the literature (Torres et al., 2014), such as 30 g oil diluted with 30 mL hexane and extracted with 10 mL MeOH:H₂O, 80:20 (v/v). After the extraction of a blank sample, analytes were added to the extract, the

extract was acidified, evaporated down to 5 mL, diluted to 50 mL with aqueous 0.01 mol L⁻¹ HCl and loaded onto the cartridge. The analytes were recovered from the SPE cartridge by passing 2 mL of MeOH; 2% NH₃ and the IS was added at this stage. However, recoveries for SeCys₂ were < 20% and only slightly higher for the other analytes, neither any significant improvement was obtained halving the EVOO amount. Thereafter, all the experiments were done with OASIS MCX, which has the same polymeric backbone of OASIS HLB, but is sulfonic acid functionalized, and can, therefore, be considered a mixed mode sorbent.

These experiments were all performed by adding the analytes to the extract, with the purpose of testing the recovery after cleanup. At this point, the analytes were added to the sample diluted with hexane and the whole procedure was performed obtaining recoveries not significantly different from those achieved by spiking the extract. Any other attempt to improve recoveries, such as acidifying the extracting mixture (0.01 mol L⁻¹ HCl) or decreasing MeOH content of the MeOH:H₂O extraction mixture (1:1, v/v), failed. This behavior might be the results of ion pairing or other unexpected interactions between seleno-amino acids and some compounds in the complex matrix. From a practical point of view, it was not a problem, as the extract can be acidified post-extraction before MCX cleanup.

Table 2

Experimental conditions tested during seleno-amino acids method optimization for preconcentration using Oasis MCX.

Condition	SPE	EVOO amount (g)	Loading	Washing 1	Washing 2	Elution
A	MCX	30	pH 2 by HCl	5 mL 0.01 mol L ⁻¹ HCl	5 mL MeOH	2 mL MeOH, 3% NH ₃
B	MCX	15	pH 2 by HCl	5 mL 0.01 mol L ⁻¹ HCl	5 mL MeOH	2 mL MeOH, 3% NH ₃
C	MCX	15	pH 2 by HCl	5 mL 0.050 mol L ⁻¹ HCl	5 mL MeOH	2 mL MeOH, 3% NH ₃
D	MCX	15	pH 2 by HCl	5 mL 0.005 mol L ⁻¹ HCl	5 mL MeOH	2 mL MeOH, 3% NH ₃
E	MCX	15	pH 2 by HCl	2 mL water	5 mL MeOH	2 mL MeOH, 3% NH ₃

Table 3

Linear regression of solvent standard (SS), matrix matched (MM) and matrix assisted (MA) calibration curves and matrix effect (ME, %), absolute recovery (RE, %) and process efficiency (PE, %) for the investigated compounds. Data from three experimental replicates and two technical replicates. Trueness, expressed as apparent recovery (%); intermediate precision, expressed as relative standard deviation (RSD, %); method detection limit (MDL); and method quantification limit (MQL); n = 5.

Compound	SS y	R ²	MM y	R ²	MA y	R ²	ME (%)	RE (%)	PE (%)	Apparent recovery (RSD) %		MDL ($\mu\text{g kg}^{-1}$)	MQL ($\mu\text{g kg}^{-1}$)
										2 $\mu\text{g kg}^{-1}$	10 $\mu\text{g kg}^{-1}$		
L-MeSeCys	3592x + 2429	0.9992	2720x + 2761	0.9943	1731x + 2325	0.9930	76	64	49	87 (6)	93 (4)	0.7	0.8
L-SeMet	25078x + 11269	0.9992	21366x + 10672	0.9865	13943x + 4940	0.9900	85	65	55	101 (4)	99 (2)	0.2	0.2
D-SeMet	25234x + 9671	0.9994	21648x + 11332	0.9870	15873x + 6132	0.9946	92	63	58	105 (7)	107 (2)	0.2	0.2
L-SeCys ₂	1448x - 203	0.9990	1346x - 225	0.9999	1302x - 281	0.9983	90	97	87	118 (4)	121 (6)	0.1	0.1
meso-SeCys ₂	1305x - 223	0.9892	1301x - 133	0.9615	1258x - 107	0.9792	100	97	97	126 (9)	125 (7)	0.1	0.1
D-SeCys ₂	1336x + 111	0.9999	1234x - 95	0.9998	1183x - 336	0.9995	90	96	86	113 (7)	118 (3)	0.05	0.05

3.4. Linearity and process efficiency

After instrumental linearity was assessed in a wider range (see Experimental Section), the linearity of the method was proved in a range within which concentrations in EVOO could be expected. All the calibration curves for the selected analytes showed a linear shape with $R^2 > 0.9995$. PE (%), RE (%) and ME (%), were calculated as described in the Experimental section (Table 3). PE for L-MeSeCys and both SeMet enantiomers was about 50%, due to both partial recovery and partial ion suppression; PE was > 85% for SeCys₂ enantiomers and diastereoisomer, as they were eluted later. This fact may introduce some problems in the determination of trueness (see later) because the isotopic IS was fully suitable only for MeSeCys and SeMet.

3.5. Trueness, precision, method detection limit, and method quantification limit

Trueness and precision were estimated in spiked samples at two concentration levels, i.e. 2 and 10 $\mu\text{g kg}^{-1}$, based on the expected concentration levels (Table 2). Apparent recoveries for SeCys₂ enantiomers, which are more retained by the MCX than SeMet, ranged 113–126%, due to the different chemical structure of the isotopic IS. As intermediate precision is high, a correction factor could be introduced, avoiding the MA calibration for SeCys₂ quantification.

MDL and MQL assessment in LC-MS/MS is a rather controversial issue. In estimating these two validation parameters, we followed: first, the European Commission Decision 2002/657/EC concerning the performance of analytical methods and the interpretation of results (European Commission, 2002) and second, the interpretation of this directive and some recommendations reported in the tutorial review (Kruve et al., 2015). First of all, MDL and MQL are variable parameters, especially when MS is used for the measure and should be recalculated following the instrumentation response fluctuation. Therefore, it can be more or less roughly estimated in condition of routine use, for example at the end of a series of real sample analysis, just before scheduled source cleaning, to have a conservative value. MDLs and MQLs are characteristic of a certain matrix, so they must be determined for the selected matrix.

The definite subdivision of the two transitions registered in SRM mode in quantifier and qualifier somehow contradicts the meaning of the “two transition rule”, as without confirmation, quantification is meaningless because the identity of the analyte becomes uncertain. Therefore, MDL must be calculated for the less abundant confirmatory ion. When a noise can be measured, the criterion of S/N ratio = 3 can be applied, otherwise other criteria should be tested. As far as MQL is concerning, it is defined as the lowest concentration of analyte that can be determined with an acceptable repeatability and trueness. However, also in this case, when a noise can be measured, the criterion of the S/N ratio = 10 is widely accepted. Obviously, the S/N evaluation must be performed for concentration close to the limits. Moreover, the MQL

cannot be lower than MDL, thus sometime the MDL also determines the MQL for the reason expressed above. The values reported in Table 3 for MDL and MQL have been calculated following these criteria, and appear low enough to measure concentrations of the selected compounds that can be of some biological significance.

Even if the method was investigated regardless of analyte chirality, results were finally compared to a previous work on seleno-amino acids preconcentration in oil (Torres et al., 2014) taking into consideration only the common analytes (i.e. MeSeCys and SeMet), and the same spiking level (10 $\mu\text{g kg}^{-1}$). The recovery in this work is lower, 64% for MeSeCys vs 93% and 62–63% for SeMet vs 84%. The apparent recoveries, obtained by correction with the IS, were, nevertheless, the same for MeSeCys and better for SeMet (99% vs 84%). Precision was better in the present work ($\leq 4\%$ vs approximately 10%). MDLs and MQLs were lower in (Torres et al., 2014), 0.01 $\mu\text{g kg}^{-1}$ and 0.09 $\mu\text{g kg}^{-1}$, respectively.

3.6. Analysis of EVOO samples,

Thirty-two EVOO samples of various certified geographic origin (Table S1, Fig. S1) were analyzed for both total Se and seleno-amino acids. With respect to a previous work, in which seven EVOO samples produced in Argentina were analyzed by microwave-assisted digestion-ICP-MS (Torres et al., 2014), the total Se content of our samples was very different. In the previous work, five samples showed a Se concentration in the range 62.8–117.4 $\mu\text{g kg}^{-1}$, while in two samples, Se was < 0.02 $\mu\text{g kg}^{-1}$.

Our 32 samples showed a Se concentration range of < 0.5–9.1 $\mu\text{g kg}^{-1}$ (Table 4 and Table S3). As both total Se and seleno-amino acid analytical methods were well validated, these differences should not be ascribed to the different method used for analysis. Additionally, it should also be underlined that, as an example, (Table S3 and Fig. S1) EVOO 31 and 32 samples, originating from the same district, have very different total Se content, and, more in general, there is no correlation between the Se in soil and in EVOO due to a complex hydrogeology.

Table 4

Results of total Se and seleno-amino acid quantification in EVOO samples, n = 3 (results where seleno-amino acid quantification was < MDL were omitted, but they are available in Table S4).

Oil sample	Total Se ($\mu\text{g kg}^{-1}$)	L-SeMet ($\mu\text{g kg}^{-1}$)
32	9.1 \pm 0.5	1.42 \pm 0.04
27	5.9 \pm 0.4	0.72 \pm 0.02
20	4.6 \pm 0.3	0.50 \pm 0.05
29	4.3 \pm 0.5	0.46 \pm 0.04
21	4.2 \pm 0.4	0.42 \pm 0.06
19	4.0 \pm 0.8	0.34 \pm 0.06
30	3.7 \pm 0.3	0.28 \pm 0.07
23	3.5 \pm 0.4	< MQL

Among the seleno-amino acids selected for this study, only *l*-SeMet was detected and could be quantified in 7/32 samples. As an example, Fig. 1B shows a chromatogram relative to SRM used for quantitation of SeMet by the present method ($0.72 \mu\text{g kg}^{-1}$). This finding does not agree with the only available previous report (Torres et al., 2014), where MeSeCys was the only detected compound. This difference cannot be explained by the geographic provenience “*per se*”, but total Se content might be the determining factor. Both SeMet and MeSeCys were synthesized in plant starting from SeCys; however, Se exceeding the toxic level increases the biosynthesis of SeCys, activating the detoxifying enzyme Se-cysteine methyltransferase, which consequently methylates SeCys, which is in turn transformed to volatile dimethylselenide (Schiavon & Pilon-Smits, 2017).

Another interesting finding is the very good correlation ($R^2 = 0.996$) between total Se and SeMet (Fig. S3) which accounts for 4–6% of total Se. This correlation cannot be explained easily. It has been reported for total protein content in EVOO a value of $100\text{--}500 \mu\text{g L}^{-1}$ (Hidalgo, Alaiz, & Zamora, 2001), and methionine accounted for about 2% of the amino-acidic composition, that corresponds to $2\text{--}10 \mu\text{g L}^{-1}$, while cysteine was only 0.8% ($0.8\text{--}4 \mu\text{g L}^{-1}$). In addition, it has also been reported in normal soils a ratio S/Se ranging about 500/3000, and that the ratio S/Se in hydroponic culture is more or less maintained in leaves (White, Bowen, Marshall, & Broadley, 2007). From these data, it could be expected that Se incorporated into proteins should be in the approximate maximum amount of 15ng L^{-1} , therefore, as reported elsewhere (López-García, Vicente-Martínez, & Hernández-Córdoba, 2013), most of Se should be bonded or carried by the lipid fraction or other minor EVOO compounds in the form of selenite, selenate and selenolipids.

4. Conclusions

A new method for determination of seleno-amino acids in EVOO was described which includes the enantioresolution of seleno-amino acid isomers. The method, based on HPLC-ESI-MS/MS, was developed and validated, while a method previously developed and validated for total Se determination in human serum by open-vessel acid digestion followed by HG-AFS, was adapted with few modification to analyze total Se. Thirty two samples coming from different Italian regions were analyzed: the range of total Se concentration was $0.5\text{--}9.1 \mu\text{g kg}^{-1}$ and *l*-SeMet was the only seleno-amino acid identified, which was detected in only seven samples at a concentration in the range $0.2\text{--}1.42 \mu\text{g kg}^{-1}$. Although the concentration of total Se ascribable to *l*-SeMet was only 6–7% of the total, a good correlation was found between these two parameters. A comparison with other samples was not possible, because only one study regarding seven Argentinean EVOO is present in the literature, where 2 samples out of 7 did not contain measurable amount of neither total Se, nor seleno-amino acids, whereas the other 5 samples were relatively rich in total Se (62.8 to $117.4 \mu\text{g kg}^{-1}$) and MeSeCys was found the only seleno-amino acid identified. Moreover, there was no correlation between these parameters.

The ability of the chromatographic column to separate all the enantiomers in this kind of sample did not produce unexpected results, however, it might be useful for other matrices, where seleno-amino acids racemization may occur.

Acknowledgments

The project was funded by Cariplo Foundation within the “Agroalimentare e Ricerca” (AGER) program. Project AGER2-Rif.2016-0169, “Valorization of Italian OLIVE products through Innovative analytical tools – VIOLIN”.

Conflict of interest

The authors declare no conflict of interest.

Appendix A. Supplementary data

Supplementary data to this article can be found online at <https://doi.org/10.1016/j.foodchem.2018.11.053>.

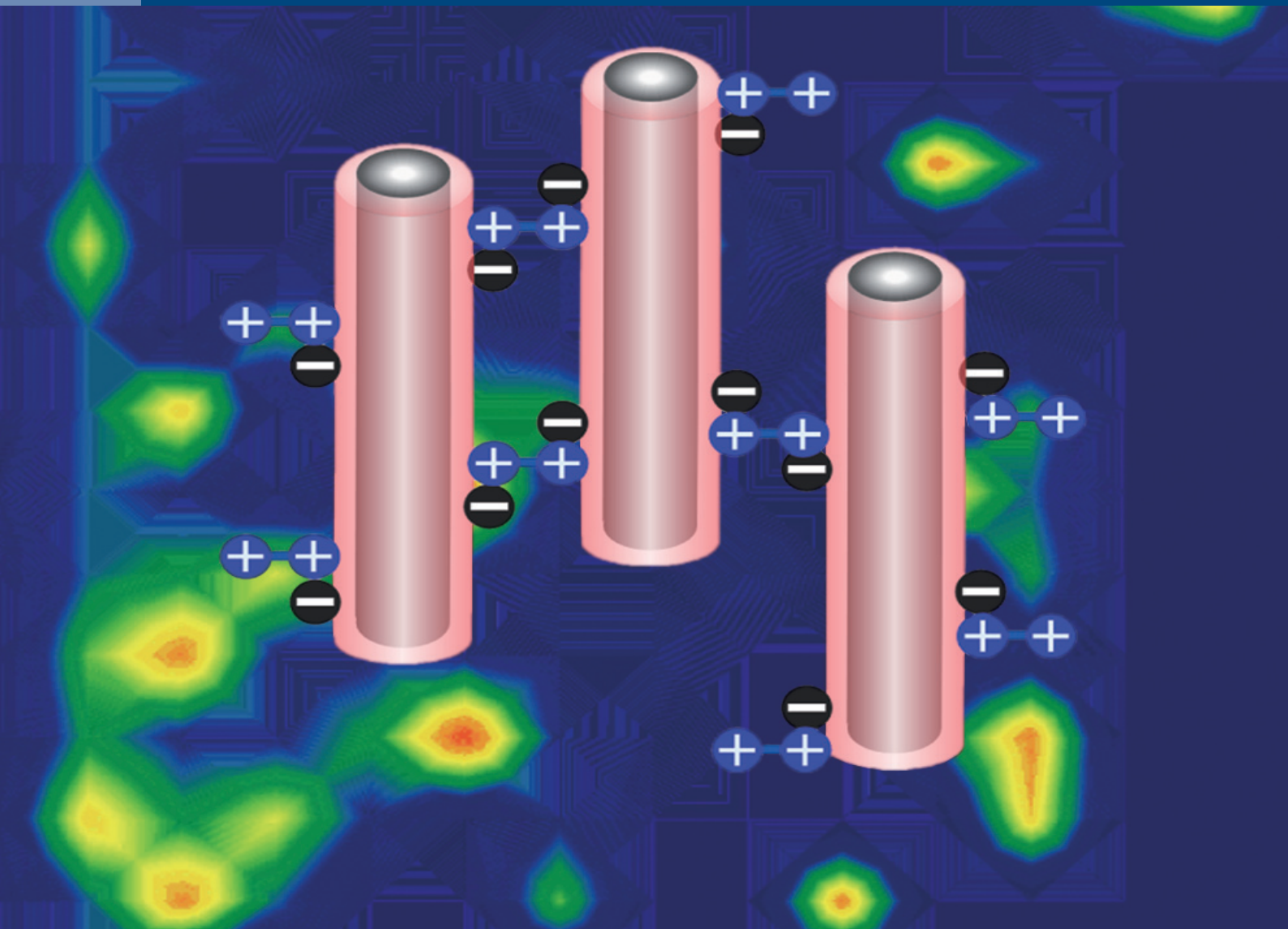
References

- Amoako, P. O., Uden, P. C., & Tyson, J. F. (2009). Speciation of selenium dietary supplements; formation of S-(methylseleno)cysteine and other selenium compounds. *Analytica Chimica Acta*, 652(1–2), 315–323. <https://doi.org/10.1016/j.aca.2009.08.013>.
- Arnaudguilhem, C., Bierla, K., Ouerdane, L., Preud'homme, H., Yiannikouris, A., & Lobinski, R. (2012). Selenium metabolomics in yeast using complementary reversed-phase/hydrophilic ion interaction (HILIC) liquid chromatography-electrospray hybrid quadrupole trap/Orbitrap mass spectrometry. *Analytica Chimica Acta*, 757, 26–38. <https://doi.org/10.1016/j.aca.2012.10.029>.
- B'Hymer, C., & Caruso, J. A. (2006). Selenium speciation analysis using inductively coupled plasma-mass spectrometry. *Journal of Chromatography A*. <https://doi.org/10.1016/j.chroma.2006.02.063>.
- Bernal, J., Ares, A. M., Pól, J., & Wiedmer, S. K. (2011). Hydrophilic interaction liquid chromatography in food analysis. *Journal of Chromatography A*. <https://doi.org/10.1016/j.chroma.2011.05.004>.
- Berthod, A., Chen, X., Kullman, J. P., Armstrong, D. W., Gasparrini, F., D'Acquarica, I., ... Carotti, A. (2000). Role of the carbohydrate moieties in chiral recognition on toplanin-based LC stationary phases. *Analytical Chemistry*, 72(8), 1767–1780. <https://doi.org/10.1021/ac9911004t>.
- Capriotti, A. L., Cavaliere, C., Crescenzi, C., Foglia, P., Nescatelli, R., Samperi, R., & Laganà, A. (2014). Comparison of extraction methods for the identification and quantification of polyphenols in virgin olive oil by ultra-HPLC-QToF mass spectrometry. *Food Chemistry*, 158, 392–400. <https://doi.org/10.1016/j.foodchem.2014.02.130>.
- Capriotti, A. L., Cavaliere, C., Foglia, P., Piovesana, S., & Ventura, S. (2015). Chromatographic methods coupled to mass spectrometry detection for the determination of phenolic acids in plants and fruits. *Journal of Liquid Chromatography and Related Technologies*, 38(3), 353–370. <https://doi.org/10.1080/10826076.2014.941263>.
- Capriotti, A. L., Montone, C. M., Antonelli, M., Cavaliere, C., Gasparrini, F., La Barbera, G., ... Laganà, A. (2018). Simultaneous preconcentration, identification, and quantitation of selenoamino acids in oils by enantioselective high performance liquid chromatography and mass spectrometry. *Analytical Chemistry*, 90(14), 8326–8330. <https://doi.org/10.1021/acs.analchem.8b02089>.
- D'Amato, R., Petrelli, M., Proietti, P., Onofri, A., Regni, L., Perugini, D., & Businelli, D. (2018). Determination of changes in the concentration and distribution of elements within olive drupes (cv. Leccino) from Se biofortified plants, using laser ablation inductively coupled plasma mass spectrometry. *Journal of the Science of Food and Agriculture*, 98(13), 4971–4977. <https://doi.org/10.1002/jsfa.9030>.
- Di Dato, C., Gianfrilli, D., Greco, E., Astolfi, M., Canepari, S., Lenzi, A., ... Giannetta, E. (2017). Profiling of selenium absorption and accumulation in healthy subjects after prolonged l-selenomethionine supplementation. *Journal of Endocrinological Investigation*, 40(11), 1183–1190. <https://doi.org/10.1007/s40618-017-0663-5>.
- El-Ramady, H., Abdalla, N., Taha, H. S., Alshaal, T., El-Henawy, A., Faizy, S. E. D. A., ... Schnug, E. (2016). Selenium and nano-selenium in plant nutrition. *Environmental Chemistry Letters*. <https://doi.org/10.1007/s10311-015-0535-1>.
- European Commission, 2002. COMMISSION DECISION of 12 August 2002 implementing Council Directive 96/23/EC concerning the performance of analytical methods and the interpretation of results. OJ L 221, 17.8.2010, pp. 8–36. doi:10.1017/CBO9781107415324.004.
- Friedman, M., & Levin, C. E. (2012). Nutritional and medicinal aspects of D-amino acids. *Amino Acids*, 42(5), 1553–1582. <https://doi.org/10.1007/s00726-011-0915-1>.
- Gammelgaard, B., Jackson, M. I., & Gabel-Jensen, C. (2011). Surveying selenium speciation from soil to cell-forms and transformations. *Analytical and Bioanalytical Chemistry*. <https://doi.org/10.1007/s00216-010-4212-8>.
- Gómez-Ariza, J. L., Bernal-Daza, V., & Villegas-Portero, M. J. (2007). First approach of a methodological set-up for selenomethionine chiral speciation in breast and formula milk using high-performance liquid chromatography coupled to atomic fluorescence spectroscopy. *Applied Organometallic Chemistry*, 21(6), 434–440. <https://doi.org/10.1002/aoc.1239>.
- Gómez-Ariza, V., García-Barrera, T., Garbayo, I., Vílchez, C., & Gómez-Ariza, J. L. (2012). Metallomic study of selenium biomolecules metabolized by the microalgae *Chlorella sorkiniana* in the biotechnological production of functional foods enriched in selenium. *Pure and Applied Chemistry*, 84(2), 1. <https://doi.org/10.1351/PAC-CON-11-09-18>.
- Hidalgo, F. J., Alaiz, M., & Zamora, R. (2001). Determination of peptides and proteins in fats and oils. *Analytical Chemistry*, 73(3), 698–702. <https://doi.org/10.1021/ac000876o>.
- Jagtap, R., & Maher, W. (2016). Determination of selenium species in biota with an emphasis on animal tissues by HPLC-ICP-MS. *Microchemical Journal*. <https://doi.org/10.1016/j.microc.2015.07.014>.
- Jagtap, R., Maher, W., Krikowa, F., Ellwood, M. J., & Foster, S. (2016). Measurement of selenomethionine and selenocysteine in fish tissues using HPLC-ICP-MS. *Microchemical Journal*, 128, 248–257. <https://doi.org/10.1016/j.microc.2016.04.021>.
- Krueve, A., Rebane, R., Kipper, K., Oldekop, M. L., Evard, H., Herodes, K., ... Leito, I. (2015). Tutorial review on validation of liquid chromatography-mass spectrometry

- methods: Part I. *Analytica Chimica Acta*. <https://doi.org/10.1016/j.aca.2015.02.017>.
- La Barbera, G., Capriotti, A. L., Cavaliere, C., Montone, C. M., Piovesana, S., Samperi, R., ... Laganà, A. (2017). Liquid chromatography-high resolution mass spectrometry for the analysis of phytochemicals in vegetal-derived food and beverages. *Food Research International*, 100, 28–52. <https://doi.org/10.1016/j.foodres.2017.07.080>.
- Langrock, T., Czihal, P., & Hoffmann, R. (2006). Amino acid analysis by hydrophilic interaction chromatography coupled on-line to electrospray ionization mass spectrometry. *Amino Acids*, 30(3 SPEC. ISS.), 291–297. <https://doi.org/10.1007/s00726-005-0300-z>.
- Lombi, E., & Susini, J. (2009). Synchrotron-based techniques for plant and soil science: Opportunities, challenges and future perspectives. *Plant and Soil*. <https://doi.org/10.1007/s11104-008-9876-x>.
- López-García, I., Vicente-Martínez, Y., & Hernández-Córdoba, M. (2013). Nonchromatographic speciation of selenium in edible oils using dispersive liquid-liquid microextraction and electrothermal atomic absorption spectrometry. *Journal of Agricultural and Food Chemistry*, 61(39), 9356–9361. <https://doi.org/10.1021/jf4027537>.
- Marrubini, G., Appelblad, P., Maietta, M., & Papetti, A. (2018). Hydrophilic interaction chromatography in food matrices analysis: An updated review. *Food Chemistry*, 257(August 2017), 53–66. <https://doi.org/10.1016/j.foodchem.2018.03.008>.
- Matuszewski, B. K., Constanzer, M. L., & Chavez-Eng, C. M. (2003). Strategies for the assessment of matrix effect in quantitative bioanalytical methods based on HPLC-MS/MS. *Analytical Chemistry*, 75(13), 3019–3030. <https://doi.org/10.1021/ac020361s>.
- Muñoz Olivas, R., Quevauviller, P., & Donard, O. F. X. (1998). Long term stability of organic selenium species in aqueous solutions. *Presenius' Journal of Analytical Chemistry*, 360, 512–519. <https://doi.org/10.1007/s002160050751>.
- Nathanail, A. V., Syvähuoko, J., Malachová, A., Jestoi, M., Varga, E., Michlmayr, H., ... Peltonen, K. (2015). Simultaneous determination of major type A and B trichothecenes, zearalenone and certain modified metabolites in Finnish cereal grains with a novel liquid chromatography-tandem mass spectrometric method. *Analytical and Bioanalytical Chemistry*, 407(16), 4745–4755. <https://doi.org/10.1007/s00216-015-8676-4>.
- Oguri, S., Kumazaki, M., Kitou, R., Nonoyama, H., & Tooda, N. (1999). Elucidation of intestinal absorption of D, L-amino acid enantiomers and aging in rats. *Biochimica et Biophysica Acta - General Subjects*, 1472(1–2), 107–114. [https://doi.org/10.1016/S0304-4165\(99\)00110-5](https://doi.org/10.1016/S0304-4165(99)00110-5).
- Piovesana, S., Capriotti, A. L., Cavaliere, C., La Barbera, G., Samperi, R., Zenezini Chiozzi, R., & Laganà, A. (2017). A new carbon-based magnetic material for the dispersive solid-phase extraction of UV filters from water samples before liquid chromatography-tandem mass spectrometry analysis. *Analytical and Bioanalytical Chemistry*, 409(17), 4181–4194. <https://doi.org/10.1007/s00216-017-0368-9>.
- Prinsen, H. C. M. T., Schiebergen-Bronkhorst, B. G. M., Roeleveld, M. W., Jans de Sain-van der Velden, J. J. M. G. M., Visser, G., ... Verhoeven-Duif, N. M. (2016). Rapid quantification of underivatized amino acids in plasma by hydrophilic interaction liquid chromatography (HILIC) coupled with tandem mass-spectrometry. *Journal of Inherited Metabolic Disease*, 39(5), 651–660. <https://doi.org/10.1007/s10545-016-9935-z>.
- Rayman, M. P. (2012). Selenium and human health. *The Lancet*, 379(9822), 1256–1268. [https://doi.org/10.1016/S0140-6736\(11\)61452-9](https://doi.org/10.1016/S0140-6736(11)61452-9).
- Rayman, M. P., Infante, H. G., & Sargent, M. (2008). Food-chain selenium and human health: Spotlight on speciation. *British Journal of Nutrition*. <https://doi.org/10.1017/S0007114508922522>.
- Ruszczyńska, A., Konopka, A., Kurek, E., Torres Elguera, J. C., & Bulska, E. (2017). Investigation of biotransformation of selenium in plants using spectrometric methods. *Spectrochimica Acta - Part B Atomic Spectroscopy*, 130, 7–16. <https://doi.org/10.1016/j.sab.2017.02.004>.
- Sanchez-Rodas, D., Mellano, F., Morales, E., & Giraldez, I. (2013). A simplified method for inorganic selenium and selenoaminoacids speciation based on HPLC-TR-HG-AFS. *Talanta*, 106, 298–304. <https://doi.org/10.1016/j.talanta.2012.11.005>.
- Schiavon, M., & Pilon-Smits, E. A. H. (2017). The fascinating facets of plant selenium accumulation – biochemistry, physiology, evolution and ecology. *New Phytologist*. <https://doi.org/10.1111/nph.14378>.
- Spadoni, M., Voltaggio, M., Carcea, M., Coni, E., Raggi, A., & Cubadda, F. (2007). Bioaccessible selenium in Italian agricultural soils: Comparison of the biogeochemical approach with a regression model based on geochemical and pedoclimatic variables. *Science of the Total Environment*, 376(1–3), 160–177. <https://doi.org/10.1016/j.scitotenv.2007.01.066>.
- Stoffaneller, R., & Morse, N. L. (2015). A review of dietary selenium intake and selenium status in Europe and the Middle East. *Nutrients*. <https://doi.org/10.3390/nu7031494>.
- Sutton, K. L., Ponce de Leon, C. A., Ackley, K. L., Sutton, R. M. C., Stalcup, A. M., & Caruso, J. A. (2000). Development of chiral HPLC for selenoamino acids with ICP-MS detection: Application to selenium nutritional supplements. *The Analyst*, 125(2), 281–286. <https://doi.org/10.1039/a907847i>.
- Torres, S., Cerutti, S., Raba, J., Pacheco, P., & Silva, M. F. (2014). Preconcentration of seleno-amino acids on a XAD resin and determination in regional olive oils by SPE UPLC-ESI-MS/MS. *Food Chemistry*, 159, 407–413. <https://doi.org/10.1016/j.foodchem.2014.03.045>.
- White, P. J., Bowen, H. C., Marshall, B., & Broadley, M. R. (2007). Extraordinarily high leaf selenium to sulfur ratios define “Se-accumulator” plants. *Annals of Botany*, 100(1), 111–118. <https://doi.org/10.1093/aob/mcm084>.
- Zembrzuska, J., Matusiewicz, H., Polkowska-Motrenko, H., & Chajduk, E. (2014). Simultaneous quantitation and identification of organic and inorganic selenium in diet supplements by liquid chromatography with tandem mass spectrometry. *Food Chemistry*, 142, 178–187. <https://doi.org/10.1016/j.foodchem.2013.05.004>.

JOURNAL OF SEPARATION SCIENCE

10 | 19



Methods
Chromatography · Electroseparation



Applications
Biomedicine · Foods · Environment

www.jss-journal.com

WILEY-VCH

RESEARCH ARTICLE

Investigation of free and conjugated seleno-amino acids in wheat bran by hydrophilic interaction liquid chromatography with tandem mass spectrometry

Carmela Maria Montone | Michela Antonelli | Anna Laura Capriotti  | Chiara Cavaliere |
Giorgia La Barbera  | Susy Piovesana | Aldo Laganà

Dipartimento di Chimica, Sapienza Università di Roma, Rome, Italy

Correspondence

Professor Anna Laura Capriotti, Dipartimento di Chimica, Sapienza Università di Roma, Box no 34 - Roma 62, Piazzale Aldo Moro 5, 00185 Rome, Italy.

Email: annalaura.capriotti@uniroma1.it

An analytical method for determining seleno-methionine, methyl-seleno-cysteine, and seleno-cystine in wheat bran was developed and validated. Four different extraction procedures were evaluated to simultaneously extract endogenous free and conjugated seleno-amino acids in wheat bran in order to select the best extraction protocol in terms of seleno amino acid quantitation. The extracted samples were subjected to a clean-up by a reversed phase/strong cation exchange solid-phase extraction and analyzed by chiral hydrophilic interaction liquid chromatography-tandem mass spectrometry. The optimized extraction protocol was employed to validate the methodology. Process efficiency ranged from 58 to 112% and trueness from 73 to 98%. Limit of detection and limit of quantification were lower than 1 ng/g. Four wheat bran samples were analyzed for both total Se and single seleno-amino acids determination. The results showed that Se- seleno-methyl-L-selenocysteine was the major seleno-amino acid in wheat bran while seleno-methionine and seleno-cysteine were both minor species.

KEYWORDS

enantioselective high-performance liquid chromatography, mass spectrometry, seleno-amino acids, total selenium, wheat bran

1 | INTRODUCTION

Selenium (Se) is an essential micronutrient for human health, as it is part of the detoxification system of the body against oxidative stress [1] and several other functions were attributed to it, such as immunological, and anti-inflammatory properties [2]; additionally, it is an essential cofactor for enzyme

systems in humans [3]. As a consequence, selenium supplementation has been suggested to improve several conditions and diseases [4]. The biological activity of Se depends on its speciation. Recently, it was demonstrated that even though animals can equally assimilate both inorganic and organic naturally occurring seleno-compounds [5], higher anticancer activity and lower cytotoxicity have been reported for the organic forms of selenium [6].

Se content in food sources varies from plant to plant. It depends upon Se uptake and accumulating capacity of plant, soil Se content, which varies according to geographical locations and presence of other elements in soil. Fruits generally contain low amount of Se compared to vegetables. Cereals, such as rice and wheat, contain high concentration

Article Related Abbreviations: CRM, certified reference material; FL, fortification level; ME, matrix effect; PE, process efficiency; RE, recovery; RT, room temperature; Se, selenium; Se-AA, seleno amino acid; Se-Cys, seleno-cystine; Se-MeSeCys, methyl-seleno-cysteine; Se-Met, seleno-methionine; SRM, selected reaction monitoring; SS, standard in solvent; TCA, trichloroacetic acid.

of Se ranging between 10 and 550 ng/g [7,8]. Wheat, with a worldwide production of 749.5 million metric tonnes in 2016, is the third cereal cultivation in the world [9], mainly utilised for human consumption and livestock feed. A wheat kernel comprises three principal fractions—bran, germ and endosperm. The outer layers are all parts of the bran which is a by-product of milling and it has been usually employed in non-food applications. However, in the last decade wheat bran has been also used for human consumption as it is an abundant source of dietary fibre, which has been linked to improved bowel health and possible prevention of some diseases such as colon cancer [10].

Most of the papers dealing with the Se determination do not distinguish the specific seleno-compounds. Quantitative determination of Se species in biological samples usually involves hyphenated techniques [7,11]. From an analytical perspective, most organic seleno-compounds are amino acids or derivatives. Chirality in selenoamino acids (Se-AAs) is expected to play an important role as well. Most of the Se-AAs present in food have at least one chiral centers which can give rise to D- and L-enantiomeric forms if both are produced. In particular, the stereoisomers are D- and L-selenomethionine, Se-methyl-L-selenocysteine and D-, L- and meso-selenocystine. It is usually the L-enantiomer that is assimilated into the body, which is also less toxic compared to the D-form [12].

If on one hand most approaches exploited derivatization into diastereoisomers to separate Se-AA racemates [13], on the other hand the direct analysis has the advantage of skipping the derivatization step, with possible related analyte loss, unsuitability for very low abundant samples and extensive sample processing [14]. Direct approaches, which enable enantiomer separation without derivatization, were described for Se-AA analysis in complex samples. Direct approaches exploited the use of enantioselective chromatography, based on CHIROBIOTIC T [15–19], chiral ligand-exchange stationary phases [20] and chiral crown ether chiral stationary phase (CSP) [12,21]. Recently, in our research group a 5 cm long chiral macrocyclic glycoprotein stationary phase (CHIROBIOTIC TAG) column was employed for enantioresolution of Se-AAs (D- and L-selenomethionine, Se-methyl-L-selenocysteine, D-, L- and meso-selenocystine) in oil samples [22]. Despite the advance of instrumental techniques since biological samples such as food or whole plant usually contain a complex mixture of proteins [23] appropriate sample pretreatment steps are often required prior to the analysis of Se-AAs which could be free or conjugated to proteins. The presence of 15% high-quality proteins in wheat bran causes the integration of Se-AAs in these molecules [24]. Distinguishing between free Se-AAs and Se-AAs conjugated to proteins is relevant from a nutritional point of view, considering that free Se-AAs are more readily available for human beings absorption than Se-AAs conjugated to proteins [25].

Some papers in the literature have already studied free or conjugated Se-AAs in mung bean sprouts, which had been cultivated under Se-enriched condition [23], and in Brassica juncea but without any preconcentration system which is fundamental for the identification of all species present in the sample at relatively low concentrations (ppb) [26]. The aim of this work deals with the development of an analytical method for simultaneous extraction, preconcentration, identification, and quantitation of free and conjugated Se-AAs in wheat bran. In particular, four different extraction methods were compared and two different enzymes, namely Proteinase K and protease XIV, were tested to digest and obtain conjugated Se-AAs. The samples were purified and enriched by solid-phase extraction and analysed by means of HPLC-ESI-MS/MS. The method was then validated in the raw matrix.

2 | MATERIALS AND METHODS

2.1 | Chemicals and reagents

Proteinase K from *Tritirachium album* (CAS 39450-01-06); protease from *Streptomyces griseus* (CAS 9036-06-0); standards of (S)-2-amino-4-(methylseleno)butyric acid (Se-L-methionine) $\geq 98\%$; Se-DL-methionine $\geq 99\%$; (R)-2-amino-3-(methylselenanyl)propanoic acid hydrochloride (Me-Se-L-cysteine hydrochloride) $\geq 95\%$; 3,3'-(diseleno)bis[(R*)-2-aminopropanoic acid] (Se-DL-cystine) 95%; were obtained by Sigma Aldrich, now Merck (Darmstadt, Germany). Once analyzed with a chiral stationary phase (see later), this last standard showed three peaks with the area ratio $\sim 1:2:1$ which were attributed to L, meso, and D SeCys₂ forms, respectively. Pierce Bicinchoninic acid (BCA) Protein Assay Kit was purchased from Thermo Fisher Scientific. Reagent grade methanol, HCl (37%, w/w), NH₃ (28–30%, w/w) Tris (hydroxymethyl) aminomethane (Tris), trifluoroacetic acid (TFA), Sodium Dodecyl Sulfate (SDS); Formic acid 95–97%, ammonium formate $\geq 99.995\%$; were from Merck. Ultrapure water (resistivity 18.2 M Ω cm) was obtained by an Arium water purification system (Sartorius, Florence, Italy). LC-MS grade water methanol and acetonitrile (ACN) were purchased from VWR International (Milan, Italy). Oasis MCXTM (150 mg) cartridges were from Waters (Milford, MA, USA). The Astec CHIROBIOTICTM TAG column (50 \times 4.6 mm id, 5 μ m particle size) was provided by Sigma-Aldrich.

2.2 | Standard solutions

Stock solutions of Se-L-Met, Se-DL-Met and Me-Se-Cys hydrochloride were prepared at 1000 μ g/mL in water. Se-DL-cystine was prepared in 10% v/v formic acid at the same concentration. A composite standard stock solution was prepared by combining aliquots of each individual standard solution

and diluting with water to the final concentration of 5 µg/mL while for L and D SeCys₂ it was 2.5 µg/mL. All the stock solutions were subdivided in aliquots and stored at -20°C in amber glass vials and brought to room temperature (RT) just before use. Working standard solutions were prepared from stock standards by suitable dilution with water, stored at 4°C when not in use and renewed weekly. Structures of Se-AAs are shown in Supporting Information Figure S1.

2.3 | Total Se measurement

Total Se content was measured by microwave-assisted closed vessel acid digestion (MWD; Ethos 1 Touch Control Milestone srl., Sorisole, Bergamo, Italy) followed by hydride generation atomic fluorescence spectroscopy following a slightly modified procedure reported elsewhere [27]. Briefly, about 200 mg of each wheat bran sample was treated with 2 mL of 67% HNO₃ and 1 mL of 30% H₂O₂, and then heated with microwave energy for 40 min. The obtained solution was brought to a volume of 10 mL with ultrapure water and diluted with 36% HCl (1:2, v/v) before hydride generation atomic fluorescence spectroscopy analysis. A 5% HCl solution was used as carrier and 2% NaBH₄ in 0.5% NaOH as the reducing agent. All the samples were analyzed in duplicate. A five-point matrix-matched external standard calibration was performed by diluting a standard solution in 15% HNO₃ to obtain solutions in the concentration range 0.5–15 µg/L. Both SeO₄²⁻ and L-SeMet were used to obtain this calibration graph. The absence of significant matrix effects was confirmed after spiking with SeO₄²⁻ or L-SeMet at 2 ng/g, by evaluating the recovery (103 and 96%, respectively) after the spike of Se at 2 ng/g, and R₂ (0.9978 and 0.9958, respectively). The method detection limit (LOD, 0.1 ng/g) and the method quantification limit (LOQ, 150 ng/g) were calculated as three and ten times of the standard deviation of the blank determination, respectively (eight replicates). The operative blank value was subtracted to all measurements.

2.4 | Samples and sample extraction

Samples of wheat bran were obtained from local wholesale feed store of the Lazio region (Italy). The plant tissues were weighed, frozen in liquid nitrogen to break the cell walls, ground with pestle and mortar, and stored at 4°C in the refrigerator in a 50 mL polypropylene tube which was sealed and wrapped with aluminum foil until extraction or digestion.

Four different extraction protocols were compared. For all tested protocols, 50 mg of wheat bran was treated.

In protocol A, sample was extracted using 150 mg of acid-washed glass beads and 1.5 mL of water. The samples were submitted to two cycles of 1 h vortexing at RT and 1 h

ultrasonication at 55°C; then, the suspension was centrifuged at 24°C for 15 min, at 11 000× g. The supernatant was withdrawn and transferred into a 15 mL centrifuge tube, while the residue was resuspended and washed with 1 more mL of water, centrifuged again and the supernatant added to the extract. Ten mL of a solution of CH₃OH containing 10 mmol/L HCl was added to the extract. The tube was vortexed and incubated for 1 h at 4°C to promote protein precipitation. Supernatant contained free Se-AAs, while pellet contained conjugated Se-AAs. The pellet was collected by centrifugation (18 400× g for 15 min at 4°C), washed two times with 1 mL of CH₃OH:H₂O (80:20, v/v). Protocol B used the same reagents employed in protocol A with a slight difference in ultrasonication which was performed in ice rather than at 55°C. Protocol C was based on a literature method [22] and wheat bran samples were directly digested as described in the paragraph 2.5. In Protocol D wheat bran extracts were prepared by glass beads lysis method [28]. Briefly, 50 mg of wheat bran was added to 150 mg of acid washed glass beads and 1 mL of lysis buffer (60 mmol/L Tris pH 9 and 2% w/v SDS). The samples were placed in an ultrasonic bath for 4 h with intermittent vortexing (1 h) every 30 min, then they were incubated for 30 min at 100°C and finally the insoluble material was removed by centrifugation at 4°C for 15 min at 11 000× g. The supernatant coming from experiment was transferred into a new centrifuge tube and subjected to protein precipitation using a solution consisting of 10% w/v trichloroacetic acid (TCA) in acetone.

2.5 | Protein digestion

Pellets coming from protocol A, B and D were dissolved in 2 mL of 8 mol/L urea in Tris-HCl 60 mmol/L (pH 8.8) and diluted fourfold. All extracted samples were quantified by the BCA assay using bovine serum albumin (BSA) as standard following the manufacturing instruction (<https://www.thermofisher.com/order/catalog/product/23225>) and stored at -80°C until digestion. The protein percentage for the four employed protocols was in the range of 11.2 ± 0.8%. The digestion was carried out as follow. Two different proteolytic enzymes were used, namely Proteinase K and Protease XIV. For each sample, 6 mg of protein were in vitro digested. In the Proteinase K digestion experiments, 2 mg enzyme were added (1:3, enzyme/protein ratio) and the samples were digested by stirring continuously for 24 h in the dark using a wrist-action shaker (Burrell, Pittsburgh, PA, USA). In the experiment carried out with Protease XIV, 20 mg of enzyme (ratio enzyme:substrate 10:3) was added to the sample and the digestion was carried out overnight at 37°C. Enzymatic digestion was quenched by TFA to reach pH 2. For a more comprehensive explanation in Table 1 are reported all analyzed samples coming from the four different protocols.

TABLE 1 Summary of the extraction protocols

Extraction Protocol	Obtained Samples	Brief Method Description
Protocol A	A_free A_Proteinase K A_Protease XIV	This protocol allowed to identify free and conjugated Se-AA. Sonication temperature 55°C
Protocol B	B_free B_Proteinase K B_Protease XIV	This protocol allowed to identify free and conjugated Se-AA. Sonication in ice bath.
Protocol C	C_Proteinase K C_Protease XIV	Digestion was carried out directly on wheat bran. No free Se-AAs analyzed.
Protocol D	D_Proteinase K D_Protease XIV	Proteomic experiment. Only conjugated Se-AAs were analyzed.

2.6 | Solid phase extraction

The extracts were purified by an Oasis MCXTM SPE cartridge previously sequentially washed with 5 mL of CH₃OH and 5 mL of 10 mmol/L HCl solution, by gravity, according to our previous work [29]. After samples loading, the cartridge was washed with 2 mL ultrapure water followed by 5 mL of MeOH (by gravity) then, the analytes were eluted with 2 mL of CH₃OH, 3% NH₃ into a clean vial. The solvent was evaporated down to 150 µL in a Speed-Vac SC 250 Express (Thermo, Holbrook, NY, USA) maintained at 25°C; finally, 100 µL of ACN containing 0.5% HCOOH were added; the obtained solution was filtered using PTFE syringe filter and 200 µL were transferred to the autosampler vial.

2.7 | LC-MS/MS Analysis

LC-MS/MS analysis was performed according to our previous work carried out on oil samples in which an enantioselective hydrophilic interaction liquid chromatography-tandem mass spectrometry was performed. An Ultimate 3000 UHPLC system connected via a heated ESI source to a TSQ VantageTM triple-stage quadrupole mass spectrometer (Thermo Fisher Scientific, Bremen, Germany) were used. The UHPLC system consisted of a binary pump equipped with a degasser, a thermostated microwell plate autosampler, set at 14°C and a thermostated column oven. The Astec CHIROBIOTICTM TAG analytical column (50 × 4.6 mm id, 5 µm particle size) was kept at 50°C. Mobile phase A was MeOH/ACN/H₂O, 45:45:10 v/v/v, 10 mmol/L ammonium formate and 0.5% formic acid; mobile phase B was ACN/H₂O, 20:80 v/v, 20 mmol/L ammonium formate at pH 4. Gradient elution started with a 2 min isocratic step at 0% B. Then, B was linearly increased to 15% in 2 min, from 15 to 100% in 10 min and kept constant for 5 min. Finally, B was decreased linearly to 0% in 0.5 min and equilibrated for 5 min. The flow rate was set at 500 µL/min and 10 µL of the final extract was injected. The ESI source was operated in positive ionization and SRM

mode. The source settings were: spray voltage 3 kV, vaporizer temperature 280°C, and the capillary (ion-transfer tube) temperature 280°C. Sheath gas pressure, ion sweep gas pressure, and auxiliary gas pressures were set to 40, 0, and 20 (arbitrary units), respectively. Source conditions, lens parameters and analyte transitions were optimized by infusing standard solutions at 10 ng/µL in mobile phase A at 10 µL/min. The [M+H]⁺ ions were selected by the first quadrupole and fragmented in the collision cell with the optimized collision energy. The two transitions showing the highest S/N were selected for SRM. The UHPLC-MS system was managed by Xcalibur software (v.2.1, Thermo Fisher Scientific).

2.8 | Precautions

During the preparation of the samples, plastics, especially polyethylene, were avoided as much as possible, to avoid loss of the analytes by absorption. All the solutions were stored in amber glass vials to prevent degradation of the analytes by light. Another critical point of the experimental procedure is the removal of the solvent from the extract, since degradation of the most labile compounds may occur. Therefore, all the evaporation steps were performed in a rotary evaporator at RT, avoiding the complete drying of the extract. All solutions contained 1% ascorbic acid in order to avoid the oxidation of the Se-AAs. Thermal and light losses were avoided by carrying out all the evaporation steps in the dark.

2.9 | Method performance

The method validation was performed using wheat bran aliquots. The calibration curves were constructed in matrix, to perform quantitative liquid chromatography selected reaction monitoring (LC-SRM) analysis. The validation of the method also included the study of selectivity, recoveries, accuracy, LOD and LOQ. Two transitions were acquired as indicated in Supporting Information Table S1 according to FDA guidelines. (Guidance for industry: bioanalytical

method validation, 2018) SRM transition showing the highest S/N ratio was used for quantification (Q) purposes and the transition showing the second highest S/N ratio for purpose of identification/confirmation (q). In Supporting Information Table S1 there are reported precursor and product ions monitored for the investigated Se-AAAs. S-lens values for each precursor ion and collision energy for each transition are also reported. Scan width was kept at 0.5 *m/z* for all the transitions. Linear regression, averages and standard deviations were calculated using Microsoft Excel 2010. For recovery experiments, spiking was carried out directly on wheat bran for free Se-AA and before digestion for conjugated Se-AAAs.

2.9.1 | Calibration graphs

Three sets of calibration graphs were prepared. They were named standard in solvent (SS), matrix matched, and matrix assisted. To construct the SS calibration graph, standard calibration solutions were prepared at six different concentration levels by appropriate dilution of the Se-AA mixture solution H₂O/HCOOH 99.9:01 *v/v*. The levels were in the range 0.25–50 ng/mL. Each solution was prepared in duplicate and injected twice, at random; the results were averaged to obtain a single calibration graph for each Se-AA compound. For all Se-AAAs, the peak area of each analyte was plotted against the concentration of the corresponding analyte. The matrix matched curves were prepared by spiking individual extracts obtained from 50 mg aliquot of samples. The fortification levels (FLs) were in the range 0.25–50 ng/mL, corresponding to 1.25–250 ng/g of solid samples. The MA calibration curves were prepared by spiking 50 mg aliquots of the same sample before extraction. Note: no analyte-free sample was available.

2.9.2 | Recovery

Process Efficiency, Recovery and Matrix Effect (PE, RE, ME) were evaluated as in a previous work [30]. Matrix solutions spiked with Se-AAAs standards before and after extraction were named as sample set 1 and set 2, respectively, while neat standard solutions prepared in pure solvents were named as sample set 3. The matrix solutions without spike were named set 4. Three FLs were used for these evaluations. The first FL was set to 1 µg/g for methyl-seleno-cysteine, seleno-L-methionine, seleno-D-methionine and seleno-meso-cystine and 0.5 µg/g for seleno-L-cystine and seleno-D-cystine. The other two levels were 2xFL and 5xFL.

For each analyte, the absolute peak area was measured. The RE was assessed according to the following equation:

$$RE (\%) = (\text{Area set 1} / \text{Area set 2}) \times 100 \quad (1)$$

ME was estimated according to the following equation:

$$ME (\%) = (\text{Area set 2} - \text{Area set 4}) / \text{Area set 3} \times 100 \quad (2)$$

PE was estimated according to the following equation:

$$PE (\%) = (\text{Area set 1} - \text{Area set 4}) / \text{Area set 3} \times 100 \quad (3)$$

2.9.3 | Trueness and precision

Since Se-AAAs are endogenous compounds and no certified reference material (CRM) is available, trueness was estimated through recovery calculation. Therefore, it was calculated at the three FLs, by Eq. 1.

Precision of the method was assessed as within-laboratory precision, both intraday (repeatability) and interday (reproducibility), at the three concentration levels used for trueness estimation, by calculating RSD. The intraday precision was expressed as RSD_I of the trueness values of five spiked samples, for each concentration level, analyzed in the same day. The interday precision was expressed as RSD_R of the recovery values of five spiked samples, for each concentration level, analyzed in five consecutive days.

2.9.4 | LOD and LOQ

For each analyte, LOD was calculated on the q transition, after estimating the endogenous concentration of each analyte. LOD was intended as the amount of substance that, after extraction from a real sample, it was able to produce a chromatographic peak three times higher than the chromatographic baseline noise (i.e. S/N, 3:1). For the calculation of the LOQ, the following conditions had to be satisfied simultaneously: i) an S/N reporting ≥ 10:1 for the transition Q; ii) q was to be detected with an S/N ratio ≥ 3:1.

3 | RESULTS AND DISCUSSION

3.1 | Extraction protocol optimization

In this work, four different extraction procedures were evaluated for the simultaneous extraction and identification of free and conjugated Se-AAAs in wheat bran because a significant amount of Se is conjugated to proteins, therefore the enzymatic hydrolysis is mandatory to break the peptide bonds and release the Se-AAAs within the protein molecule. To the best of our knowledge, this study is the only one carried out on this matrix by HPLC-MS/MS analysis, as a previous work on whole wheat grains was performed by ion chromatography dynamic reaction cell inductively coupled plasma mass spectrometry without any differentiation between free and conjugated Se-AAAs [31].

The first issue to be considered with plant samples is the recalcitrant nature of plant tissues, which makes it necessary to grind the tissue as finely as possible to obtain a high recovery of compounds of interest before any solvent extraction. Compared to the previous papers [23,26], the

samples analyzed in this work were first stirred with glass beads. The use of a mechanical extraction method promotes the solubilization of the Se-AAAs.

After the mechanical maceration of the samples, different aqueous buffer can be used. The extraction of Se-AAAs from different matrices was widely studied in the literature [23,32,33] and considering the polar nature of these compounds, hot water extraction is one of the most used strategy. Different water temperatures were already tested highlighting that a temperature of 55°C resulted to be the best choice. For this reason, in protocol A this temperature was adopted. Considering the issues related to the instability of these analytes, such as UV radiation, slow oxidation by atmospheric oxygen accelerated by light, heat and alkalinity [34] a second extraction in ice (Protocol B) was also performed in order to understand if the temperature was responsible of Se-AAAs degradation. Alongside, a protocol already carried out [26] was tested digesting directly the wheat bran with two different enzymes (Protocol C). The method was employed in order to compare a literature method to our procedures even if it was not possible to obtain the free fractions of Se-AAAs. In the last protocol employed (Protocol D) a stronger extraction buffer, consisting in a detergent like SDS, was tested. In this experiment only digested fractions were obtained, as the supernatant contained high quantity of salts and interfering compounds and could not analyzed by mass spectrometry.

The results of the four extractions are summarized in Table 2 which shows the Se-AAAs extracted in ng/g and in (Supporting Information Table S2) that shows the total Se in ng/g. The evaluation of the extraction protocol was based on the identification performance of the target Se-AAAs. Three experimental replicates were performed for each condition, to assess the variability of each extraction procedure. A good reproducibility was observed for all the tested protocols, as the relative standard deviation was below 10%. As it can be observed in the Tables, higher Se-AA concentration levels were found in protocol B where the sample was

extracted by ice sonication cycles. In particular, Me-Se-L-Cys was identified only in protocols A and B in the fractions containing free Se-AAAs. The highest Me-Se-L-Cys amount was obtained in protocol B (3.66 ng/g). A lower amount was obtained by protocol A (2.91 ng/g); in all the other fractions this Se-compound was not detectable. Se-L-Met was detected in all the extracts, showing that the highest amount of this compound was bound to the proteins. While the amount of this compound was roughly the same in the free fractions, 7.98 and 8.82 ng/g for protocol A and B respectively, a considerable difference was highlighted in the two digested fractions. In protocol A 4.28 and 4.60 ng/g were quantified for digestion by proteinase K and protease XIV, while in protocol B the concentrations were 70 and 98.90 ng/g. This could be ascribed to the Se functional group degradation during the high temperature sonication. Protocol C was also quite efficient in recovering this Se-AA (78.47 and 55.06 ng/g), while Protocol D was found to be less valuable (12.80 and 3.40 ng/g). A possible explanation to the lower recoveries obtained in Protocol D could be ascribed to the degradation of the functional groups containing selenium at high temperature. It has been recorded that Se-AAAs are degraded at temperatures higher than 60°C (see Supporting Information Figure S2). Se L-Met is the only Se compound found in all extraction protocols. This result is not surprising since L-isomer of Se-Met is a major natural food-form. Se-L-Met is considered a useful chemical form for Se nutritional supplementation and it is widely used for its antioxidant and chemopreventive properties. Se-Met is also shown to increase glutathione peroxidase activity in cardiomyocytes [35]. An apparently astonishing result was the recovering of Se-D-Met in Protocol B (36.70 and 35 ng/g in Proteinase K and protease XIV digested fractions, respectively). It is well known that D-AAAs are not naturally found in eukaryotic organisms but they are commonly synthesized by bacteria. However, amino acid racemization can occur when food matrices are exposed to high temperature or fermentation during industrial

TABLE 2 Results of Se-AAAs quantification in wheat bran samples for the four compared extraction methods. Results are provided with RSD

Treatment Extraction/hydrolysis	Methyl-seleno-L cysteine (ng/g) ± SD	Seleno-L-methionine (ng/g) ± SD	Seleno-D-methionine (ng/g) ± SD	Seleno-L-cystine (ng/g) ± SD	Seleno-meso-cystine (ng/g) ± SD
A_free	2.91 ± 0.22	7.98 ± 0.21	<LOD	<LOD	<LOD
A_proteinase K	<LOD	4.28 ± 0.37	<LOD	<LOD	<LOD
A_protease XIV	<LOD	4.60 ± 0.30	<LOQ	<LOD	<LOD
B_free	3.66 ± 0.31	8.82 ± 0.51	<LOD	<LOD	<LOD
B_proteinase K	<LOD	70 ± 1.50	36.70 ± 0.91	7.74 ± 0.31	1.22 ± 0.058
B_protease XIV	<LOD	98.90 ± 1.70	35 ± 0.86	<LOD	<LOD
C_proteinase K	<LOD	78.47 ± 0.98	<LOD	<LOD	<LOD
C_protease XIV	<LOD	55.06 ± 0.78	<LOD	<LOD	<LOD
D_proteinase K	<LOD	12.80 ± 0.54	<LOD	<LOD	<LOD
D_protease XIV	<LOD	3.40 ± 0.34	<LOD	<LOD	<LOD

TABLE 3 Recovery (RE, %), Matrix Effect (ME, %) and Process Efficiency (PE, %) for the investigated compounds, obtained using 50 mg of wheat bran. Fortification level (FL) was set to 1 µg/g for methyl-seleno-cysteine, seleno-L-methionine, seleno-D-methionine and seleno-meso-cystine and 0.5 µg/g for seleno-L-cystine and seleno-D-cystine

Compound	FL			2 x FL			5 x FL		
	RE (%)	ME (%)	PE (%)	RE (%)	ME (%)	PE (%)	RE (%)	ME (%)	PE (%)
Methyl-seleno-cysteine	96	102	98	98	110	108	95	118	112
Seleno-L-methionine	95	88	84	98	90	88	92	90	83
Seleno-D-methionine	93	117	109	96	100	96	90	110	99
Seleno-L-cystine	74	80	59	80	85	68	73	87	64
Seleno-meso-cystine	73	79	58	82	87	71	74	80	59
Seleno-D-cystine	75	81	61	85	81	69	73	81	59

TABLE 4 Trueness and within-laboratory precision, expressed as relative standard deviation (intraday, RSD_I; interday, RSD_R; *n* = 5); method LOD and method LOQ

Compound	Trueness free SE-AA (RSD _I , RSD _R) (%)	Trueness Proteinase K (RSD _I , RSD _R) (%)	Trueness Protease XIV (RSD _I , RSD _R) (%)	Method LOD (ng/g)	Method LOQ (g/g)
Methyl-seleno-cysteine	96 (4;7)	91 (3;4)	84 (5;10)	0.72 ± 0.110	0.81 ± 0.011
Seleno-L-methionine	95 (5;8)	88 (12;15)	88 (11;12)	0.18 ± 0.021	0.20 ± 0.012
Seleno-D-methionine	93 (5;8)	87 (12;13)	80 (2;7)	0.18 ± 0.011	0.20 ± 0.011
Seleno-L-cystine	74 (6;7)	96 (2;7)	88 (7;9)	0.16 ± 0.015	0.10 ± 0.017
Seleno-meso-cystine	73 (13;5)	98 (1;5)	94 (4;6)	0.11 ± 0.014	0.16 ± 0.012
Seleno-D-cystine	75 (4;6)	97 (2;6)	96 (3;7)	0.05 ± 0.010	0.06 ± 0.013

processes. Food stores prepare and sell increasing quantities of foods, such as breakfast cereals, which in some cases contain substantial quantities of D-AAAs [36]. Se-L-Cys₂ and Se-meso-Cys₂ were also detected only by protocol B extraction with proteinase K digestion. This is probably due to the different cleavage ability of the two employed enzymes. Another possible explanation of the presence of Se-L-Cys₂ and Se-meso-Cys₂ could be related to the fact that in plants and animals, the majority of AAAs incorporated in proteins are L-forms, that is the reason why the corresponding D- or meso-forms can potentially be toxic. L-Se-AAAs are usually reported in studies, but a few ones also report D-forms, for instance in formula milk where Se-D-Met was identified [19] and in selenized yeast [12]; such works, however, do not provide any explanation for the phenomenon. Finally, D-forms were reported in a study on the Se distribution in chives treated with different Se supplementation. The major enantiomers were L-forms in all cases, but D-forms could be identified when chives were supplemented with Se-Met, indicating that the distribution of Se in the different enantiomeric forms can be influenced by the type of soil enrichment applied [37]. Another possible explanation of the presence of D- and meso-forms may be procedural. Water extraction is considered a safe procedure, which does not induce racemization, but strong acids have been reported to convert 0–10% of Se-L-Met into the D-form. Enzymatic release of Se-AAAs from proteins has been reported as a safe method to achieve high

recovery without artifacts formation [38]. However, further studies should be performed to deeply understand those data.

3.2 | Method performance

The HPLC-MS/MS method for the analysis of Se-AAAs in wheat bran was performed in accordance with the main FDA guidelines. All validation results are summarized in Table 3 and Table 4. For laboratory method validation, RE and ME were determined at three spiking levels in wheat bran samples, according to Eqs. (1) and (2) (see Table 3). The overall PE was provided by Eq. (3). The RSDs were below 15% for all the analytes.

Recoveries were >73% at the lowest FL. The MEs of signal suppression affected in particular Se-meso-Cys₂. The trueness of the method was assessed by means of REs at three FLs, whereas intra-day and inter-day laboratory precision were determined by performing recovery experiments (*n* = 5) at FL (1 µg/g for all the AAAs except Se-L-cys₂ and Se-D-cys₂, for which it was set to 0.5 µg/g) in the same day and in five consecutive days, respectively (see Table 4). Trueness and precision within the laboratory were also calculated at 2xFL and 5xFL (see Supporting Information Tables S4 and S5). The LODs and LOQs were determined as described in the Section 2 (see Table 4), since by operating in SRM mode with the last generation triple quadrupole mass spectrometers, it is quite common to obtain SRM signals without noise.

The absence of carry-over was assessed by injecting ethanol after the highest point of the calibration curve and after the non-fortified real samples (C_0). It was not always possible to compare the values of LOD and LOQ because different experiments are performed with different detectors. However, compared to the work on beans [23] and diet supplements [33], the values obtained in this work possess lower LOQ and our method allowed the identification of all the isomers of the Se-AAs in question. For these reasons, our method results to be more sensitive compared to the already mentioned papers.

LODs and LOQs are adequate to detect the endogenous quantities of Se-AAs in the real samples, maintaining a high identifying power even at low concentration levels. Table 4 shows intra- and interday recoveries and within-laboratory precision. The accuracy between one run and the next was within $\pm 20\%$, in perfect agreement with FDA guidelines, recommending a threshold of $\pm 20\%$ for the lowest peak level. The exhaustive validation of a method aimed at analyzing micronutrients in foods and biological samples should provide the use of CRMs. Unfortunately, there are not commercially available CRMs containing a complete set of analyzed Se-AAs. So, in this work, an indirect validation was the only possible way to circumvent the unavailability of an appropriate CRM and to evaluate the analytical performance of the developed method.

The equations and coefficient of determination (R^2) obtained for the standard and the matrix-matched calibration graph are reported in Supporting Information Table S3.

3.3 | Application to real samples

Four wheat bran samples from different local markets were analyzed for both Se-AAs and total Se.

The chromatograms of a real sample and a sample spiked at LOQ are shown in Supporting Information Figures S3 and S4.

Our samples showed a Se concentration range of 4.41–5.36 ng/g for free Se-AAs and 45.61–53.87 ng/g for the conjugated Se-AAs (Table 5). Among the Se-AAs selected for this study, Se-L-Met was found to be the most abundant in all analyzed samples with a concentration range of 7.42–9.21 ng/g in the free fractions and 67.21–100.02 ng/g for the conjugated ones, confirming that cereals converts Se mainly into Se-Met and incorporate it into protein in place of methionine because tRNA-Met does not discriminate between Methionine and Se-Met [39]. The results for both free and conjugated fractions were consistent for all our samples, demonstrating that there is no correlation between the Se in soil and in wheat bran samples.

We finally evaluated the Se speciation in the analyzed samples finding that 7% of the total Se was represented by free Se-AA, while 60–70% belonged the conjugated fractions. The

TABLE 5 Application to real samples extracted with Protocol B

Sample	Treatment Extrac- tion/hydrolysis	Methyl-seleno-L- cysteine (ng/g)	Seleno-L-methionine (ng/g)	Seleno-D-methionine (ng/g)	Seleno-L-cysteine (ng/g)	Seleno-meso-cysteine (ng ⁻¹)	Sum Se (ng/g) \pm
1	B_Free	3.66 \pm 0.12	8.82 \pm 0.19	<LOD	<LOD	<LOD	5.07 \pm 0.30
	B_proteinase K	<LOD	69.20 \pm 0.21	36.70 \pm 0.98	7.74 \pm 0.67	1.22 \pm 0.51	46.30 \pm 0.41
	B_protease XIV	<LOD	98.90 \pm 0.97	35.00 \pm 0.57	<LOD	<LOD	53.60 \pm 0.72
2	B_Free	4.21 \pm 0.37	9.21 \pm 0.54	<LOD	<LOD	<LOD	5.46 \pm 0.21
	B_proteinase K	<LOD	72.27 \pm 0.63	34.52 \pm 0.90	7.81 \pm 0.42	1.87 \pm 0.49	47.00 \pm 0.35
	B_protease XIV	<LOD	100.02 \pm 0.62	35.42 \pm 0.51	<LOD	<LOD	53.87 \pm 0.32
3	B_Free	5.61 \pm 0.45	7.50 \pm 0.78	<LOD	<LOD	<LOD	5.37 \pm 0.31
	B_proteinase K	<LOD	69.42 \pm 0.38	35.20 \pm 0.98	8.25 \pm 0.76	1.54 \pm 0.54	46.18 \pm 0.32
	B_protease XIV	<LOD	94.23 \pm 0.99	37.40 \pm 0.65	<LOD	<LOD	52.36 \pm 0.39
4	Free	3.42 \pm 0.67	7.42 \pm 0.45	<LOD	<LOD	<LOD	4.41 \pm 0.65
	B_proteinase K	<LOD	67.21 \pm 0.35	37.71 \pm 0.56	7.20 \pm 0.34	1.10 \pm 0.32	45.61 \pm 0.56
	B_protease XIV	<LOD	94.68 \pm 0.97	37.21 \pm 0.43	<LOD	<LOD	52.46 \pm 0.37

remaining 20–30% is due to other compounds which we did not analyze.

4 | CONCLUDING REMARKS

A method for determination of endogenous free and conjugated Se-AAs in wheat bran was described which includes the comparison of four different extraction protocols and the enantioresolution of Se-AAs isomers. The method, based on HPLC-ESI-MS/MS was validated, while a method previously developed and validated for total Se determination was adapted with few modifications to analyze total Se. The main aim of this work was the development of a method able to simultaneously extract in only one extraction both free and conjugated Se-AAs. The four tested protocols were compared on the basis of Se-AAs quantification. The best extraction was found to be protocol B in which an aqueous solution buffer and ice sonication cycles were employed. This protocol allowed the recovery of high concentrations of Se-AAs avoiding loss and degradation caused by high temperatures. The best protocol was therefore applied to the analysis of four real samples collected in different local markets. The range of total Se concentration was of 4.41–5.36 for free Se-AA and 45.61–53.87 ng/g for the conjugated Se-AAs. The most abundant Se-AA found in wheat bran samples was Se-L-Met confirming that it is the main source of organic Selenium found in food matrices.

ACKNOWLEDGMENT

We would like to thank Dr. Silvia Canepari and her research group for the data of total Se content which was measured by hydride generation atomic fluorescence spectroscopy.

CONFLICT OF INTEREST

The authors have declared no conflict of interest.

ORCID

Anna Laura Capriotti 

<https://orcid.org/0000-0003-1017-9625>

Giorgia La Barbera 

<https://orcid.org/0000-0003-0583-906X>

REFERENCES

- Tinggi, U., Selenium: its role as antioxidant in human health. *Environ. Health Prev. Med.* 2008, *13*, 102–108.
- Hoffmann, P. R., Berry, M. J., The influence of selenium on immune responses. *Mol. Nutr. Food Res.* 2008, *52*, 1273–1280.
- Bellinger, F. P., Raman, A. V., Reeves, M. A., Berry, M. J., Regulation and function of selenoproteins in human disease. *Biochem. J.* 2009, *422*, 11–22.
- Li, T., Wang, Y., Li, W. J., Chen, J. M., Wang, T., Wang, W. X., Concentrations and solubility of trace elements in fine particles at a mountain site, southern China: regional sources and cloud processing. *Atmos. Chem. Phys.* 2015, *15*, 8987–9002.
- Takahashi, K., Suzuki, N., Ogra, Y., Bioavailability comparison of nine bioselenocompounds in vitro and in vivo. *Int. J. Mol. Sci.* 2017, *18*, 506.
- Deng, S., Zeng, D., Luo, Y., Zhao, J., Li, X., Zhao, Z., Chen, T., Enhancement of cell uptake and antitumor activity of selenadiazole derivatives through interaction and delivery by serum albumin. *RSC Adv.* 2017, *7*, 16721–16729.
- Gao, H.-H., Chen, M.-X., Hu, X.-Q., Chai, S.-S., Qin, M.-L., Cao, Z.-Y., Separation of selenium species and their sensitive determination in rice samples by ion-pairing reversed-phase liquid chromatography with inductively coupled plasma tandem mass spectrometry. *J. Sep. Sci.* 2018, *41*, 432–439.
- Gupta, M., Gupta, S., An overview of selenium uptake, metabolism, and toxicity in plants. *Front. Plant Sci.* 2017, *7*, 2074.
- FAO, FAOSTAT Database, http://www.fao.org/waicent/portal/statistics_en.asp.
- Onipe, O. O., Jideani, A. I. O., Beswa, D., Composition and functionality of wheat bran and its application in some cereal food products. *Int. J. Food Sci. Technol.* 2015, *50*, 2509–2518.
- Graß, B., Hergenröder, R., Neyer, A., Siepe, D., Determination of selenoamino acids by coupling of isotachopheresis/capillary zone electrophoresis on a PMMA microchip. *J. Sep. Sci.* 2002, *25*, 135–140.
- Ponce De Leon, C. A., Sutton, K. L., Caruso, J. A., Uden, P. C., Chiral speciation of selenoamino acids and selenium enriched samples using HPLC coupled to ICP-MS. *J. Anal. At. Spectrom.* 2000, <https://doi.org/10.1039/b001069n>.
- Ju, W., Li, X., Li, Z., Wu, G. R., Fu, X. F., Yang, X. M., Zhang, X. Q., Gao, X. B., The effect of selenium supplementation on coronary heart disease: A systematic review and meta-analysis of randomized controlled trials. *J. Trace Elem. Med. Biol.* 2017, *44*, 8–16.
- Choi, C. K., Dong, M. W., Sample preparation for HPLC analysis of drug products, Handbook of Pharmaceutical Analysis by HPLC, Vol 6, Academic Press, 2005, 123–144.
- Méndez, S. P., González, E. B., Sanz-Medel, A., Hybridation of different chiral separation techniques with ICP-MS detection for the separation and determination of selenomethionine enantiomers: chiral speciation of selenized yeast. *Biomed. Chromatogr.* 2001, *15*, 181–188.
- Gómez-Ariza, J. L., Bernal-Daza, V., Villegas-Portero, M. J., Comparative study of the instrumental couplings of high performance liquid chromatography with microwave-assisted digestion hydride generation atomic fluorescence spectrometry and inductively coupled plasma mass spectrometry for chiral speciation of selen. *Anal. Chim. Acta* 2004, *520*, 229–235.
- Pérez Méndez, S., Blanco González, E., Sanz Medel, A., Chiral speciation and determination of selenomethionine enantiomers in selenized yeast by HPLC-ICP-MS using a teicoplanin-based chiral stationary phase. *J. Anal. At. Spectrom.* 2000, *15*, 1109–1114.
- Ilisz, I., Ballet, S., Van Rompaey, K., De Wachter, R., Tourwé, D., Armstrong, D. W., Péter, A., High-performance liquid chromatographic separation of stereoisomers of *N*-phthaloyl-protected

- amino acids and dipeptidomimetics. *J. Sep. Sci.* 2007, 30, 1881–1887.
19. Gómez-Ariza, J. L., Bernal-Daza, V., Villegas-Portero, M. J., First approach of a methodological set-up for selenomethionine chiral speciation in breast and formula milk using high-performance liquid chromatography coupled to atomic fluorescence spectroscopy. *Appl. Organomet. Chem.* 2007, 21, 434–440.
20. Huang, X., Wang, J., Wang, Q., Huang, B., Chiral speciation and determination of DL-selenomethionine enantiomers on a novel chiral ligand-exchange stationary phase. *Anal. Sci.* 2005, 21, 253–257.
21. Sutton, K. L., Ponce de Leon, C. A., Ackley, K. L., Sutton, R. M. C., Stalcup, A. M., Caruso, J. A., Development of chiral HPLC for selenoamino acids with ICP-MS detection: application to selenium nutritional supplements. *Analyst* 2000, 125, 281–286.
22. Capriotti, A. L., Montone, C. M., Antonelli, M., Cavaliere, C., Gasparini, F., La Barbera, G., Piovesana, S., Laganà, A., Simultaneous preconcentration, identification, and quantitation of selenoamino acids in oils by enantioselective high performance liquid chromatography and mass spectrometry. *Anal. Chem.* 2018, 90, 8326–8330.
23. Tie, M., Sun, J., Gao, Y., Yao, Y., Wang, T., Zhong, H., Li, H., Identification and quantitation of seleno-amino acids in mung bean sprouts by high-performance liquid chromatography coupled with mass spectrometry (HPLC-MS). *Eur. Food Res. Technol.* 2018, 244, 491–500.
24. Baladrán-Quintana, R. R., Mercado-Ruiz, J. N., Mendoza-Wilson, A. M., Wheat bran proteins: a review of their uses and potential. *Food Rev. Int.* 2015, 31, 279–293.
25. Torres, S., Gil, R., Silva, M. F., Pacheco, P., Determination of seleno-amino acids bound to proteins in extra virgin olive oils. *Food Chem.* 2016, 197, 400–405.
26. Montes-Bayón, M., Yanes, E. G., De León, C. P., Jayasimhulu, K., Stalcup, A., Shann, J., Caruso, J. A., Initial studies of selenium speciation in Brassica juncea by LC with ICPMS and ES-MS detection: an approach for phytoremediation studies. *Anal. Chem.* 2002, 74, 107–113.
27. Di Dato, C., Gianfrilli, D., Greco, E., Astolfi, M., Canepari, S., Lenzi, A., Isidori, A. M., Giannetta, E., Profiling of selenium absorption and accumulation in healthy subjects after prolonged L-selenomethionine supplementation. *J. Endocrinol. Invest.* 2017, 40, 1183–1190.
28. Montone, C. M., Capriotti, A. L., Cavaliere, C., La Barbera, G., Piovesana, S., Zenezini Chiozzi, R., Laganà, A., Peptidomic strategy for purification and identification of potential ACE-inhibitory and antioxidant peptides in Tetrademus obliquus microalgae. *Anal. Bioanal. Chem.* 2018, 410, 3573–3586.
29. Piovesana, S., Montone, C. M., Antonelli, M., Cavaliere, C., La Barbera, G., Canepari, S., Samperi, R., Laganà, A., Capriotti, A. L., Investigation of free seleno-amino acids in extra-virgin olive oil by mixed mode solid phase extraction cleanup and enantioselective hydrophilic interaction liquid chromatography-tandem mass spectrometry. *Food Chem.* 2019, 278, 17–25.
30. La Barbera, G., Capriotti, A. L., Cavaliere, C., Foglia, P., Montone, C. M., Chiozzi, R. Z., Laganà, A., A rapid magnetic solid phase extraction method followed by liquid chromatography-tandem mass spectrometry analysis for the determination of mycotoxins in cereals. *Toxins (Basel)*. 2017, 9, 147.
31. Tsai, C.-Y., Jiang, S.-J., Microwave-assisted extraction and ion chromatography dynamic reaction cell inductively coupled plasma mass spectrometry for the speciation analysis of arsenic and selenium in cereals. *Anal. Sci.* 2011, 27, 271–6.
32. Bird, S. M., Uden, P. C., Tyson, J. F., Block, E., Denoyer, E., Speciation of selenoamino acids and organoselenium compounds in selenium-enriched yeast using high-performance liquid chromatography?inductively coupled plasma mass spectrometry. *J. Anal. At. Spectrom.* 1997, 12, 785–788.
33. Zembrzuska, J., Matusiewicz, H., Polkowska-Motrenko, H., Chajduk, E., Simultaneous quantitation and identification of organic and inorganic selenium in diet supplements by liquid chromatography with tandem mass spectrometry. *Food Chem* 2014, 142, 178–187.
34. Davies, M. J., Protein oxidation and peroxidation. *Biochem. J.* 2016, 473, 805–825.
35. Savaskan, N. E., Hore, N., Eyupoglu, I. Y., Metal Ion in Stroke. Springer New York, New York, NY 2012, pp. 525–536.
36. Genchi, G., An overview on d-amino acids. *Amino Acids* 2017, 49, 1521–1533.
37. Kapolna, E., Shah, M., Caruso, J., Fodor, P., Selenium speciation studies in Se-enriched chives (*Allium schoenoprasum*) by HPLC-ICP-MS. *Food Chem.* 2007, 101, 1398–1406.
38. Chen, B., He, M., Zhong, C., Hu, B., Chiral speciation of selenoamino acids in biological samples. *J. Chromatogr. A* 2014, 1363, 62–70.
39. DeCou, C. R., Cole, T. T., Lynch, S. M., Wong, M. M., Matthews, K. C., Assault-related shame mediates the association between negative social reactions to disclosure of sexual assault and psychological distress. *Psychol. Trauma Theory, Res. Pract. Policy* 2017, 9, 166–172.

SUPPORTING INFORMATION

Additional supporting information may be found online in the Supporting Information section at the end of the article.

How to cite this article: Montone CM, Antonelli M, Capriotti AL, et al. Investigation of free and conjugated seleno-amino acids in wheat bran by hydrophilic interaction liquid chromatography with tandem mass spectrometry. *J Sep Sci* 2019;42:1938–1947. <https://doi.org/10.1002/jssc.201900047>



The study of bioactive peptides present in various food products represents a new field of research and field of application of proteomic analysis. Some peptides are able to trigger physiological activities that promote skin health, such as stimulating collagen synthesis, controlling angiogenesis and melanogenesis and modulating cell proliferation. Peptides are often classified as multifunctional peptides, i.e. they are capable of inducing more than one physiological activity. These characteristics make them suitable for use as therapeutic agents in the pharmaceutical field or as functional compounds, food additives, bio-preservatives in the field of nutraceuticals. Therefore, the purpose of this doctoral project was to develop effective and innovative analytical strategies for the study of bioactive molecules and identification of compounds not abundant or not yet identified in different food matrices.

Ph.D. in Chemistry (XXXII cycle)

Carmela Maria Montone

Tutor: Prof Aldo Lagnà

Cordinator: Prof. Osvaldo Lanzalunga